Durham E-Theses

Late Quaternary palaeoceanography in Disko Bugt, West Greenland

Park, Laura Anne

How to cite:

Park, Laura Anne (2003) *Late Quaternary palaeoceanography in Disko Bugt, West Greenland*, Durham theses, Durham University. Available at Durham E-Theses Online: http://etheses.dur.ac.uk/1284/

Use policy

The full-text may be used and/or reproduced, and given to third parties in any format or medium, without prior permission or charge, for personal research or study, educational, or not-for-profit purposes provided that:

- a full bibliographic reference is made to the original source
- a link is made to the metadata record in Durham E-Theses
- the full-text is not changed in any way

The full-text must not be sold in any format or medium without the formal permission of the copyright holders.

Please consult the full Durham E-Theses policy for further details.

Academic Support Office, Durham University, University Office, Old Elvet, Durham DH1 3HP
e-mail: e-theses.admin@dur.ac.uk Tel: +44 0191 334 6107
http://etheses.dur.ac.uk

Late Quaternary Palaeoceanography in Disko Bugt, West Greenland

A copyright of this thesis rests with the author. No quotation from it should be published without his prior written consent and information derived from it should be acknowledged.

Laura Anne Park

Hatfield College

Thesis Submitted for the degree of Doctor of Philosophy

Department of Geography

University of Durham

September 2003

1 5 MAR 2006

For my family

Declaration

This thesis is the result of my own work. Data from other authors contained herein are acknowledged at the appropriate point in the text. All quotations have been distinguished by quotation marks and the sources of information acknowledged. A reference list is appended.

The copyright of this thesis lies with the author. No quotation from it may be published without prior consent and any information derived from it should be acknowledged.

Laura Park

Acknowledgements

Financial support for this thesis comes from the Natural Environment Research council (NERC) ARCICE Thematic Studentship Award; grant reference number GT24/1999/ARCI/0009. Fieldwork aboard the R/V *Dana* was also funded in part by EU funding awarded to Dr Antoon Kuijpers and project partners at GEUS (Geological Survey for Greenland and Denmark).

This thesis would not have been possible without the assistance and support of numerous people. I am grateful to my supervisors, Dr Jerry Lloyd and Professor Antony Long (University of Durham), for their enthusiasm, commitment and motivation. Thank you for having faith in me. I also acknowledge the support of other project members, Dr Antoon Kuijpers (GEUS) for fieldwork logistics and Karin G. Jensen (GEUS) for flexibility with core sampling and diatom discussions, Dr Andy Roberts (Southampton Oceanography Centre) for the support and assistance with core sampling, and Dr Justin Dix (SOC) for Chirp fieldwork and his family's generous hospitality. I gratefully acknowledge the access to foraminiferal data from Dr Jerry Lloyd and sedimentological data from Matthias Moros (Bjerknes Centre for Climate Research, Norway). Many thanks go to the Captains and crew aboard both the R/V *Dana* and the R/V *Porsild* for their hard work and professionalism. Thanks also to staff at the Sheriff's Highway Veterinary Practice for their help with X-raying and Colin Chilcott (University of Edinburgh) for clarifying many isotope queries.

The technicians and secretaries in the Department of Geography, University of Durham were wonderful throughout; particular thanks to Neil Tunstall, Stella Henderson and Michelle and Steven Johnson. I am extremely grateful for the help and support and encouragement from friends and colleagues in the department, particularly, Dr Toru and Achan Higuchi, Drs Kay McManus, Louise Bracken, Paul Harrison, Adam Holden, Dan Knox and Damien Laidler. A special thank you to Dr Ant Beck for always having a solution to any one of my numerous "crises". Further mention must be made of all

members of the QEC research group, especially Cal Gregory, Erin McClymont and Elizabeth Mackie. Thanks also for the great fun provided by the Monday footy crowd, and Wednesday rugby bunch.

I would like to thank Consett and District Rugby Football Club and all the lads at the 'Demi' for providing great entertainment over the last couple of years, especially Richy T, Broughy, and Mick Kent. Thanks also must go to the Geology Lot, particularly Dr Dougal Jeram, Rich Single and Gary Wilkinson for FNITNI, and for not being Geographers!

For helping me hang onto some shred of sanity, the following people made the good times great and the bad times hazy. Many thanks to Louise Hanson for her friendship no matter what, John Thompson for excellent wine and French chat, Dr Ali Quirk for her generosity, and Nancy Ockendon for keeping the MRes lot in touch. Special thanks to Alan Milne for his generous nature and fabulous computer, and Marcia Vincent for the Turkish rug and washing machine story.

Finally, thank you to my family (Carol, John and Struan). The frequent supplies of red wine, treats and cash certainly smoothed the way, but this would not have been possible without your love, support and patience. This is for you.

Laura Park

Durham, September 2003

Abstract

This thesis uses foraminiferal, sedimentological and isotope analysis from three piston cores from different depositional environments in Disko Bugt, West Greenland to understand the nature of the relationship between deglacial activity and palaeo-water mass circulation. It has increased the spatial and temporal resolution of marine multi-proxy data in the region through the development of a tight radiocarbon chronology. High resolution sampling has furthered the understanding of modes of Holocene palaeoceanographic circulation in Disko Bugt and West Greenland, and linked them to likely operating mechanisms of change. Information about past variations in the strength of the dominant water current in West Greenland (the West Greenland Current – WGC), has been successful through the application of foraminiferal water mass indicator species and isotope techniques. New dating relating to the timing of the final retreat of Jakobshavns Isbrae, the most important ice stream draining the West Greenland Ice Sheet, has been determined through evidence of meltwater and sediment fluxes from the calving margin. The high resolution records produced in this thesis clearly document the rapid instability and subsequent retreat of the ice stream to be related to rapid atmospheric warming following the well-documented "8.2 event". Mid-Holocene climatic changes are recorded in the fjord mouth setting of Kangersuneq. Despite considerable dissolution processes operating in the fjord (which are in fact a product of climatic change themselves), a high resolution record of variable and declining warmth of the WGC is recorded from *c.*6.3 ka cal BP, prior to the onset of full Neoglacial conditions around 4.1 ka cal BP. The maximum cooling during the Neoglacial period is clearly seen from *c.*3.2 to 2.2 ka cal BP in two cores. A distinct warming of the WGC takes place around 2.2 ka cal BP, which can be linked to an increased component of Irminger Current Water. This is also seen in the records from East Greenland and the Nordic Seas. The foraminiferal assemblages from one of the cores show evidence of a distinct climatic amelioration which is associated with the Medieval Warm Period. There is some evidence for a deterioration of oceanographic conditions which is linked to the onset of the Little Ice Age.

Table of Contents

List of figures

Chapter 3: Methods

Chapter 4: Results

Chapter 1: Introduction

1.1 Introduction

This thesis examines the nature of the relationship between the deglacial history of Disko Bugt in West Greenland and water mass circulation. Diagnostic foraminiferal assemblages, sedimentological data and $\delta^{18}O$ ratios are used to develop a high resolution record of Holocene modes of oceanographic circulation, focussing on the dynamics of deglaciation, Holocene rapid instabilities and the role of Jakobshavns Isbrae (the major ice stream draining the West Greenland Ice Sheet). Possible driving mechanisms for change in oceanographic circulation are explored, and links are established on a range of temporal and spatial scales with existing palaeoclimatic records from the region.

This chapter outlines the key role the Greenland Ice Sheet (GIS) has to play in climate change, and places this thesis and its research aims firmly in the context of the University of Durham ARCICE project *"Late Quaternary Ice Sheet Dynamics in West Greenland"*. The scientific rationale for this research is outlined, highlighting the current knowledge gaps, the significance of West Greenland, and the importance of Jakobshavns Isbrae. This chapter also provides a summary of the thesis structure.

1.2.1 The Greenland Ice Sheet and climate system

The Greenland Ice Sheet is an important component of the global climate system, and is one of the two large ice masses to have survived the transition to current interglacial conditions (Huybrechts, 2002). This is because it is located in the path of storms, allowing the ice sheet to receive a large moisture supply and also because of the relative warmness of near ocean surfaces (Johnson, 1997). Its volume is enough to raise sea level by 7 metres (Warrick and Oerlemanns, 1990) and, combined with an estimated summer melting of up to 60% (Weidick, 1985), it has a key role to play in climate dynamics on both a local and global scale. From 6 ka cal yr BP onwards,

Greenland is the only ice sheet left in the Northern Hemisphere, and therefore provides a laboratory for studying the interaction between climate/ice sheets and oceanography, as well as a basis for climate model validations.

1.2.2 Perturbations in the West Greenland climate system

The Greenland ice cores, e.g. GRIP (Dansgaard *et al.*, 1993; GRIP Members, 1993; Grootes *et al.*, 1993; Meese *et al.*, 1994; Steig *et al.*, 1994; Stuvier *et al.*, 1995, 1997), GISP2 (Meese *et al.*, 1994; Steig *et al.*, 1994; Stuvier *et al.*, 1995; 1997), Dye 3 (Clausen *et al.*, 1997; Dahl-Jenssen *et al.*, 1998; Johnsen *et al.*, 2001), provide a record of atmospheric climate signals which are used as a benchmark against which to correlate other global proxy palaeoenvironmental records. However, there is a relatively poor understanding of past dynamics of the ice sheet, and of changes in mass balance relating to atmospheric and ocean interactions. In general, the Holocene has been considered to be a characteristically stable period in comparison to glacial periods (Grootes *et al.*, 1993). Despite this, increasing evidence suggests that high latitude areas were more susceptible to variable climate conditions than previously thought (e.g. Bianchi and McCave, 1999; Bond *et al.*, 1997, 2001; Dahl and Nesje, 1996), and variations in freshwater flux may be a key component of these changes (Alley *et al.*, 1997; de Vernal *et al.*, 1991). As Greenland is the single remaining ice sheet in the Northern Hemisphere, there is potential for significant oceanographic and atmospheric perturbation on a local, regional and global scale given currently predicted scenarios for future climate change. These scenarios are primarily related to potential disruption to the thermohaline circulation by increased freshwater flux to the North Atlantic forced by anthropogenically-induced warming (Dansgaard *et al.*, 1993; Schmittner and Stocker, 1999; Stocker and Schmittner, 1997).

The formation of North Atlantic Deep Water is critical in driving global thermohaline circulation. The circulation of water masses in the North Atlantic region is an important conduit for heat transport. An increase in meltwater supply to the North Atlantic from Arctic and Greenlandic sources initiated by climate warming is likely to reduce surface water densities and therefore the deep-water formation rates. A resulting thermohaline circulation slow-down or collapse, initiated by changes in

meltwater flux, would impact significantly on Western Europe and Africa and have implications for the global climate system (Latif *et al.*, 2000; Seager *et al.*, 2002).

1.2.3 Localised variations in the West Greenland climate system

It is becoming increasingly apparent that seemingly localised changes in atmospheric or oceanographic conditions, such as variations in the mode of the North Atlantic Oscillation (NAO), one of the most prominent modes of variability in the Northern Hemisphere winter climate (Wanner *et al.*, 2001), may have "knock-on" effects throughout the climate system (Dawson *et al.*, 2003; Seidov and Haupt, 2003). Enhanced storm activity and moisture supply in the Labrador Sea relating to the incursion of increasing westward deflected warm water masses carried by the Irminger current are likely to have been responsible for the initiation of Canadian ice sheet re-growth at the start of the Last Glacial Maximum (Bradley, 2000; Johnson, 1997). With increased evaporative losses to the anthropogenically enhanced greenhouse effect from increased CO_2 production, estimates are that re-growth/expansion of the Canadian and Greenland ice sheets could be instigated towards the end of this century (Johnson, 1997; Ulbrich and Christoph, 1999).

Enhanced positive phases of NAO are likely to have significant effects on atmospheric and oceanographic circulation in the North Atlantic regions due to northward displacement of the Arctic front, creating anomalously high atmospheric temperatures in Europe, as far northeast as Siberia, and much lower temperatures and drier climates in West Greenland (Nesje *et al.*, 2000; Rogers, 1997; White, *et al.*, 1997). Greenland is influenced by both the Icelandic Low to the southeast and Davis Strait/Baffin Bay storms to the southwest and west. The NAO creates a "seesaw" in winter temperatures between West Greenland and Northern Europe (Barlow *et al.*, 1997; Dawson *et al.*, 2003).

1.2.4 Other climate system driving mechanisms

Other driving mechanisms such as changing solar irradiance (Bond *et al.*, 1997; Finkel and Nishiizumi, 1997) may be involved in rapid shifts and instabilities in the climate system during the Holocene. Bond *et al.*, (2001) claim that clusters of sub-millennial scale variabilities in solar flux in the range of 200-500 years are the main driving mechanism for the production of the periodic ~1500 yr cyclicity known generally as 'Bond cycles' (Bond *et al.*, 1997). These Bond cycles show rather limited periodicity during the Holocene, and indeed the reported duration for Bond cycles is on the order of 1470 +/-500 yrs (Schulz, 2002; Schulz and Paul, 2002). These and other authors (e.g. Chapman and Shackleton, 1998; 2000; Grootes and Stuiver, 1997; Stuiver *et al.*, 1995) argue that ice core and marine records may rather be exhibiting Holocene climatic variations with a 550 and 900-1000 periodicity (Risebrobakken *et al.*, 2003).

1.3.1 Introduction to the ARCICE project

This thesis is part of the oceanographic component of a wider international research project entitled "*Quaternary Ice Sheet Dynamics in West Greenland*" which is funded by the NERC ARCICE programme. ARCICE is a thematic research programme that aims to enhance our understanding of, and capacity to predict, the fluctuations of Arctic sea-ice and glaciers, which influence climate and sea levels in NW Europe. The specific project based in Durham addresses a primary aim of the ARCICE programme, namely the dynamics of glaciated Arctic continental margins since the Last Glacial Maximum (LGM). It involves collaboration with other institutions on a national and international basis; the University of Copenhagen, the Geological Survey of Greenland and Denmark (GEUS), the Southampton Oceanography Centre, and Toronto University.

The multidisciplinary ARCICE project has two main strands; the first is terrestrially based, and the second is marine based. The terrestrial component is related to Holocene relative sea level (RSL) changes in West Greenland, investigating glacio-isostatic adjustment and ice margin fluctuations by establishing a new generation of

well-constrained RSL curves based on isolation basin and coastal stratigraphic data. These data are then used to test models and existing chronologies for ice-margin fluctuations since the Last Glacial Maximum (LGM) (Long *et al.*, 1999, 2003; Long and Roberts, 2002, 2003; Rasch, 2000).

1.3.2 Terrestrial based component

In recent years there has been an increase in the research investigating ice margin fluctuations of the Greenland Ice Sheet since the Last Glacial Maximum (LGM). This research has tended to focus on the relatively wide ice-free terrestrial margins of west Greenland. The accepted chronology was proposed in the 1970's by workers such as Weidick (1968, 1972) and Ten Brink (1974, 1975), with more recent valuable contributions from Kelly (1985); Ingólfsson *et al.* (1990); Van Tatenhove *et al.* (1995, 1996); Funder and Hansen (1996), and has recently been updated by Bennike and Björck (2002). This research has been based largely on geomorphological mapping of major moraine complexes of West Greenland, with the deglacial chronology developed using relative sea-level (RSL) curves, radiocarbon dated by shells and other carbonaceous material. Recent work by Long *et al.* (1999) and Long and Roberts (2002) used isolation basin methodology to increase the accuracy of RSL reconstructions.

1.3.3 Overview of the marine based component

The key aim of the marine component was to identify 'rapid instabilities' of the Greenland Ice Sheet in Disko Bugt, West Greenland (Figure 1.1), which may be linked to topographic morphology, pinning points of the ice sheet, and meltwater and sediment fluxes. This has been achieved by undertaking a coring programme directed by seismic data acquisition to identify sites for palaeoceanographic reconstructions using foraminiferal, oxygen isotope and other sedimentological techniques. Analysis of the data produced using these techniques has produced a centennial to millennial timescale record of palaeoceanographic change in terms of meltwater/iceberg and

sediment fluxes since the LGM. This can then be directly linked to Greenland ice core records (e.g. GRIP, GISP2).

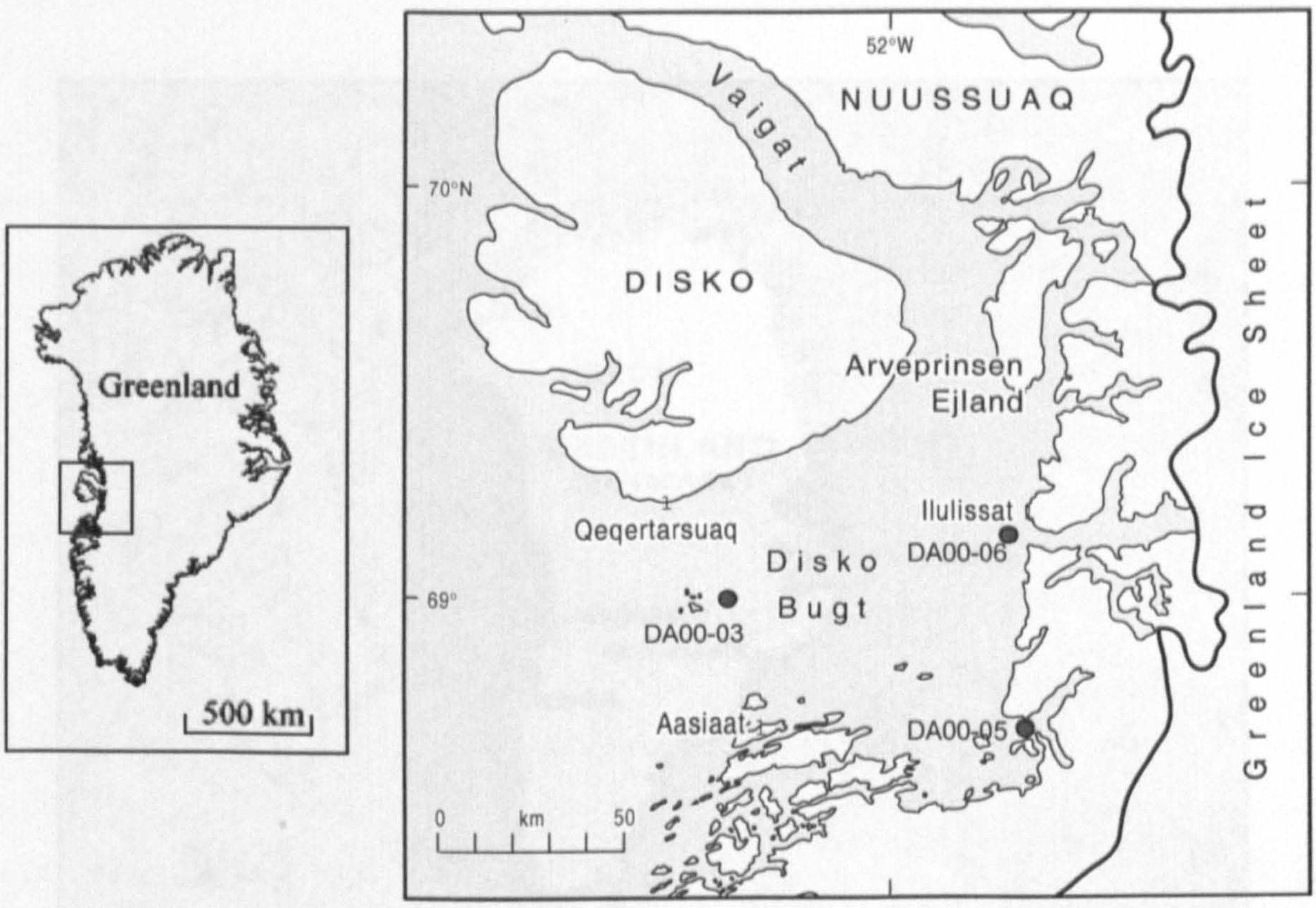

Figure 1.1: Location map of research area, Disko Bugt, West Greenland. Blue dots mark the location of the long piston cores (DA00-03, DA00-05, DA00-06) used in this thesis.

Thermohaline circulation allows vast quantities of mid latitude heat to be transported to the North Atlantic Ocean by the "conveyor belt circulation system". Despite significant increases in the understanding of its contemporary behaviour, as well as its activity over long time periods during the last glacial and postglacial transition (e.g. Bond *et al.,* 1997; Broecker *et al.,* 1997; Dixon and Lanzante, 1999; Grotzner *et al.,* 1999; McManus *et al.,* 2002; Rassmussen *et al.,* 2003), changes in past ocean circulation during the Holocene are more poorly documented (Duplessy *et al.,* 2001). Records of ocean circulation and climate change in high latitudes during the Holocene are concentrated in the Nordic and Greenland Seas (e.g. Duplessy *et al.,* 1992; Fronval and Jansen, 1996; Hald and Aspeli, 1997; Koç *et al.,* 1993; Veum *et al.,* 1992), and despite an increasing body of research on the Greenland margin (e.g. Andrews *et al.* 1994, 1996, 1997, 1998a, 199b; de Vernal *et al.*, 1992; Dowdeswell *et al.,* 1998; Feyling-Hanssen and Funder, 1990; Funder and Weidick, 1991; Jennings

and Helgadottir, 1994; Jennings and Weiner, 1996; Kuijpers *et al.* 2003; Levac *et al.*, 2001), there is a significant knowledge gap in terms of the offshore record of oceanographic change in central West Greenland.

Figure 1.2: Overall diagram showing location of the different seas (Nordic Seas: Barents Sea, Norwegian Sea, Greenland Sea, and the Labrador Sea) in the area in relation to Greenland. Adapted from http://wwp.greenwichmeantime.com/time-zone/north-america/greenland/map.htm

Disko Bugt, in central West Greenland is a large marine embayment, and is an important location in relation to the Greenland Ice Sheet because it receives the iceberg and meltwater flux from the Jakobshavns Isbrae ice stream. Jakobshavns Isbrae is one of a series of massive outlets, which are important conduits for meltwater/icebergs and sediment transfer from the Greenland Ice Sheet to the continental shelf. At the present day Jakobshavns Isbrae is the fastest flowing ice stream in the world; it drains approximately 7% of the Greenland Ice Sheet and discharges 30 to 40 $km^3\ a^{-1}$ (Bindschadler 1984), this is equivalent to approximately one-third of the calving budget for the whole of central West Greenland (Reeh, 1984).

1.3.4 Model testing of the marine based component

The marine component of the ARCICE project was initially designed to test two possible scenarios of ice sheet fluctuations. The first related to the two-stage model of deglaciation proposed by Funder and Hansen (1996). These authors proposed that rapid rising RSL allowed destabilisation of the marine based portion of the ice sheet between 14 and 10 ka BP (Figure 1.3), followed by a slower retreat of the terrestrially based portions from the inner-lying coastal areas to a position behind the present ice margin. Following the climatic optimum, a readvance is thought to have occurred, but evidence has been limited.

The second scenario aimed to test the behaviour of Jakobshavns Isbrae during the mid to late-Holocene. Glaciological reconstructions by Weidick *et al.* (1990) estimated that between 2.7-4.7 ka. cal BP the margin of the Inland Ice at Jakobshavn was approximately 15 km behind its current position, close to a deep bedrock trough extending 1200-1500 m below sea level and continuing over 100 km inland (Figure 1.4). They proposed ameliorated climate conditions which showed consistency with archaeological occupation of southwest Greenland Inuit sites.

Due to the age of preliminary core basal dates, it is likely that destabilisation of the marine-based portion of the ice sheet on the shelf is likely to pre-date the longest core record (DA00-06) available, and the original ARCICE aims of understanding pre-Holocene deglacial history could not be addressed. The resulting resolution of DA00-06, proximal to Jakobshavns Isbrae has limited the ability of this research to specifically address Weidick *et al.'s* (1990) model, and as can be seen from the cartoon in Figure 1.3, Funder and Hansen (1996) do not address ice margin activity during the Holocene in their model.

By documenting possible oceanographic effect of halts or readvances of the Inland Ice following the initial recession of the marine based portion of the ice sheet from the continental shelf, the suggestion that the Greenland Ice Sheet may have undergone catastrophic drawdown through the ice stream during the deglacial process could be addressed.

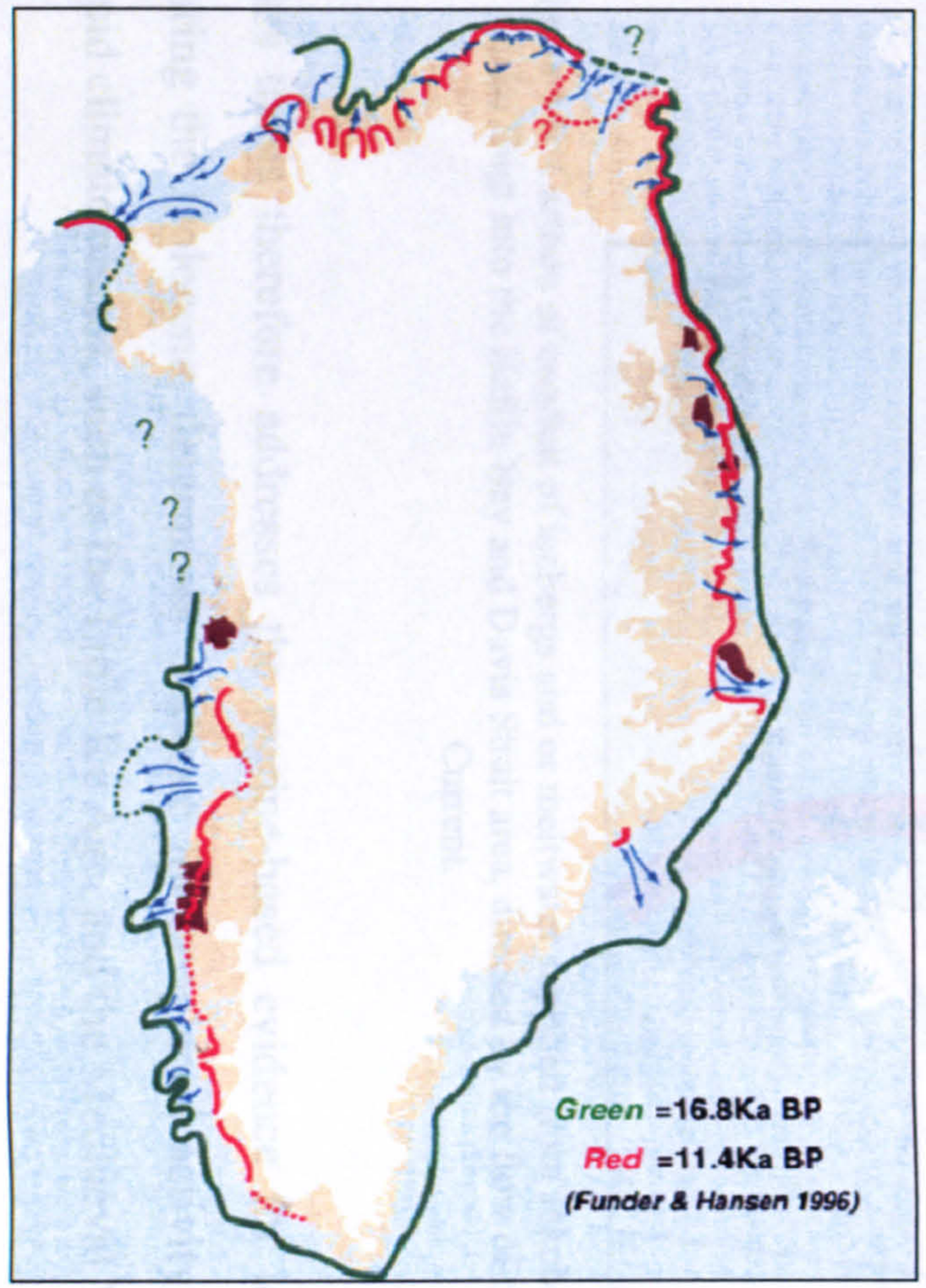

Figure 1.3: Cartoon of 2-stage model of marine-based deglaciation. Green line shows estimated position of ice margin at 16.8 ka cal BP and red line shows estimated position of ice margin at 11.4 cal ka BP (From Funder and Hansen, 1996).

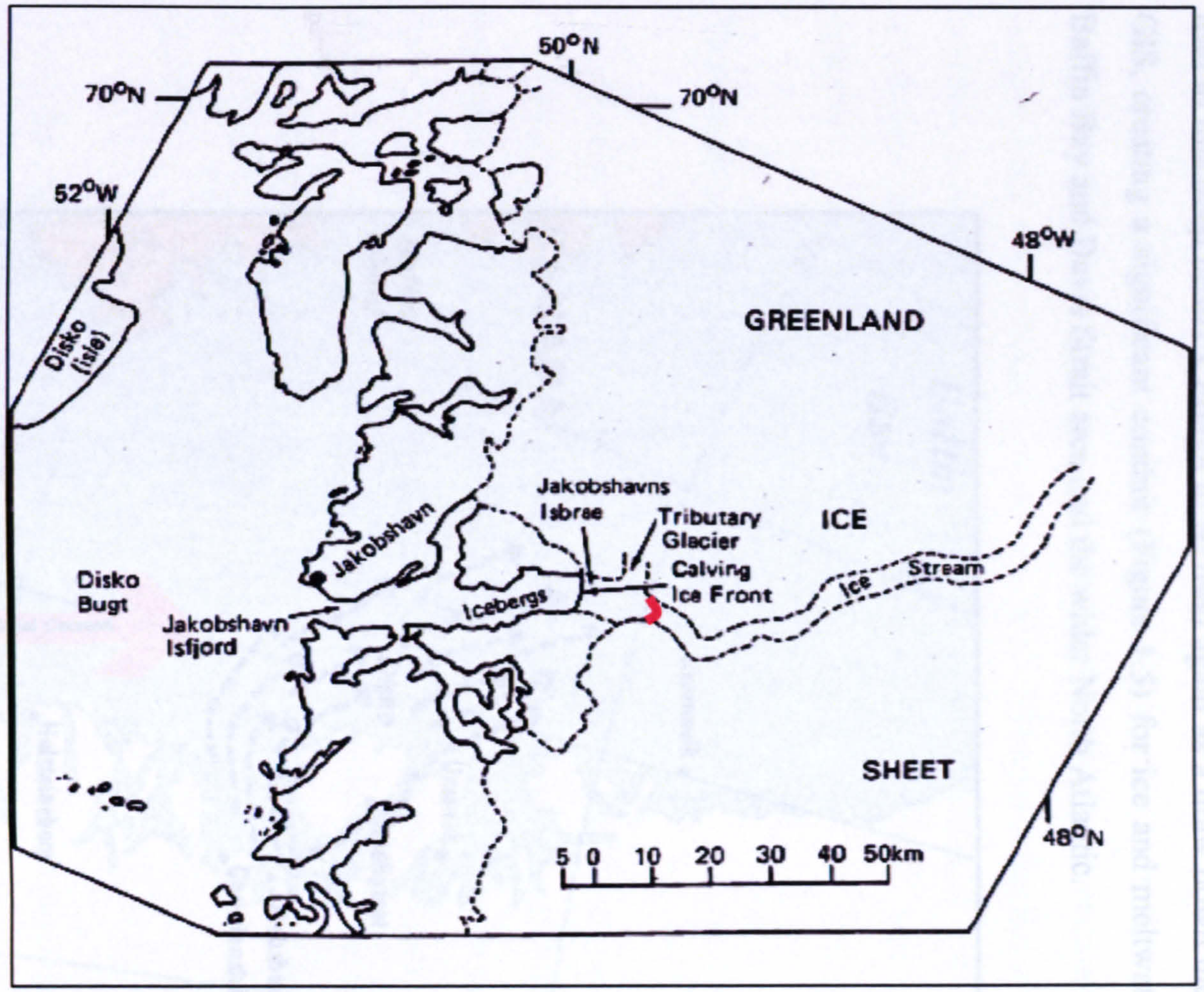

Figure 14: Diagram of the possible position of the ice margin 4.7-2.7 ka BP. The red line on this figure marks the possible position of the ice margin 4.7-2.7 ka cal BP (From Weidick *et al.*, 1990)

This scenario has important implications, as predicted rises in future warming may lead to this deep bedrock trough to be used again as a draw down mechanism for the GIS, creating a significant conduit (Figure 1.5) for ice and meltwater fluxes to the Baffin Bay and Davis Strait area and the wider North Atlantic.

Figure 1.5: Cartoon of conduit of icebergs and or meltwater supplied from Jakobshavns Isbrae through Disko Bugt into the Baffin Bay and Davis Strait area, directed by the flow of the West Greenland Current.

This thesis therefore addresses the marine-based evidence for ice stream activity during the Holocene, determines evidence for neoglacial activity, and more recent rapid climate phases, such as the Little Ice Age, and the Mediaeval Warm Period.

1.4.1 Thesis aims and objectives

This PhD thesis is concerned with the oceanographic component of the ARCICE project. It is important that an accurate record of palaeoceanographic change complements the terrestrial record of West Greenland deglaciation. This work presents a continuous high-resolution decadal to bidecadal record of Holocene palaeoceanographic changes from foraminiferal, isotopic and sedimentological analysis.

The overall aim of this research is:

To develop a high resolution record of Holocene modes of palaeoceanography, focussing on the dynamics of deglaciation, Holocene rapid instabilities and the role of Jakobshavns Isbrae using foraminiferal, sedimentological and oxygen isotope data from three pistons cores at locations in Disko Bugt (see Figure 1.1). This will contribute to producing a centennial to millennial timescale record of palaeoceanographic change in terms of meltwater/iceberg and sediment fluxes since the LGM that can be directly linked to Greenland ice core records (e.g. GRIP, GISP2).

From this, specific objectives were developed to meet the requirements of the project as a whole:

1. To determine the deglacial history of Disko Bugt, West Greenland, and variation of the composite water masses of the West Greenland Current (WGC), using marine records from three piston cores in Disko Bugt.

2. To evaluate the discharge history of Jakobshavns Isbrae during the Holocene.

3. To establish a high resolution record of Holocene water mass changes within Disko Bugt from faunal and isotopic records.

4. To develop a tight chronology for these palaeoenvironmental records through radiocarbon dating.

5. To compare these results to established global climate records such as GRIP and GISP2, as well as to previous work from the North Atlantic region.

1.4.2 Rationale behind specific thesis objectives

The specific rationale for each of these objectives is discussed below.

1. Advances in the understanding of the deglaciation of West Greenland have been made through terrestrial based investigations (e.g. Long and Roberts, 2002, 2003, Long *et al.*, 1999; Rasch *et al.*, 1997). However, there is limited marine based information about the timing and behaviour of Jakobshavns Isbrae as it retreated from Disko Bugt. While there is a body of knowledge about the timing and re-instigation of present day water mass circulation in the region, the data are often limited to relatively low resolution studies in shallow coastal fjord sites. The key findings of this thesis will link the terrestrial record of ice sheet change and Jakobshavns Isbrae's deglacial activity to the oceanographic story. This has not been attempted previously.

2. This objective examines whether meltwater and sediment flux from Jakobshavns Isbrae during the past has been constant. Currently, Jakobshavns Isbrae drains approximately 7% of the Greenland Ice Sheet. It is possible that this proportion has varied during the Holocene. This may relate to deglaciation of Disko Bugt, ice stream response to changes in global temperature, and ice stream response to driving mechanisms such as global isostatic adjustment (GIA), and possible variations in moisture supply derived from changes in the atmospheric system over the North Atlantic region.

Examination of the core sediments may reveal if there have been fluctuations in the dominance of this ice stream, with ice rafted debris (IRD) 'episodes' recorded at different locations in the Bugt. Linkages with the records of warmer or colder water

masses can be made with the IRD records to determine whether any IRD events can be connected to climate signals of a more regional nature, or whether the shifts are reflecting changes in local sediment delivery and meltwater/iceberg production conditions.

3. Changes in the faunal assemblages and isotopic record of foraminiferal tests in Disko Bugt will reveal the variation in water mass conditions throughout the Holocene. It is likely that in core locations proximal to Jakobshavns Isbrae changes in oxygen isotope ratios will reflect variations in intensities of meltwater input from the ice stream into Disko Bugt, and thus document the deglacial history of Jakobshavns Isbrae. Isotopic variations may also be linked to changes in the strength of (individual components of) the West Greenland Current, the dominant surface current along the west coast of Greenland (Figure 1.6). This brings a more regional oceanographic dimension to the bay.

Changes in faunal composition of sediments can be related to changes in bottom water conditions (temperature, salinity, preservation potential). Certain species can be linked for example, to ice proximal or ice distal conditions, which will reveal changes in the proximity of Jakobshavns Isbrae during deglaciation and the Holocene. Some species may also be found to be indicative of changes in the proportion of the two composite surface water currents which combine to form the West Greenland Current. It is likely that distribution of species may also be controlled by availability of food, which could be a possible indication of changing pack ice conditions.

Regional and local influences will be differentiated by changing faunal compositions. It is important to acknowledge that possible complications of the faunal records may arise through a regional climate change causing a local and a regional response. Distinguishing these may be addressed by careful comparisons with the IRD and isotopic records produced in this thesis, and the other palaeoenvironmental data currently being produced (Jensen, *et al., submitted* and Jensen *et al., in press*, Morros, *unpublished data)*. Comparison with ice core records and further regional studies will further resolve possible signal complications.

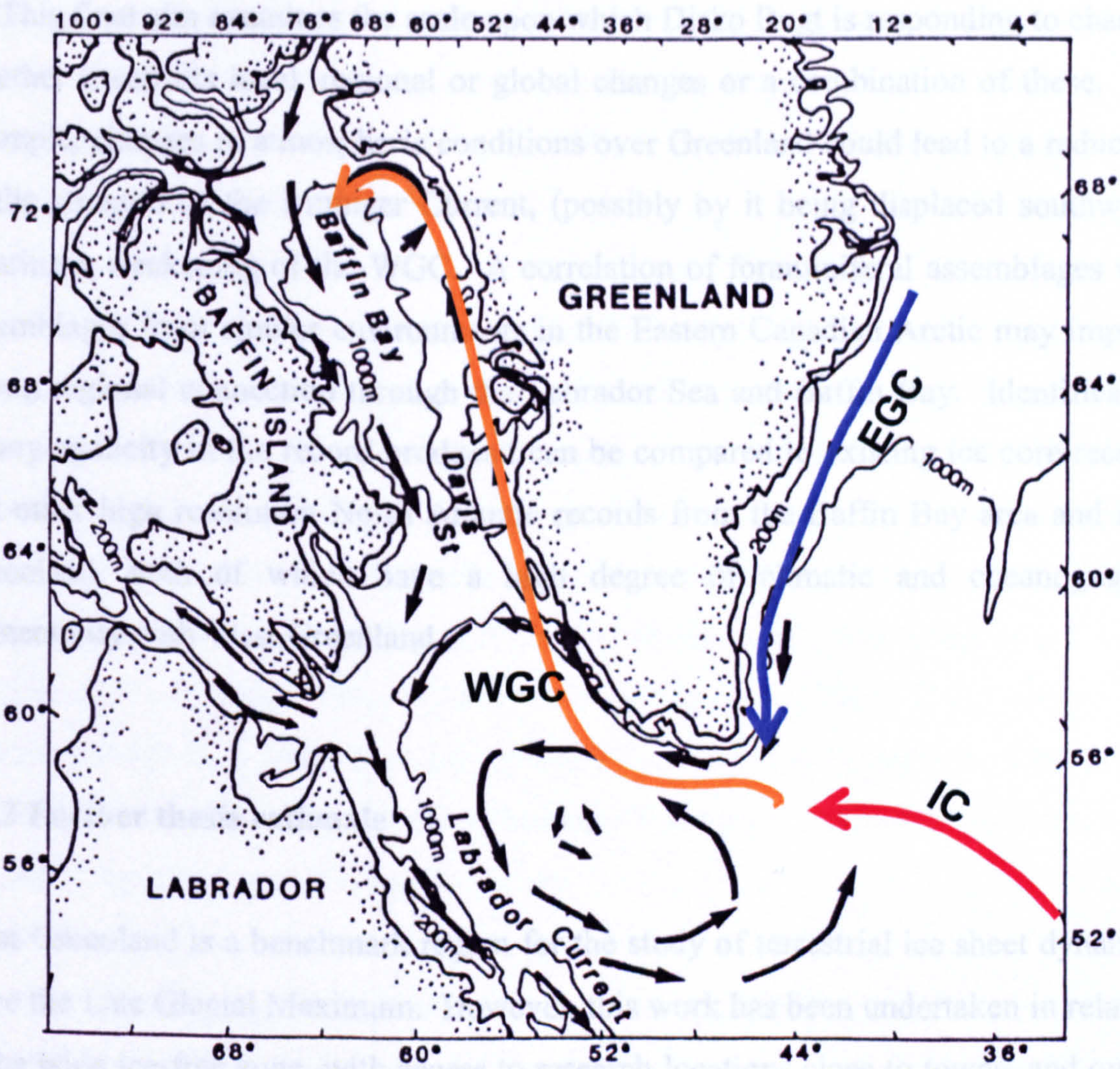

Figure 1.4: Cartoon of dominant surface current in West Greenland. West Greenland Current: WGC (Warm, depicted as orange), East Greenland Current: EGC (Cold, depicted as blue), Irminger current: IC (Warmest, depicted as red). (Adapted from Osterman and Nelson, 1989).

4. Tight chronological control is of the utmost importance. Reliable age-depth models are vital for correlation of any sort, especially in complex sedimentary environments, and in relation to the other aims given here. Without a tight chronological framework, results are merely descriptive, and cannot be directly compared to other records. Throughout this NERC project, and in this thesis in particular, emphasis has been on generating well-constrained, high resolution paleoenvironmental data. These relate to identification of rapid instabilities or events, such as massive drawdown of the Greenland Ice Sheet. As far as possible, with the materials available, this has been achieved, and the chronology of the three cores involved is presented in Chapter 4.

5. This final aim examines the scale upon which Disko Bugt is responding to change; whether it reflects local, regional or global changes or a combination of these. For example, changes in atmospheric conditions over Greenland could lead to a reduction in the strength of the Irminger Current, (possibly by it being displaced southward) creating a weakening of the WGC. A correlation of foraminiferal assemblages with assemblages from similar environments in the Eastern Canadian Arctic may imply a strong regional connection through the Labrador Sea and Baffin Bay. Identification of any cyclicity in the record produced can be compared to existing ice core records and other high resolution North Atlantic records from the Baffin Bay area and East Greenland, both of which have a high degree of climatic and oceanographic connectivity with West Greenland.

1.4.3 Further thesis rationale

West Greenland is a benchmark region for the study of terrestrial ice sheet dynamics since the Late Glacial Maximum. However, this work has been undertaken in relation to the wide ice-free zone, with access to research locations close to towns, and out of the research base on Disko Island. The region has a long history of relative sea level (RSL) research, and archaeological research of occupation of this wide, presently ice-free zone by Greenlandic Inuit cultures. This research has been based on terrestrial sequences, some of which include marine sediments now above sea level, but the offshore palaeoceanographic component of the region has not been addressed. High resolution palaeoceanography of the West Greenland margin has been relatively poorly investigated in comparison to the East Coast and the north Icelandic Shelf. This current research from Disko Bugt is the first to have generated a high-resolution palaeoceanographic record of the region.

1.5.1 Identifying the knowledge gap

Previous work in terms of foraminiferal research in west coast sites has been limited to an early 1970's paper on palaeotemperatures in a small southwest fjord (Hermann, 1972), taxonomic efforts by Feyling-Hansen and Funder (1990) based in the north of

Greenland, and a fjord-based study on Disko Island (Øhlenschlager, *unpublished MSc thesis*, 2000). Most foraminiferal studies are confined to the east coast (Jennings and Helgadottir, 1994, Jennings and Weiner 1996), or the Eastern Canadian Arctic (Vilks, 1989; Osterman and Nelson, 1989).

Back on the west coast of Greenland, good RSL results and terrestrial chronologies have been generated (Long *et al.*, 1999; Long and Roberts 2001, 2003; Rasch, 1997). Increasingly intensive work has been carried out on the glaciology of Jakobshavn Isbrae itself, and the subsequent modelling of its behaviour, ice flow and velocities, and iceberg production (e.g. Abdalatti and Krabil, 1999; Bamber *et al.*, 2000a, 2000b; Joughin *et al.*, 2001; Letreguilly *et al.*, 1991; Matsumoto, 1996; Sohn *et al.*, 1998; Sugden, 1987; Thomas *et al.*, 1998; Warren and Hulton, 1990). Early bathymetric seismic surveys were undertaken by Brett and Zarudski (1979), but these were purely descriptive, with no interpretation or linkage of surveyed bathyal features to wider aspects of local or regional ice sheet history.

Recent oceanographic research is relatively extensive, with a detailed analysis and breakdown of the West Greenland Current and adjacent currents and waters (e.g. Buch, 2000; Buch and Stein, 1987; Dunbar, 1989; Myers *et al.*, 1989; Stein, 1990, 1993). However, this research has tended to be driven by socio-economic factors, as knowledge of oceanographic conditions here is important in the assessment of environmental impact on living resources, and assessing the possibilities of living and non-living exploitation of marine resources (Buch, 2000).

The major aspect that has not been investigated in any high resolution detail previously is the palaeoceanographic evolution of the West Greenland margin, and specifically Disko Bugt. There is currently no comprehensive palaeoceanographic record against which to compare these other terrestrial palaeo-records and contemporary process investigations, or to provide reliable marine-based evidence to complement their findings. In recent years it has become very obvious that in order to further understanding of past climates and environments all aspects of the palaeorecords must be investigated. This is especially true in an ice marginal location such as this where the role of the ocean has been divorced from the surrounding

environment, especially in light of the increasing awareness of the part played by ocean circulation in determining climate fluctuations on a variety of scales.

1.5.2 Relevance to future climate scenarios

From palaeoclimatological perspectives, knowledge of ice sheet or ice stream behaviour and its interaction with the ocean during interglacials, as well as glacials, is important, especially in relation to iceberg and meltwater flux on ocean circulation in the North Atlantic. Understanding the nature of water mass changes is also important in order to realistically quantify freshwater flux as a forcing mechanism in the ocean component of general circulation models (Matsummoto, 1996). High resolution records of relationships between the ice sheet, climate and ocean circulation in the past, such as this thesis seeks to present, is crucial to furthering the understanding of mechanisms operating today, and in modelling the responses of the ice sheet to potential future climate perturbations.

Knowledge of past perturbations and rapid short lived climate changes such as those that may have been operating in the Holocene interglacial is essential for climate model prediction, as the resolution of current models is often too coarse to derive confident predictive outputs for future climatic scenarios, particularly in relation to forcings of meltwater flux variations. Stocker (2000) describes freshwater discharge into the ocean as the primary agent to trigger abrupt (climate) changes. Short lived periods such as the Medieval Warm Period (MWP) and the Little Ice Age (LIA) are able to be related in part to changes in oceanographic circulation and water mass transport and states of atmospheric pressure (Domack and Mayewski, 1999; Jennings and Weiner, 1996; Jennings *et al.*, 2002; Hui Jiang *et al.*, 2002; Lassen *et al.*, 2002), rather than just global atmospheric temperature changes.

Increasing the resolution of marine (and terrestrial) multi-proxy palaeoenvironmental data, as well as enhancing the spatial resolution of marine sites in the North Atlantic to include regions such as West Greenland, is ultimately required to further resolve the issues of periodicity and rapid scale changes during this present interglacial. The

proximity of coastal and offshore West Greenland to well-established high-resolution and globally significant records such as the Greenland ice cores is essential for addressing these issues. The location of Jakobshavns Isbrae as the most important ice stream draining the Greenland Ice Sheet (GIS) (see Figure 1.1), and its connectivity to the wider regional oceanography of Baffin Bay and the North Atlantic, means it is well placed for identifying phases of palaeoceanographic or palaeoclimatic change on a range of spatial and temporal scales.

1.6 Chapter summary and thesis structure

This introduction has provided an outline of the scientific rationale for undertaking this research. The importance of the location of Greenland and its relationship with the atmospheric and climate systems have been identified, as well as possible responses to driving mechanisms of change in the past, and in relation to future climate scenarios. The justification and aims of this thesis have been outlined in the context of the wider thematic ARCICE project and existing relevant palaeoenvironmental work in the West Greenland and Disko Bugt area.

This thesis is structured as follows. Chapter 2 examines the prevailing oceanographic circulation system, dominant in West Greenland at the present time, with reference to knowledge of past circulation, which this research aims to develop. Chapter 3 outlines the methods used to generate data for this thesis, concentrating on site selection, sampling methods, and analytical techniques. Results from the three piston cores used within this research are presented in Chapter 4, and relate to foraminiferal distributions, stable isotope results, sedimentological data and the development of a Holocene marine chronology for Disko Bugt, West Greenland.

Palaeoenvironmental interpretation of these core results from Disko Bugt is discussed in Chapter 5, identifying significant foraminiferal assemblages which can be related to the specific water mass components of the West Greenland Current (WGC). Chapter 6 develops these discussions to establish the palaeoceanographic record of West Greenland during the Holocene. These two interpretation chapters focus on the nature of the relationship between the deglacial history of Jakobshavns Isbrae in Disko Bugt,

West Greenland, and water mass circulation, and develop a high resolution record of Holocene modes of the WGC activity. Possible driving mechanisms for change are explored, and links on a range of temporal and spatial scales are established with existing palaeoclimatic records. Thesis conclusions are presented in Chapter 7, as well as acknowledgement of thesis research limitations. Finally, suggestions are made regarding possible future research paths stemming from this original investigation.

Chapter 2: West Greenland study area

2.1.1 Introduction

This chapter discusses the West Greenland study area, and highlights current research and prevailing knowledge about present and past processes operating in the area. Specific attention is paid to the advances made in relative sea level work, and a detailed examination of West Greenland oceanography is made.

2.1.2 Breadth of previous West Greenland research

West Greenland has been the subject of varying degrees of investigation and research. Mid-century diatom investigations by Foged (1953, 1955, 1958, 1972, 1977), provide taxonomic information, but little connection is made to palaeoenvironmental records. Glaciological investigation of ice streams (specifically Jakobshavns Isbrae) and modelling of these (Warren and Hulton 1990; Warren 1991; Reeh *et al.,* 1999) has been a focus for terrestrial research.

Low resolution coastal fjord studies have been carried out in Southwest Greenland (e.g. Bennike *et al.*, 1994; Donner and Jungner, 1975; Feyling-Hanssen and Funder, 1990; Funder and Weidick, 1991; Ingolfsson *et al.*, 1990; Kelly, 1979, 1985; Levac, 2001; Osterman and Nelson, 1989). However, these marine based studies have not extended to Disko Bugt, or linked findings to possible terrestrial or glacial operating mechanisms. Fjord investigations in Disko Bugt itself have been poorly developed in the area, with only two significant studies based in fjords of Disko Island rather than the mainland (Desloges *et al.,* 2002; Gilbert *et al.,* 1998), which concentrate on sedimentological processes.

Further terrestrial processes that have received attention include rock glacier formation (Humlum, 1999), and more recently, limnological research (Anderson *et al.,* 1999, 2001; Brodersen and Anderson, 2000, 2002; Ryves *et al.,* 2002; Willemse and Tornqvist, 1999). These latter authors are concerned with developing transfer

functions from diatoms and chironomids to assess changes in precipitation and evapotranspiration during the late Quaternary. This achievement will be useful in furthering the understanding of moisture supply to coastal terrestrial areas and has possible implications for comprehending West Greenland's response to atmospheric circulation changes such as amplified phases (positive or negative) of the North Atlantic Oscillation (NAO).

2.2.1 West Greenland landscape

West Greenland is taken to be the 150 km to 200 km wide ribbon of ice-free land that stretches from Kap Alexander (78° N) to Kap Farvel (60° N). Disko Bugt is centrally located (between 68°30'N and 69°15'N and 50°00'W and 54°00'W), and is the largest (40,000 km^2) (Long and Roberts, 2002) marine embayment on the west coast (Figure 2.1).

Figure 2.1: Map of extent of West Greenland from Kap Farvel to Kap Alexander.

Precambrian gneisses account for much of the mainland bedrock geology, while Disko Island and areas of the Nuussuaq peninsula are composed of relatively soft Tertiary basalts (Chalmers *et al.,* 1999). Morphologically, the landscape is very similar to the classic fjord landscape of western Norway (Ten Brink, 1975). For the most part, the terrestrial coastal landscape is hilly upland, with cirques and plateau remnants with elevations from 300 to 1500 m. The landscape is further typified by exposed and deeply abraded bedrock and thin Quaternary deposits (Funder, 1989; Sugden, 1974), often with small lakes or isolation basins present above and below the marine limit (Long *et al.,* 2003). During the last glacial maximum (LGM), termed the Sisimuit glaciation or Sisimuit Stade by Kelly (1985), the presently low-lying ice-free coastal area was covered by the Greenland Ice Sheet (GIS), and Disko Bugt was occupied by a large ice stream (Ingólfsson *et al.,* 1990). The ice shelf extended out into Baffin Bay (Bennike *et al.,* 1994; Funder, 1989), and is likely to have been grounded 30-50 km offshore (Kelly, 1985).

Figure 2.2: Diagram showing the possible extent of the Sisimuit glaciation during the Last Glacial Maximum (Blue line). Filled in area represents the large ice stream likely to have been occupying Disko Bugt at the time.

2.2.2 West Greenland bathymetric features

Seismic surveys carried out nearly 50 years ago (Holtzscherer and Bauer, 1954 in: Funder, 1989) found the presence of deep subglacial channels extending more than 200 km inland from the ice margin and it is thought that these are related to a preglacial fluvial drainage system. Immediately north of Disko Bugt, the landscape is dominated by a complex drainage pattern derived from high mountain plateaux dissected by steep valleys and cirques. The bathymetric features of the area are described by Brett and Zarudzki (1979) from their shallow geophysical survey on the West Greenland continental shelf. These are rather generalised, as their survey was limited to Disko Bugt itself.

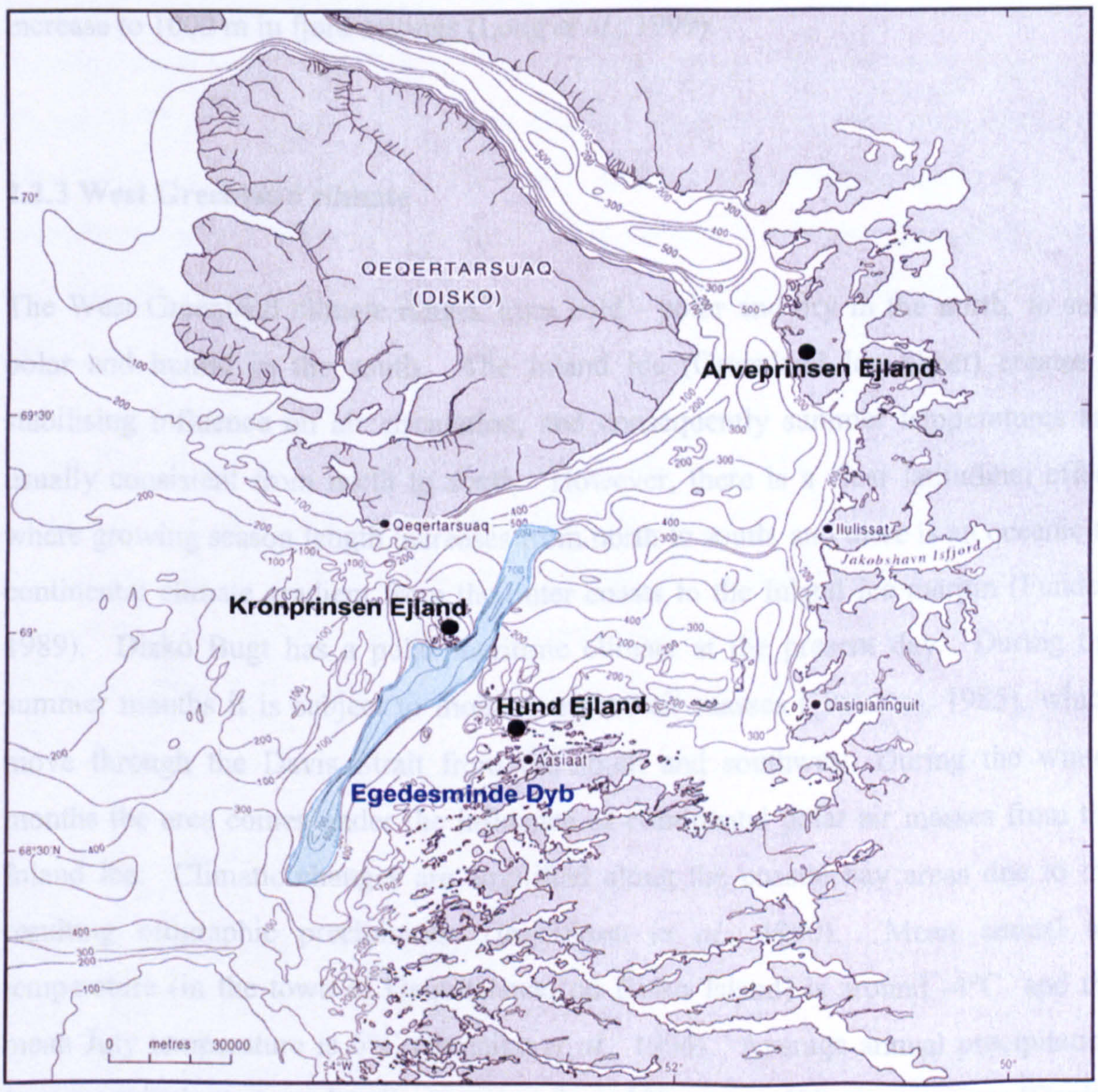

Figure 2.3: Seabed contour map of Disko Bugt [from Long and Roberts, 2003. Contours are given in metres below sea level. Data are based on interpolation between soundings detailed in admiralty maps (Royal Danish Hydrographic Office, 1954)]. Egedesminde Dyb, the deepest transverse channel extending from the West Greenland coastline is highlighted in blue above.

The Brett and Zarudzki survey extended from 64°N to just north of 69°N and revealed a broad platform of gently westward sloping banks from near the coastline to the shelf break. A series of deep transverse channels dissects the shelf into individual banks, the largest of which, Egedesminde Dyb, extends westwards from Disko Bugt, between Kronprinsen Ejland and Hunde Ejland (Zarudzki, 1979). Figure 2.3 (above) shows the bathymetric features of Disko Bugt itself. These channels seem to display the main features of glacial valleys, and are thought to be a product of the Quaternary glaciation of the banks. The floor of Disko Bugt itself displays very rugged topography, incised by a dendritic pattern of deep valleys up to 990 metres, which Brett and Zarudzki (1979) ascribe to southwestwardly flowing glaciers. Water depths in the eastern and western part of the Disko embayment vary typically between 200 and 400 m (Kuijpers *et al.*, 2001; Long and Roberts, 2002), although locally this may increase to 1000 m in fjord settings (Long *et al.*, 1999).

2.2.3 West Greenland climate

The West Greenland climate ranges from cold - polar and dry in the north, to sub-polar and humid in the south. The Inland Ice (Greenland Ice Sheet) creates a stabilising influence on air circulation, and consequently summer temperatures are usually consistent from north to south. However, there is a clear latitudinal effect where growing season length increases from north to south, and there is an oceanic to continental climate gradient from the outer coasts to the Inland Ice margin (Funder, 1989). Disko Bugt has a polar maritime climate at the present day. During the summer months it is subject to moist maritime air masses (Humlum, 1985), which move through the Davis Strait from the south and southwest. During the winter months the area comes under the influence of continental polar air masses from the Inland Ice. Climatic changes are amplified along the coastal bay areas due to the resulting orographic precipitation (Ingólfsson *et al.*, 1990). Mean annual air temperature (in the town of Qeqertarsuaq on Disko Island) is around -4°C, and the mean July temperature is 6°C (Bennike *et al.*, 1994). Average annual precipitation (water equivalent at sea level) can range from 100 mm to 500 mm per year (Danish Meteorological Institute, 1962-1985 in: Rasch & Nielsen, 1995; Ingólfsson *et al.*, 1990). Marine climatic change along the coast of West Greenland is brought about by

variations in the intensity of the West Greenland Current (WGC) that brings warm Atlantic water to Disko Bugt, and the bay is typically ice-free between mid-April and mid-January (Long and Roberts, 1999; 2002).

2.3.1 Fluctuations of the West Greenland Ice Sheet

A lowering of eustatic sea level exceeded isostatic subsidence in this area during the last glaciation. During the Last Glacial Maximum, the ice margin was land based on the inner shelf, 30 to 50 km from the present coastline, but towards the shelf break flowed large calving outlet glaciers. While the extent of the ice on the shelf differed from area to area (Funder, 1989), at the mouth of Disko Bugt, side scan sonar surveys (Brett and Zarudzki, 1979; Larsen, 1983) have shown that iceberg scouring commonly occurred down to depths of 350 m. These scours extended up to 4 km in length, and measured 75 m in width. This means that the ice in this location must have been extended out into, and beyond Disko Bugt. The origin of the icebergs must have been from the ice sheet on the shelf, as the depth of the scours indicates that iceberg depth was too great to have originated from the mouth of Jakobshavn and escape the fjord lips.

In the Disko Bugt area of central West Greenland, the Inland Ice margin is presently 25 to 40 km inland of the coast (Ingólfsson *et al.*, 1990). The fjords connect the Inland Ice margin with the marine environment through actively calving outlet glaciers such as Jakobshavns Isbrae. It is estimated that around 40% of the Greenland Ice Sheet's mass loss occurs in these calving regions (Weidick, 1990).

2.3.2 Jakobshavns Isbrae

Jakobshavns Isbrae is located at 69°10' N on the West Coast of Greenland. It is the fastest moving glacier in the world with speeds of up to 7 km a^{-1} (Clarke and Echelmeyer, 1996), with its outlet in Disko Bugt. Two ice streams feed the glacier; one of these is 100 km long, draining between 4.0 and 5.8% of the Greenland Ice Sheet (Pelto and Hughes, 1989). As a whole, it drains 6.5% of the Inland Ice (Fastook

et al., 1995), covering a large area of the western slope of the margin (Weidick, 1992).

The dynamics of Jakobshavns Isbrae exhibit similar characteristics to those outlets draining the West Antarctic Ice Sheet and into the Amundsen Sea. However, the large ice thickness and steep surface gradient leading to high basal shear stresses of Jakobshavns (200 to 300 kPa) distinguish it from the comparatively long and flat ice streams of West Antarctica (Clarke and Echelmeyer, 1996). The ice tongue varies in thickness from 600 to 1100 m thick, and floats in the fjord which is 100 to 1500 m deep (Clarke and Echelmeyer, 1996). Calving at the end of the 10 to 14 km long floating terminus (Clarke and Echelmeyer, 1996) can produce bergs up to 2 km^3, which at present drift predominantly to the north. Large icebergs (600 m deep) often get stuck on the submarine shoal at Illulisat (Jakobshavn) (~200 to 300 m deep) which extends approximately 5 km into Disko Bugt (Figure 2.4). Here they stagnate to melt and break up behind the sill (Echelmeyer *et al.*, 1991).

Figure 2.4: Aerial photograph of blocked up icebergs in Jakobshavn Isfjord, looking east up towards Jakobshavns Isbrae.

Analysis of surface velocity data taken over a 22-year period at the calving front by a number of workers (Carbonnell and Bauer, 1968, Lingley *et al.*, 1981 in: Pelto and Hughes, 1989) has yielded a mean velocity of 20.6 m d^{-1} and an estimated volume flux into the fjord of 37 km^3 a^{-1}. The calculation of these authors indicated that the mass balance of the glacier during the 1980's was near equilibrium, although a minor negative balance was observed.

A rapid retreat has been assigned to the glacier from its LIA position in 1850 (Figure 2.4), retreating 27 km in just over 100 years (Fastook *et al.*, 1995) although this is not as fast as the recent rate of the Alaskan Columbia Glacier retreat of 0.5 to 1.7 km a^{-1} (Echelmeyer *et al.*, 1991). From trimlines at the 1850 position, Echelmeyer *et al.* (1991) estimate that the thickness of the coastal marginal ice was 25% greater during the LIA than the present estimate of 700 to 800 m. Historical retreats of the terminus of Jakobshavns Isbrae are illustrated in Figure 2.5.

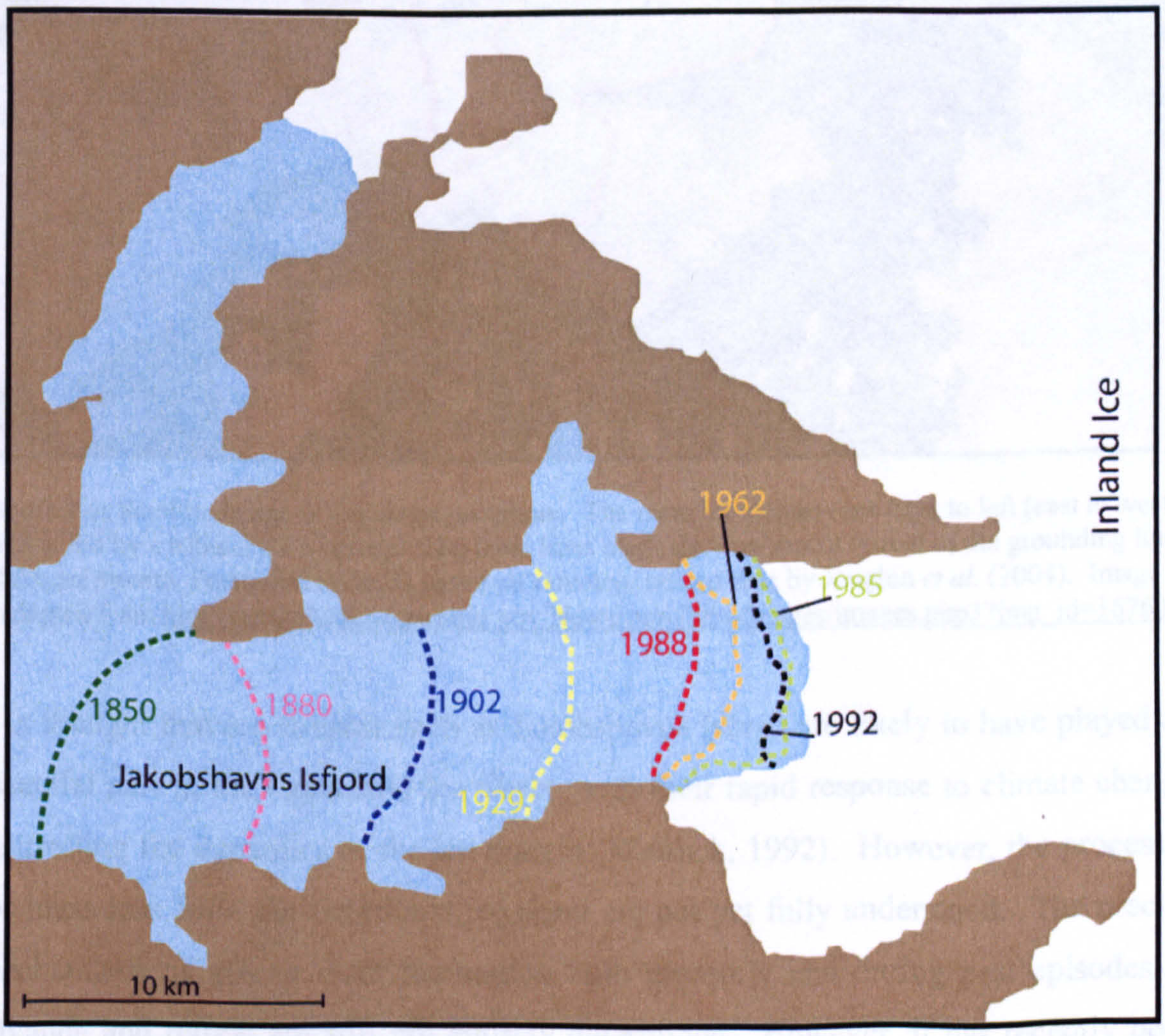

Figure 2.5: Historical ice sheet margin fluctuations based on four different remote sensing data sets (1962, 1985, 1988, 1992), and terrestrial evidence of ice margin halts and re-advances (1850, 1880, 1902, 1929). Adapted from Weidick (1992).

After a slowing down period during the late 1980's and 1990's, the rate of discharge of icebergs into the Davis Strait from the calving front has varied significantly. Velocity has decreased from 6.7 km yr^{-1} in 1985 to 5.7 km yr^{-1} in 1992. By 2000, this had increased to 9.4 km yr^{-1}, and by 2003 the velocity had nearly doubled that of 1985 with 12.6 km yr^{-1} (Joughin *et al.*, 2004). This increase in velocity is shown in the satellite image in Figure 2.6.

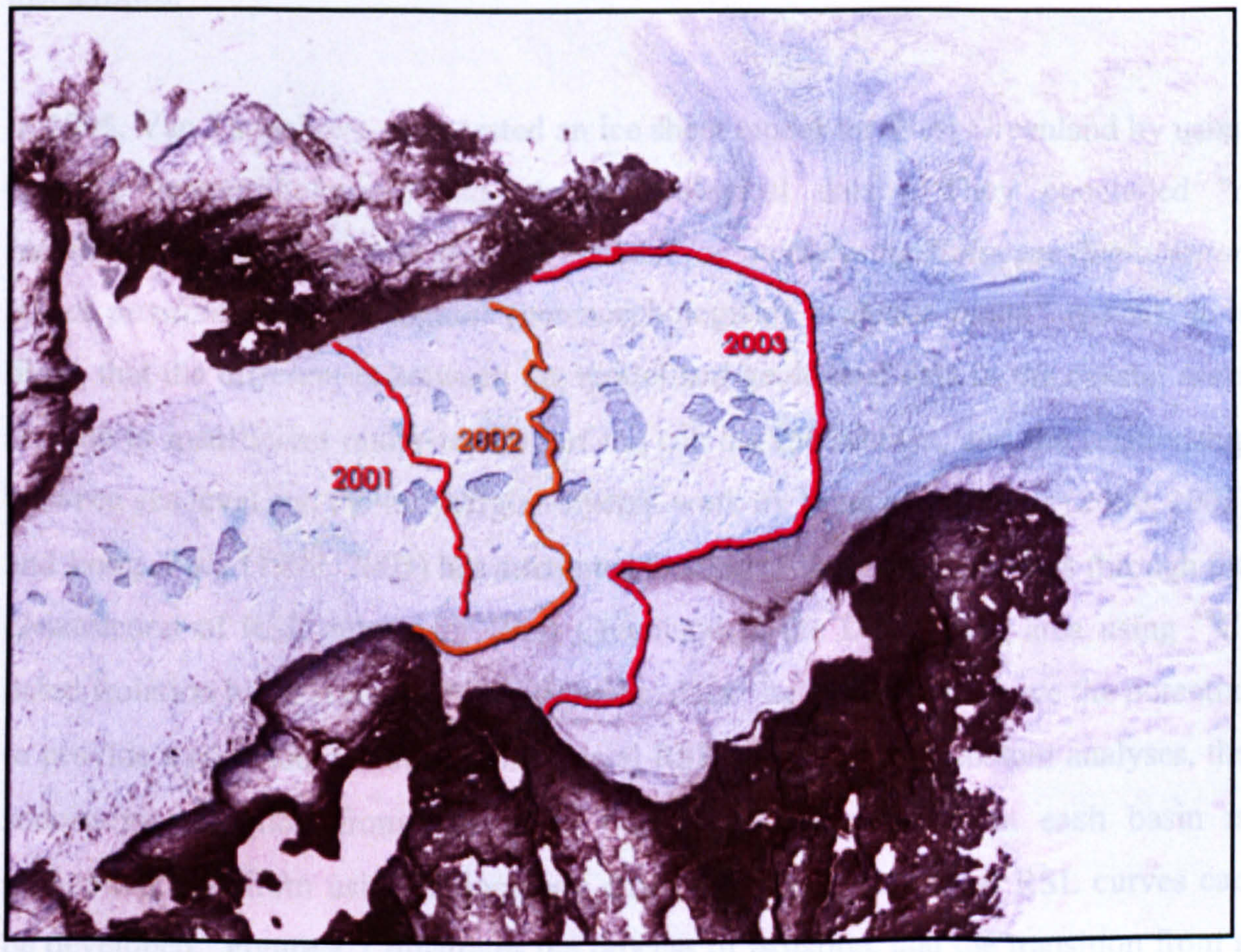

Figure 2.6: Satellite image of Jakobshavns Isbrae. The main ice stream runs right to left (east to west), and is fed by a tributary ice stream. The three lines mark the very recent retreat of the grounding line of the ice stream. Positional lines are based on remotely sensed data by Joughin *et al.* (2004). Image is adapted from http://earthobservatory.nasa.gov/Newsroom/NewImages/images.php3?img_id=16760

It is thought that ice streams such as Jakobshavns Isbrae are likely to have played an essential part in the Greenland Ice Sheet, with their rapid response to climate change controlling the dynamics of the ice margin (Weidick, 1992). However, the processes for mass loss from the Greenland ice sheet are not yet fully understood. The precise mechanisms of glacier front fluctuation both presently and during past episodes of advance and retreat are still not entirely determined. However, it has recently been identified that near-coastal thinning is likely to be responsible for mass loss from the

Greenland ice sheet (Rignot and Thomas, 2002). While Weidick (1992) advocates gradual retreat and advance from the pinning points during the Holocene (approximately 20 m a^{-1}), post 'Little Ice Age' retreat has been shown to be much faster (see Figures 2.5 and 2.6 above). Identifying controls on ice sheet dynamics has so far been limited, as previous work has only been derived from terrestrial evidence. This generally provides only minimum age estimates for ice limits, and does not engage with marine evidence for the nature and mechanisms for ice margin instabilities.

In 1995, Van Tattenhove *et al.* tested an ice sheet model for West Greenland by using existing geomorphological and glacial geological data. They concluded "*a reconstruction of the volume of the Greenland ice sheet during Holocene deglaciation is not possible using geological* (geomorphological) *evidence alone*" (p326). It is likely that the differences between the model and geological data in the coastal areas are due to insufficient understanding of the calving mechanism, and the relationship between sea level and the ice margin. Recent work by Long and Roberts (2000, 2003) and Long *et al.*, (1999, 2003) has attempted to address these shortcomings through the construction of RSL curves for West Greenland in the Disko Bugt area using ^{14}C-dated isolation basin and coastal stratigraphic data. Isolation basins have the potential to provide a complete record of post-glacial RSL change. Using diatom analyses, the successive transition from marine to freshwater environments in each basin is pinpointed, and from using radiocarbon dates, high resolution local RSL curves can be developed. Figure 2.7 illustrates the process of isolation, and the transition from a fully marine depositional environment to fully freshwater conditions during a fall in sea level.

Further discussion of post-glacial relative sea level change in West Greenland take place in this chapter in sections 2.5.1 and 2.5.2.

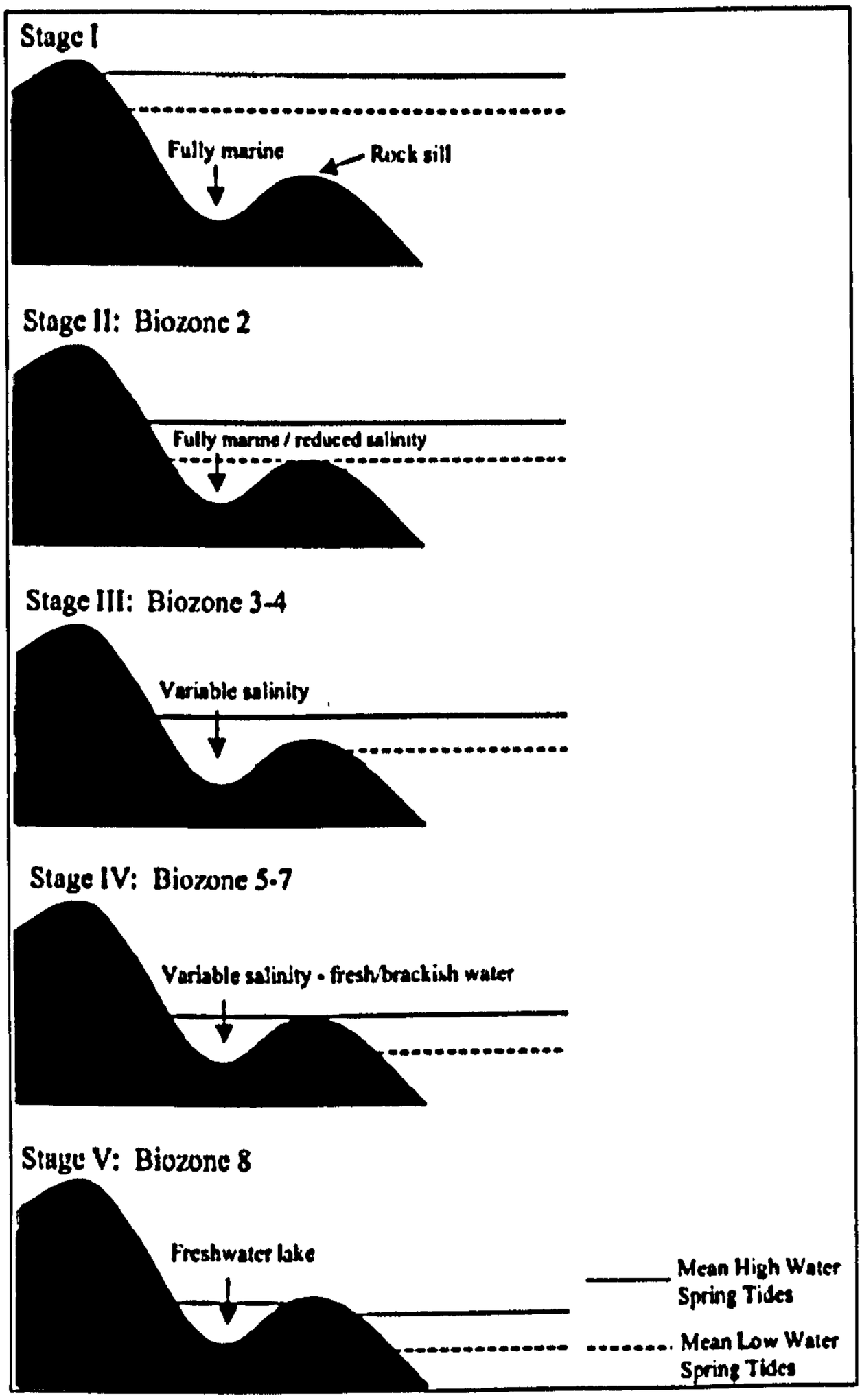

Figure 2.7: Schematic representations of an isolation basin during a fall in sea-level. During Stage I the basin is inundated during all stages of the tidal cycle and is fully marine, by Stage V the basin is isolated at all stages of the tidal cycle and is a freshwater lake. Stages II to IV represent intermediate stages when the basin is isolated during various proportions of the tidal cycle and has a variable but generally decreasing salinity (adapted from Lloyd, 2000).

2.4 Sedimentary processes

The characteristics of fjord drainage basins, and the degree of exposure of their waters to the open sea, have a direct effect on sedimentary regime (Gilbert *et al.*, 1998). Sediment depositional processes in glacial marine environments can be highly complex as a direct result of the ocean-glacier interaction (Smith and Andrews, 2000). Sediment deposition in a glacial marine environment takes place either by sediment rain-out or reworking by sediment gravity flows such as debris flows and turbidity

currents (Eyles *et al.*, 1985). Figure 2.8 describes the general model of glacio-marine sedimentation operating in the Disko Bugt area.

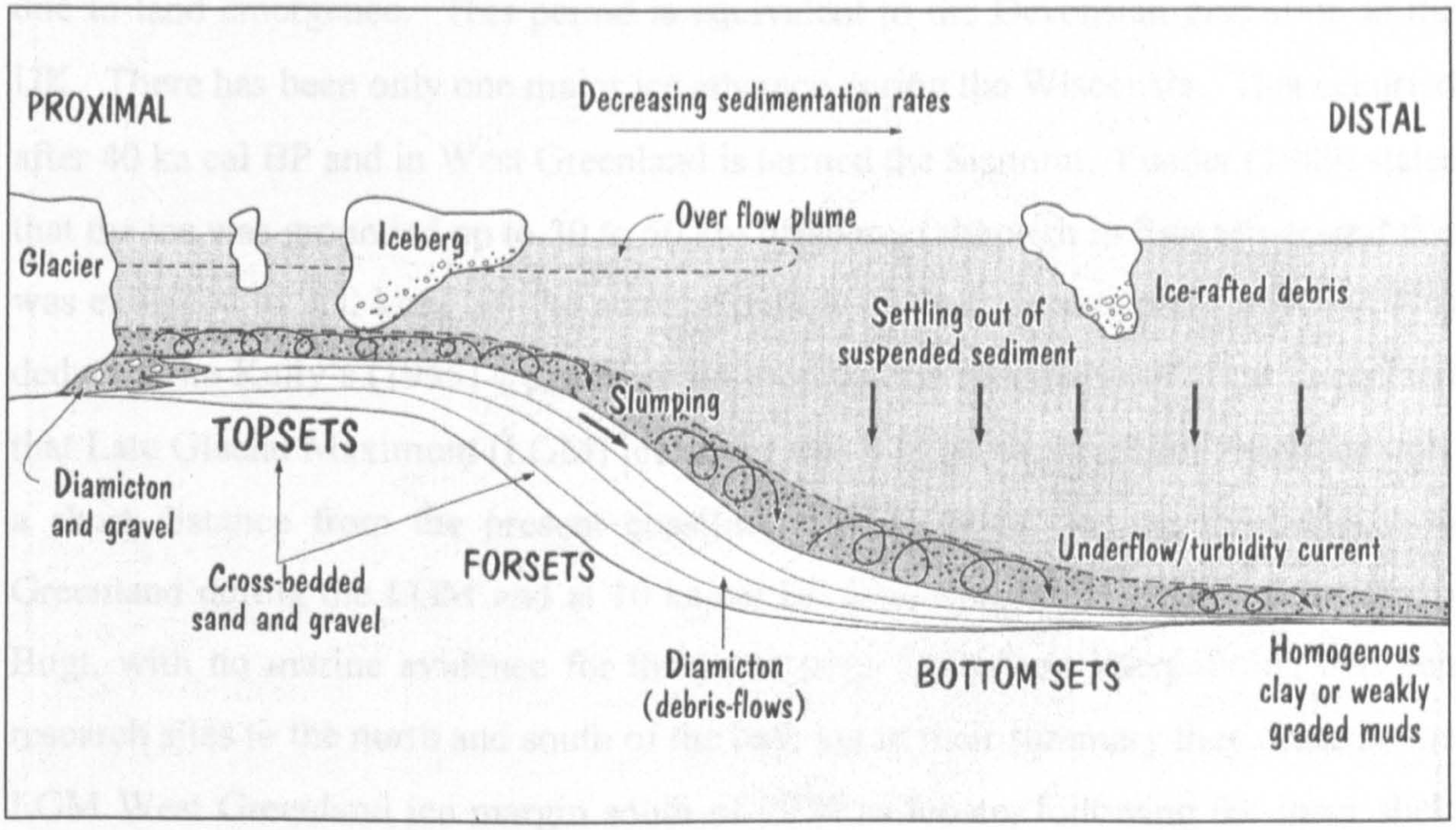

Figure 2.8: Model of glacio-marine sedimentation operating in the Disko Bugt area. Sediment in the cores analysed in this thesis has been deposited through the processes illustrated above. Deposition of sediment is primarily through (IRD) from iceberg rainout, and settling out of suspended sediments. (From Hambrey, 1994 in: Siegert, 2001).

Iceberg ploughing or scouring is often evident in fjords; it is significant in Scoresby Sund, Jakobshavns Isbrae's east coast counterpart, and is thought to occur in Jakobshavn Isfjord as well (Dowdeswell *et al.*, 1993), however no evidence of this has been found, and indeed knowledge of debris production from the Greenland Ice Sheet is limited (Knight *et al.*, 2002). Due to this complexity, the value of sedimentary records of arctic fjords in contributing to understanding of palaeoenvironmental change in Greenland has not been fully explored. Those that have been undertaken (e.g. Andrews *et al.*, 1997, 1998; and Jennings and Weiner, 1996) have concentrated on the east coast, while Desloges *et al.*, (2002) and Gilbert *et al.*, (1998) working on the west coast, have concentrated on smaller scale system processes around Disko Island itself. While these studies have focussed on the nature of the sedimentary records of the fjords and shelves and the processes operating, they do not engage with the mechanisms involved for ice margin and ice stream or glacier instability, which this study seeks to address.

2.5.1 Sea level change

Relative sea level has fallen in all areas of Greenland since the Wisconsin glaciation due to land emergence. This period is equivalent to the Devensian glaciation in the UK. There has been only one major ice advance during the Wisconsin. This occurred after 40 ka cal BP and in West Greenland is termed the Sisimiut. Funder (1989) states that the ice was grounded up to 30 to 50 km offshore, (although in East Greenland this was extended to 200 km), but the actual extent is unclear; Funder and Hansen (1996) deduce from Kelly's (1985) weathering limit on coastal mountains of West Greenland that Late Glacial Maximum (LGM) ice cover was thin on the coast and extended only a short distance from the present coastline. Their model for ice sheet extent in Greenland during the LGM and at 10 ka cal BP (See Chapter 1) is limited for Disko Bugt, with no marine evidence for these tentative limits, and interpolation between research sites to the north and south of the bay; yet in their summary they describe the LGM West Greenland ice margin south of 72°N as lobate, following the inner shelf with outlets through transverse channels. These transverse channels located by Brett and Zarudzki (1979) imply that the ice was extended much further out in the Disko Bugt area.

2.5.2 Investigations of the deglacial history of the Inland Ice margin

Investigations of the deglacial history of the Inland Ice margin to date have been based on a variety of studies. Relative sea level information in western Greenland has been continually sought since early archaeological observations during the 1940's (Gabel-Jørgensen & Egedal, 1940; Roussel 1941) and early tidal measurements and observations (Gabel-Jørgensen and Egedal, 1940; Saxov 1958). Subsequent data has been obtained from other sources, but have been derived mainly from geological and geomorphological investigations (e.g. Kelly, 1985, Rasch *et al.*, 1997, Weidick, 1990, 1992), and more recently, this has been produced in conjunction with palaeoecological records (e.g. Long and Roberts 2002; 2003; Long *et al.*, 1999; 2003) from isolation basins.

The importance of relative sea-level change (RSL), and its relationship to deglacial history since the LGM and specifically during the Holocene has become increasingly apparent over recent times (Funder and Hansen, 1996). The complex RSL and isostatic history of West Greenland holds important implications for understanding modes and mechanisms of deglaciation, and the interrelationship with oceanographic circulation. A detailed understanding of RSL may go a long way to providing a key to understanding the elements involved in iceberg calving and ice sheet retreat.

The major obstacle in reconstructing relative sea level changes at present appears to be the uneven distribution of data based on ^{14}C dates from shells and other carbonaceous material, which can only provide minimum age or altitude estimates due to issues such as those concerning reworking, for example. Extrapolation of these data for interregional comparisons has meant that the complexity of the RSL change and isostatic rebound history in response to ice sheet dynamics has been lost due to the likely significant differential crustal regime in the different areas. This is emphasised by the recent evidence of Long *et al.*, (1999) that there is a substantial north-south gradient to the isostatic record of the relatively small area of eastern Disko Bugt, resulting in variations in RSL of up to 20 m at 7.8 to 6.8 ka cal BP. One hypothesis is that sea level rise could cause floating of grounded marine based ice tongues, followed by catastrophic collapse. Another is that instigation of the West Greenland Current bringing Atlantic-sourced, warm, saline basal water could have caused basal melting of the ice sheet, allowing surging and increased calving leading to collapse and melting.

2.5.3 Current scenario of ice sheet retreat

The current model of ice sheet retreat and instability that has been proposed for the Inland Ice margin is that two discrete phases occurred, probably initiated some time after c. 15 ka cal BP, between 14 and 10 ka cal BP, (Funder and Hansen, 1996). From c. 14 ka cal BP, rising RSL is attributed to destabilisation of the marine-based ice on the shelf and in major inlets. This first stage is thought to have been driven by calving, and Funder and Hansen (1996) see this scenario allowing the ice front to retreat to a position approximating the present day coastline. The next (second) stage

began with a minor advance between c. 10 and 9.5 ka cal BP. This stage relates to the terrestrial based ice retreating quickly to achieve a mid-Holocene position behind the present ice margin. Weidick *et al.*, (1990) suggest this was possibly more than 15 km behind the present position, although more recent evidence in the form of moraine dating in the Kangerlussuaq area by Van Tattenhove *et al.*, (1996) has allowed the possibility that the retreat could in fact have been 10's of kilometres behind.

These two steps attempt to explain the behaviour of the glacial retreat, although currently there is limited evidence for this in Disko Bugt. The marine based stages of retreat have been inferred only from the intersection of marine deposits on land, providing minimum age estimates at best, and there is no oceanographic record of ice margin fluctuations in terms of speed of retreat, and specific timing of movements. Timing of the terrestrial based portion of the Ice Sheet has been further constrained by the work of Long and Roberts (2002, 2003) and Long *et al.*, (2003). Figure 2.9 shows the minimum dates for terrestrial retreat.

From the mid-Holocene (around 4 ka cal BP), the ice sheet is thought to have readvanced (Weidick, 1990). However, evidence becomes less clear from this time, with poor preservation of geomorphological features, and a lack of investigation on a local or regional scale. Again this seems to highlight the need for inter-site comparisons as opposed to interregional. A range of driving mechanisms are put forward in response to widespread evidence for RSL rise - as a crustal response to neoglacial readvance (Weidick *et al.*, 1993; 1996), or to the effects of forebulge collapse from the Greenland and Laurentide Ice Sheets (Rasch *et al.*, 1997), (Rasch and Jensen, 1997). The most recent RSL studies do not correlate with the regional forebulge collapse hypothesis, but follow the scenario of crustal subsidence due to ice sheet readvance during the neoglacial.

Figure 2.9: Minimum radiocarbon dates for terrestrial deglaciation (Long *et al.*, 2003) given in mean cal kyr BP. (Data are from Rasch, 1997 supplemented with data from Bennike, 2000; Long and Roberts 2002; Long *et al.*, 1999, 2003).

Long *et al's* (1999) data show that RSL fell continuously from the marine limit at approx. 70 m at c. 9.9 ka cal BP to approx. -5 m 2.8 ka cal BP. From then, RSL has risen by around 5 m due to a switch from emergence to submergence. Their most recent development of localised RSL curves for Disko Bugt region in West Greenland based on isolation basin stratigraphy (see section 2.3.2 this chapter) is illustrated in Figure 2.10. Figure 2.11 shows the locations in West Greenland where the isolation basin fieldwork took place.

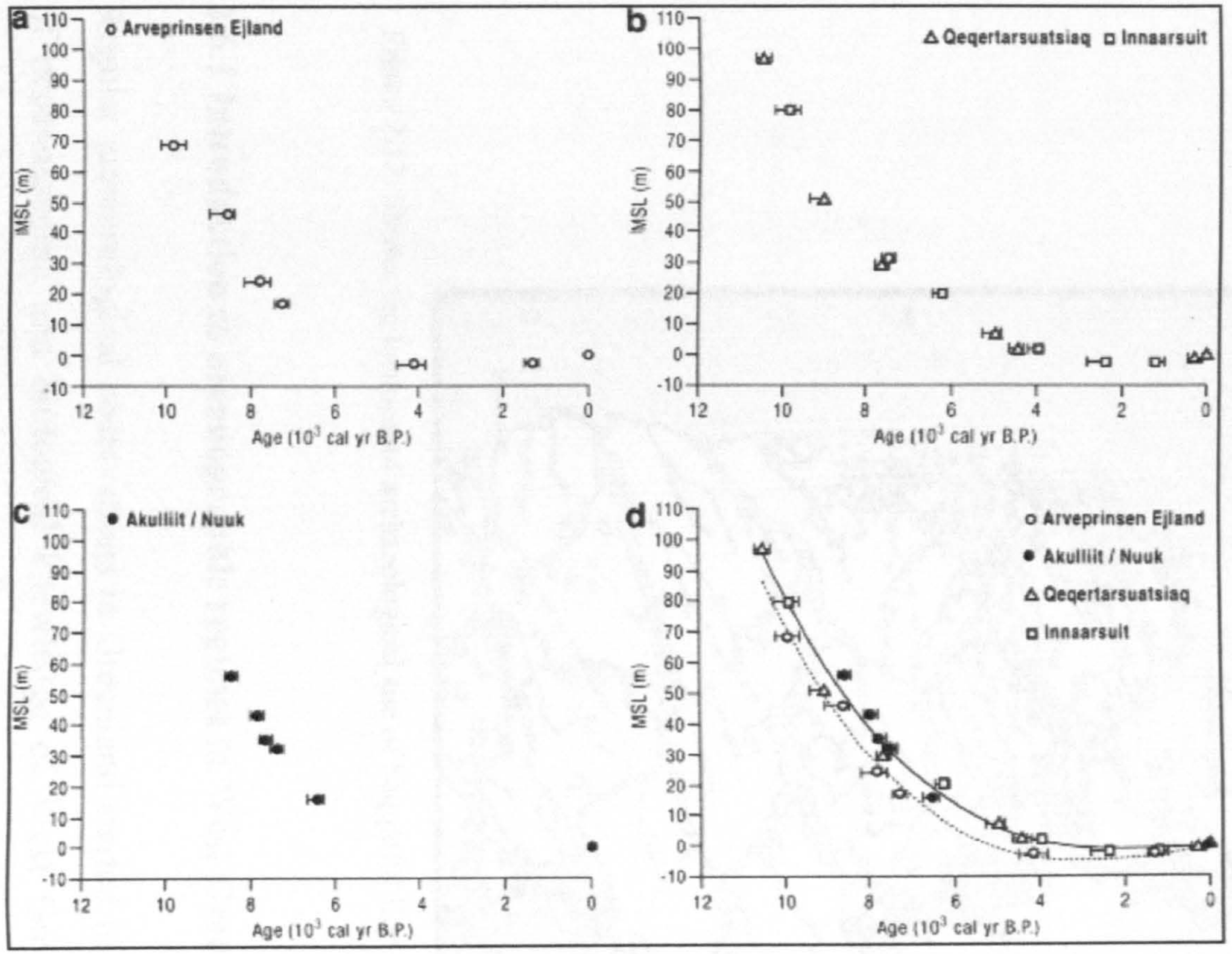

Figure. 2.10. RSL graphs depicting Mean Sea Level during the Holocene from the study area shown in Figure 2.11. The Innarssuit and Qeqertarsuatsiaq data are very similar and were combined by the authors (Long *et al.,* 2003) as a single dataset (d). The trend lines summarising the data from Arveprinsen Ejland, and the combined Innarsuit and Qeqertarsuatsiaq data, are best-fit third-order polynomials. The *x*-axis error bar is equal to the 2sigma calibrated age range of each index point Other data are from (Long and Roberts, 2003) (Qeqertarsuatsiaq), (Long and Roberts, 2002) (Akulliit/Nuuk), and (Long *et al.,* 1999) (Arveprinsen Eijland.)

Figure 2.11: Locations in West Greenland where Long *et al's.,* isolation basin fieldwork took place. The four fieldwork sites are marked with black dots.

The record of Rasch *et al.*, (1997) in western Disko Island showed that the early-middle Holocene periods was characterised by a decline in RSL, to be later followed by late Holocene rise. Interpretation of coastal features at Saqqarliit Ilorliit (location show in Figure 2.12) suggest that after c. 2.5 ka cal BP a transgression occurred that lasted until around 1.0 ka cal BP, and was repeated between 0.7 ka cal BP and the present. It is possible that the most recent transgression comprised three distinct minor phases. The production of local RSL records such as these should not be stand-alone investigations, and the previous trend for regional investigations should be redirected into the development of detailed local RSL curves with tight chronological control.

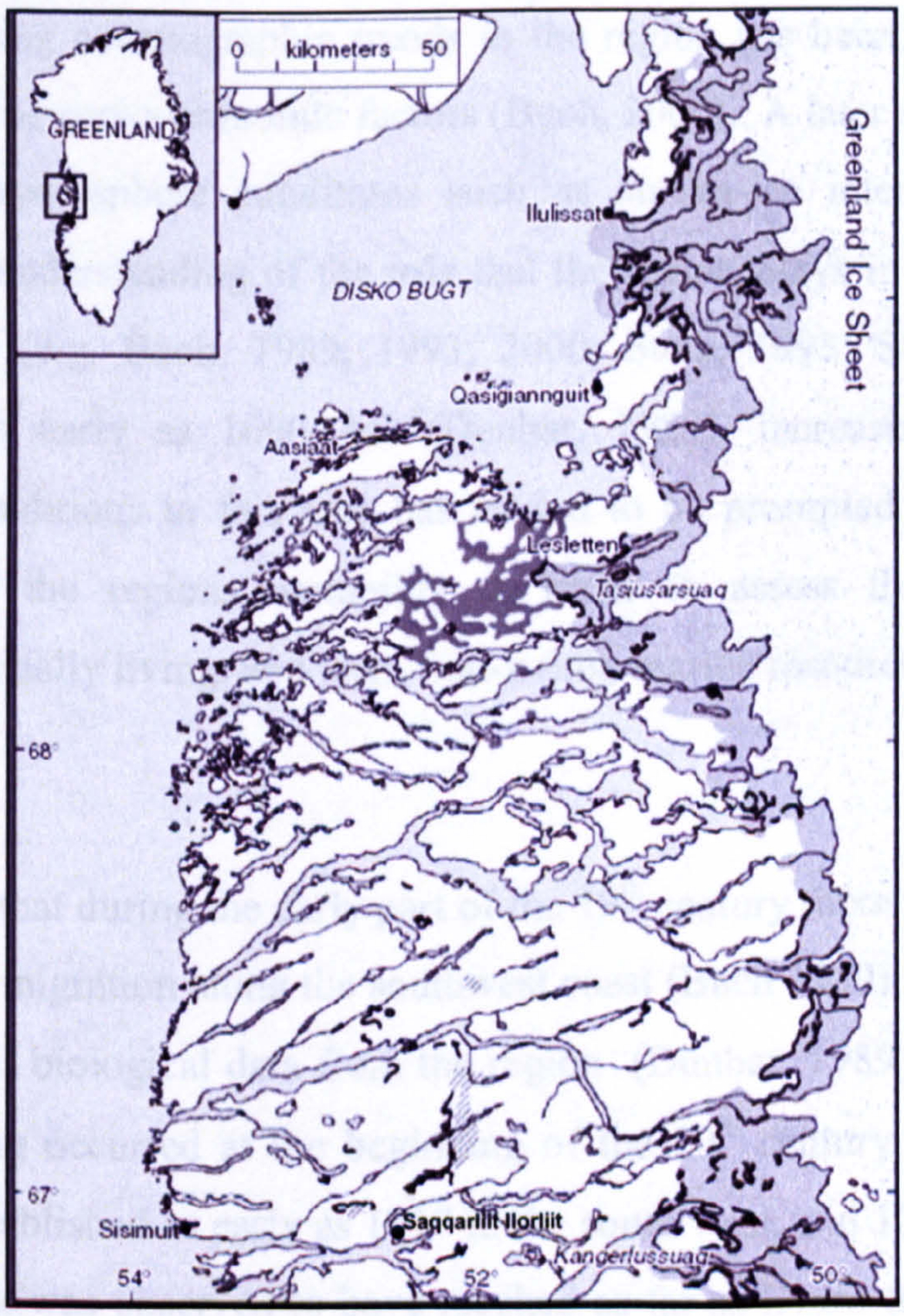

Figure 2.12: Shows the location of archaeological site of Saqqarliit Ilorliit in relation to Disko Bugt.

2.6.1 Introduction to oceanographic regimes in West Greenland

Regular meteorological observations in Greenland started in 1873, and the collection of oceanographic and biological knowledge of West Greenland waters began in

earnest with the Danish and American expeditions in 1928 of the "*Godthaab*" and the "*Marion*" and the "*General Greene*" respectively (Dunbar, 1989). This early research sought quantitative oceanographic information in relation to locally observed occurrences and movements of economically exploitable fish species. Since the mid 20th century, further economically- (and latterly academically-) prompted regular vessel-based hydrographical observations have been undertaken by Danish and German researchers (Buch and Stein, 1987).

2.6.2 Recent oceanographic trends

Research concerning oceanographic trends in the region has been, and continues to be, driven mainly by socio-economic factors (Buch, 2000). A later emphasis has been on determining hydrosphere conditions such as air-sea-ice interactions that may contribute to the understanding of the role that the region plays in relation to global climate scenarios (e.g. Buch, 1989; 1993; 2000; Stein, 1993; Stein and Wegner, 1990). Since as early as 1600 AD (Dunbar, 1989), increasing knowledge of oceanographic conditions in this area has tended to be prompted by furthering the understanding of the regions variability in order to assess the possibilities of exploitation of, initially living, and later, non-living, marine resources (Bradley, 2000; Buch, 2000).

Local knowledge that during the early part of the 19th century there were brief periods of significant cod migration along the southwest coast (Buch 1989), prompted interest in temperature and biological data from the region (Dunbar, 1989). Cod movement and later spawning occurred at the beginning of the 20th century, with commercial fisheries being established as early as 1917 in the south west, and 10 to 15 years later, the fish movement was observed to have reached as far as Disko Bugt, and recorded further north as well (Dunbar, 1989). A similar increase in Atlantic salmon was also noted, although lagging behind the cod trend. Both fish species are associated with Atlantic (Irminger) water, and to some extent a mixture of Atlantic and Arctic water (Dunbar, 1989).

Dunbar and Thompson (1979) associated the salmon distribution with the climatic warming of the WGC, and have linked historical records of salmon abundance in West Greenland waters to warm periods recorded in the Greenland ice cores from Camp Century. These periods are sub-centennial in cyclicity (75-76 years).

2.6.3 Oceanographic conditions in West Greenland waters

Oceanographic conditions in West Greenland waters, including the Labrador Sea and Davis Strait, are a result of varying scales of circulation of elements of the North Atlantic and Arctic Oceans (Stein, 1993). Exchange between the Arctic and adjoining oceans by water mass transport by the East Greenland Current (EGC) and branch components of the North Atlantic Current system create the West Greenland Current system (WGC) which has a powerful control on the temperature over Greenland and resulting ice sheet dynamics (Buch, 2000). This northwestern arm of the Atlantic Ocean consists of a large counter-clockwise oceanographic gyre, operated by a "warm", northward flowing, and "cold", southward moving surface current (Stein, 1993) (Figure 2.13 and Figure 2.14).

The hybrid West Greenland Current system (WGC) directs circulation along the West Greenland margin and Labrador Sea (Stein, 1993), and contributes to the cyclonic circulation in Baffin Bay (Ingram and Prinsenberg, 1998). Its influence through its relatively warm water effects extends from Kap Favel at the southern tip of Greenland, and up through Baffin Bay as far as the northwest continental margin of Greenland (Buch, 1993; Lewis *et al.*, 1996; Steffen, 1985). The WGC is complemented by the southward flowing Baffin Current (BC), and Labrador Current (LC), providing a surface outflow of low salinity Arctic water from the Canadian Archipelago (Ingram and Prinsenberg, 1998; Jacobs *et al.*, 1985).

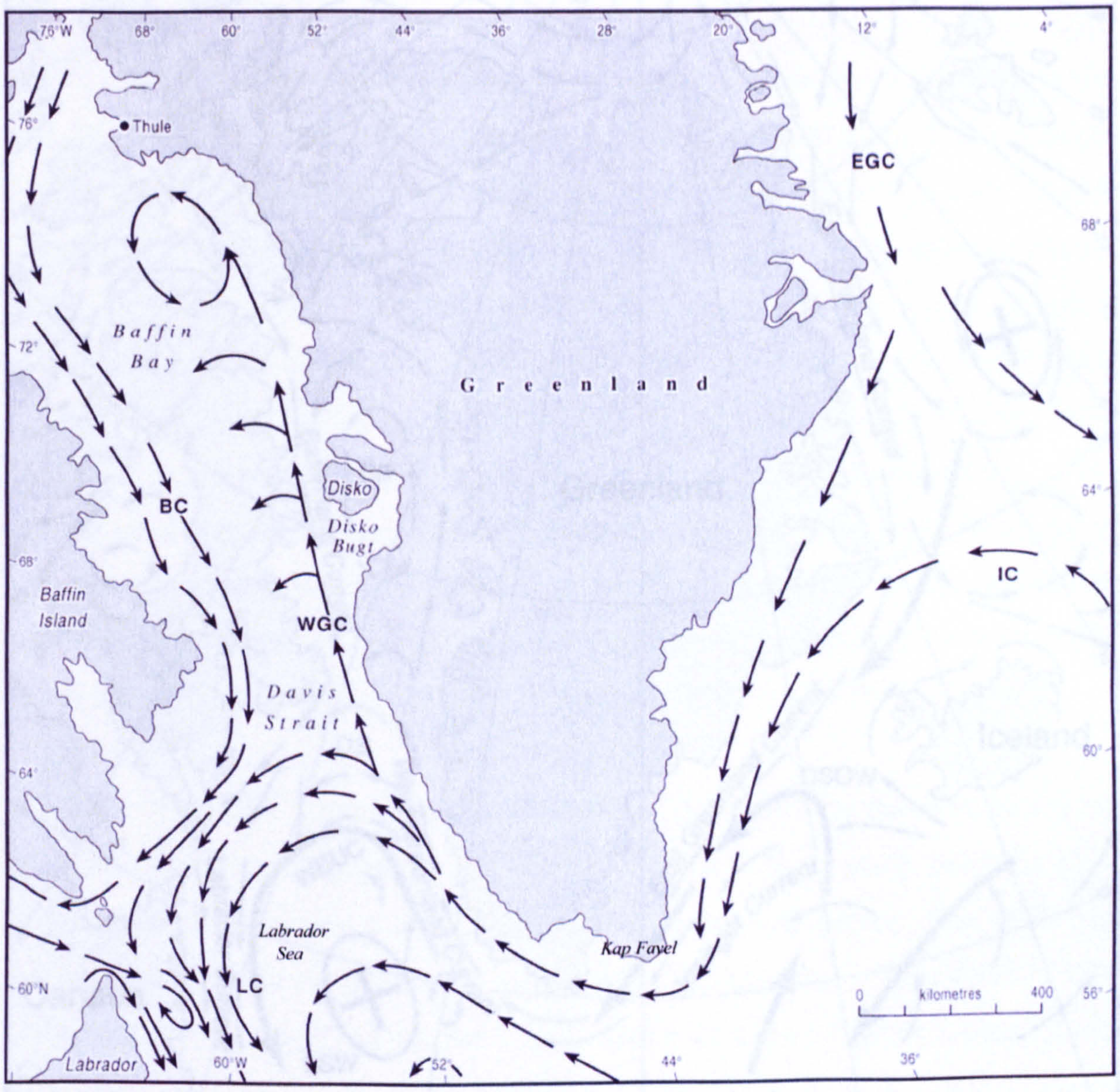

Figure 2.13: The component currents of the WGC, and its northward flow along the West Greenland coast. LC – Labrador Current, IC – Irminger current, WGC – West Greenland Current, BC – Baffin Current, EGC – East Greenland Current. (Modified from Lloyd *et al., submitted*).

While surface current velocities vary throughout the region, the WGC is much weaker than its west coast counterpart, the Baffin Current flowing down past Baffin Island and the Labrador Coast (Jacobs *et al.*, 1985). Both currents however, have surface speeds in excess of 30 cm/s (Myers *et al.*, 1990).

The WGC is also linked by wind stress and heat forcing (Eden and Böning, 2002) to smaller scale events such as the generation of meanders and eddies (Eden and Böning, 2002; Stein, 1993) to the west and northwest in the Labrador Sea and Davis Strait.

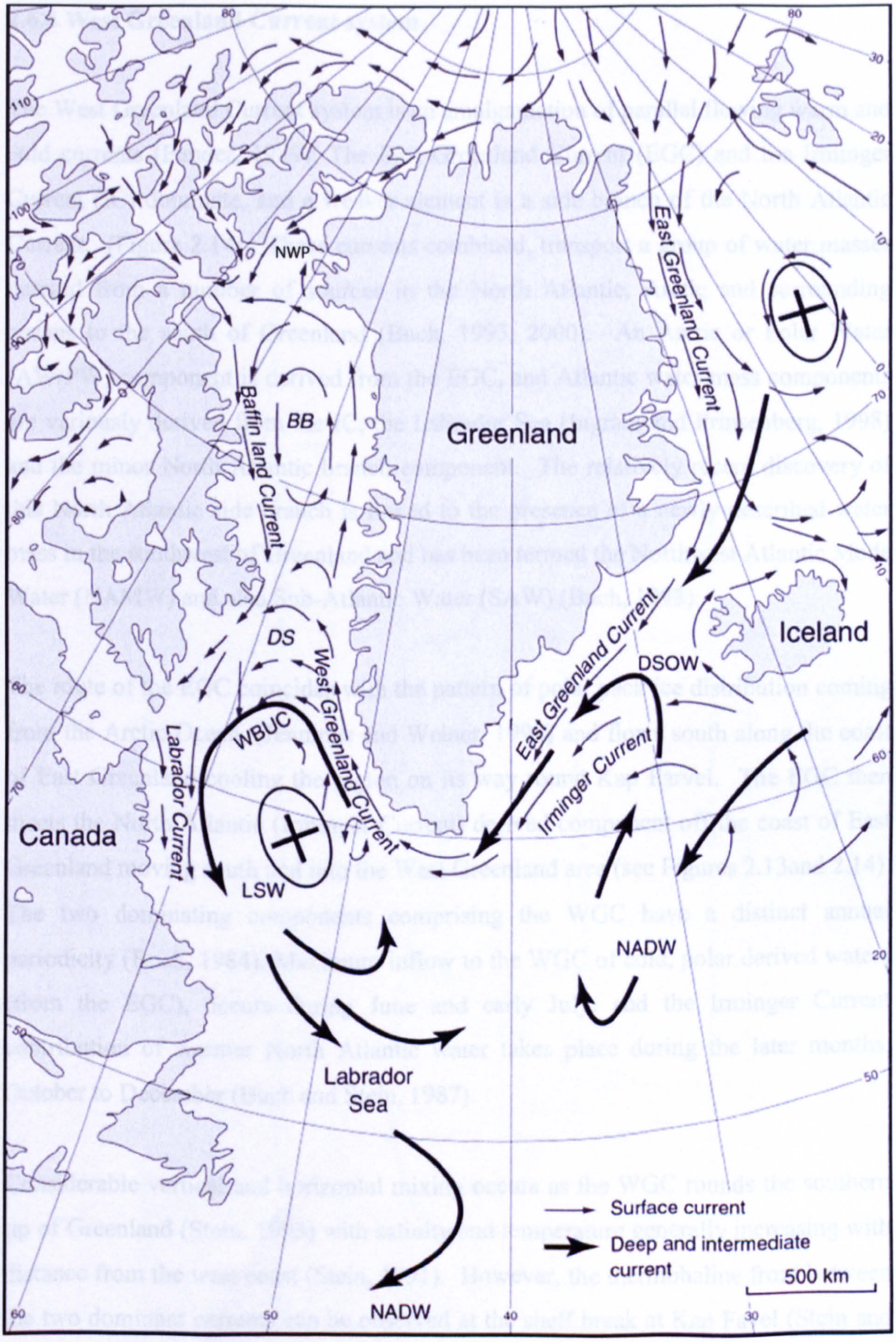

Figure 2.14: Detailed map of sources of water mass influences in West Greenland. This shows the wider oceanographic circulation in terms of surface as well as deep and intermediate currents around Greenland. BB - Baffin Bay. DS - Davis Strait. NWP – North Water Polynya. NADW – North Atlantic Deep Water. LSW – Labrador Sea Water. WBUC – West Boundary Under Current. DSOW – Denmark Strait Overflow Water. Ellipses with crosses in the centre mark gyres and areas of deep water convection.

2.6.4 West Greenland Current system

The West Greenland Current system is an amalgamation of parallel flowing warm and cold currents (Funder, 1989); The East Greenland Current (EGC) and the Irminger Current (IC) dominate, and a weaker element is a side branch of the North Atlantic Current. (Figure 2.14). These currents combined, transport a group of water masses derived from a number of sources in the North Atlantic, Arctic and surrounding oceans to the south of Greenland (Buch, 1993, 2000). An Arctic or Polar Water (AW/PW) component is derived from the EGC, and Atlantic water mass components are variously derived from the IC, the Labrador Sea (Ingram and Prinsenberg, 1998) and the minor North Atlantic branch component. The relatively recent discovery of this North Atlantic side branch is linked to the presence of a newly described water mass in the southwest of Greenland and has been termed the Northwest Atlantic Mode Water (NAMW) and also Sub-Atlantic Water (SAW) (Buch, 1993).

The route of the EGC coincides with the pattern of polar pack ice distribution coming from the Arctic Ocean, (Jennings and Weiner, 1996) and flows south along the coast of East Greenland cooling the region on its way round Kap Farvel. The EGC then meets the North Atlantic (Irminger Current) derived component off the coast of East Greenland moving south and into the West Greenland area (see Figures 2.13and 2.14) The two dominating components comprising the WGC have a distinct annual periodicity (Buch, 1984). Maximum inflow to the WGC of cold, polar derived waters (from the EGC), occurs during June and early July, and the Irminger Current contribution of warmer North Atlantic water takes place during the later months, October to December (Buch and Stein, 1987).

Considerable vertical and horizontal mixing occurs as the WGC rounds the southern tip of Greenland (Stein, 1993) with salinity and temperature generally increasing with distance from the west coast (Stein, 1991). However, the thermohaline front between the two dominant currents can be observed at the shelf break at Kap Favel (Stein and Wegner, 1990) and the separate components can still be recognised up along the southwest and west coasts of Greenland (Buch, 1989, 2000; Myers *et al.,* 1989; Stein, 1993; Stein and Buch, 1985).

2.6.5 West Greenland Current components

By the time the WGC reaches Disko Bugt, these separate components are difficult to distinguish. This is supported by an example of contemporary temperature, salinity and depth (CTD) data from Disko Bugt, which shows a warm, saline water mass underlying the colder and fresher "mixed Disko Bugt water layer" (Figure 2.15), suggesting that the WGC in this area of West Greenland is relatively homogenous.

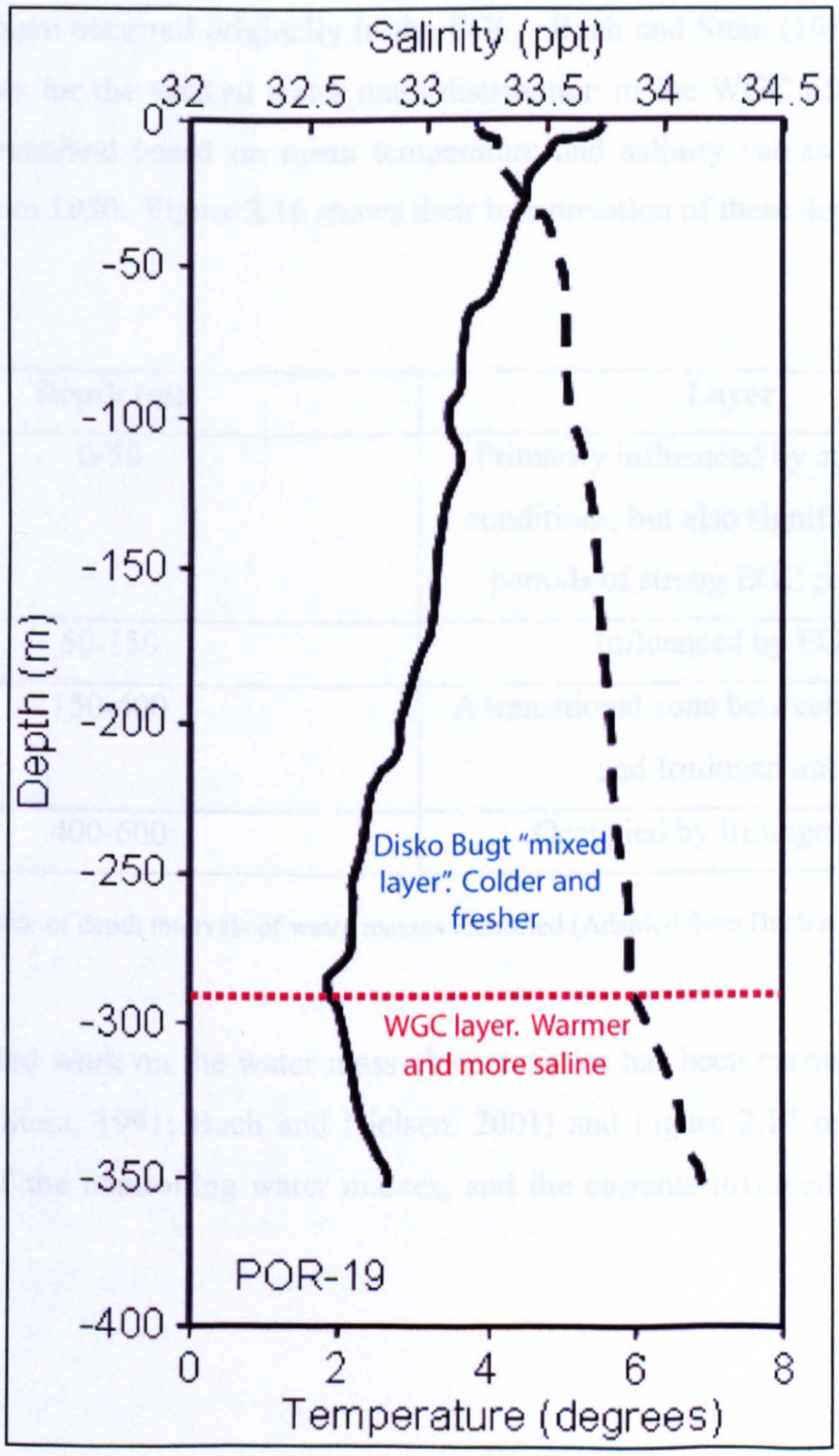

Figure 215: CTD data profile from east of Disko Bugt in front of Jakobshavns Isbrae, collected in 1999 field season by Kuijpers and Lloyd, referenced to Kuijpers *et al.*, 2001

When the maximum intensity of inflow is attained by either of the two main current components, the centre of the presiding current is located between 150-200 m water depth. However, hydrographic conditions of the upper surface layer also become influenced by the presence of the current components due to the Coriolis effect forcing the water masses eastward against the outer slopes of the West Greenland banks (Buch and Stein, 1987).

Stein (1993) found it possible to trace thermal events in the WGC system, which were observed to have occurred originally in the EGC. Buch and Stein (1987) calculated depth intervals for the vertical water mass distribution of the WGC off the coast of southwest Greenland based on mean temperature and salinity values for July and November from 1950. Figure 2.16 shows their interpretation of these depth intervals.

Depth (m)	Layer
0-50	Primarily influenced by atmospheric conditions, but also significant during periods of strong EGC polar water
50-150	Influenced by EGC
150-400	A transitional zone between polar water and Irminger water
400-600	Occupied by Irminger water

Figure 2.16: Table of depth intervals of water masses identified (Adapted from Buch and Stein, 1987).

Further detailed work on the water mass characteristics has been carried out, (Buch, 1993, 2000; Stein, 1991; Buch and Nielsen, 2001) and Figure 2.17 provides a full description of the controlling water masses, and the currents involved in the WGC system.

Water Mass	Temp (°C)	Salinity (‰)	Comments
Polar Water (occurs in surface layer 0-200m)	<1°C. Summer temperatures may rise to 3-5°C	<33.75-34.0	Surface layer, close to coast. Characteristics differ from pure Polar Water, due to slight mixing with surrounding water masses during transportation by EGC.
Irminger Water (200-300m) this and above depth data from Stein, 1991.	*c.*4.5°C	>34.95	Originating from North Atlantic Current (transported by IC). In this pure form only occasionally present in area.
Irminger Mode Water	*c.* 4°C	34.85-34.95	Formed by Irminger Water mixing with surrounding water, accounting for slightly lower temperature and salinity. Always present off SW Greenland.
Northwest Atlantic Mode Water	>2°C. Late autumn temperatures may rise to >5°C	34.5-34.85	Originates in northern part of North Atlantic Current from mixing of North Atlantic and Labrador Currents. Low salinities due to LC influence.

Figure 2.17: Table of details of composition of the water masses found at Southwest Greenland (Adapted from Buch, 1993, 2000; Stein, 1991; Buch and Nielsen, 2001).

Lewis *et al.*, (1996) provided temperature-salinity data strongly suggesting that the WGC can penetrate as far north as the North Water area in the far northern part of Baffin Bay (shown in Figure 2.14). Here, a large polynya appears in Smith Sound between Greenland and Ellesmere Island

This North Water polynya is thought to be produced by removal of the ice by wind or surface currents (latent heat effects), and warm-water upwelling (sensible heat effect). On the discovery of surface warm water cells above freezing point, Steffen (1985)

postulated that this warm water was likely to be sourced from the WGC. This concurred with Ross' later current meter mooring data of currents and temperature within Baffin Bay (Ross, 1990a; b, 1991 in: Ingram and Prinsenberg, 1998). Lewis *et al.'s* (1996) temperature and salinity profiles from the coast of Greenland towards the Canadian coast identified a warm layer along the coast, which became progressively cooler and thinner to the north and west. While the mechanisms involved in the initial opening of the polynya have yet to be determined, it is likely that the during the early months, the North Water is initially a latent heat polynya, with sensible heat effects becoming more developed in the latter part of the spring (Darby *et al.*, 1994).

2.7 Oceanography and atmospheric connections

Interannual and seasonal variability in oceanographic conditions are considerable. There are close links with the North Atlantic Oscillation index (NAO) and the climate of Greenland, as well as other areas in the North Atlantic and Europe. Changes in sea ice cover, and subsequent effects on oceanographic temperature and salinity conditions are significant factors affecting contemporary oceanographic conditions. Changes in all of these elements can be linked to distributions of marine species, both historically and today.

2.7.1 The North Atlantic Oscillation

The NAO is an index that represents the anomalies in sea level pressure between the Icelandic low pressure system in the subpolar Atlantic and the Azores high pressure system in the subtropical Atlantic (Shabbar, 1997) and is one of the major modes of winter climate variability in the Northern Hemisphere atmosphere (Buch, 2000). When the pressure difference between the two locations is high, the index is said to be in a positive phase (NAO+) and when the difference in pressure is small the index is in a negative phase (NAO-). The index varies on a yearly basis, can also maintain one phase of state for periods lasting several years. Winter is the season that tends to display the greatest interdecadal variability between the two phases (Hurrell, 1995).

The following diagram (Figure 2.18) shows the general characteristics of the two phases of the NAO index.

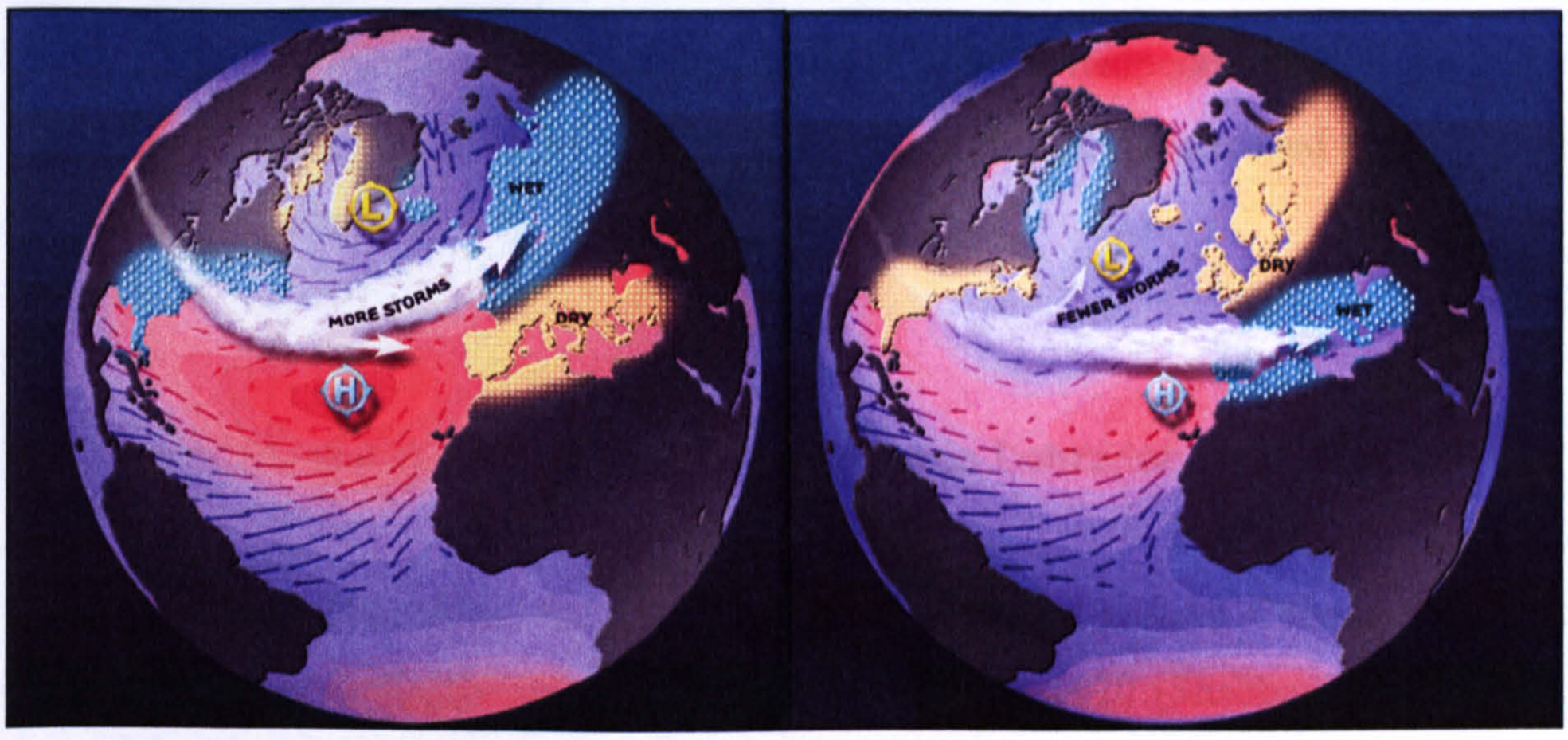

Figure 2.18: The two phases of the NAO index. The left-hand diagram shows the effects of a positive NAO index; The Icelandic low and Azores high intensify as Arctic pressure drops. This intensifies the Westerlies and brings warm moist air further north. The right-hand cartoon depicts the results of a negative NAO index; Arctic pressure increases and the subtropical high and the Icelandic low are weak. Storminess is weakened and brings warm, moist air to southern Europe. Images adapted from http://www.ldeo.columbia.edu/NAO/

Positive NAO: During the positive NAO index, the Icelandic low is strong, and there is an increase in the strength of the North Atlantic Westerlies. This means that warm, moist air is carried further and there is a subsequent northward shift in storm activity (Stein, 1997). Northern Europe and Eurasia become warmer and wetter, and the Eastern United States also becomes wetter. Southern Europe is likely to experience much drier conditions as the Mediterranean area is deprived of moisture. Northern Canada, the Labrador Sea, Baffin Bay area and West Greenland become cooler and drier, as cold air is diverted further north over the North American continent (Dorn *et al.*, 2003), with evaporation exceeding precipitation (Hurrell, 1995). Enhanced storm activity affects Southern Greenland, Iceland and into Northern Europe due to the increased northerly storm tracks crossing the Atlantic.

Negative NAO: During the negative NAO index, there is a much weaker subtropical high and Icelandic low. This results in a reduced pressure gradient between the two areas. Storminess is reduced, in terms of strength and frequency, and movement of

storm tracks is more east to west (Rogers, 1997), so the Mediterranean areas are wetter, and cold air flows over Northern Europe and the eastern United States experienced cooler drier conditions. The Labrador Sea area becomes warmer and wetter, and Greenland as a whole experiences milder temperatures and moisture increases, with South and West Greenland having particularly increased precipitation (Dorn, 1997; Stein, 1997).

2.7.2 The NAO and recent atmospheric patterns in Labrador and Greenland

Winter surface temperature data from stations on coastal eastern Canada and west Greenland show detectable decadal cooling since about 1970 (Shabbar *et al.*, 1997). Decadal cooling in winter in coastal Canada, especially the Labrador area is thought to be associated with decadal salinity anomalies (Dickson *et al.*, 1988; Mysak *et al.*, 1990), and/or variations in the NAO. According to Hurrell (1996), the majority of the European and northwest Atlantic cooling over the past 25 years can be statistically explained by the interannual variability of the NAO.

A strongly sustained positive phase of the NAO index has been evident since the early 1980's (Buch, 1993, 2000), and the significant cold conditions experienced in southwest Greenland for the last thirty years have meant the virtual disappearance of cod from the fishing banks area (Dunbar, 1989; Stein, 1993; Buch, 2000). Dawson *et al.*, (2003) link late-Holocene climatic "seesaws" first conclusively identified by van Loon and Rodgers (1978), with storminess changes in the north Atlantic region and GISP2 palaeoclimatic records. They show that in general, when winters in West Greenland are colder than average, conditions are characterised by enhanced positive NAO, and negative NAO indices are associated with above average temperature and moisture supply in Greenland (Jones *et al.*, 1997).

2.7.3 Temperature and salinity changes in West Greenland waters

The cold atmospheric conditions created by a persistently positive NAO phase are transferred to the oceanographic upper water mass conditions, whereby the strength of

the westerlies in a preceding winter is negatively correlated with baroclinic transport in the WGC and the LC relative to the upper 100 m during the summer months (Myers *et al.*, 1989, 1990). Hydrographic data from the coast of southwest Greenland since 1950 reveal two distinct periods, 1968-73 and 1981-84, with strong negative temperature and salinity anomalies up to depths of 500 m (Buch and Stein, 1987).

During the late 1960's/early 1970's anomaly, July readings showed relatively cold and fresh conditions in the upper 150 metres, indicating a greater than normal inflow of cold Polar Water from the EGC. The presence of a very cold air mass centred over Egedesminde, West Greenland from February 1982 to November 1984 is thought to have been responsible for the negative temperature and salinity anomaly documented by Buch and Stein (1987). Low winter temperatures produced extremely large quantities of sea ice, and prevention of normal Irminger Water inflow to the area. This restriction of Irminger Water allowed even the deeper layers (150-400 m and 400-600 m) to exhibit negative temperature and salinity anomalies in the latter part of the period.

The well-documented "Great Salinity Anomaly" (GSA) (Kerr, 1992), first observed in 1968 (Dickson *et al.*, 1988) was a widespread general cooling, and period of significantly decreased salinity (Dickson *et al.*, 1988) of the upper 500-800 m layer (Myers *et al.*, 1990) in the North Atlantic during the 1970's into the early 1980's. The GSA is thought to have resulted from the migration of the East Greenland Front (EGF), located between the EGC and the IC prompted by a period of exceptionally strong and sustained northerly winds over the Arctic Ocean and northern North Atlantic during the preceding decade (Buch, 2000, Myers *et al.*, 1990), derived from a build up of extremely high air pressure over Greenland, and a marginal decrease over the eastern parts of the Norwegian and Barents Seas (Buch and Stein, 1987). This southeast migration was accompanied by an influx of PW, sea ice and generally colder temperatures to the area (Jennings and Weiner, 1996).

The advection of this cold, low salinity water mass and sea ice passed along the banks of southwest Greenland in 1969 (Buch and Stein, 1987). Air temperatures following the 1960's have decreased to the early 1990's at Nuuk in West Greenland, as well as at stations on the Labrador coast (Stein, 1993) and high amplitude cold events were

recorded both east and west of the Labrador Sea on a near decadal scale in the early 1970's, 1980's and 1989-90 (Stein, 1993).

Buch (2000) also described the anomalous cold conditions in the upper 400 m at southwest Greenland as being well below normal for both summer and winter during the two sustained cold periods, 1981-84 and 1989-94. Similar results were found by Stein (1993), identifying significantly colder than average temperatures at the same oceanographic station for the depth layers between 0 and 200 m, for the years 1982-84 and 1989.

Myers *et al.* (1989) examined seasonal and interannual variability of the Labrador and West Greenland Currents along the coast of southwest Greenland by constructing water current transport estimates using temperature and salinity data from 1950 to the late 1980's. They were able to distinguish between short and long term fluctuations in the strength of the currents. Large scale wind forcing (Dunbar, 1989; Myers *et al.*, 1988; Thompson *et al.*, 1986) is likely to be responsible for the interannual variation in water mass density off the West Greenland shelf. This emphasises the role that atmosphere-ocean connections play in this region.

The dynamic nature of the area is highlighted by the large-scale interannual changes in salinity (Buch, 1987; Dickson *et al.*, 1988; Kerr, 1992), deep-water formation in the Labrador Sea (Clarke and Gascard, 1983, Lazier, 1988), and variations in sea ice formation (Buch, 1993, 2000; Mysak and Manak, 1989; Deser *et al.*, 2002). Temperature and salinity data relating the Labrador Current and the West Greenland Current from Myers *et al.* (1989) shows a freshening in the upper 200 metres of the Labrador Sea at three times on a near decadal scale at 1960, 1971, and 1984. The 1971 fresh phase corresponds with the widespread GSA (Buch, 1987; Dickson *et al.*, 1988; Kerr, 1992). All three correspond with increases in Arctic sea ice production and extent (Buch 2000; Mysak and Manak, 1989). Statistical analysis, (Stein, 1993) shows that a coupling of thermohaline events can occur on both sides of the Labrador Sea.

Temperature anomalies observed in the waters of West Greenland are not as a singular result of overall climatic warming involving only air temperature increases in

the area itself (Stein, 1991, 1993), but are related to changes in the relative amount of the Arctic and Atlantic water in the West Greenland Current. It has recently been recognised that the seasonal and interannual variability of the Greenland waters can be considerable. An example of this is the exceptional cold and dry conditions over Greenland brought on by a persistent and strong positive phase of the NAO since the early 1980's. This was mirrored in the waters off the south west Greenland coast in the two distinct cold periods, 1982-84 and 1989-94, where temperatures were well below normal in the upper 400 m surface layer (Buch, 2000). While data is from survey locations up to 100 nautical miles off the southwest coast, conditions like this will be transported and the effect may be detectable within the water masses entering Disko Bay (Buch and Stein, 1987; Dunbar, 1989; Myers *et al.*, 1989).

2.7.4 Explaining the changes in the WGC water mass components

It is likely that fluctuations in the WGC components are related to atmospheric conditions, and, indirectly to surface winds and sea ice formation (extent and duration). Dunbar and Thompson hypothesised the following scenario in 1979; entry of Atlantic and Arctic water into the West Greenland region becomes restricted when westerly winds prevail to the south. This occurs during periods when the Iceland Low is at its highest latitude. This position is created by intense strong zonal westerly circulation (Loder *et al.*, 1998). The warming effect is created by the increasing importance of the participation of the Labrador Sea water (which is Atlantic sourced), which dominates in the WGC north of Ivigtut. This restriction of entry of cold, lower salinity Polar sourced surface water, was further qualified by Stein and Buch (1985) to be not only restricted, but also perhaps also laterally relocated by the winds.

The opposite effect appears when the Icelandic zonal circulation is shifted to lower latitudes; eastern "anomaly" winds dominate in the south of Greenland (Dunbar, 1989, Loder *et al.*, 1998). This leads to an intensification of the Irminger Current and East Greenland Current components of the WGC during their respective dominant seasonal phases. An increase in flow, and total cooling effect, shifts the Labrador Sea gyre and the point at which the WGC begins to turn west towards Baffin Bay northwards (Buch, 2000).

As early as 1985, Stein suggested that the presence of the very cold airmass centred over Egedesminde in the Davis Strait area and thought to be responsible for the 1981-1984 negative salinity and temperature anomaly could be a teleconnection to the El Niño events of the early 1980's, but this possibility has not been explored fully. Further explanations are related to dust and volcanic activity in Mexico and Washington State, USA (Buch and Stein, 1987). While periods or phases such as the ones described above may appear to be extreme yet short lived, general, "warming" or "cooling" trends, i.e. changes in the composition of the components of the West Greenland Current may also occur. For example, archaeological midden investigations of the "Saqqaq" Inuit culture, active between 2400 BC and 1400 BC (the Neoglacial period), in Disko Bugt, show an overwhelming presence of Atlantic cod and salmon, but little of another fish species, the capelin. While this is attributed to the manner of consumption of the capelin, the abundance of the two Atlantic species may also be linked to a strong Atlantic/Irminger Current water influence, or weaker Arctic/East Greenland current influence (Dunbar, 1989).

Recent work by Shabbar *et al.*, (1997) investigating decadal variability of surface temperatures in the coastal east Canada and West Greenland area invokes the presence of the BWA index (Baffin Island-West Atlantic), a new sea level pressure index (SLP) to account for the winter decadal cooling relationship with the circulation pattern over northeastern North America, specifically the Canadian Polar Trough (CPT). This BWA index better explains the surface climate changes in the Baffin Bay-Davis Strait area than the NAO index, which is more directly related to changes in the eastern part of the North Atlantic.

However, the NAO index is still relevant to the West Greenland area in terms of the characteristics of the water masses being delivered to the area that originate from, or are transported through, regions that come under the influence of the NAO index. Stein's (1993) data show that in modern times, that during long observational periods (>3 yrs), East and West Greenland stations are able to show an east-west connectivity and consistency between the cold and warm signals in water masses. These changes in water mass characteristics are likely to be related in turn to atmospheric conditions

operating at the time. At present there appears to be a coupling of thermal events of both sides of the Labrador Sea.

The Labrador Sea is one of only two areas in the Northern Hemisphere where deep-water formation occurs (Kuijpers *et al.*, 2001), and the connectivity of coastal West Greenland with coastal Eastern Canada through water mass transportation suggests that changes in meltwater and iceberg volumes sourced from the West Greenland portion of the Greenland ice sheet may have implications for oceanographic circulation and deep-water formation in the region.

2.7.5 Sea ice in West Greenland waters

Over the past two decades, Marko *et al.*, (1994) detected an increase in sea ice cover in the Davis Strait in the January months, combined with the presence of unusually strong northerly surface winds that have been acting over the Labrador Sea during the winter months from the mid 1970's. This leads to both a cooling of the surface waters, and an intensification of the post-winter southward sea ice drift from western Davis Strait on the Labrador Current. "Westice" is first year sea ice and formation begins in September in northern Baffin Bay and Davis Strait, and in the following months it continues to obstruct considerable portions of the Northwest Greenland coast (Buch, 1987; Ingram and Prinsenberg, 1998; Prinsenberg *et al.*, 1997).

During the majority of the time window (1981-1997) considered by Buch (2000), the sea ice limit reached southward as far as Aasiat on the shores of Disko Bugt during December-January, with the winter sea ice extent retreating to northern Baffin Bay each summer (Deser *et al.*, 2002). It does not usually reach the Southwestern Greenlandic waters due to the warmer water masses originating in the Atlantic having their peak inflow during the later autumn months (Buch and Stein, 1989).

The other type of sea ice that dominates in the region is "Storis", multi-year ice (Buch, 2000), which originates in the Arctic and is transported to the area by the EGC (Jennings and Weiner, 1996, Mysak and Manak, 1989). Storis delivery is subject to considerable variability and is determined by the outflow, sea ice and meteorological

conditions in the Arctic Ocean, Greenland Sea, Iceland Sea and the Irminger Sea. The two extremely cold periods documented in 1983-84 and 1989-94 allowed the development of much greater that normal quantities of westice, and the highly unusual event of the two sea ice formations co-joining (Ingram and Prinsenberg, 1998; Myers *et al.*, 1989; Stein, 1993), was able to occur several times in bays in the southwest of Greenland (Buch, 2000)

2.8 Chapter summary

Disko Bugt is a large marine embayment on the West Coast of Greenland. Bathymetric and geological features in the bay are directly related to West Greenland Ice Sheet activity during the Last Glacial Maximum. Interrelated RSL responses to ice margin retreat following this period and subsequent possible margin fluctuations have recently been heavily investigated to further constrain early estimates by Funder and Hansen (1996). The most recent chronology suggests that Jakobshavns Isbrae retreated later than previously estimated from Disko Bugt (around 10.2 ka cal BP cal BP), and was able to survive rapid rates of sea level rise and meltwater pulses (Fairbanks, 1989; Long and Roberts, 2003) during the last deglaciation. The advancements in knowledge of terrestrial based palaeoenvironmental change relating to deglaciation and the Holocene require consolidating with this oceanographic investigation.

The West Coast of Greenland is characterised by complex hybrid oceanographic and atmospheric connections. Changes in the WGC may be driven by changes in the component currents (EGC and IC). From recent hydrographic and oceanographic investigations it is suggested that these changes may be forced by fluctuations in the Arctic atmospheric and oceanic Fronts in East Greenland, situated between the EGC and the IC, prompted by enhanced positive phases of NAO. Increased positive NAO conditions are suggested to lead to increases in the Arctic ice flux and the Polar Water component of the EGC as well as increasing the limits and extent of seasonal pack ice. This is reflected in the WGC as a significant decrease in temperature and salinity.

Distribution of species of marine flora and fauna appear to be affected by perturbations of the oceanographic regime by atmospheric forcing mechanisms. This is seen, for example, during the enhanced positive phases of NAO during the 1990's which has led to the decline of cod. Fish fauna relating to colder Arctic waters are noticeably absent from archaeological middens in southwest Greenland. It should therefore be possible to track changes in the strength (salinity and temperature) of the WGC through the palaeoclimatic record with the high resolution techniques employed in this thesis.

Chapter 3: Methods

3.1 Introduction

Recent and current progress in developing relative sea-level records for West Greenland (e.g. Long and Roberts 2002, 2003; Long *et al.*, 1999; Rasch, 1997) has refined the deglacial chronology of the area, but it is vital that this work is complemented by palaeoceanographic and sedimentological studies. Little work of this type has been undertaken specifically in West Greenland. The majority of West Greenland oceanographic work relates to the post-glacial colonisation by molluscs of coastal sites in the south of Greenland (e.g. Donner and Jugner, 1975; Funder and Weidick, 1991), with a recent localised fjord sedimentation study in Disko Island (Desloges *et al.*, 2002; Øhlenschlager, *unpublished data*). New data is currently being gathered relating to palaeohydrographic changes in sites around Greenland including West Greenland (Jensen *et al.*, submitted; Jensen *et al.*, in press). However this is limited to changes in surface waters (using diatoms), and some early results indicate that preservation has been a severely restraining factor in these studies, and consequently sampling resolution is not very consistent (K.G. Jensen, pers. comm., 2002). Work relating to foraminiferal, IRD and isotopic analysis has not previously been attempted in this location, and as a result, this thesis is the first to produce a marine record of palaeoceanographic changes, post-glacial ice margin retreat and sediment/iceberg/meltwater fluxes in this area.

This chapter gives details of fieldwork locations, the rationale for site selection and sampling strategy. The investigative methods used are outlined and analytical techniques described. The use of foraminifera for palaeoceanographic reconstruction is appraised.

3.2. Preliminary 1999 field season sampling strategy

As this PhD is part of a wider NERC ARCICE research project (*Quaternary Ice Sheet Dynamics in West Greenland*), the selection of fieldwork locations was to some extent already fixed, in that sampling sites were to be located within Disko Bugt in order to

be able to meet the research aims and objectives (see Chapter 1). The first field season took place prior to the initiation of the period of PhD study, so there existed evidence and data upon which to base the PhD site selection and sampling strategy for the main season of data collection. The first field season relating to this project took place in 1999 using the *R/V Porsild*, when a coring and conductivity, temperature and depth (CTD) programme was carried out. Figure 3.1 shows the location of these coring and CTD cast sites.

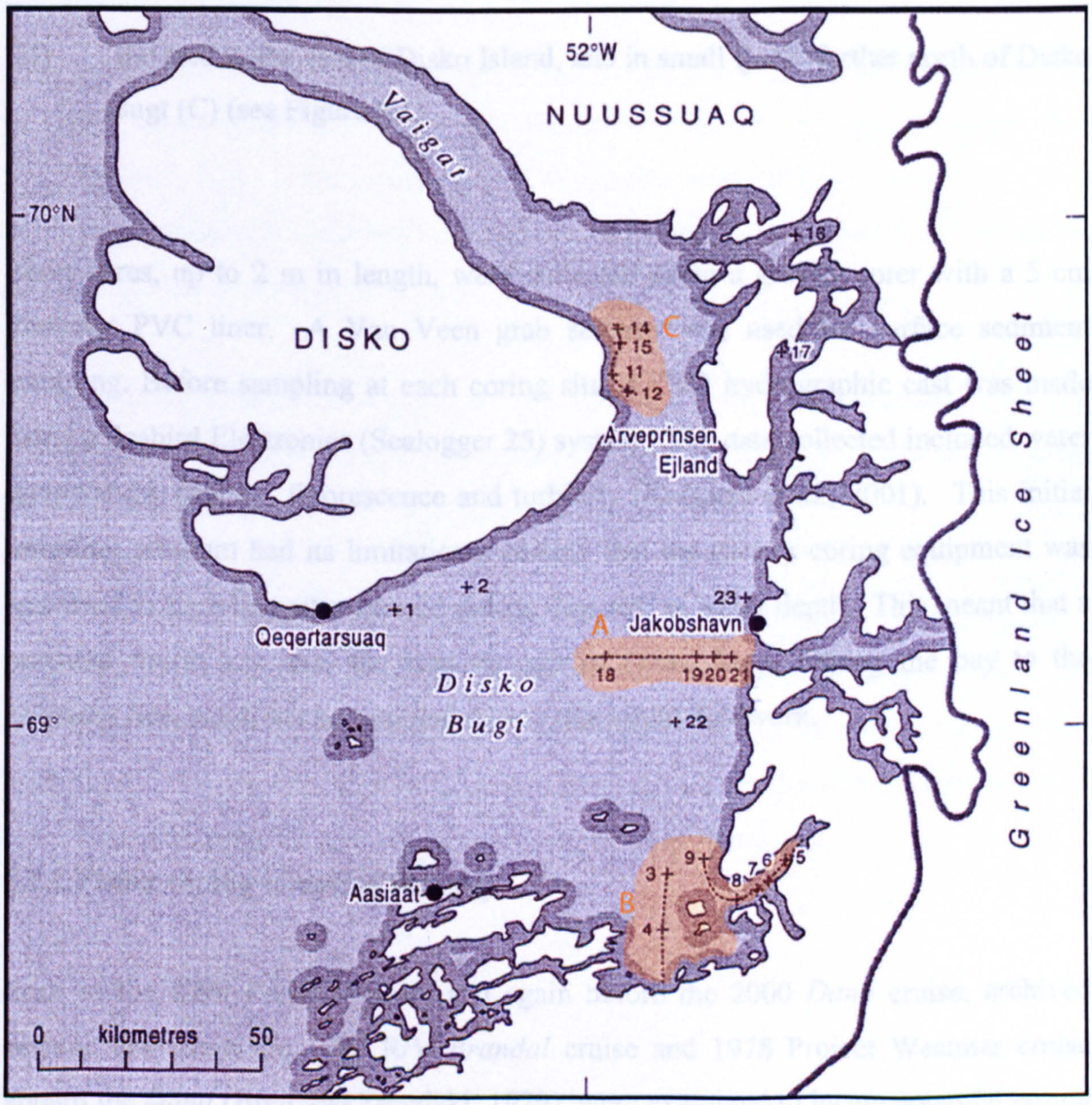

Figure 3.1: Survey site locations from the 1999 field sampling season. CTD and gravity cores taken at each site. A: Area in front of Jakobshavns Isbrae, B: Large sediment fan and into Kangersuneq Fjord, C: East of Disko Island.

The sampling strategy adopted during this initial field season by Kuijpers and Lloyd (1999 pers. com.) was to use a large spread of sampling stations to gather estimates of sediment coverage throughout Disko Bugt, with three key areas to be targeted for this survey.

These were:

i) the areas directly in front of Jakobshavns Isfjord (A)

ii) a large sediment fan to the southeast of the bay (B), and

iii) the area to the east of Disko Island, and in small fjords further north of Disko Bugt (C) (see Figure 3.1).

Short cores, up to 2 m in length, were collected using a gravity corer with a 5 cm diameter PVC liner. A Van Veen grab sampler was used for surface sediment sampling. Before sampling at each coring site, a CTD hydrographic cast was made using a Seabird Electronics (Sealogger 25) system. The data collected included water temperature, salinity, fluorescence and turbidity (Kuijpers *et al.*, 2001). This initial sampling program had its limitations, namely that the gravity coring equipment was restricted to sampling sites located in less than 400 m water depth. This meant that a potential fourth key site, the western part of Disko Bugt, linking the bay to the Labrador Sea, could not be sampled during this initial fieldwork.

3.2.2 Piston coring sampling strategy

Prior to the 1999 *Porsild* cruise, and again before the 2000 *Dana* cruise, archived seismic data from the 1972 R/V *Brandal* cruise and 1978 Project Westmar cruise aboard the *Dana* (Brett and Zarudzki, 1979), were examined to locate potential coring sites. The seismic systems used during these early cruises were a single channel analogue sparker, a small (up to 40in^3) airgun system, and a 1.5-3.5 kHz subbottom profiler. These investigations revealed that the majority of presumed Quaternary sediment accumulation was in the eastern part of the bay, apart from a thick infill in

the western part of Disko Bugt in the base of a deep channel running north-east – south-west (Egedesminde Dyb, see Figure 3.2). This trough is envisaged as being a conduit for meltwater and calved icebergs, and allowing massive downdraw of the ice sheet (Long and Roberts, 2003). Kronprinsen Ejland to the north, and Hunde Ejland to the south of the Dyb were thought to mark pinning points for the ice stream during deglaciation (Funder and Hansen, 1996), but recent dating of isolation basin work by Long *et al.* (1999, 2003) and Long and Roberts (2002, 2003) shows that, once deglaciation began from the outer shelf, there was no significant delay in retreat caused by these potential pining points.

Bathymetric and seismic evidence also reveal the presence of a large shallow sloping sediment fan, located in Sydosbugten to the south of the bay in front of Kangersuneq fjord (Figure 3.2). This major spread of glaciomarine sediment suggests that a significant conduit for sediment/water must have existed here at some point during the region's glacial or postglacial history.

By combining data collated from the old seismic surveys with the data from the preliminary 1999 cruise, three key locations were identified within Disko Bay to fulfil the main research aims and objectives of this thesis.

This thesis is concerned with identifying periods of instability and change in Disko Bugt by constructing a high resolution record of Holocene modes of palaeoceanography and the dynamics of Jakobshavns Isbrae. In order to address the key aim and objectives of this research (Chapter 1), core site locations were chosen to give the best possible coverage of these scales in Disko Bugt.

Figure 3.2: Seabed contour map of Disko Bugt [from Long and Roberts, 2003. Contours are given in metres below sea level. Data are based on interpolation between soundings detailed in admiralty maps (Royal Danish Hydrographic Office, 1954)]. Egedesminde Dyb, the deepest transverse channel extending from the West Greenland coastline is highlighted in blue above. Kanersuneq is highlighted with the sediment fan Sydosbugten highlighted in orange.

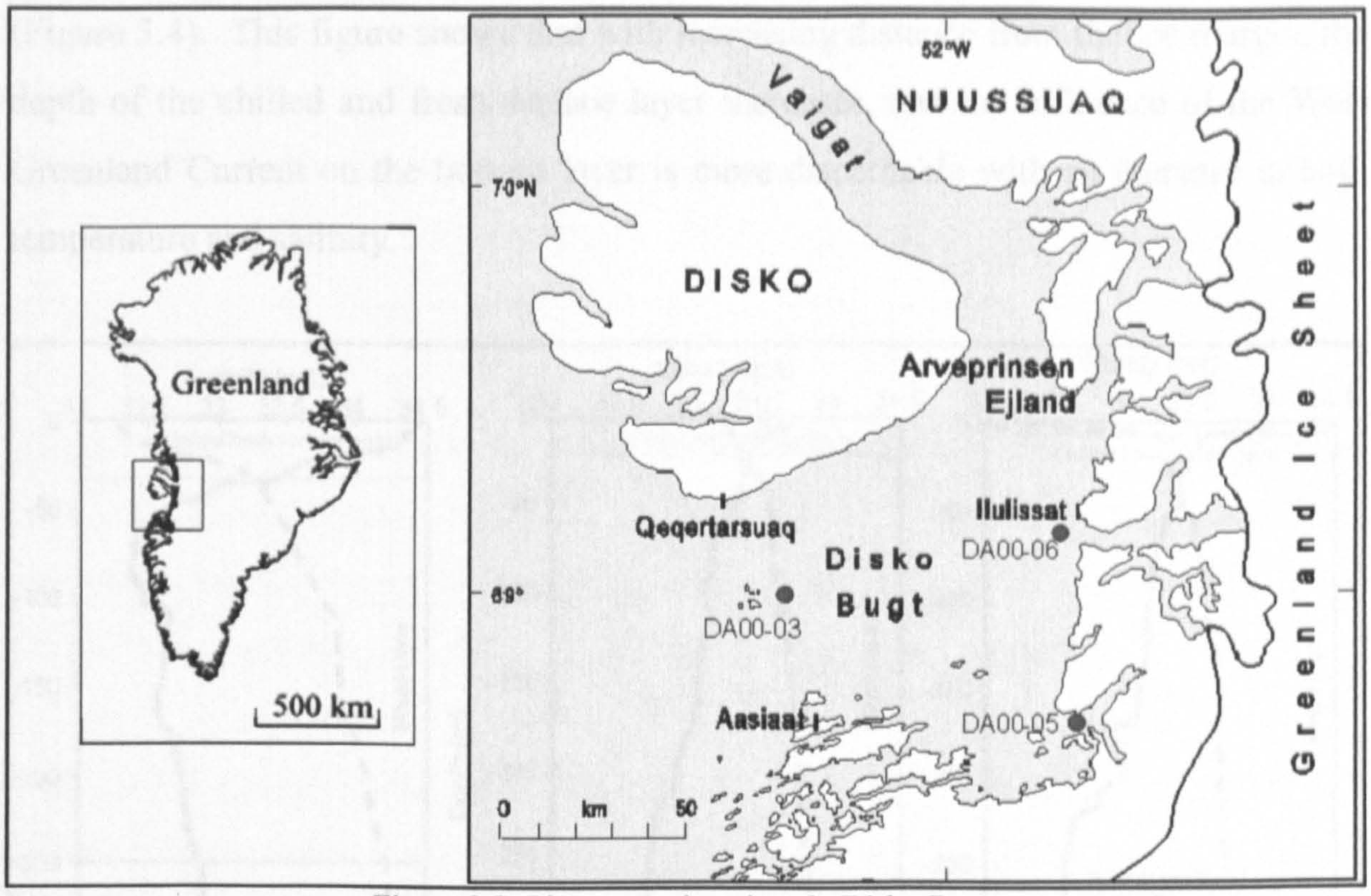

Figure 3.3: Piston core locations in Disko Bugt.

1. Firstly a coring site at the mouth of Jakobshavns Isfjord was chosen (DA00-06, Figure 3.3), to investigate an *ice proximal* environment to reveal information about the deglacial history of Jakobshavns Isbrae, and its interaction with West Greenland Current waters during the Holocene. Jakobshavns Isbrae has already been identified as one of the most important ice streams draining the West Greenland Ice Sheet (Chapter 1). Significant advances have been made about the terrestrial deglacial chronology from the work of Long and Roberts (2002; 2003) and Long *et al.* (1999; 2003), but information about the marine based portion of the West Greenland Ice Sheet is required to further explain the retreat of the ice from Disko Bugt.

This core site location was chosen because preliminary evidence from the gravity core analyses indicated that sediments in front of Jakobshavns Isfjord extended to at least 10.2 ka cal BP (Lloyd *et al.*, submitted). Coring point selection at this site aimed to give as long a core record as possible to generate high resolution records of fluctuations in the ice stream deglacial activity. The proximity of this site to Jakobshavns Isbrae meant that changes in sediment and meltwater delivery to the bay from the ice stream would be recorded before it potentially got diluted in the Bugt, and mixed with underlying water masses to form a widespread mixed layer in Disko Bugt. This had been identified from CTD casts during the 1999 *R/v Porsild* cruise

(Figure 3.4). This figure shows that with increasing distance from the ice margin, the depth of the chilled and fresh surface layer increases, and the influence of the West Greenland Current on the bottom layer is more discernable with an increase in both temperature and salinity.

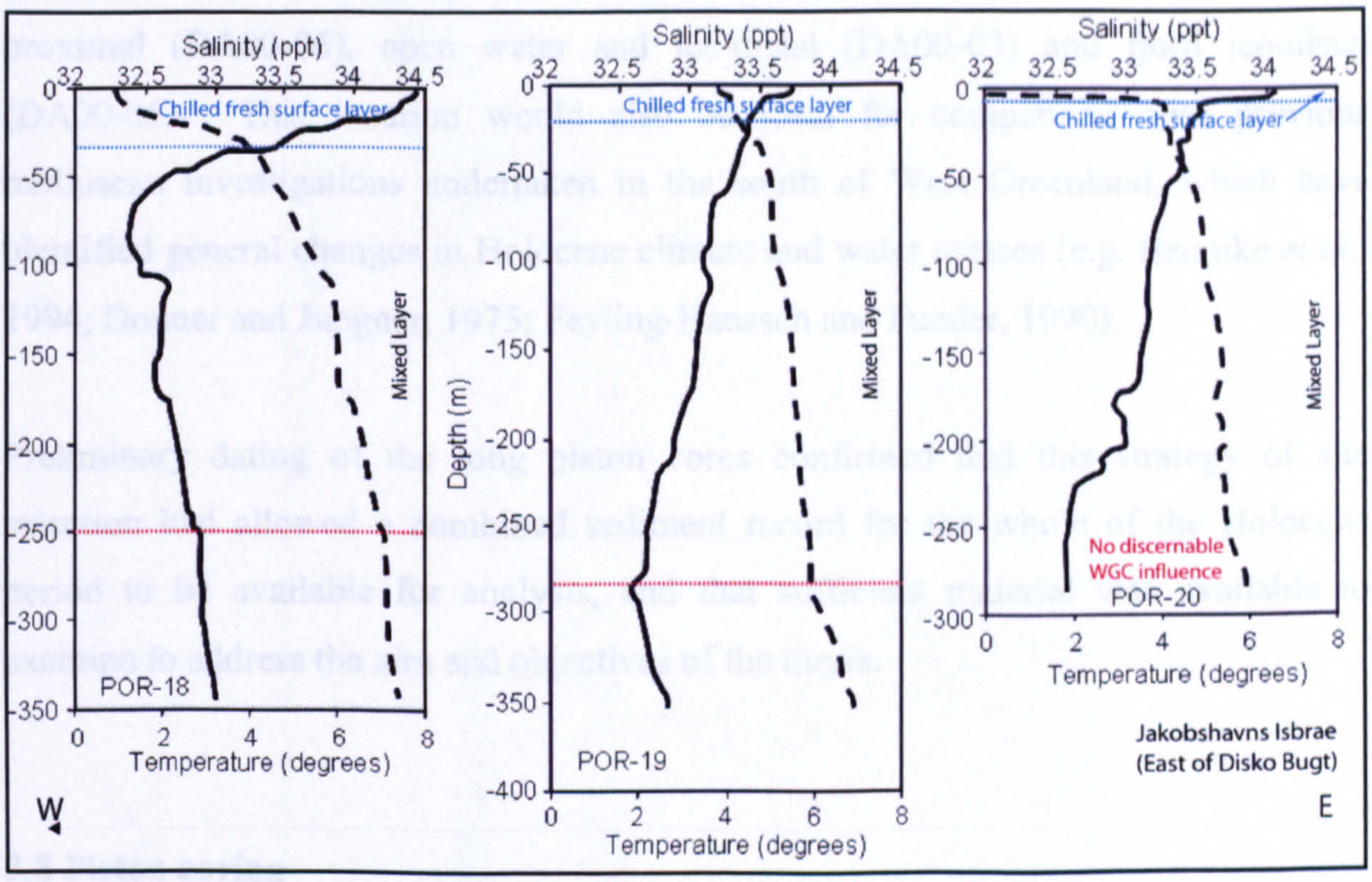

Figure 3.4: Examples of temperature and salinity profiles from a transect taken by Kuijpers and Lloyd in 1999 in front of Jakobshavns Isbrae - POR18 to 20, West to East (see Figure 3.1 for locations). Blue line indicates depth of chilled fresh layer, red line indicates when WGC influence is discernable in the profile.

2. A second core location in the deep troughs *(ice distal)* was chosen to provide a more regional view of palaeoceanographic changes in Disko Bugt (DA00-03, Figure 3.3). This site was chosen as there is a large thickness of sediment in the deep troughs, identified from the old seismic surveys during the previous year. It was anticipated that these sediments would have the potential to reveal long records of more regional oceanographic change such as fluctuations in the strength of the West Greenland Current and its components, the Irminger Current and the East Greenland Current. This was due to the outer bay location, at some distance from the potentially overwhelming meltwater dominated influence of Jakobshavns Isbrae. If core records were temporally extensive, then this site would be ideal for identifying the potential role of changes in regional palaeoceanography in deglaciation.

3. A third core site location in the southeast of Disko Bugt would allow examination of possible changes of dominance in ice streams, and would provide a detailed study of a large West Greenland *distal* fjord environment. This core site is located at the mouth of Kangersuneq fjord (DA00-05 Figure 3.3), and its inclusion in the coring program meant that three marine environments were investigated in the region; ice-proximal (DA00-06), open water and ice-distal (DA00-03) and fjord ice-distal (DA00-05). This location would also be ideal for comparison with previous molluscan investigations undertaken in the south of West Greenland, which have identified general changes in Holocene climate and water masses (e.g. Bennike *et al.*, 1994; Donner and Jungner, 1975; Feyling-Hanssen and Funder, 1990).

Preliminary dating of the long piston cores confirmed that this strategy of site selection had allowed a combined sediment record for the whole of the Holocene period to be available for analysis, and that sufficient material was available to examine to address the aim and objectives of the thesis.

3.3 Piston coring

Piston coring took place aboard the R/V *Dana* on the 3rd-6th August 2000. The coring equipment consisted of a 2-ton corer, 12 m in length with an inner liner diameter of 9.8 cm. Using a cradle, together with 20 mm steel cable from the trawl winch, the corer was deployed 6 times (see Figure 3.5). Coring at the sampling station off Jakobshavns was attempted twice. The first attempt (DA00-01) was unsuccessful due to the very coarse IRD in the top section of the core, which destroyed the core catcher upon entry and, on retrieval of the core barrel, sediment failed to be trapped and was lost.

Figure 3.5: Deployment of piston corer from R/V *Dana*, August 2000.

To remain on cruise schedule, the ship moved to the second coring location where two cores were taken in the outer part of the bay in the thick sediment infill of the deep troughs. Coring here was straightforward and the longest cores of the cruise, DA00-02 and DA00-03 were retrieved. With excellent weather and water conditions two further coring stations were engaged at the mouth and lower end of Kangersuneq fjord. With successful equipment deployment, two further cores were retrieved, DA00-04 and DA00-05. In order to complete the fieldwork aims, the Jakobshavns Isbrae location was re-visited and core DA00-06 was successfully collected (Kuijpers *et al.*, 2001).

3.4 Shallow seismic surveying

Marine seismic reflection techniques use high-frequency sound sources to image the ocean floor, and allow the sediments and geology below to be mapped. Sub-bottom acoustic profilers emit low frequency acoustic energy that penetrates the seabed providing a cross-section of the underlying (geological) sediments. While some systems are limited by their image resolution, the development of the towed, digital, wideband, frequency-modulated (FM) sonar system called 'Chirp' allows high resolution penetration of the ocean floor and its sediments, that is rapid and non-invasive (Quinn *et al.*, 1997a; 1997b). The device can penetrate up to 50 m in soft silts and clays, providing high quality acoustic data that can be used to characterise sediment properties, often creating detailed images of palaeo-landscapes. This seismic surveying technique has been successfully used in similar circumstances in West Antarctica, where high-resolution seismic profiles and piston cores were collected from Maxwell Bay in the South Shetland Islands to investigate the complex glacimarine sedimentation processes and glacial history of the area (Yoon *et al.*, 1997).

3.4.1 R/V *Dana* Chirp

Chirp surveying was carried out in two phases. Aboard the R/V *Dana,* when moving between piston core locations during the R/V *Dana* cruise, Chirp data was continuously taken to aid in choosing specific core sites at the various locations. The Chirp record revealed the characteristics of potential sites, and from examination of the traces, ideal sites showing smooth sea floor topography, with undisturbed sedimentation, and possible parallel bedding were identified. Figure 3.6 shows the seismic tracks, and coring, surface sampling and CTD cast sites for the 1999 and 2000 cruises.

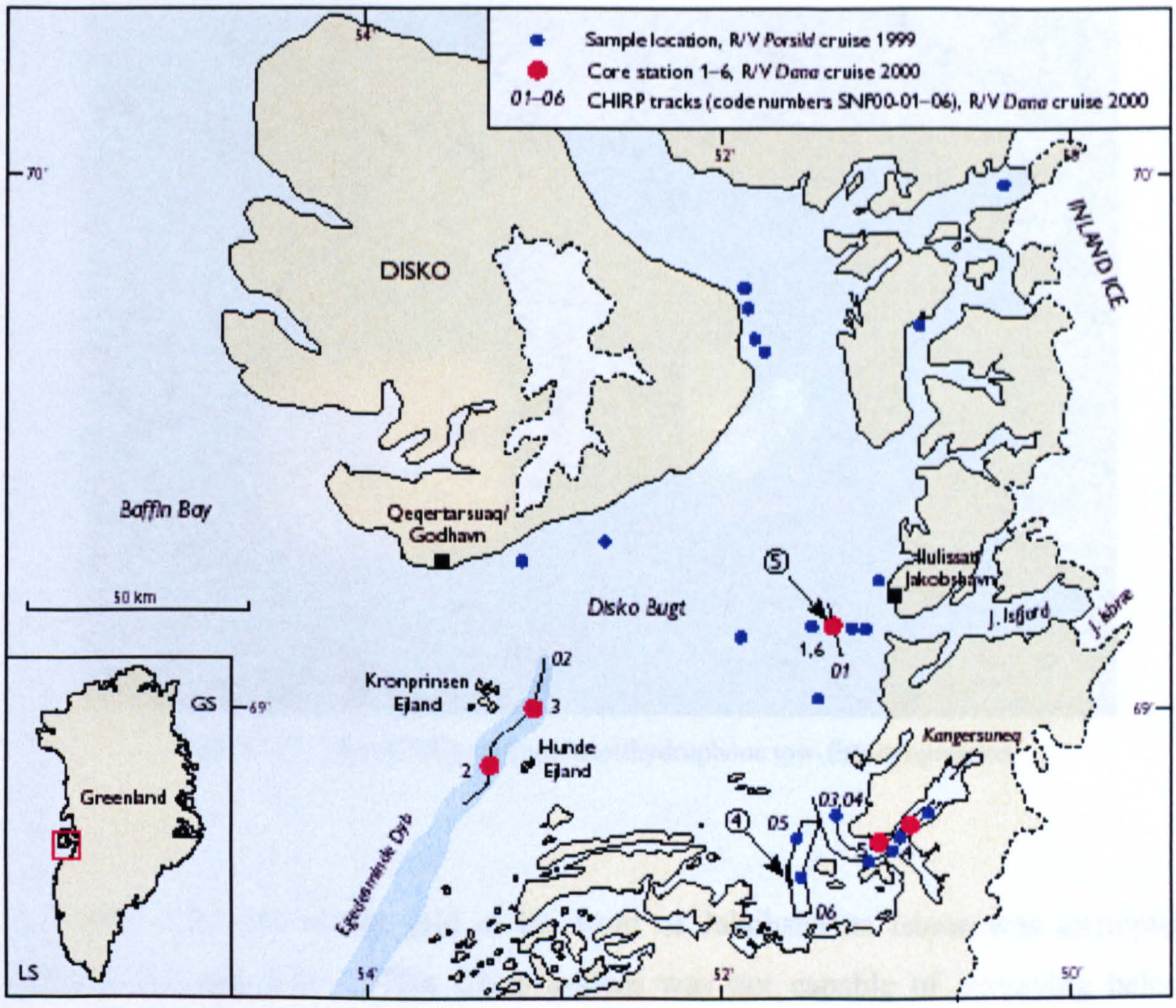

Figure 3.6: Combined sampling locations for core material, surface sample and seismic tracks during the R/V *Porsild* (1999) and R/V *Dana* (2000) fieldwork cruises. Blue dots mark the sites used during 1999 sampling and red dots mark the sites used during the 2000 fieldwork (from Kuijpers *et al.*,2001).

3.4.2 R/V *Porsild* Chirp

In collaboration with Dr Justin Dix, Southampton Oceanography Centre (SOC), a detailed program of shallow seismic surveying was also carried out on the R/V *Porsild* in 2000 to map the seabed topography and sediments in the vicinity of the Jakobshavns Isfjord mouth. The GEOChirp system consisted of a transducer/hydrophone tow-fish and a transceiver/processing system with a digital and analogue recording facility (Figure 3.7). This was lowered into the water using the automatic winch and the portside access gate and towed at a depth of between 4 and 8 m below the sea surface at a maximum speed of five knots in survey lines.

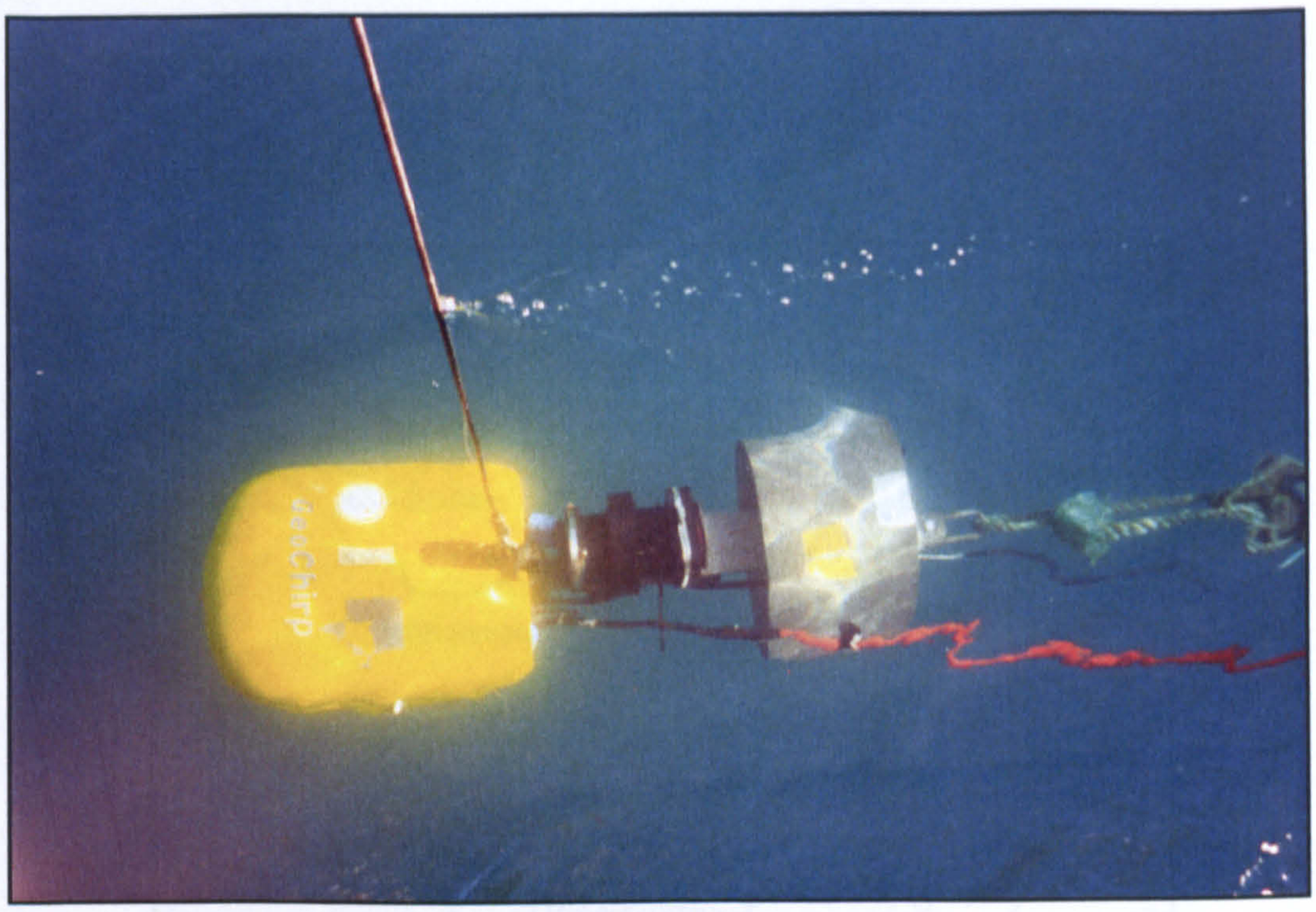

Figure 3.7: The GEOChirp transducer/hydrophone tow-fish in operation.

A 10 km x 20 km survey grid at the front of Jakobshavns Isbrae was attempted (Figures 3.8 and 3.9). This Chirp system was not capable of surveying below approximately 340 m, and frequent changes in water depth meant that periodic halts and adjustments to the delay time had to be made, and in survey lines close in to the edge of the Isfjord care had to be taken to guard against mini-ice floes which threatened the security of the steel winch cable and the stability of the 'fish' below.

This survey was the first of its kind to be carried out in water depths of more than approximately 50 m and will allow an initial mapping of sediment architecture and facies types to be developed for a grid of approximately 200 km^2 in front of Jakobshavns Isfjord (Dix, *unpublished data*). The survey grid covered the location of piston core DA00-06 (shown in Figure 3.3), as well as the short cores POR20 and POR 21 taken in 1999 by Kuijpers and Lloyd (J Lloyd pers. comm. 2003) and correlations between sediment types and seismic reflections have been made (Dix, *unpublished data*) which allows fingerprinting of the seismic amplitudes. For example, core sediment loaded with IRD gives a much stronger signal than fine-grained sediment. No Chirp data can be presented in this thesis as analysis and processing of the information is currently being undertaken (J. Dix pers. comm. 2003).

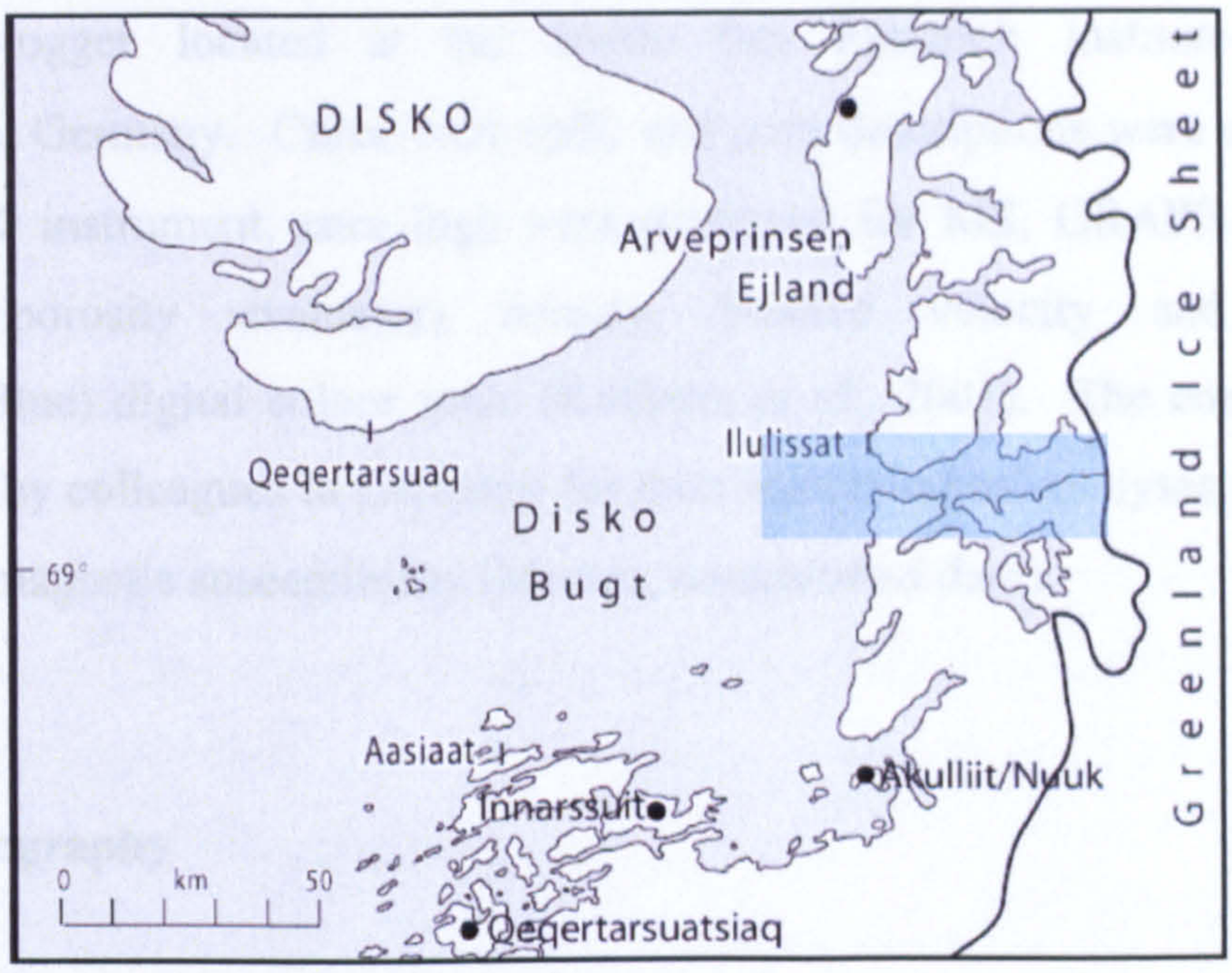

Figure 3.8: Site of Chirp survey grid undertaken during the R/V *Porsild* 2000 cruise.

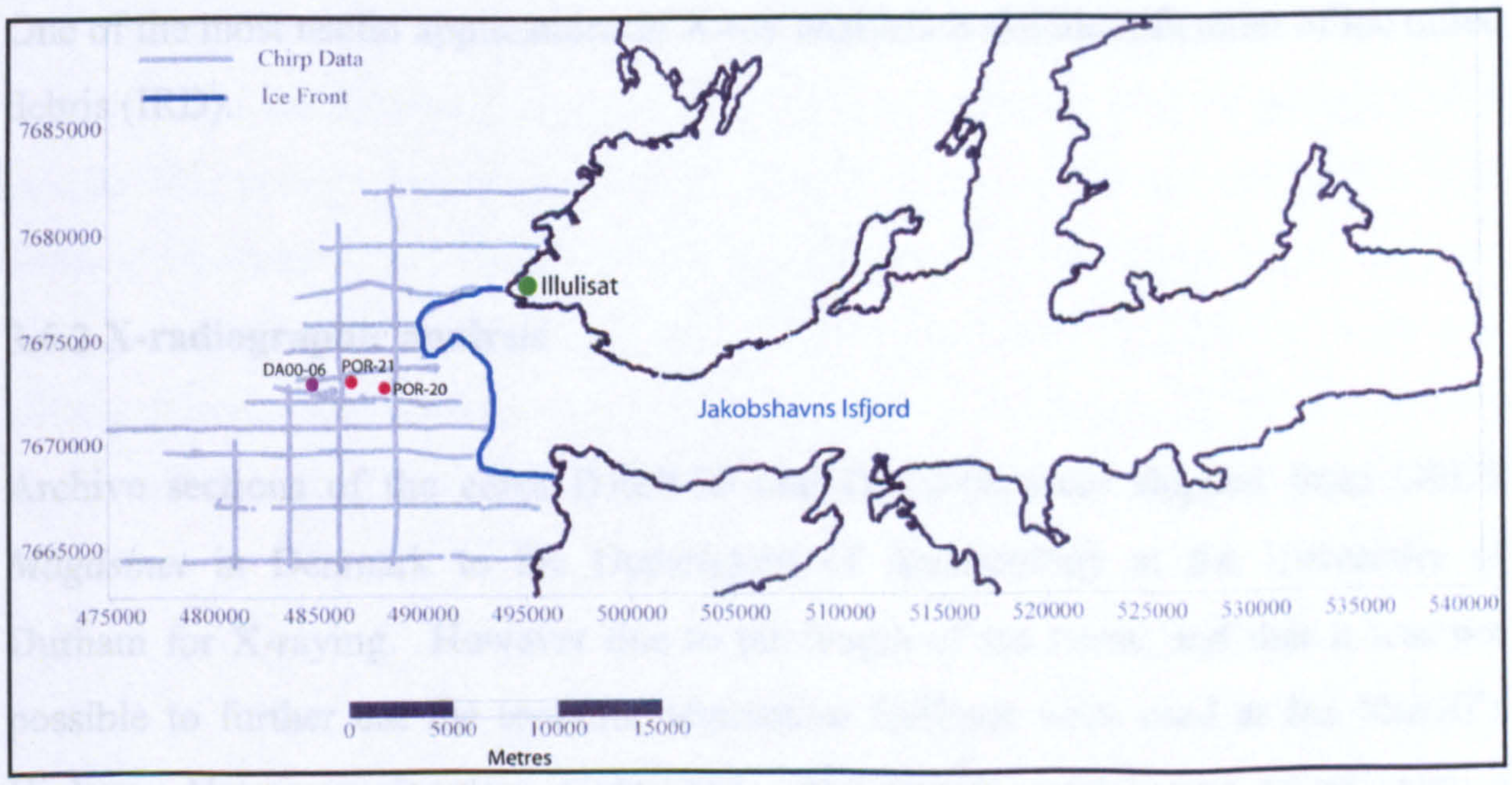

Figure 3.9: The Chirp survey grid in front of Jakobshavns Isbrae. Cores POR-20 and POR-21 are marked with a red dot and DA00-06 is marked with a purple dot. At the relevant core site locations.

3.5 Sedimentological analysis

Prior to opening, the cores were logged by technicians using the GEOTEK multi-sensor core-logger located at the Baltic Sea Research Institute (BSRI) in Warnemünde, Germany. Cores were split, and core descriptions were made. Using the GEOTEK instrument, core logs were produced for MS, GRAPE (gamma ray attenuation porosity evaluator) density, P-wave velocity and the RGB (Red/Green/Blue) digital colour scale (Kuijpers *et al.*, 2001). The cores were then sub-sampled by colleagues in Germany for their mineralogical analyses; particle size, density, and magnetic susceptibility (Morros, *unpublished data*).

3.6.1 X-radiography

X-ray photography is an established tool in core assessment and analysis (Dowdeswell *et al.*, 1998; Ó Cofaigh and Dowdeswell, 2001). Sediment structures and patterns of sediment architecture such as laminations that often cannot be derived from simple core logging often become apparent from the high resolution imagery. One of the most useful applications of X-ray analysis is the identification of ice rafted debris (IRD).

3.6.2 X-radiographic analysis

Archive sections of the cores DA00-03 and DA00-06 were shipped from GEUS *Magasinet* in Denmark to the Department of Archaeology at the University of Durham for X-raying. However due to the length of the cores, and that it was not possible to further cut the sections, alternative facilities were used at the Sheriff's Highway Veterinary Practice, Gateshead. The X-radiographs were taken using a Picker International ME20MC X-ray machine. It had a Kv (voltage) range of 30-125, and an MAS (milliamps per second) range of 0.5-50. The machine had a 100 cm film focussing distance. Test exposures were taken from the top, middle and bottom of each core, as adjustments had to be made to obtain the maximum photographic contrast between sediments of differing density. Final settings were 60 Kv at 0.15

MAS. Films were taken at 25 cm intervals on two sections of core at a time, with an overlap between each film of at least 1-2 cm together with lead markers to allow end matching for image reassembly.

Upon visual examination of the cores after splitting them, Kuijpers (pers. comm., 2001) documented that bioturbation was present in two of the three cores used; DA00-03 and DA00-05. However, my detailed examination of the X-rays suggested that bioturbation was not a significant problem, as no evidence of burrowing in the X-ray films which would indicate reworking of the sediment, and affect the stratigraphy. This was backed up by there being no evidence of date inversions in the established core chronology. In conjunction with the derived rapid sedimentation rates (see Chapter 4); the problems of altered chronology and diminished resolution associated with reworking are greatly reduced.

Analysis of the X-ray films took place using a custom built light box and a cardboard viewer to eliminate exterior light pollution. IRD was measured and counted at 2 cm intervals down the core, and these counts were categorized in three sections; 2-5 mm, 5-10 mm and >10 mm diameter. This would allow comparison of results in terms of total IRD (greater than 2 mm) with other authors (see discussion of IRD in Section 3.6.3). From the different size categories, calving proximity may be revealed, with coarser IRD perhaps indicating closer proximity of Jakobshavns Isbrae, or increased meltwater/sediment flux phases. Once the IRD counts were completed, the films were developed to produce contact prints for later comparison with the palaeoenvironmental analyses (e.g. Figure 3.9). At the same time, the presence of any shells visible on the films was also noted for later use for dating material.

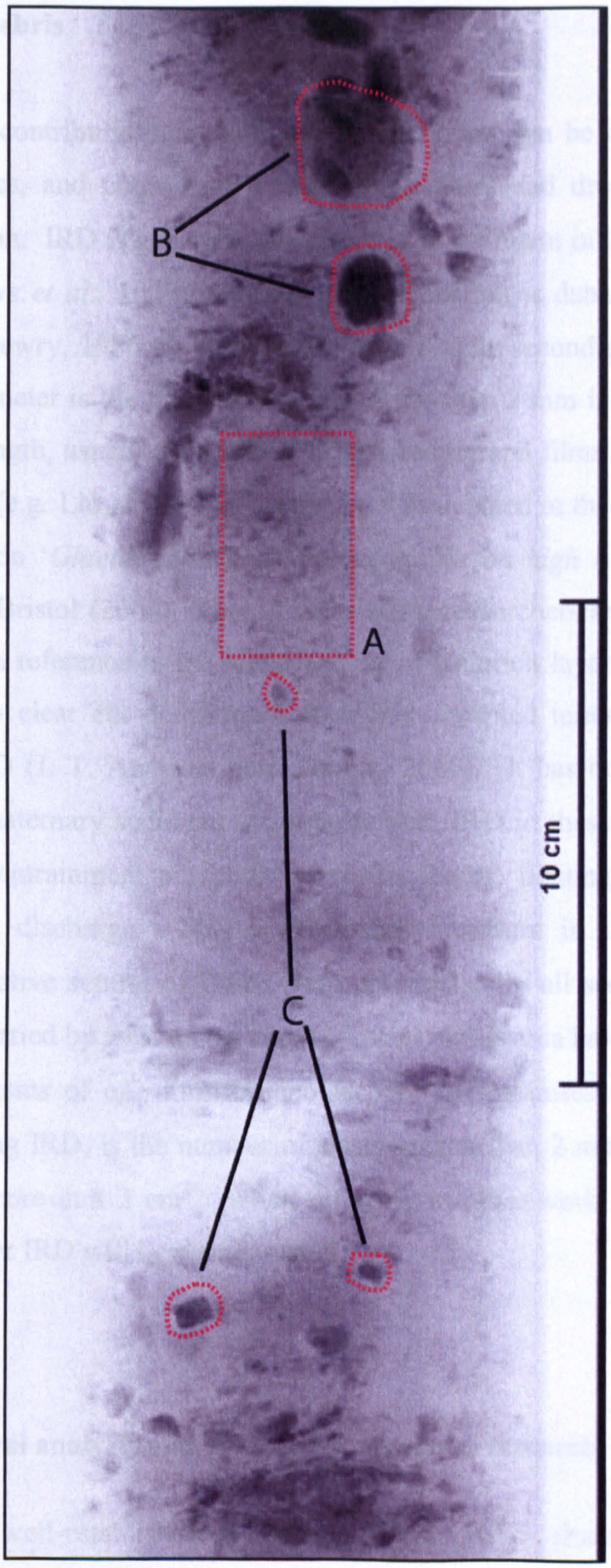

Figure 3.10: IRD detected in X-ray photograph taken from top part of the core DA00-06 (at approximately 20-50cm depth). **A**: fine IRD < 2mm. **B**: Clast between 2 and 5mm. **C**: Clasts > 5mm.

3.6.3 Ice rafted debris

Ice rafted debris contributions to sediment accumulation can be quantified through grain-size analyses, and counting the number of clasts and dropstones to a pre-determined fraction. IRD is generally associated with sediment in the sand-size range (>63μm) (Andrews *et al.,* 1997), although this distinction is debated (Andrews and Matsch, 1983; Drewry, 1986; Syvitski *et al.,* 1996). The second generally accepted particle size parameter is the number of clasts larger than 2 mm in 1 to 2 cm section sample of core length, usually determined from x-radiograph films of the undisturbed sections of cores (e.g. Lloyd, 1996). This topic was debated at the recent Geological Society meeting on '*Glacier influenced sedimentation on high latitude continental margins'* held in Bristol (2000). One of the leading researchers in the field recently raised the point in reference to the identification of Heinrich layers, mentioning that there was still no clear cut definition and widely accepted terms and quantifiable parameters of IRD (J. T. Andrews pers. comm., 2000). It has been suggested that technically *all* Quaternary sediment could be termed IRD in these environments, its origin being the entrainment of debris in ice, i.e. bergs, floating ice tongues, and loaded meltwater discharge. This is particularly relevant in the relatively ice-proximal investigative setting of Disko Bugt, as practically all sediment is at some point eroded or carried by ice. As the core sediment in this area has all come from ice transport mechanisms of one form or another, for the purposes of this thesis, the criteria for defining IRD, is the number of clasts greater than 2 mm counted visually from X-rays per core unit 2 cm^2. When referring to other work and literature, the defining criteria for IRD will be clearly stated.

3.7.1 Foraminiferal analysis and palaeoenvironmental research

Foraminifera are well-established indicators of water mass characteristics. Much information relating to changes in oceanographic regimes, water mass differences and ice sheet movements, can be determined from contemporary and palaeo-faunal assemblages and from their associated oxygen isotope record. The study area of Disko Bugt comprises mainly shallow water environments, (and benthic species are

dominant at all core locations) in both modern and palaeoenvironments (J.M. Lloyd pers. comm., 2000).

Fossil assemblage data from the three piston core sites are used to characterise water mass differences and bottom water conditions in particular, changes in temperature and salinity associated with the West Greenland Current. Also, changes in productivity, perhaps relating to extended phases of seasonal pack ice are identified. The three core sites are characterised by quite different present day conditions and, therefore, can be used to address different aims (Chapter 1). All three core sites are representative of distinct environments, with DA00-06 recording palaeo ice-proximal conditions, DA00-05 representing a fjord environment under influence from both meltwater and possibly varying intensity of incoming water masses, and DA00-03 providing the connection between the bay and the more regional water masses of the Labrador Sea.

Identifying present day distribution of species allows a comparison of contemporary faunal distributions with the assemblages recorded through the core sequences, if the modern analogues are represented in the fossil record. If there is disparity between a modern and fossil assemblage, the fossil benthic record will still be able to reveal information about changes in bottom waters, and productivity fluctuations, especially in shallow marine environments such as Disko Bugt, based on published studies. Modern assemblages for Disko Bugt are being determined as part of the wider NERC project (Lloyd, *in prep.*) and can be used for comparison, together with contemporary data from similar environmental studies (e.g. Jennings and Helgadottir, 1994; Jennings and Weiner, 1996; Madsen and Knudsen, 1994; Osterman and Nelson, 1989).

Previous work on foraminifera in the region is limited, with only general taxonomic investigations by Feyling-Hanssen (1990a, 1990b), and most of the palaeoenvironmental studies being restricted to the fjords of eastern Greenland (e.g. Jennings and Helgadottir, 1994; Jennings and Weiner, 1996; Madsen and Knudsen, 1994). However, Osterman and Nelson's (1989) work on the eastern Baffin Island continental shelf has comparative data regarding the influences of different water masses on dissolution, and ecological data. Further comparisons can also be made

with studies further a field in the Nordic Seas (e.g. Hald and Korsun, 1997; Hald and Steinsund, 1992), as similar conditions (water mass characteristics, environmental niches and depths) are likely to be found.

3.7.2 Collection and preparation of samples

The long piston cores were shipped to GEUS for storage, and split, with one half of each kept as an archive section, and the other as a working section for multiple analyses by project members (Mathias Morros (BSRI); sedimentological analyses, Karin Jensen (GEUS); diatom analysis) . Samples for foraminiferal analyses were taken from the working sections of cores DA00-03 and DA00-06 at an 8 cm interval and DA00-05 at a 10 cm interval. As these were working sections, there was a constraint on the maximum sediment available for analysis. Prior processing of the 1999 short gravity core samples provided a guide to the volume of sediment required, and it was seen that assuming sedimentation rate and associated foraminiferal abundance was relatively constant, a minimum of 5 cm^3 of sediment would be required for a 300 test foraminiferal count. Where there was minimal sediment, such as at core breaks, or or where sediment had been removed by project partners for other proxy methods, a sample was taken from the closest available location. Sediment was removed using disposable syringes, stored in sealable plastic bags and refrigerated until being transported back to the UK for further processing.

Samples were soaked over-night to disaggregate fine-grained sediment, and carefully wet-sieved through 500 μm and 63 μm sieves. Wet sieving was used due to general test fragility, particularly of the agglutinated specimens, which are not as robust as calcareous tests when dried. Material greater than 500 μm was discarded. Apart from samples from the upper metre of core DA00-06 there were few samples that had significant sediment greater than 500 μm in size. There is considerable debate about the correct mesh size to use to concentrate foraminiferal tests from samples from late-glacial/Holocene settings (Knudsen and Austin, 1996 in: Andrews *et al.*, 1996). At the 1995 workshop on Late Quaternary palaeoceanography of the North Atlantic Margins, most participants advocated the use of the 125 μm mesh size. The small test size, particularly of agglutinated species, in the Disko Bugt samples encouraged the

use of the 63 μm sieve size in this thesis. The workshop recommended that the benthic-deep water assemblages, particularly from the High Arctic should be assessed using the smaller mesh sizes, as using the 63 μm sieve reduced low count possibilities in the likelihood of fluctuating sediment accumulation rates and productivity.

Samples were prepared in batches of 10 or 12 for analysis under the light microscope at a magnification between x 15 and x 50 and stored in sealed polyethylene vials. Samples were wet-picked from a tray with a fine haired brush, then using dilute adhesive, selected specimens were attached to a Chapman slide. This was to create type slides for species identification, as certain species were notorious for taxonomic similarities with others (e.g. *Islandiella norcrossi*).

Initial sample identification was carried out every 24 cm to allow the production of skeleton information, which, in conjunction with radiocarbon chronology would lead to further refining of the sampling at convenient intervals (e.g. 12 cm, 8 cm 2 cm etc.).

With this information, especially in relation to the age-depth models that became available as material was processed, it became apparent that the initial strategy of an 8 cm interval would be the most appropriate as this would yield a resolution of between 10 and 20 years per sample. The initial skeleton information showed that more sediment would be required to be processed for viable taxonomic counts.

Archive sections of the cores DA00-03 and DA00-06 were sub sampled after X-ray analysis at Durham before being returned to GEUS. Following the X-ray procedures, samples were taken from the cores using a sharp palette knife every 2 cm. Sample volume ranged typically between 5 ml and 15 ml, equivalent to a section *c.* 2 cm of core length.

3.7.3 Foraminiferal sample size

Where possible, 300 specimens were counted from each sample according to standard practice (Patterson and Fishbein, 1989). This allowed a 95% confidence level that the possibility of finding a new species in the count would not affect the overall assemblage pattern. This was not possible in approximately half of the samples analysed. While sedimentation rates appeared constant according to the age-depth model, foraminifera concentrations vary. It is possible that this was due to preservation issues and foraminifera productivity. Counts varied between <3 tests per ml to >45 tests per ml. Full lisst of species abundances are given in Appendices 2 and 3 (core DA00-06); 8 and 9 (DA00-05); and 11 and 12 (DA00-03).

3.7.4 Assumptions and limitations of foraminiferal analysis

As with all palaeoenvironmental investigative techniques there are limitations to be aware of. With foraminifera, as with other micro and macro fossil techniques, there are issues of post-depositional and post mortem changes, including bioturbation, selective preservation and dissolution. The effects of bioturbation are in this case negligible due to the high sedimentation rate, and the absence of evidence from the X-ray analysis. Preservation and dissolution of species are significant though, from dissolution of calcareous species due to changes in water temperature and chemistry, as well as possible destruction of both agglutinated and calcareous test as a result of high-energy depositional environments. It is clear that dissolution of calcareous foraminifera is important in some sections due to corrosive bottom waters as evidenced by the presence of test linings in samples. This issue is discussed in more detail in Chapter 5.

3.8.1 Oxygen isotope analysis

Oxygen isotope analysis is a widely used palaeoenvironmental reconstruction method on a variety of spatial and temporal scales (Sen Gupta, 1999). Calcareous foraminifera are preserved in many ocean sediments, and the oxygen isotopic composition of their tests reflects the isotopic composition of the ocean at the time the carbonate was precipitated. Changes in the isotopic composition of seawater through time will be reflected by changes preserved in the foraminiferal test. Thus, changes to water mass characteristics may then be related to temperature/salinity of Disko Bugt water masses. While often employed to allow global correlation of ocean sediments (Patience and Kroon, 1991), oxygen isotopes are used here to identify changes in water mass (and subsequent temperature and salinity) and also possible meltwater flux within Disko Bugt. This enables local/regional palaeoceanographic reconstruction and correlation with Greenland ice core records (GISP2, GRIP). There are various factors that influence the oxygen isotope signal preserved in the tests of the foraminifera. These are outlined below;

1) Ice volume effect

The balance between low latitude evaporation and high latitude precipitation and continental based ice storage is responsible for significant variations in the oxygen isotope ratio of the oceans. During glacial periods mid latitude ice sheets store large quantities of water on land. Evaporation of this water from the oceans preferentially removes the lighter ^{16}O isotope. The ratio of $\delta^{18}O/\delta^{16}O$ in the oceans is therefore subject to significant fluctuations based on the growth and decay of mid latitude ice sheets. Berger (1979) estimated that the difference in oceanic oxygen isotopic ratio between a full glacial and an interglacial cycle to be 1.0‰. These variations are recorded in the tests of foraminifera living at the time and preserved in the ocean sediment.

2) Temperature effect

The oxygen isotopic content of the foraminiferal tests is derived from the isotopic composition of the water from which the precipitation occurs, this precipitation is temperature dependent (Patience and Kroon, 1991). At low temperatures there is greater fractionation of the heavier isotope relative to the lighter one, and the test will

contain a greater amount of ^{18}O than would be the case at a higher temperature. The temperature effect is a 0.2‰ isotope change per 1°C temperature change. So for example if marine waters in which the foraminifera are living cools by 5°C, the isotopic composition of the foraminiferal calcite will be 1‰ heavier. In general planktic species are subject to significantly greater temperature fluctuations (Sen Gupta, 1999). Benthic specimens from the deep are often assumed not to be influenced by temperature because the bottom water are already close to freezing, so do not vary significantly (Murray, 1991). This is not the case in Disko Bugt, however, due to the WGC bringing warmer deep waters in to the bay. This water depth is relatively shallow, and so temperature does change significantly.

3) Salinity

Salinity effects are also influential factors in the oxygen isotope ratio of foraminifera. Tropical and temperate waters have higher $\delta^{18}O/ \delta^{16}O$ ratios than polar waters. These difference are not only due to the temperature effect, but also are closely linked to the surface ocean water salinity distribution (e.g. Duplessy *et al.*, 1992), where the higher the salinity the higher the $\delta^{18}O/ \delta^{16}O$ ratio, due to preferential removal of the lighter ^{16}O isotope during evaporation. Both salinity and the $\delta^{18}O/ \delta^{16}O$ ratio of surface waters are reduced when meltwater or precipitation depleted in $H_2{}^{18}O$ enters the ocean, while increased evaporation concentrates the heavier $H_2{}^{18}O$ and increases salinity.

4) Species vital effects

Large variations in oxygen isotope ratios can be found between species. This is due to physiological differences that influence the degree to which the individual species precipitate $CaCO_3$ in isotopic equilibrium with the ambient seawater. Variations in isotope ratio are also attributed to the effects of the developmental stage of the foraminifera as the juvenile and adult stages display differences in the extent of oxygen isotope fractionation. Migration of some species during different stages of their life cycle within the water column is also found (Murray, 1991). A combination of these vital effects can give variations of up to 1.2‰. However, this may be countered by using homogenous test sizes in a sample, and comparing with species for which the vital effects have been established (Patience and Kroon, 1991; Sen Gupta, 1999). This has not yet been established for the species used in this research,

as, to date, no foraminiferal oxygen isotope analysis has been carried out in Greenland, or similar areas using the same species. It is therefore extremely difficult to minimise its impact (if any) within this thesis.

3.8.2 Carbon isotope analysis

Benthic foraminiferal reflect $\delta^{13}C$ in bottom waters and pore waters in the upper centimetres of marine sediment. Despite the fact that pore-water $\delta^{13}C$ gradients may be depleted by up to 1‰ per cm of sediment depth due to sedimentary organic decomposition (Rohling and Cooke, 1999), this limitation is not relevant in this study, as variations in isotope ratios are discussed only relatively, as there are no details available regarding modern water chemistry and present day ratios. Despite variations in isotope ratios arising from the complex disequilibria, microhabitat and vital effects (see Chapter 4) benthic carbon isotope ratios have the potential to reveal information about changes in water mass characteristics and productivity in Disko Bugt.

Lowered $\delta^{13}C$ values in benthic foraminifera when higher ones are expected may relate to increases in surface productivity with the influx or increase in proportion of warmer more saline Atlantic waters. The effect of meltwater on the benthic foraminiferal ratios is to decrease the $\delta^{13}C$ composition of the waters by the addition of isotopically light terrestrial sourced organic material release during increased meltwater release or melting of pack ice, or increases in seasonal algae (e.g. diatom) blooms from within pack ice, this organic matter sinks to be re-oxidised at depth. The presence of increased amounts of fresher meltwater may also act as a lid, suppressing surface water ventilation, reducing the degree of thermal equilibrium with the atmosphere.

Higher $\delta^{13}C$ values in benthic foraminiferal can indicate strengthening of circulation processes, for example, higher $\delta^{13}C$ values are produced during an interglacial period than during a glacial where circulation is sluggish during glacial periods (Lloyd *et al.*, 1996).

3.8.3 Oxygen isotope sampling

In order to determine the palaeoceanographic changes in the study area, continuous records of $\delta^{18}O$ ratios were required. Following the initial skeleton assemblage counts, an informed decision could be made regarding the relative abundance of specific calcareous species, which had the most continuous presence throughout a core. In the case of core DA00-03 this proved straightforward, and the species *Nonionellina labradorica* was chosen to provide mono-specific oxygen isotope ratios. This species has a relatively large and robust test (Feyling-Hanssen 1990), and so even in cases of low test concentration, analyses were still viable. To meet the target weight of 100μg, the minimum number of tests per sample was 5.

Core DA00-06 was more complicated, as low foraminiferal abundance and sample preservation data from the skeleton counts showed that there was no single species continually present in an adequate state of preservation throughout the core. Therefore two primary species were chosen, *Cassidulina reniforme* and *Islandiella norcrossi,* with *N. labradorica* tests used where they were abundant. These species are all infaunal. *C. reniforme* is one of the smallest calcareous species present in this core (Feyling-Hansen, 1990), and obtaining adequate tests numbers was difficult due to low test numbers, especially in the upper part of the core and also that it seems to be particularly susceptible to dissolution. *I. norcrossi* is known to have a large size range (Murray, 1991), and care had to be taken when picking this species, as taxonomic distinctions between it and other benthic species is often not clear.

No epifaunal species such as *Cibicides lobatulus* or *Cibicides wullerstorfi,* which are preferentially used for benthic isotopic measurements, were available in sufficient quantities through the core for oxygen isotope analysis. It is likely therefore, that the three species used may reflect changes in isotopic pore water concentration as well as changes in the overlying water mass. Using three species, the offset in $\delta^{18}O$ per mil could be monitored, and assuming the isotope record of each species showed a relative trend with each other, the record from these species could be spliced together to produce a more complete record. Overlapping sections could be used to check whether a relatively constant offset exists between the species.

Samples were wet-picked using a light microscope, and placed on a dry counting tray and allowed to nearly dry. Using an extremely fine brush, these individual specimens were counted and transferred to sample vials, labelled, and in batches sent to the department of Geology and Geophysics at the University of Edinburgh for analysis. A stable isotope record was not collected from DA00- 05. This was due in part to financial and temporal constraints (extra samples were run for DA00-06 than were anticipated due to the discontinuous nature of the species and poor preservation), as well as the initial apparent lack of calcareous species in DA00-05 itself.

3.9 Chronology

A range of techniques was used in obtaining material for radiocarbon dating. Materials included plant and other organic fragments, intact shells, both gastropods and complete bivalves. Also, mixed species of benthic foraminifera were removed from the cores at various stages of other analyses. Radiocarbon dates were run at East Kilbride (NERC) radiocarbon laboratory. Samples were also run at Leibniz Labor für Altersbestimmung, Christian-Albrechts Universität, in Kiel, Germany, as well as at the AMS laboratory in the Institute of Physics and Astronomy, University of Aarhus, Denmark.

Radiocarbon dates from foraminifera were derived from handpicked mixed species of benthic tests. The procedure of picking test is the same as that for oxygen isotopes. The minimum weight of forams needed for AMS dating is 10 mg, and depending on the sizes of different species tests this meant each individual sample contained from 500 to 1600 tests. Where the availability of tests was poor, the section of the core sample was extended, to a maximum of 6 cm. However, the degree to which this affected the dating resolution was limited, due to the very high sedimentation rates present in the cores. A full table of radiocarbon dates is provided in Chapter 4 together with age depth models. All radiocarbon dates are presented in calibrated years BP (cal BP). The calibration program used is CALIB 4.3 (Stuiver and Reimer, 1993; Stuiver *et al.*, 1998) and all calibrated dates are cited with a 2-sigma age range.

3.10 Marine reservoir correction

A standard marine reservoir correction was applied to all radiocarbon dates of marine origin. The large carbon reservoir of the oceans creates a difference between the radiocarbon ages of marine samples and terrestrial ones, with the variations in ocean circulation creating regional differences within the reservoir correction. The marine carbon reservoir effect occurs globally, and is the apparent older age of marine samples created by the mixing of normal ^{14}C activity surface waters with low activity bottom waters. In the waters around Greenland, the mixing of Arctic and Atlantic sourced water creates the reservoir effect (Rassmussen and Rahbek, 1996). Water from the Arctic Ocean has a lower ^{14}C activity as long-term ice cover prevents atmospheric-oceanic CO_2 exchange.

The reservoir effect is known to influence radiocarbon dating of marine materials (and occasionally terrestrial) such as mollusc shells, mammals, fish, or foraminifera, creating an ageing effect so that samples measured return ages several hundred years older. In order for comparison with terrestrially procured dates, a correction is required. The ubiquitous correction is 400 years (Rasmussen and Rahbek, 1996), and any further regional reservoir effect (the apparent age) is determined according to determination of the apparent age of a variety of marine organisms still alive at the time of sampling (pre-bomb) depending on material type and location.

In West Greenland, eight coastal samples tested for an additional regional reservoir effect as part of the marine calibration dataset (Stuiver *et al.*, 1998) yield an additional mean regional correction for West Greenland of -22 ±23 cal yrs (Stuiver *et al.*, 1998). Throughout this thesis then, the apparent age of this regional reservoir effect is taken to be zero. This is in line with the findings of Rasmussen and Rahbek (1996), and other authors (Jensen *et al., in press*; Lloyd *et al., in press*; Long *et al.*, 2003) working in the region.

3.11 Chapter summary

This chapter outlines the methods used in data collection, production and analysis in this thesis. An overview of the preliminary 1999 R/V *Porsild* fieldwork season has been given, and the rationale for the later piston core site selection has been discussed in relation to this. This chapter has considered the sampling strategy used within this thesis, in terms of the collection and preparation of samples for sedimentological, foraminiferal, and isotopic analyses, and the subsequent methods of data analysis. There has been an informative discussion highlighting the inherent problems associated with the topic of Ice Rafted Debris (IRD), as well as limitations relating to isotope analysis. This chapter also acknowledges the requirement for applying marine reservoir corrections to radiocarbon dating, and justifies the use of the standard (400 yr) correction to ^{14}C dates produced within this body of work.

Chapter 4: Results

4.1 Introduction

This chapter presents the results of foraminiferal, oxygen isotope and IRD analysis from the three piston cores in Disko Bugt, West Greenland. Discussion of foraminiferal results is based upon species assemblage diagrams and stratigraphically constrained cluster analysis produced using Tilia and Tiliagraph, (Grimm, 1986). Stable isotope ratio results are shown for three species from DA00-06, and one species from DA00-03. No oxygen isotope record is available for DA00-05. IRD results are given for DA00-06, however, no IRD was detected in X-ray analysis for DA00-03, and no X-rays are available for DA00-05. Core chronology and the age depth models for Disko Bugt upon which interpretation in Chapters 5 and 6 are based are also presented.

4.2.1 DA00-06 foraminiferal analysis

Core DA00-06 is split into three foraminiferal assemblage Zones based on stratigraphically constrained cluster analysis shown in fig 4.1.

Zone 1 (960-290 cm) is the largest zone in the core and is dominated by three calcareous species; *Stainforthia feylingi* (15-50%), *Cassidulina reniforme* and *Elphidium excavatum* (both 20-40%). *Islandiella norcrossi* is also present in low values, typically 5-10%, with the higher percentages at the base of the zone. Other calcareous species present in this zone have abundances less than 5% (*Bolivina pseudopunctata, E. excavatum f. clavata, Nonionellina labradorica* and *Stainforthia concava*). There are few or no organic foraminiferal test linings in this zone, and the foraminiferal test count varies between 100 and 300 counts. From a radiocarbon date (AAR-6839) near to the core base (891 cm), the start of this zone can be dated to 7843 ±72 ^{14}C yrs BP (8154-8416 cal yr BP).

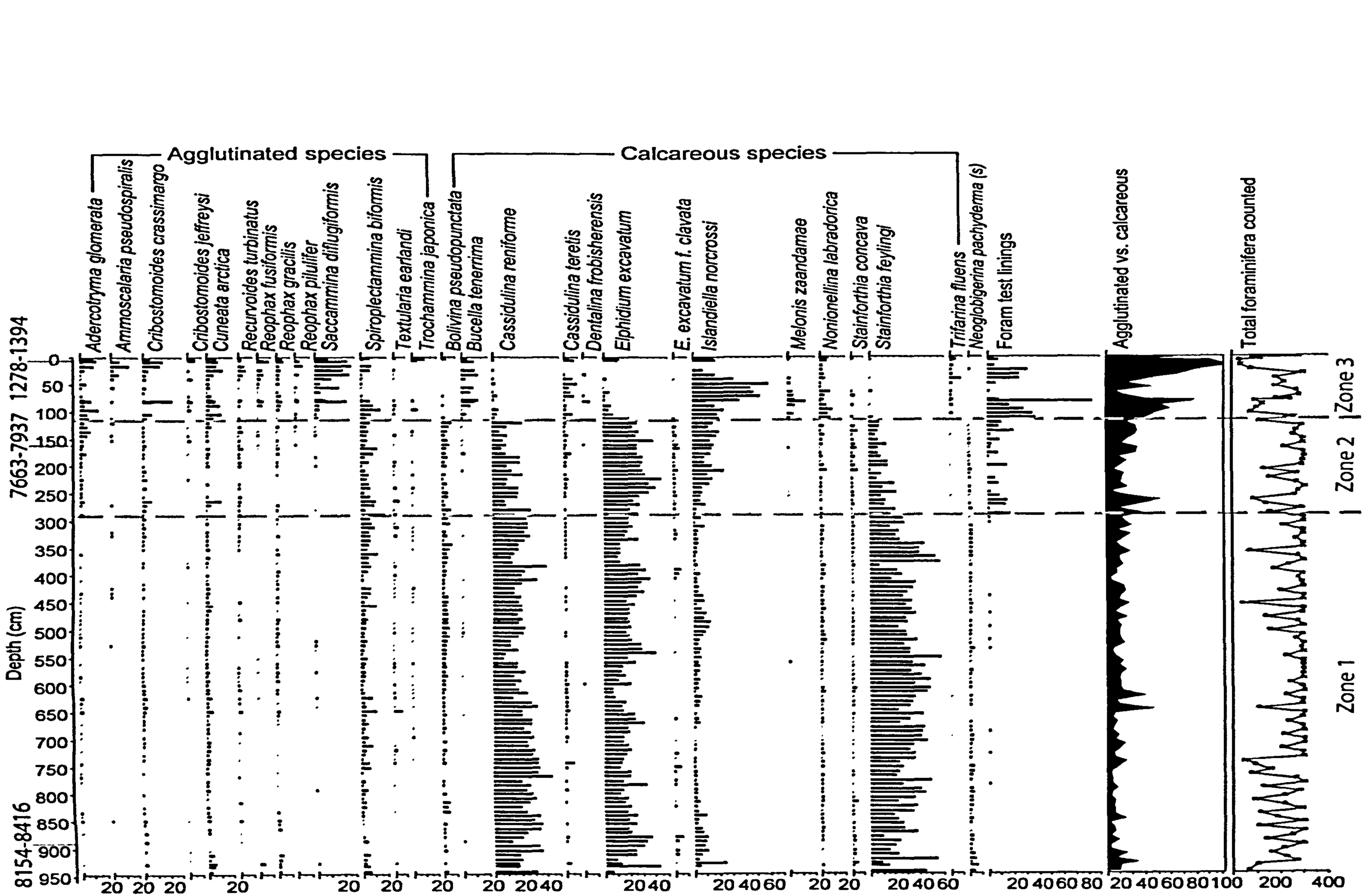

Figure 4.1: Foraminiferal assemblage data from DA00-06, only species >5% shown. Zone boundaries marked in green based on stratigraphically constrained cluster analysis. Radiocarbon dates shown in red, given in cal yr BP.

Zone 2 (290-115 cm) is dominated by *E. excavatum* (25-40%). There is also a decrease in dominance of both *C. reniforme* (10-20%) and *S. feylingi* (5-20%) through the zone, which is accompanied by an increase in frequencies of *I. norcrossi* (5-20%). Other calcareous species are present, but in small amounts, the greatest being *B. pseudopunctata* (up to 10%). The two most common agglutinated species are *A. glomerata* and *S. biformis*, although both have abundances of less than 10%. This zone shows a notable increase in the foraminiferal test linings counted (typically between 5-20 per sample). There is an even weaker presence of the planktic species *N. pachyderma (s)* in this zone. A radiocarbon date (AAR-6837) at 159 cm within the zone gives a date of 7350 ±68 ^{14}C yrs BP (7663-7937 cal yr BP).

Zone 3 (115-0 cm) is characterised by an increase in frequencies of the calcareous taxa. *I. norcrossi* (20-60%) followed by the agglutinated *Saccammina diflugiformis* (10-25%). Species diversity of the agglutinated taxa has increased. *A. glomerata, Cribostomoides crassimargo, Cuneata arctica, S. biformis* are all present (5-15% each) with lower amounts in the middle of the zone. Lower abundances (around 5%) of other agglutinates also occur e.g. *Ammoscalaria pseudospiralis, Recurvoides turbinatus, Reophax fusiformis* and *Reophax gracilis*. While there are somewhat lower and more variable foraminiferal test counts in this zone, counts of the organic walled test linings are at their highest in this zone. The top of the zone and end of the core contains a radiocarbon date (KIA-17925) at 5 cm of 1500 ±90 ^{14}C yrs BP (1278-1394 cal yr BP). There is no core top due to a loss of the top part of the sediment as a result of the coring process.

4.2.2 DA00-06 Foraminiferal species diversity

Benthic foraminiferal species diversity varies throughout the core. Data are presented in Figure 4.2. The core average species diversity is 17 species per sample, averaging seven agglutinates and ten calcareous species. In general, total species diversity is relatively stable until a slight increase in the agglutinated species between 688 cm and 400 cm. Diversity remains relatively constant for both groups until around 210 cm when there is an increase in diversity levels to approximately 25 per sample for total species diversity until the end of the core.

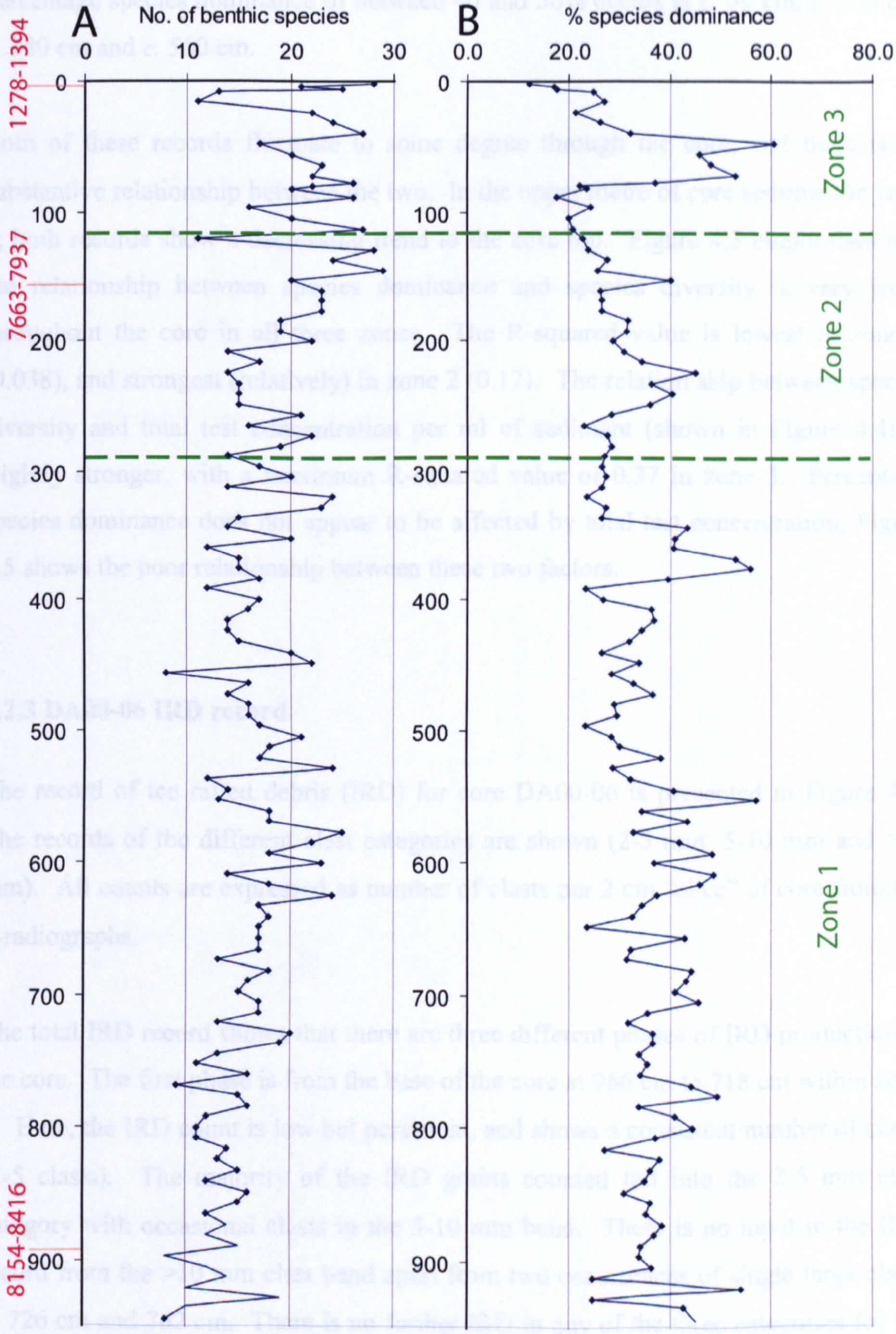

Figure 4.2: Benthic species diversity and species dominance for core DA00-06. A: Species diversity, B: % species dominance. Zones 1-3 (green dashed lines) are foraminiferal zone boundaries from Figure 4.1. Radiocarbon dates (in red) are given in cal yr BP.

Average species dominance is 34 %, and is relatively constant through the core. Peak percentage species dominance of between 40 and 50% occurs at *c.* 50 cm, *c.* 250 cm, *c.* 380 cm and *c.* 560 cm.

Both of these records fluctuate to some degree through the core, and there is no substantive relationship between the two. In the upper metre of core sediment in zone 3, both records show a decreasing trend to the core top. Figure 4.3 emphasises that the relationship between species dominance and species diversity is very weak throughout the core in all three zones. The R-squared value is lowest in zone 3 (0.038), and strongest (relatively) in zone 2 (0.17). The relation ship between species diversity and total test concentration per ml of sediment (shown in Figure 4.4) is slightly stronger, with a maximum R-squared value of 0.37 in zone 3. Percentage species dominance does not appear to be affected by total test concentration; Figure 4.5 shows the poor relationship between these two factors.

4.2.3 DA00-06 IRD record

The record of ice rafted debris (IRD) for core DA00-06 is presented in Figure 4.6. The records of the different clast categories are shown (2-5 mm, 5-10 mm and >10 mm). All counts are expressed as number of clasts per 2 cm "slice" of core from the x-radiographs.

The total IRD record shows that there are three different phases of IRD production in the core. The first phase is from the base of the core at 956 cm to 718 cm within zone 1. Here, the IRD count is low but persistent, and shows a consistent number of clasts (2-5 clasts). The majority of the IRD grains counted fall into the 2-5 mm clast category with occasional clasts in the 5-10 mm band. There is no input to the IRD record from the >10 mm clast band apart from two occurrences of single large clasts at 726 cm and 762 cm. There is no further IRD in any of the three categories for the rest of zone 1.

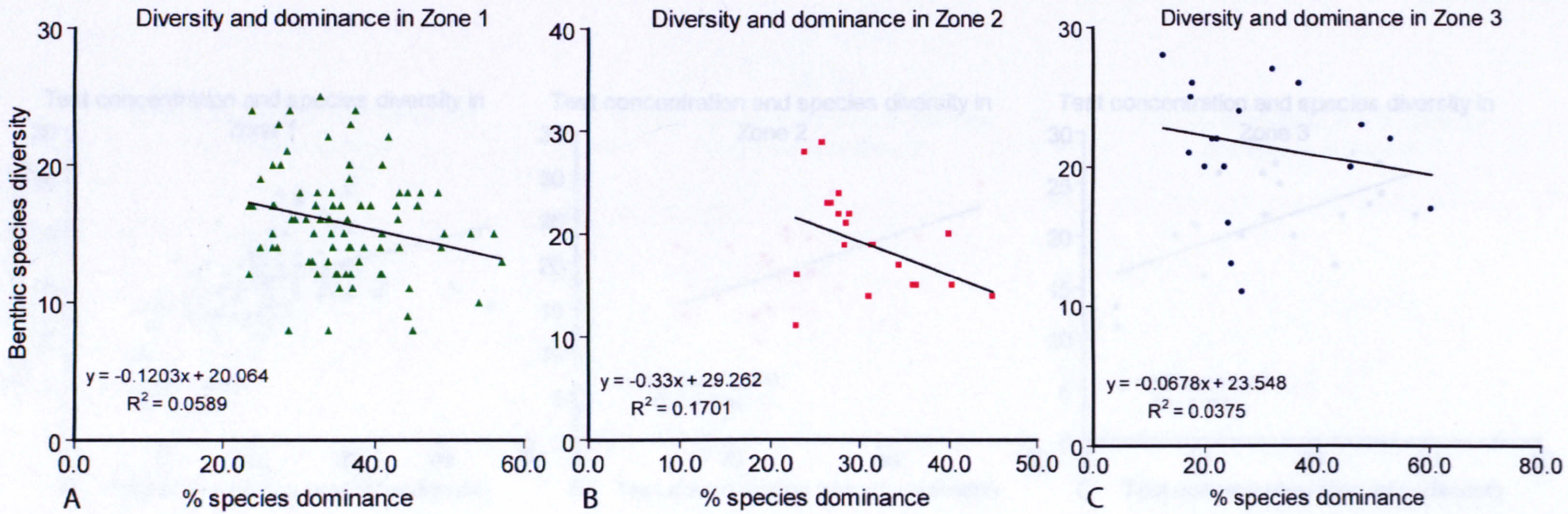

Figure 4.3: Plots of relationship between benthic species dominance and diversity in core DA00-06. A: dominance vs. diversity in zone 1. B: dominance vs. diversity in zone 2. C: dominance vs. diversity in zone 3. (Zones are based on foraminiferal assemblage zones shown in figure 4.1).

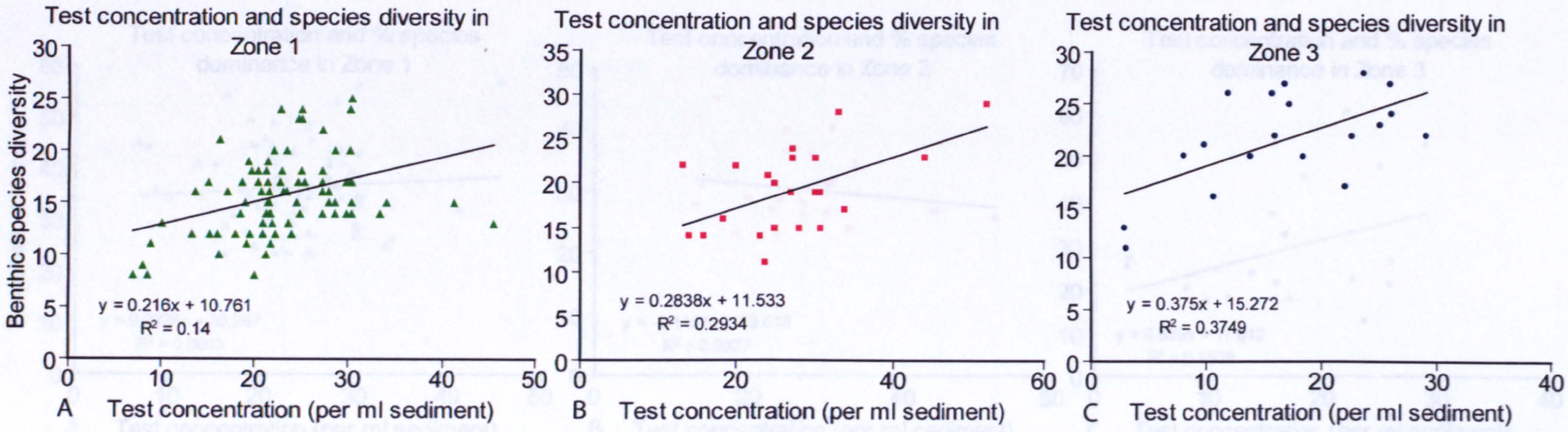

Figure 4.4: Plots of relationship between benthic test concentration and species diversity in core DA00-06. A: test concentration vs. diversity in zone 1. B: test concentration vs. diversity in zone 2. C: test concentration vs. diversity in zone 4. (Zones are based on foraminiferal assemblage zones shown in figure 4.1).

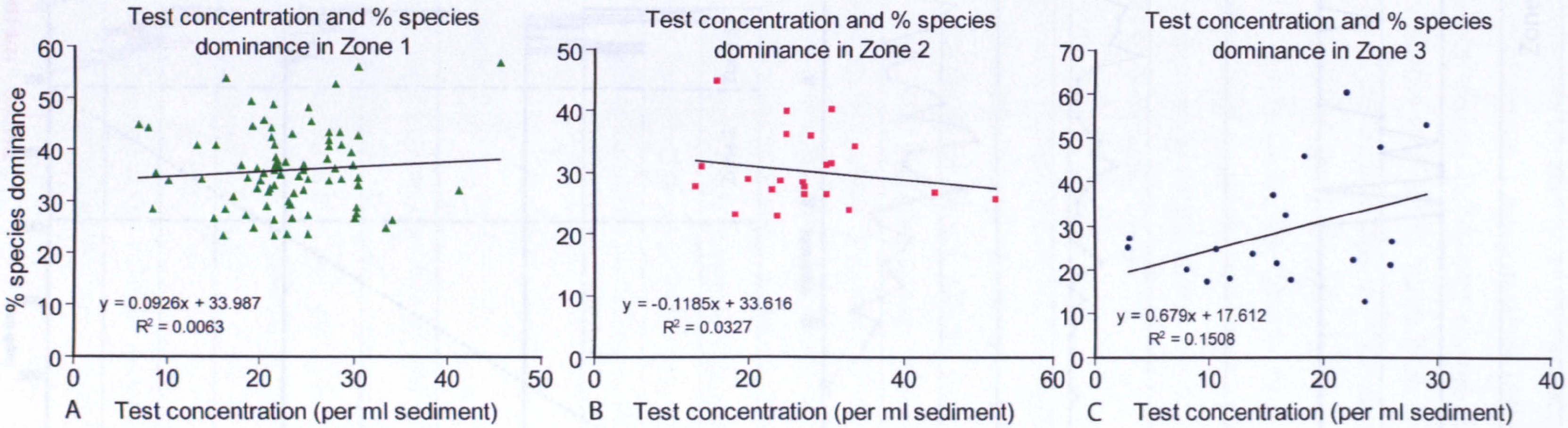

Figure 4.5: Plots of relationship between benthic test concentration and % species dominance in core DA00-06. A: test concentration vs. dominance in zone 1. B: test concentration vs. dominance in zone 2. C: test concentration vs. dominance in zone 3. (Zones are based on foraminiferal assemblage zones shown in figure 4.1).

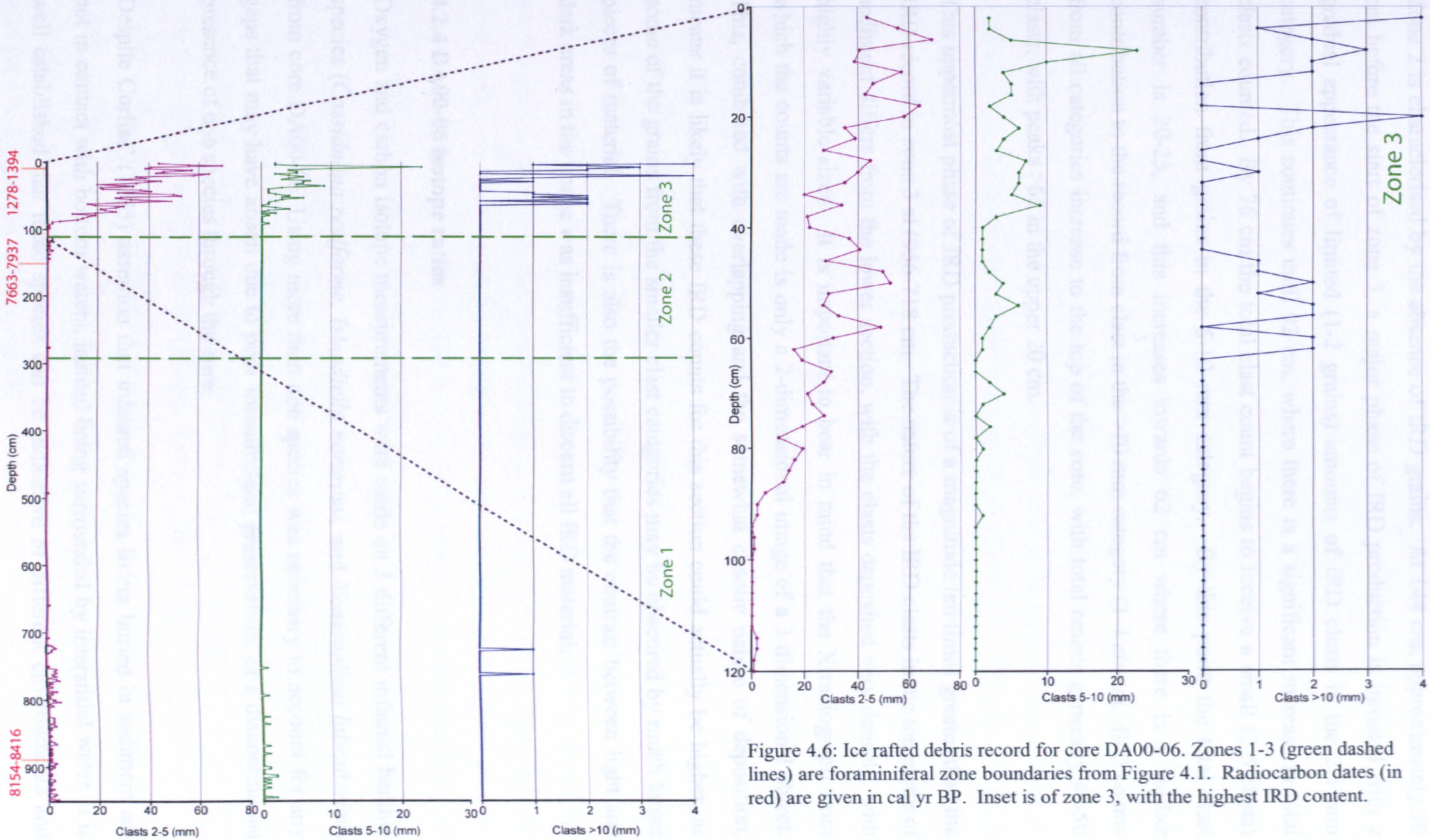

Figure 4.6: Ice rafted debris record for core DA00-06. Zones 1-3 (green dashed lines) are foraminiferal zone boundaries from Figure 4.1. Radiocarbon dates (in red) are given in cal yr BP. Inset is of zone 3, with the highest IRD content.

Zone 2 is characterised by the absence of IRD grains. At 144 cm, approximately 30 cm before the start of zone 3, a major phase of IRD production is initiated with a gradual appearance of limited (1-2 grains) amounts of IRD clasts in the 2-5 mm category. This continues until 92 cm, where there is a significant increase in total clasts counted. By 76 cm the total clast count begins to receive a small (2-5 clasts) contribution from grains in the 5-10 mm category. By this point the total clast number is 20-25, and this increases towards 62 cm where there is a further contribution to the record from clast in the >10 mm category (1-4 clasts). IRD counts from all categories increase to the top of the core, with total counts generally 40-50 clasts, with peaks >65 in the upper 20 cm.

This uppermost phase of IRD production is of a magnitude ten times greater than the IRD record in zone 3 at (956-718 cm. The nature of the IRD clasts in the top metre of sediment differs from the lower section, with the clasts deposited very densely, with highly variable sizes. It is important to bear in mind that the X-radiograph from which the counts are made is only a 2-dimensional image of a 3-dimensional object. This, combined with overlapping and the somewhat chaotic nature of deposition, means it is likely that these IRD counts for this section could actually be higher, as some of the grains from the smaller clast categories may be obscured by much larger pieces of material. There is also the possibility that the contrast between light and dark areas in the image was insufficient to discern all IRD material.

4.2.4 DA00-06 isotope ratios

Oxygen and carbon isotope measurements were made on 3 different infaunal benthic species (*Cassidulina reniforme, Islandiella norcrossi,* and *Nonionellina labradorica*) from core DA00-06. Using more than one species was necessary to account for any gaps that may have arisen due to poor foraminiferal preservation, or a discontinuous presence of one species through the core.

Despite Corliss' (1985) assertion that infaunal species living buried in sediment are not in contact with bottom waters, instead being surrounded by interstitial water, it is well established that these species can be indicative of different environments and

water mass conditions (e.g. Andrews *et al.*, 1993; Hald and Korsun, 1997; Osterman and Nelson, 1989; Schafer and Cole, 1982). There were no other epifaunal calcareous species present in sufficiently high quantities, and using three species will identify whether this holds true for these particular examples.

Using three species allows identification of offsets between species. The species generally used for isotopic measurements from benthic foraminifera is *Cibicides wullerstorfi,* but this tends to found only at much greater water depths. *Cibicides lobatulus* has also been used for surface sediment isotope measurements (Vilks and Deonarine, 1988), and another of the *Islandiella* species (*I. helenae*) has been used from a core on the northeastern Newfoundland Shelf (Scott *et al.*, 1984 in: Vilks and Deonarine, 1988) but neither of these species is present here. As far as possible, measurements were made on samples for which foraminiferal counts were also being made.

4.2.5 DA00-06 oxygen isotope record

The $\delta^{18}O$ isotope records of the 3 species are plotted in Figure 4.7. Zonation is based upon the foraminiferal assemblages zones described in section 4.2.1. Overall the three curves show similar trends. *I. norcrossi* represents the longest $\delta^{18}O$ record but has the poorest sample resolution in the lower part of the core. *C. reniforme* has the most continuous record in the lower half of the core, as it is present in most samples, but the record does not extend beyond 128 cm. *N. labradorica* has the poorest record of all 3 species in terms of sample resolution and sample coverage through the core.

Zone 1 A radiocarbon date from near to the base of the core at 891 cm gives a date of 8154-8416 cal yr BP for the start of zone 1. The *C. reniforme* record is the most shows the least scatter in this zone, and shows an overall increase in the $\delta^{18}O$ ratio with three progressively heavier sustained steps at 896-856 cm (3.12-3.18 ‰), 800-774 cm (3.38-3.37 ‰) and 736-680 cm (3:57-3.51 ‰), with a decline at 396 cm and a steady increase to a peak at the start of zone 2 at 290 cm. In the lower part of this zone,there are no data available for *N. labradorica* and data for *I. norcrossi* is poor, with gaps in the record and likely outliers.

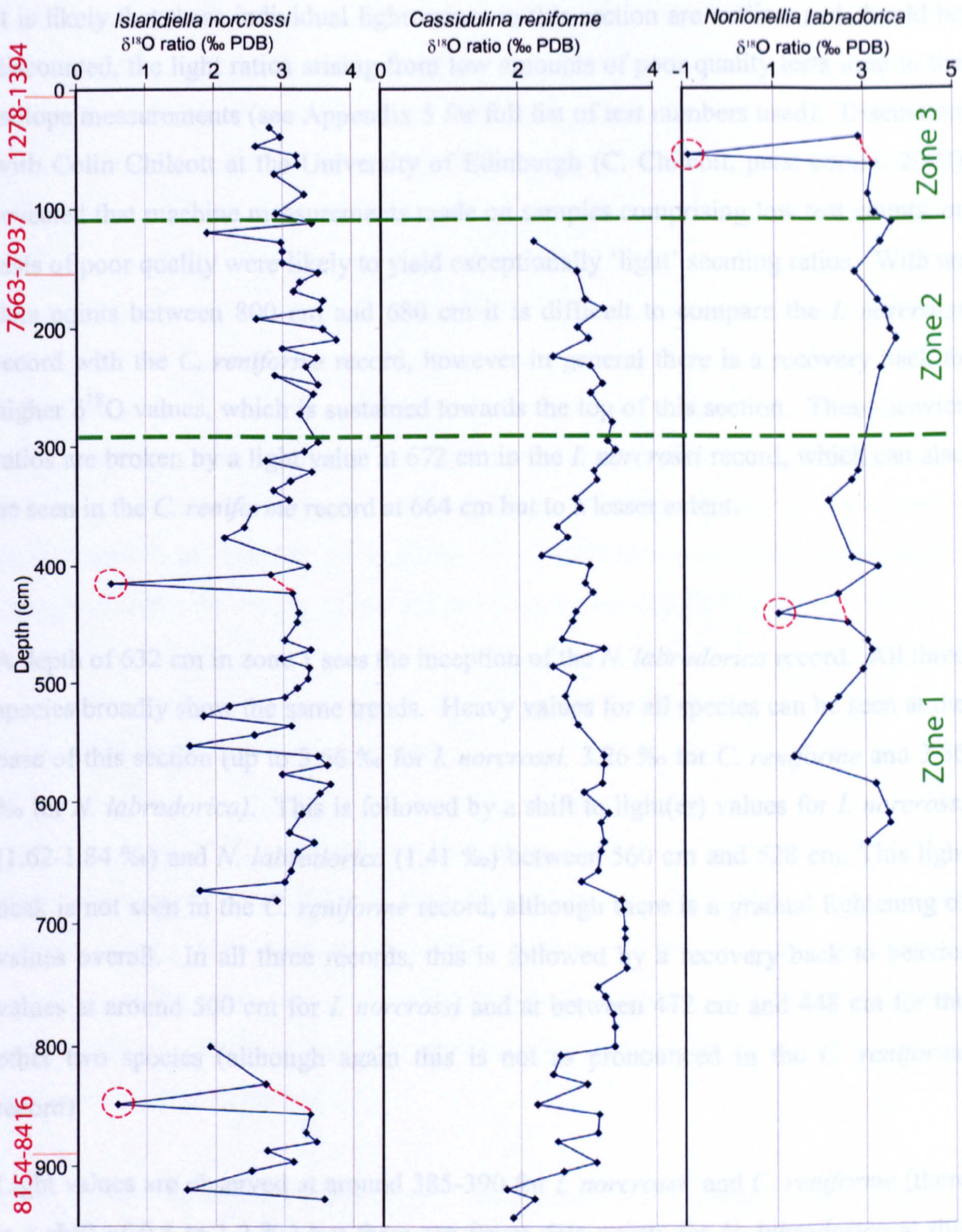

Figure 4.7: oxygen isotope ratios for DA00-06. 3 species used, *I. norcrossi, C.reniforme, N. labradorica*. Outliers are highlighted with a red dashed circle, and a red dashed line indicates interpolation between confident data points. Zonations are show in green and are based on foraminiferal data assemblages determined using cluster analysis. Radiocarbon dates are shown in red and are given in cal yr BP.

It is likely that these individual light values in this section are outliers and should be discounted, the light ratios arising from low amounts of poor quality tests used in the isotope measurements (see Appendix 5 for full list of test numbers used). Discussion with Colin Chilcott at the University of Edinburgh (C. Chilcott, pers. comm. 2002) revealed that machine measurements made on samples comprising low test counts, or tests of poor quality were likely to yield exceptionally 'light' seeming ratios. With no data points between 800 cm and 680 cm it is difficult to compare the *I. norcrossi* record with the *C. reniforme* record, however in general there is a recovery back to higher $\delta^{18}O$ values, which is sustained towards the top of this section. These heavier ratios are broken by a light value at 672 cm in the *I. norcrossi* record, which can also be seen in the *C. reniforme* record at 664 cm but to a lesser extent.

A depth of 632 cm in zone 1 sees the inception of the *N. labradorica* record. All three species broadly show the same trends. Heavy values for all species can be seen at the base of this section (up to 3.66 ‰ for *I. norcrossi*, 3.26 ‰ for *C. reniforme* and 3.56 ‰ for *N. labradorica)*. This is followed by a shift to light(er) values for *I. norcrossi* (1.62-1.84 ‰) and *N. labradorica* (1.41 ‰) between 560 cm and 528 cm. This light peak is not seen in the *C. reniforme* record, although there is a gradual lightening of values overall. In all three records, this is followed by a recovery back to heavier values at around 500 cm for *I. norcrossi* and at between 472 cm and 448 cm for the other two species (although again this is not as pronounced in the *C. reniforme* record).

Light values are observed at around 385-390 for *I. norcrossi* and *C. reniforme* (there is a shift of 0.5 to 1.2 ‰) but there are fewer data points for *N. labradorica* at this stage in the zone, and the data are more scattered. Following these lighter values, the records are characterised by an increase to a peak in $\delta^{18}O$ values; from approximately 370 cm oxygen isotope values for all three species steadily increase to a heavy peak at the top of zone 1 and the start of zone 2 at 290 cm. This peak has the heaviest ratios for *I. norcrossi* and *N. labradorica* at 3.57 ‰ for both, however it is not the highest peak for *C. reniforme* (2.90-3.29 ‰).

Zone 2 At the start of zone 2, following these heavier values, the record of all three species becomes lighter until around 150 cm, when the record for *C. reniforme* ends.

I. norcrossi and *N. labradorica* then show a stabilisation of $\delta^{18}O$ values back to between 2.61 and 3.21 ‰ for *I. norcrossi* and 2.89-3.20 ‰ for *N. labradorica.* A radiocarbon date near to this points at 157 cm gives a date for the end of the *C. reniforme* record and stabilisation of the other two species of around 7663-7937 cal yr BP.

Zone 3 There is no record for *C. reniforme* in this zone, and poor temporal coverage of data for *N. labradorica.* It is likely that the very light isotope value for *N. labradorica* at 56 cm is an outlier due to the very low test count the measurements were based upon (see Appendix 5), which as mentioned previously tends to show in the data as an excessively 'light' value. *I. norcrossi* and *N. labradorica* reach the end of their records at 32 and 40 cm respectively. A radiocarbon date from the top of this core gives a date for the end of this section at approximately 1278-1394 cal yr BP.

4.2.6 DA00-06 carbon isotope record

Carbon isotope ($\delta^{13}C$) measurements were made at the same time as the $\delta^{18}O$ ratios. The carbon isotope records for all three species are show in Figure 4.8. The carbon isotope records have been divided into the same zones using the foraminiferal zonations in the same way as the oxygen isotope records. All three records show similar trends, with the overall pattern being increasingly heavy $\delta^{13}C$ ratios from the bottom of the core to the top.

Zone 1 From 944 to 632 cm in zone 1, there is only a $\delta^{13}C$ record from *I. norcrossi* and *C. reniforme.* Both species start at the base of this section with values between –1.53 ‰ and 1.72 ‰. A radiocarbon date from near to the base of the section approximates a date of 8154-8416 cal yr BP. Values for *C. reniforme* decrease between 920 cm and 824 cm to ratios around –2.5 ‰. *I. norcrossi* only shows a brief excursion to these lighter values at 920cm then continues up the section until 848 cm with ratios around -1.6 ‰. This is followed by a decrease in $d^{13}C$ ratios to –2.5 ‰ at 800 cm. There is poor sample resolution for *I. norcrossi* record from here but the general trend is for increasingly heavier values between –1.25 ‰ and 1.65 ‰. The *C.*

reniforme record also shows recovery after around 800 cm to heavier ratios between –1.7 ‰ and –1.4 ‰

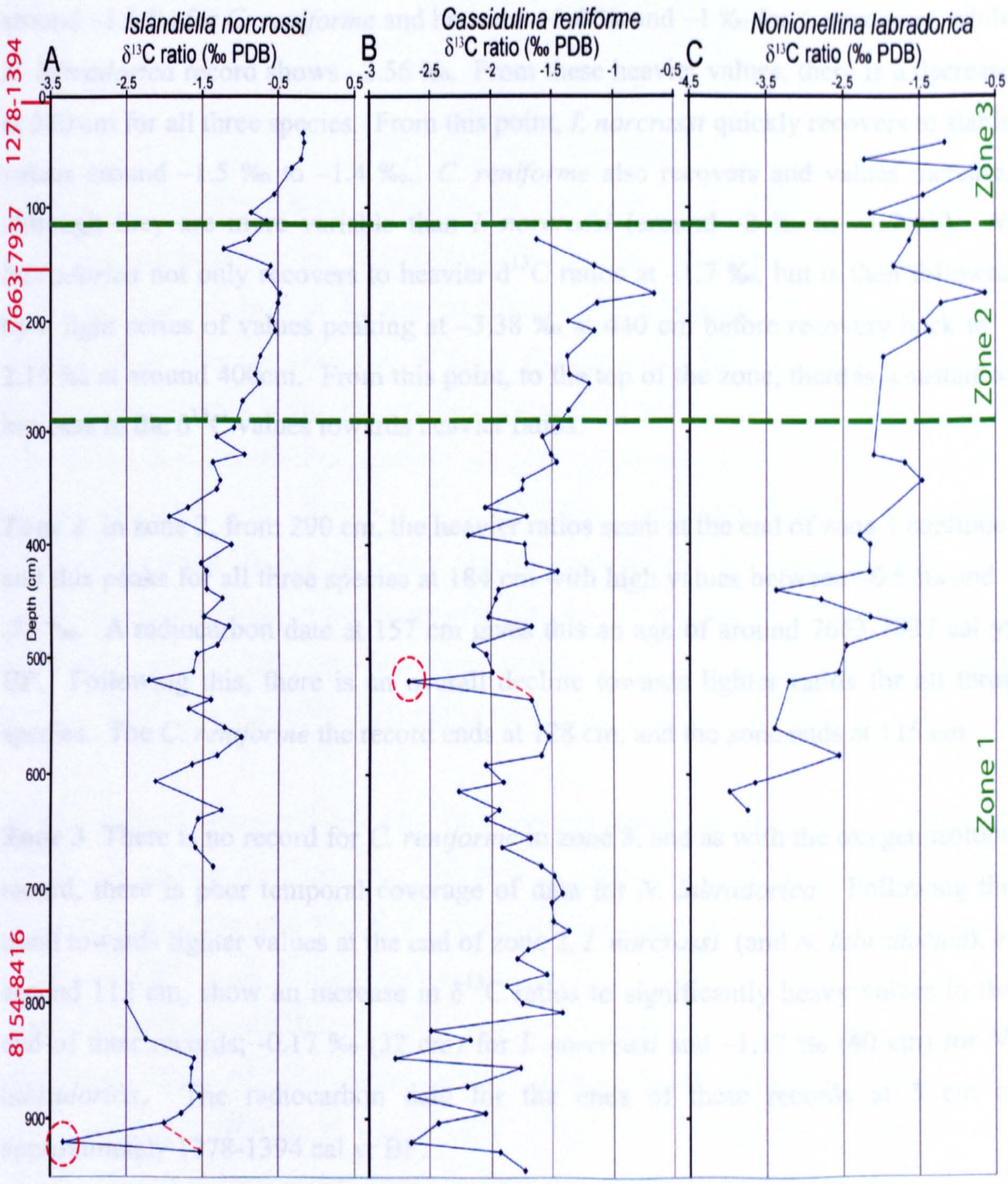

Figure 4.8: Carbon isotope ratios DA00-06. 3 species used, *I. norcrossi, C.reniforme, N. labradorica.* Outliers are highlighted with a red dashed circle, and a red dashed line indicates interpolation between confident data points. Zonations are show in green and are based on foraminiferal data assemblages determined using cluster analysis. Radiocarbon dates are shown in red and are given in cal yr BP.

From 632 cm to the top of the zone at 290 cm, there is a carbon isotope record for all three species. There are 4 features characteristic of this part of the zone, and all three

species show the first 3 trends in a similar fashion. At 632 cm, there is a light excursion with values for *C. reniforme* and *I. norcrossi* around –2 ‰ and *N. labradorica values* as low as –3.92 ‰. Following this, there is a move towards heavier values, resulting in a peak between 592 cm and 560 cm. Ratios here are around –1.5 ‰ for *C. reniforme* and between –1.6 ‰ and –1 ‰ for *I. norcrossi*, while *N. labradorica* record shows –2.56 ‰. From these heavier values, there is a decrease at 520 cm for all three species. From this point, *I. norcrossi* quickly recovers to stable values around –1.5 ‰ to –1.4 ‰. *C. reniforme* also recovers and values increase, although they are more variable than *I. norcrossi* (around –2 ‰ to –1.7 ‰). *N. labradorica* not only recovers to heavier $d^{13}C$ ratios at –1.7 ‰, but is then followed by a light series of values peaking at –3.38 ‰ at 440 cm before recovery back to –2.15 ‰ at around 400cm. From this point, to the top of the zone, there is a sustained increase in the $\delta^{13}C$ values towards heavier ratios.

Zone 2 In zone 2, from 290 cm, the heavier ratios seem at the end of zone 1 continue, and this peaks for all three species at 184 cm with high values between –0.5 ‰ and -.75 ‰. A radiocarbon date at 157 cm gives this an age of around 7663-7937 cal yr BP. Following this, there is an overall decline towards lighter ratios for all three species. The *C. reniforme* the record ends at 128 cm, and the zone ends at 115 cm.

Zone 3 There is no record for *C. reniforme* in zone 3, and as with the oxygen isotope record, there is poor temporal coverage of data for *N. labradorica*. Following the trend towards lighter values at the end of zone 2, *I. norcrossi* (and *N. labradorica*), at around 112 cm, show an increase in $\delta^{13}C$ ratios to significantly heavy values to the end of their records; -0.17 ‰ (32 cm) for *I. norcrossi* and –1.17 ‰ (40 cm) for *N. labradorica*. The radiocarbon date for the ends of these records at 5 cm is approximately 1278-1394 cal yr BP.

4.3.1 DA00-05 foraminiferal analysis

Based on stratigraphically constrained cluster analysis, core DA00-05 can be split into two main zones. Zone 1 extends to 545 cm from the base of the core at 1030 cm, and is separated into 3 sub-zones. This again is based on stratigraphically constrained

cluster analysis. It is characterised by the presence of calcareous species. Zone 2 is characterised by the absence of calcareous foraminifera and extends from this near mid-core point at 545 cm to the core top and is further divided into 4 sub-zones. The foraminiferal data and zonation are shown in Figure 4.9.

Zone 1

Zone 1a (1030-965 cm) is dominated by the calcareous species *Islandiella norcrossi,* and to a much lesser extent, by *S. feylingi. I. norcrossi* increases in abundance from values of 5% at the base of the zone to values >60% at the top. *S. feylingi* values at the base of the zone are more than 20%, but this reduces to less than 5% very quickly. *E. excavatum* species is also present but in quantities of less than 10%. *Nonionellina labradorica* and *Stainforthia. concava* are also consistently present in this zone, but only represent between 5 and 10% of benthic taxa. Agglutinated species account for <20% of the assemblage in this zone, and the value is typically nearer to 10%. Two species, *Cribostomoides crassimargo* and *Reophax arctica* are the most common. A radiocarbon date (AAR-6836) from near the base of the core at 1017 cm gives a date of 6253±73 ^{14}C yrs BP (6378-7035 cal yr BP) for the onset of this zone.

Zone 1b (965-655 cm) is defined by an increase in species diversity, mainly due to an increase in agglutinated species. The zone is dominated by *I. norcrossi* (20-40%) reaching peak values of 60%. *E. excavatum* is also common (10-20%). Agglutinated species diversification is high, with the dominant taxa being *C. crassimargo* and *R. gracilis* (both generally 10-20%). *Saccammina diflugiformis* is intermittently present, but reaches values of 20%. Other calcareous taxa that are consistently present with values of around 10% are *B. tenerrima, C. reniforme, G. inequalis, N. labradorica, and S. feylingi.* Test linings increase from the previous sub-zone with counts of between 20 and 40. No radiocarbon date is available for the top of this zone but a mid-zone date at 812 cm (AAR-6840) gives an age of 4926±80 ^{14}C yrs BP (5558-5883 cal yr BP.)

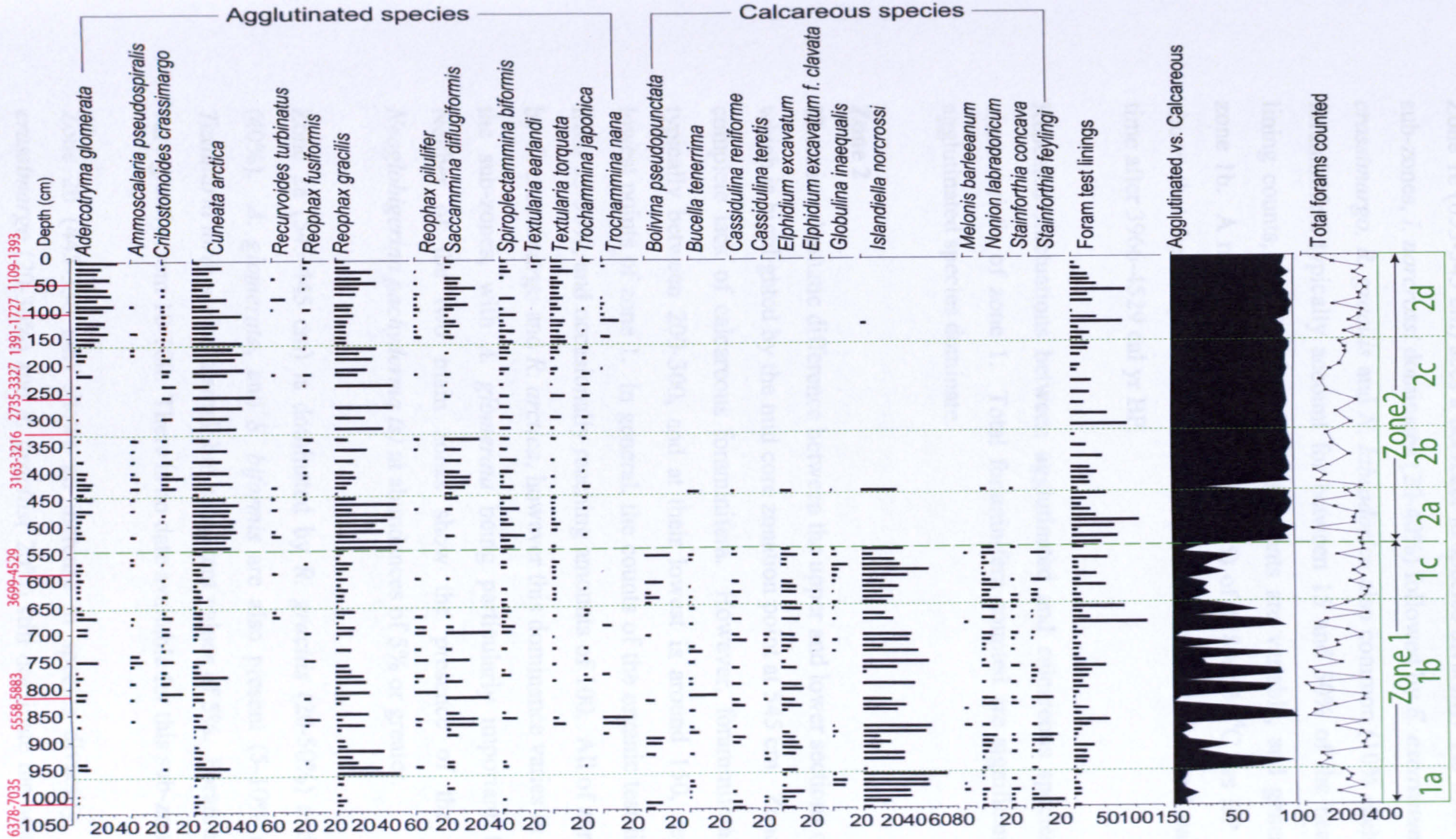

Figure 4.9: Foraminiferal assemblage data from DA00-05, only species >5% shown. Zone boundaries marked in green based on stratigraphically constrained cluster analysis. Radiocarbon dates shown in red, given in cal yr BP.

Zone 1c (655-545 cm) sees a decrease in species diversity. As with the previous two sub-zones, *I. norcrossi* dominates (20-40%) followed by *E. excavatum* (20%). with *C. crassimargo, R. gracilis* and *N. labradorica* also common (10% each). Agglutinated foraminifera typically account for between 15 and 50% of the benthic taxa. Test lining counts, and foraminiferal test counts are variable, and generally lower than zone 1b. A radiocarbon date (AAR-6835) of 4189±53 ^{14}C yrs BP within this zone shows that the abrupt end of this sub-zone, and the end of zone 1 can be dated some time after 3966-4529 cal yr BP.

Repeated fluctuations between agglutinated and calcareous species are a defining characteristic of zone 1. Total foraminifera counted are significantly lower where agglutinated species dominate.

Zone 2

There is a dramatic difference between the upper and lower sections of core DA00-05, which is highlighted by the mid core zonation point at 545 cm. Zone 2 has an almost complete lack of calcareous foraminifera. However, foraminiferal test counts are typically between 200-300, and at their lowest is around 150, never reaching the lowest points of zone 1. In general, the counts of the organic test linings are higher, from 25-50%, and occasionally reaching amounts of 100. All of zone 2 is dominated by *C. crassimargo* and *R. arctica*, however this dominance varies in intensity through the sub-zones, with *A. glomerata* being particularly important towards the top. Neither of the two main zones show the presence of the planktic species *Neoglobigerina pachyderma (s)* at abundances of 5% or greater.

Zone 2a (545-445 cm) is dominated by *R. gracilis* (20-50%) and *C. crassimargo* (40%). *A. glomerata*, and *S. biformis* are also present (5-10% each) along with *Textularia torquata* with small but consistent values of 5%. Foraminiferal test linings vary greatly from 10-100. There is no date available for this sub-zone.

Zone 2b (445-330 cm) shows an increase in species diversity, and although *C. crassimargo* (20-30%) and *R. gracilis*(20%) still dominate the assemblage, they are joined by *S. diflugiformis* (15-20%). *A. glomerata* decreases through this sub-zone

from 10% to 5%. There is no radiocarbon date for the onset of this sub-zone, but the top of it can be accurately dated at 327 cm (AAr-6838) to 3155±120 ^{14}C yrs BP (3163-3716) cal yr BP.

Zone 2c (330-165 cm) is characterised by a return to the co-dominance of *C. crassimargo* (20-40%) and *R. gracilis* (20-50%). The base of this zone is accurately dated to 3163-3716 cal yr BP, and although no date is available for the top of this zone, a date from the 262 cm (AAR-7511-b) gives a date of 3200±60 ^{14}C yrs BP (2735-3327 cal yr BP).

Zone 2d (165-0 cm) is dominated by three species. *C. crassimargo* (10-40%), *A. glomerata* and *R. gracilis* (both 10-30%). *S. biformis* values again lie in the 5-10% bracket, but *C. arctica* values have fallen to <5%. *S. diflugiformis* and *T. torquata* increase in abundance too with values between 5 and 20%. There is a radiocarbon data (AAR-7510-a) at 1.06 cm of 2004±36 ^{14}C yrs BP (1391-1727 cal yr BP). The top of this sub-zone and zone 2 as a whole can be dated at 5 cm (AAR-7509) to 1705±38 ^{14}C yrs BP (1109-1393 cal yr BP).

4.3.2 DA00-05 Species diversity

Species diversity and species dominance are plotted with depth in Figure 4.10. Agglutinated species diversity in DA00-05 is relatively constant throughout the length of the core. From 1030 cm at the base, agglutinated diversity values are 5-10 species per sample. This stable pattern is maintained until 695 cm where there is an increase to 10-15 species per sample. This trend lasts until the core top is reached.

There is a significant difference in the calcareous species diversity record. From the base of the core, species diversity values vary from 2 to around 15 per sample. There are samples with no calcareous species, as well as samples with species diversity as high as 17. This lasts until 545 cm where there is a dramatic and sudden drop in species diversity. Apart from sample 440 cm, calcareous species diversity is 0-2 species for the rest of the core. As the agglutinated species do not display this unusual trend, plots of the agglutinated and calcareous species are shown in Figure 4.11 to

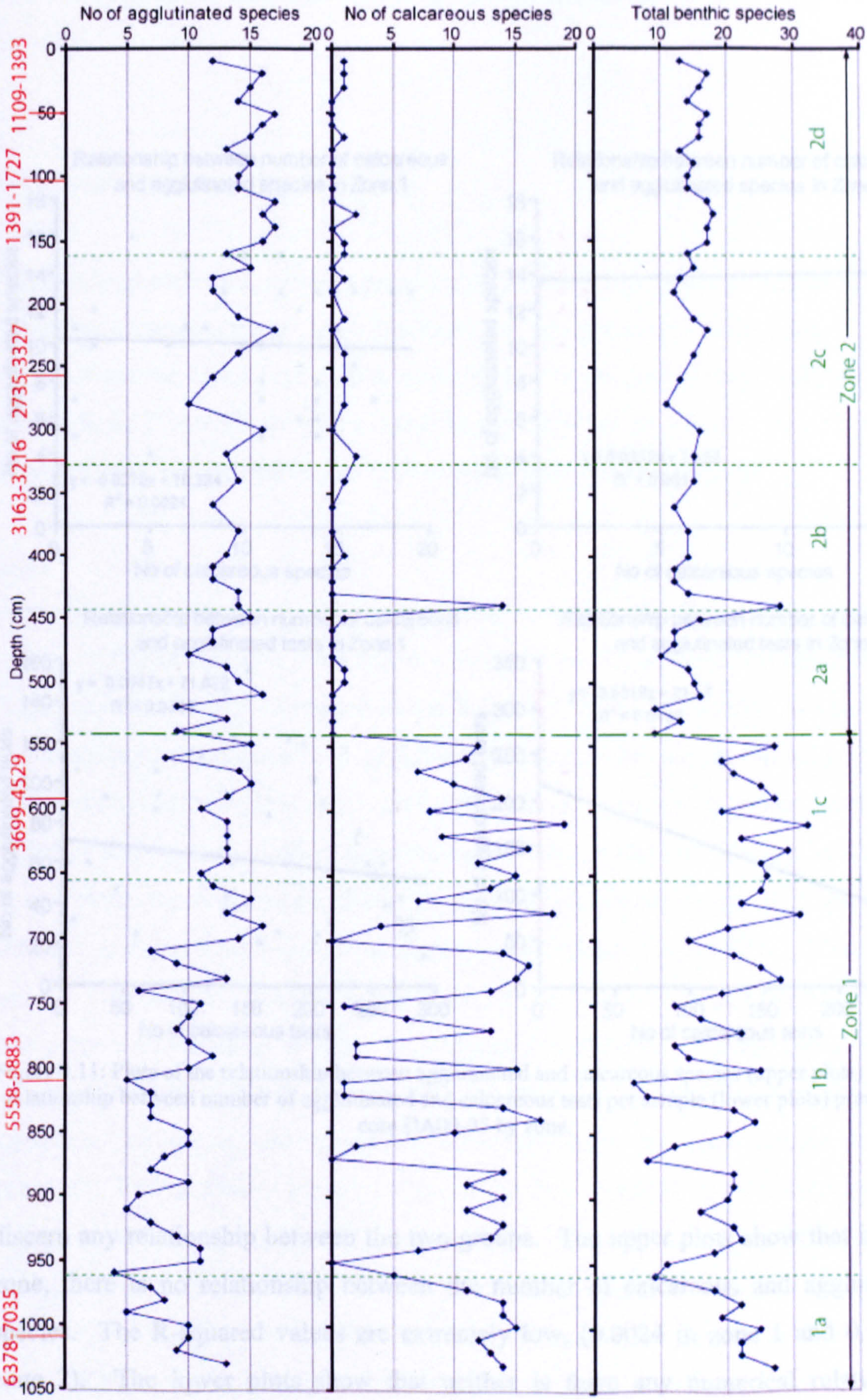

Figure 4.10: Benthic species diversity in core DA00-05. Number of agglutinated species are plotted first, then calcareous species. Total species are plotted on the far right. Zones 1-3 (green dashed lines) are foraminiferal zone boundaries based on the foraminiferal cluster analysis. Radiocarbon dates (in red) are given in cal yr BP.

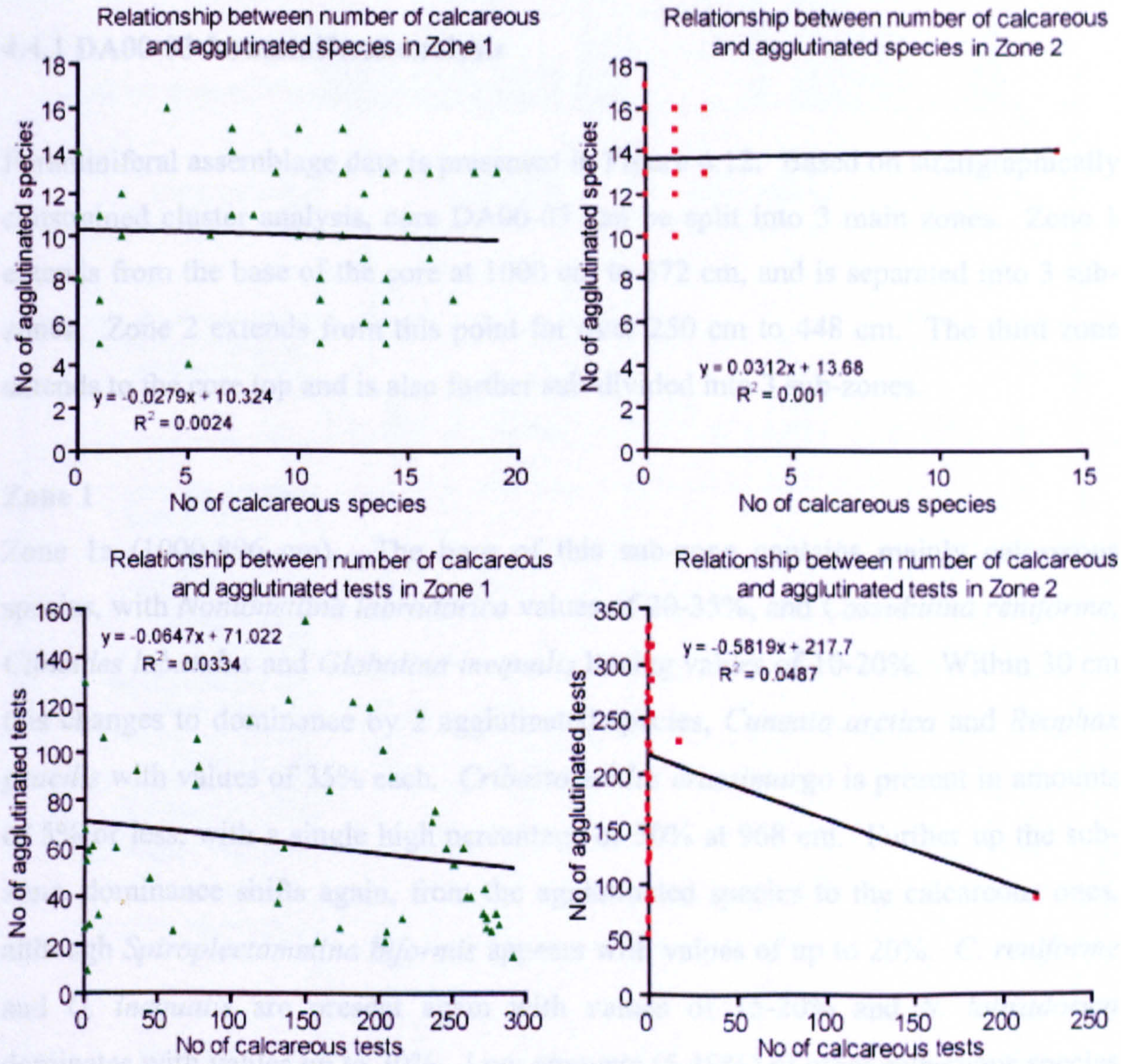

Figure 4.11: Plots of the relationship between agglutinated and calcareous species (upper plots) and the relationship between number of agglutinated and calcareous tests per sample (lower plots) present in core DA00-05 by zone.

discern any relationship between the two groups. The upper plots show that in each zone, there is no relationship between the number of calcareous and agglutinated species. The R-squared values are extremely low, (0.0024 in zone 1 and 0.001 in zone 2). The lower plots show that neither is there any numerical relationship between the number of calcareous and agglutinated tests in either of the zones. This suggests that there is an external factor controlling the presence and distribution of the calcareous species. This may point to an issue of dissolution, and will be discussed in further in Chapter 5.

It can be highlighted here that there is no isotope data available for core DA00-05 to present.

4.4.1 DA00-03 foraminiferal analysis

Foraminiferal assemblage data is presented in Figure 4.12. Based on stratigraphically constrained cluster analysis, core DA00-03 can be split into 3 main zones. Zone 1 extends from the base of the core at 1000 cm to 672 cm, and is separated into 3 sub-zones. Zone 2 extends from this point for over 250 cm to 448 cm. The third zone extends to the core top and is also further sub-divided into 3 sub-zones.

Zone 1

Zone 1a (1000-896 cm). The base of this sub-zone contains mainly calcareous species, with *Nonionellina labradorica* values of 20-35%, and *Cassidulina reniforme, Cibicides lobatulus* and *Globulina inequalis* having values of 10-20%. Within 30 cm this changes to dominance by 2 agglutinated species, *Cuneata arctica* and *Reophax gracilis* with values of 35% each. *Cribostomoides crassimargo* is present in amounts of 5% or less, with a single high percentage of 30% at 968 cm. Further up the sub-zone, dominance shifts again, from the agglutinated species to the calcareous ones, although *Spiroplectammina biformis* appears with values of up to 20%. *C. reniforme* and *G. inequalis* are present again with values of 15-20% and *N. labradorica* dominates with values up to 30%. Low amounts (5-10%) of other calcareous species are also present at the top of this sub-zone, the most notable of which are *C. lobatulus, Elphidium excavatum* and *Islandiella norcrossi,* with the other species showing extremely low amounts (<5%). Counts of foraminiferal test linings are low throughout this sub-zone, usually less than 20. A radiocarbon date (AA-44949) taken from the core catcher sample below the core base at approximately 1020 cm gives a date of 3351±44 ^{14}C yrs BP (3075-3327) cal yr BP, and a date from near the core base (AAR-6834) at 982 cm using an articulated bivalve yields a date of 3245±49 ^{14}C yrs BP (2948-3218 cal yr BP). There is no date available for the top of this sub-zone.

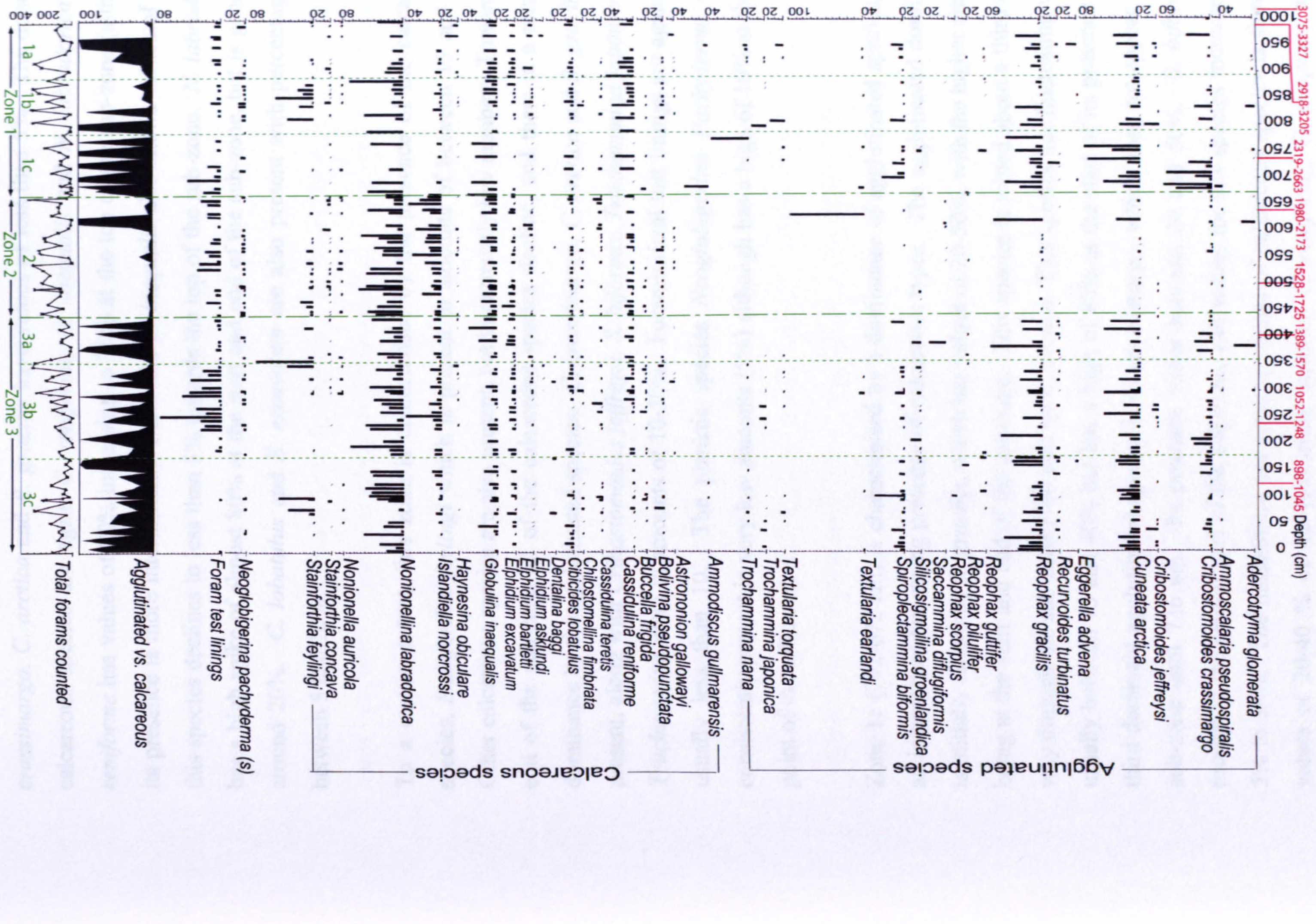

Figure 4.12: Foraminiferal assemblage data from DA00-03, only species >5% shown. Zone boundaries marked in green based on stratigraphically constrained cluster analysis. Radiocarbon dates shown in red, given in cal yr BP.

Zone 1b (896-792 cm) shows a similar pattern to the start of zone 1a with an initially poor presence of agglutinated species, and a dominance of 4 calcareous species. *C. crassimargo, C. arctica* and *R. gracilis* have values of less than 5%. The dominant calcareous species are again *C. reniforme, G. inequalis* and *N. labradorica. C. reniforme* has values of 20% increasing to 35% at the top of the sub-zone (although its presence is more intermittent), and while *G. inequalis* also shows values of 20%, this species declines to less than 5% towards the top of the sub-zone. *N. labradorica* has a high spike of almost 80% at the start and end of the sub-zone, but is generally around 20%. *C. lobatulus* and *E. excavatum* are also present with percentages of between 5 and 10%.

To a certain extent, this zone is characterised by the presence of the calcareous species, *Stainforthia feylingi* which is present in amounts of between 15 and 50%. Other calcareous species are also present, but in extremely low numbers. Towards the end of the sub-zone all of the calcareous species decline, and there is a return to dominance by the agglutinated species. *C. crassimargo, C. arctica* and *R. gracilis* are present, along with *Cribostomoides jeffreysi, S. biformis, Trochammina japonica,* and *Trochammina nana* in amounts of 10-20%. Foraminiferal test linings are again low, usually less than 10. The planktic species *Neoglobigerina Pachyderma (s)* is consistently present in very low amounts (5%) although has a high of 10% at the mid point of the sub-zone.

Zone 1c (792-672 cm) is characterised by a dominance of agglutinated species, with an intermittent but strong presence of calcareous types. The agglutinated dominance is initially shown by *R. gracilis*, which has values of 20-50%, with the higher amounts being at the start and end of the sub-zone. This species is joined about a third of the way through the sub-zone (760 cm) by *C. arctica.* This species has fluctuating values usually between 15 and 40% but has a high of 80% at the start of its presence. The third dominant agglutinated species is *C. crassimargo*, which does not appear in the sub-zone until 736 cm. Its presence varies between 20 and 50%. *S. biformis* is present in the central part of the sub-zone, and values for this species increase from 5% to 30%. The intermittent yet strong presence of calcareous species is shown by values of 20-40 % of the previously common *C. reniforme, G. inequalis* and *N. labradorica.* These are accompanied by a minor (5-10%) presence of *C. lobatulus*

and *I. norcrossi*. Foraminiferal test lining counts are low at the start of this sub-zone, but increase towards the top and are usually between 10 and 20, although there is one high point of over 40 counts. Foraminiferal counts are inconsistent and low in this zone (10-200), which accounts for the occasional, usually high, values of species such as *T. japonica* and *T. nana*. There is a radiocarbon date (AAR-6833) taken from a bivalve shell at 738 cm (around 50 cm from the base of the sub-zone), which gives a date of 2738±50 ^{14}C yrs BP (2319-2663 cal yr BP).

Zone 2

Zone 2 (672-448 cm) sees a dramatic change in the foraminiferal assemblage. Apart from an "outlier" sample at 608 cm where the count is exceptionally low, this zone is almost completely represented by calcareous species. *N. labradorica* is the dominant foraminifer, with values between 30 and 50%. *I. norcrossi* is the next most dominant, with generally consistent values of 20-25%, although it can be as high as 40%. *C. reniforme* and *G. inequalis* are present with values of 15-20%, and there is also a small but consistent presence of *E. excavatum* at 5-10%. From the mid-point of this zone (575 cm), *S. feylingi* is present in the assemblage in amounts of 10-20%. Other calcareous species contribute in minor amounts (5% or less) in this section of the core. These are *Bolivina pseudopunctata, C. lobatulus, Elphidium bartletti, Nonionella auricola* and *Stainforthia concava*. Foraminiferal test lining counts vary between 10 and 30 in this zone, and the planktic species *N. pachyderma (s)* has consistent low values of les than 5%. A radiocarbon date (CAMS-82824) based upon an intact gastropod shell is available from near the base of this zone at 642 cm. This gives a date of 2445±40 ^{14}C yrs BP (1980-2173 cal yr BP). There is a further date (CAMS-86752) from within this zone at 500 cm, which was made on a sample of mixed benthic foraminifera. This point is dated at 20665±40 ^{14}C yrs BP (1528-1735 cal yr BP).

Zone 3

Zone 3a (448-360 cm) is a relatively short sub-zone and sees a return to the mixed dominance between agglutinated and calcareous species. No new species have become part of the dominant assemblage. *C. arctica* is dominant at the start of the sub-zone with percentages of 40%, but this declines to 15% by the top. *R. gracilis* displays values of 10-25%, with a peak of 60% towards the end of the zone although

at this point the foraminiferal counts are very low. *C. crassimargo* is present with values of 25%, although it does not become established until halfway through the sub-zone at 408 cm. The calcareous species present in this section of the core are the ones that have been generally dominant throughout. *N. labradorica* is the most consistently abundant with values of 15-30%. *G. inequalis* fluctuates with percentages of 5-40%, and *C. reniforme* and *E. excavatum* have lower values of around 10%. Other calcareous species are not present in any significant amounts in this sub-zone. Foraminiferal test linings are relatively low, generally less than 15. The presence of *N. pachyderma (s)* is no longer significant in this sub-zone. A radiocarbon date (CAMS-91935) near to the bottom of the core at 404 cm based on an articulated bivalve yields a date of 1940±40 ^{14}C yrs BP (1389-1570 cal yr BP).

Zone 3b (360 cm-184 cm) sees a dominance of the assemblage by *N. labradorica* with values between 20 and 40%. The calcareous presence is evident through the presence of 2 main species; *C. arctica* and *R. gracilis* show values of 10-25%, although this does reach as high as 45% occasionally. *C. crassimargo* increases through the sub-zone from values of <5% at the bottom to 20% at the top. There are infrequent occurrences of agglutinated species where the test counts are low. For example, *Adercotryma glomerata, Saccammina diflugiformis, Silicosigmoilina groenlandica* and *S. biformis* all have singular or occasional occurrences of up to 20% in this section of the core. At the base of the sub-zone, *S. feylingi* has an unusually high presence with its highest values of the core (up to 80%) but this is short-lived, and is immediately absent for the rest of the sub-zone. *C. reniforme, Cassidulina teretis, C. lobatulus,* and *E. excavatum* are again present, but still in very minor amounts of around 5%. The planktic species *N. pachyderma (s)* is not present in significant amounts (<5%). A defining characteristic of this section of the core is the foraminiferal test lining count. This sub-zone has the highest test lining count at 20-50 with a high of 80. There are no radiocarbon dates near the top or bottom of this part of the core, but a date (AAR-7508) is available at 239 cm. Based upon a bivalve shell, this central part of the sub-zone yields a date of 1594±42 ^{14}C yrs BP (1052-1248 cal yr BP).

Zone 3c (184 cm-0 cm) has a similar species assemblage, but different dominances. As before, *N. labradorica* shows the greatest presence with percentage values of

between 20 and 50%. *C. arctica* and *R. gracilis* have high values of 35 and 40% respectively at the base of the sub-zone, but amounts decline to less than half of these in the middle part of the zone before recovery back to initial values towards the top of the core. Values for the species *C. crassimargo* are lower in this sub-zone. Amounts of 15-20% are evident at the bottom of the zone, but tests become sparse and intermittent on moving up through the sub-zone, with values only reaching a maximum of 5-10%. *G. inequalis* and *I. norcrossi* arre present here with values around 10%. *C. lobatulus* has a minor presence which reaches amounts of 10% in the top part of the sub-zone. In the middle part of the sub-zone there is a brief but significant occurrence of *S. feylingi* (percentages up to 50%). This is accompanied by very minor (around 5%) presence of other calcareous species such as *B. pseudopunctata, Buccella frigida, C. reniforme* and *C. teretis.* There is a notable absence of organic foraminiferal test linings, and the occurrences of *N. pachyderma (s)* have become less frequent and with poorer amounts. A radiocarbon date (CAMS-91944) made on a bivalve is available within this sub-zone at 128 cm, and gives a date of 1415±40 ^{14}C yrs BP (898-1047 cal yr BP).

4.4.2 DA00-03 species diversity

Species variations fluctuate considerably through this core. The numbers of benthic species per sample depth and % species dominance per sample are presented in figure 4.13. In zone 1, the number of benthic species shows an overall decline from between 15-20 per sample to between 2 and 5 per sample, although there are some excursions to over 15 in the top part of the zone. In zone 2, the number of species recovers to between 7 and 15. Zone 3 shows a high degree of scatter with no discernable trends; species numbers vary from 5 to over 15.

% species dominance in the core is also considerably varied. In general in zone 1 the dominance is between 20 and 30%, with excursions to over 60% in the latter part of the core. In zone 2 these amount become slightly more varied with dominance ranging between 20 and 40%, but only 2 distinct excursions to values over 60%. In zone 3 this trend of zone 2 continues, until the inception of zone 3c (at 184 cm) where the % species dominance become less 'widely' fluctuating between sample depths.

There is a considerable and sustained decline from around 100 cm to 50, with dominance dropping from approximately 50% down to below 20%.

The relationships between benthic species diversity, % species dominance and test concentration in the sample sediments are presented in figures 4.14, 4.15 and 4.16. In zone 1 there is a very weak correlation (R-squared value of 0.21) between species diversity and % species dominance, this increases significantly in zone 2 to a stronger relationship (R-squared value of 0.69). The relationship weakens in the third zone to 0.31. This suggests that in zone 2 the controlling factor on % species dominance is species diversity, i.e. that when numbers of benthic species increase, the % dominance of *one* of those species over the others is low. This is not the case in the firs and third zones, and there could be other factors controlling the strength of the presence of one species over another.

In Figure 4.15, there appears to be poor correlation between the number of foraminiferal test per ml of sediment and species diversity in zones 1 and 2. In zone 3 there is a degree of relationship (R-squared value of 0.43). This means that even when test concentration is low, the range of species found in the samples is not affected. This suggests that the lower concentration of tests may be a function of the speed of sedimentation operating in the zones.

The poor relationship between the number of foraminiferal test per ml of sediment and % species dominance per sample is shown in Figure 4.16. R-squared values are low in all three zones (never greater than 0.07). This suggests that high % species dominance is not determined by either a low or a high test concentration amount, and must be controlled by other (likely environmental) factors rather than inter-species and faunal factors.

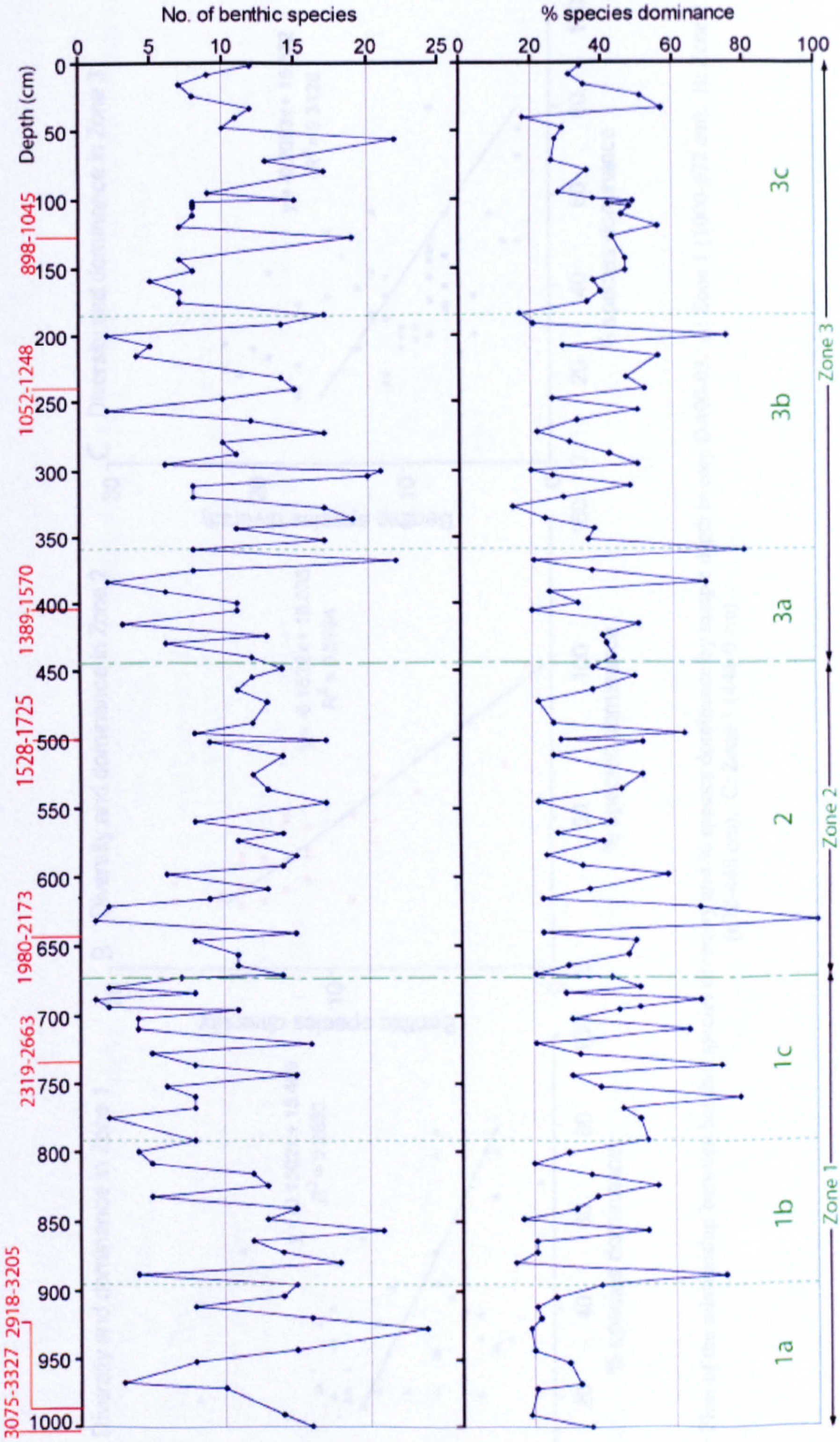

Figure 4.13: Benthic species diversity and dominance in core DA00-03. Zones 1-3 (green dashed lines) are foraminiferal zone boundaries based on the foraminiferal cluster analysis. Radiocarbon dates (in red) are given in cal yr BP

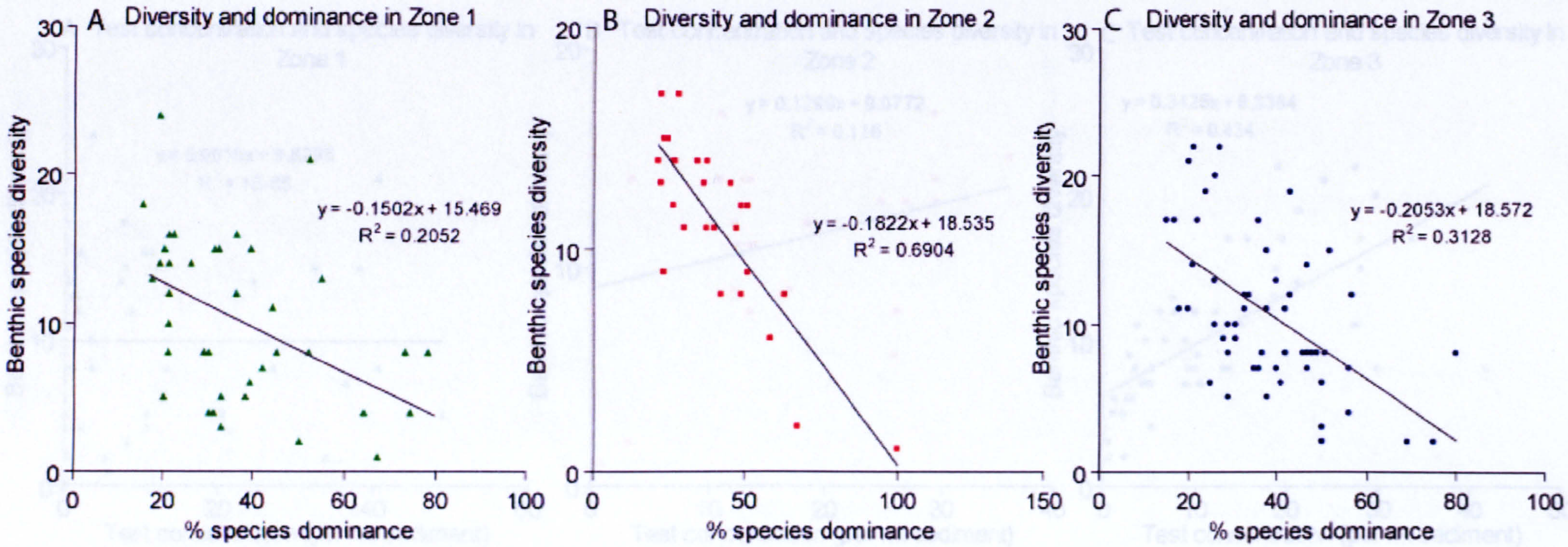

Figure 4.14: Plots of the relationship between benthic species diversity and % species dominance by sample depth in core DA00-03. A: Zone 1 (1000-672 cm). B: Zone 2 (672-448 cm). C: Zone 3 (448-0 cm)

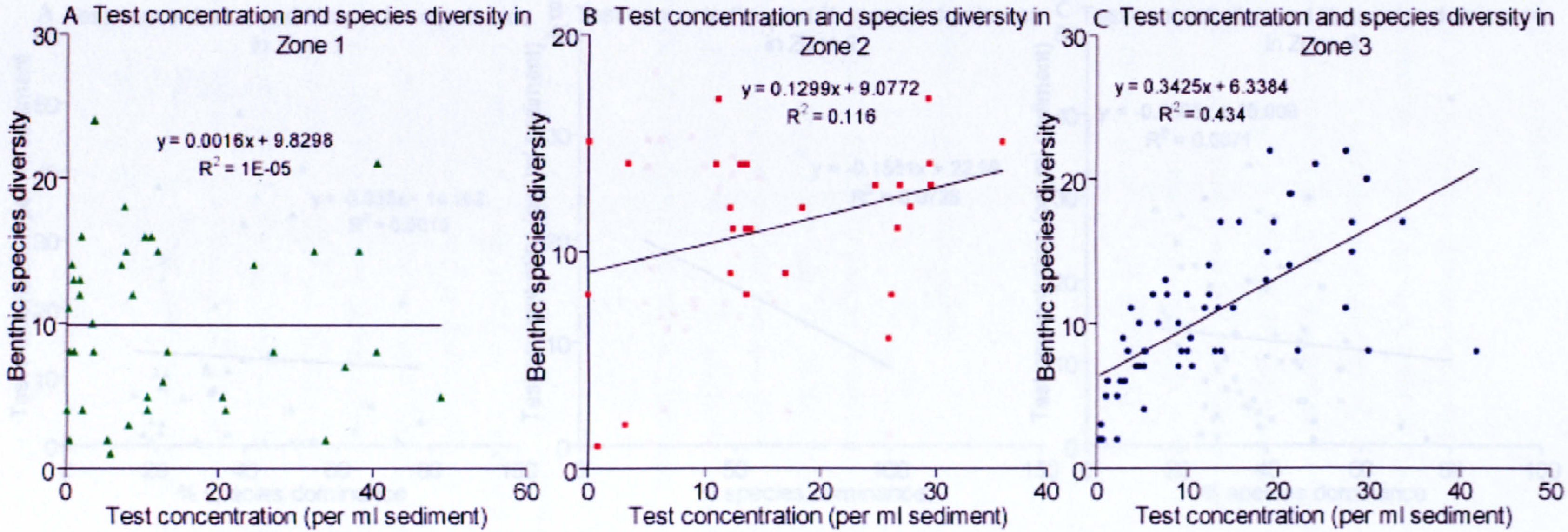

Figure 4.15: Plots of the relationship between benthic species diversity and benthic test concentration (per ml sediment) by sample depth in core DA00-03. A: Zone 1 (1000-672 cm). B: Zone 2 (672-448 cm). C: Zone 3 (448-0 cm)

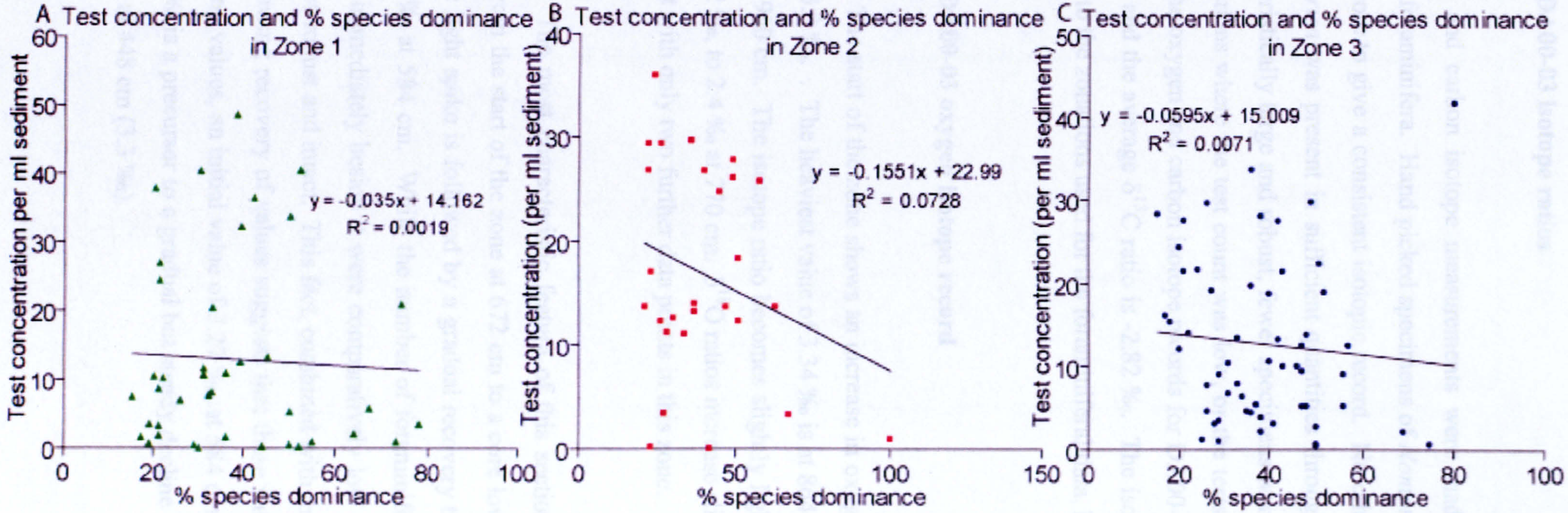

Figure 4.16: Plots of the relationship between benthic test concentration (per ml sediment) and % species dominance by sample depth in core DA00-03. A: Zone 1 (1000-672 cm). B: Zone 2 (672-448 cm). C: Zone 3 (448-0 cm)

4.4.3.1 DA00-03 isotope ratios

Oxygen and carbon isotope measurements were made using a single species of benthic foraminifera. Hand picked specimens of *Nonionellina labradorica* were used in this core to give a consistent isotopic record. No other species was required as *N. labradorica* was present in sufficient quantities throughout DA00-03. As its test is characteristically large and robust, fewer specimens were needed which was useful in core sections where the test count was low, or the tests were degraded. Figure 4.16 shows the oxygen and carbon isotope records for DA00-03. The average $\delta^{18}O$ ratio is 2.98 ‰ and the average $\delta^{13}C$ ratio is -2.82 ‰. The isotope records are described in relation to the zonations used for the foraminiferal data, based on cluster analysis.

4.4.3.2 DA00-03 oxygen isotope record

Zone 1 The start of the zone shows an increase in oxygen isotope values from 2.6 to around 3.3 ‰. . The heaviest value of 3.34 ‰ is at 864 cm and the lightest is of 2.22 ‰ is at 960 cm. The isotope ratio becomes slightly lighter from 820 cm, decreasing from 3.2 ‰, to 2.4 ‰ at 770 cm. $\delta^{18}O$ ratios increase slightly to the top of the zone to 3 ‰, but with only two further data points in this zone.

Zone 2 The most characteristic feature of this section is the steady lightening of values from the start of the zone at 672 cm to a core low of 1.13 ‰ at 608 cm. This dramatic light spike is followed by a gradual recovery to heavier ratios of between 3 and 3.6 ‰ at 584 cm. While the number of foraminiferal tests from this depth and 616 cm immediately beside it were comparatively low (8 tests, see appendix 5), the tests were robust and intact. This fact, combined with the preceding gradual decrease, and following recovery of values suggests that these values are not outliers. Despite fluctuating values, an initial value of 3.27 ‰, at 584 cm, followed by a heavier value of 3.69 ‰ is a precursor to a gradual but steady decline in isotope ratios to the end of the zone at 448 cm (3.3 ‰).

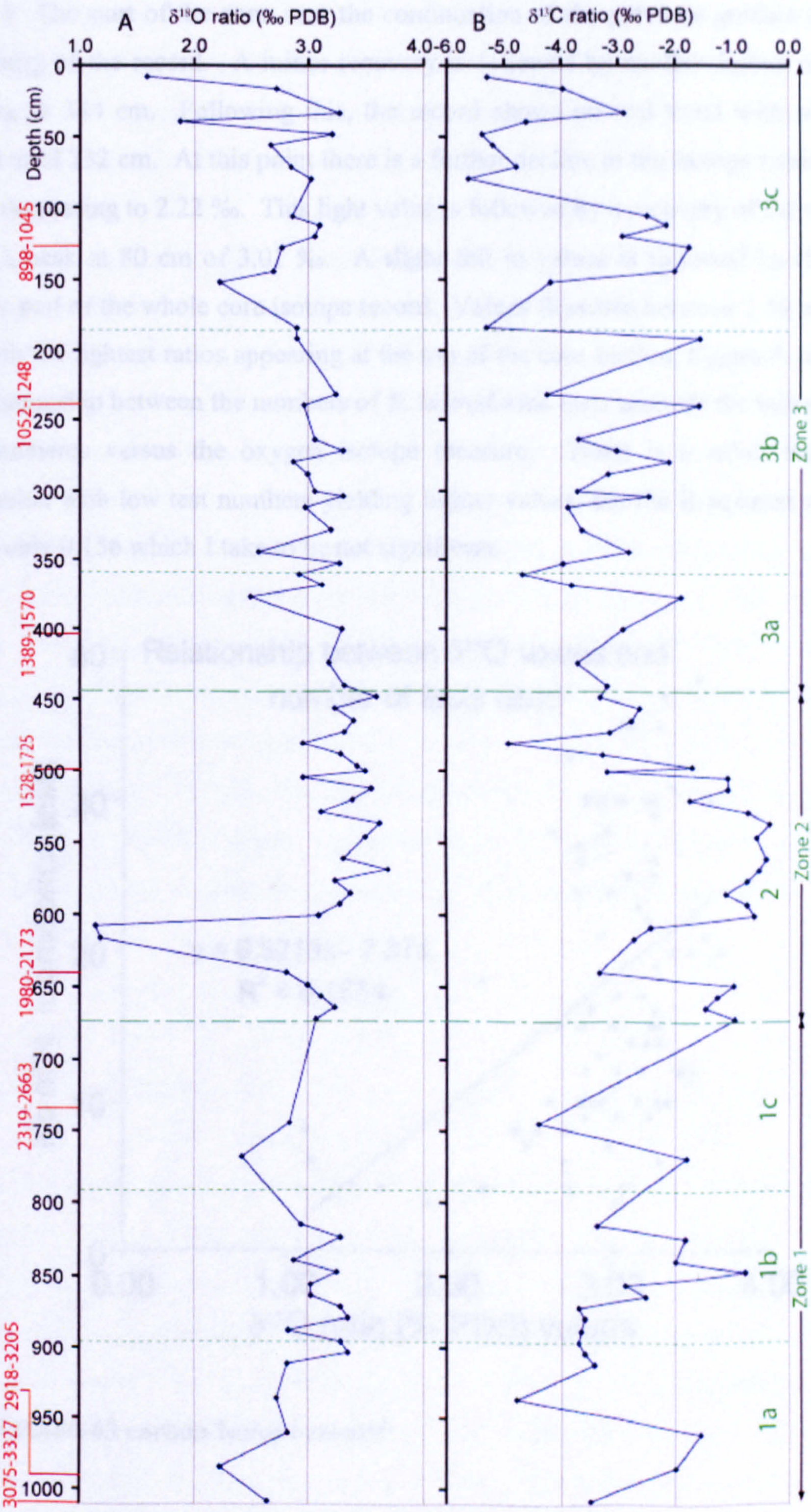

Figure 4.17 Isotope ratios for core DA00-03. Measurements made on single species foraminifera *N. labradorica*. A: Oxygen isotope ratios. B: Carbon isotope ratios. Zones 1-3 (green dashed lines) are foraminiferal zone boundaries based on the foraminiferal cluster analysis. Radiocarbon dates (in red) are given in cal yr BP.

Zone 3 The start of the zone sees the continuation of the previous gradual trend in lightening of the record. A minor recovery is followed by another lighter value of 2.52 ‰ at 344 cm. Following this, the record shows no real trend with scattered values until 232 cm. At this point there is a further decline in the isotope record, with ratios decreasing to 2.22 ‰. This light value is followed by a recovery of the ratios to reach a peak at 80 cm of 3.01 ‰. A slight fall in values is followed by the most chaotic part of the whole core isotope record. Values fluctuate between 1.59 and 3.26 ‰, with the lightest ratios appearing at the top of the core section. Figure 4.18 shows the relationship between the numbers of *N. labradorica* tests used for the isotope ratio measurements versus the oxygen isotope measure. There is a small degree of correlation with low test numbers yielding lighter values, but the R-squared value of this is only 0.156 which I take to be not significant.

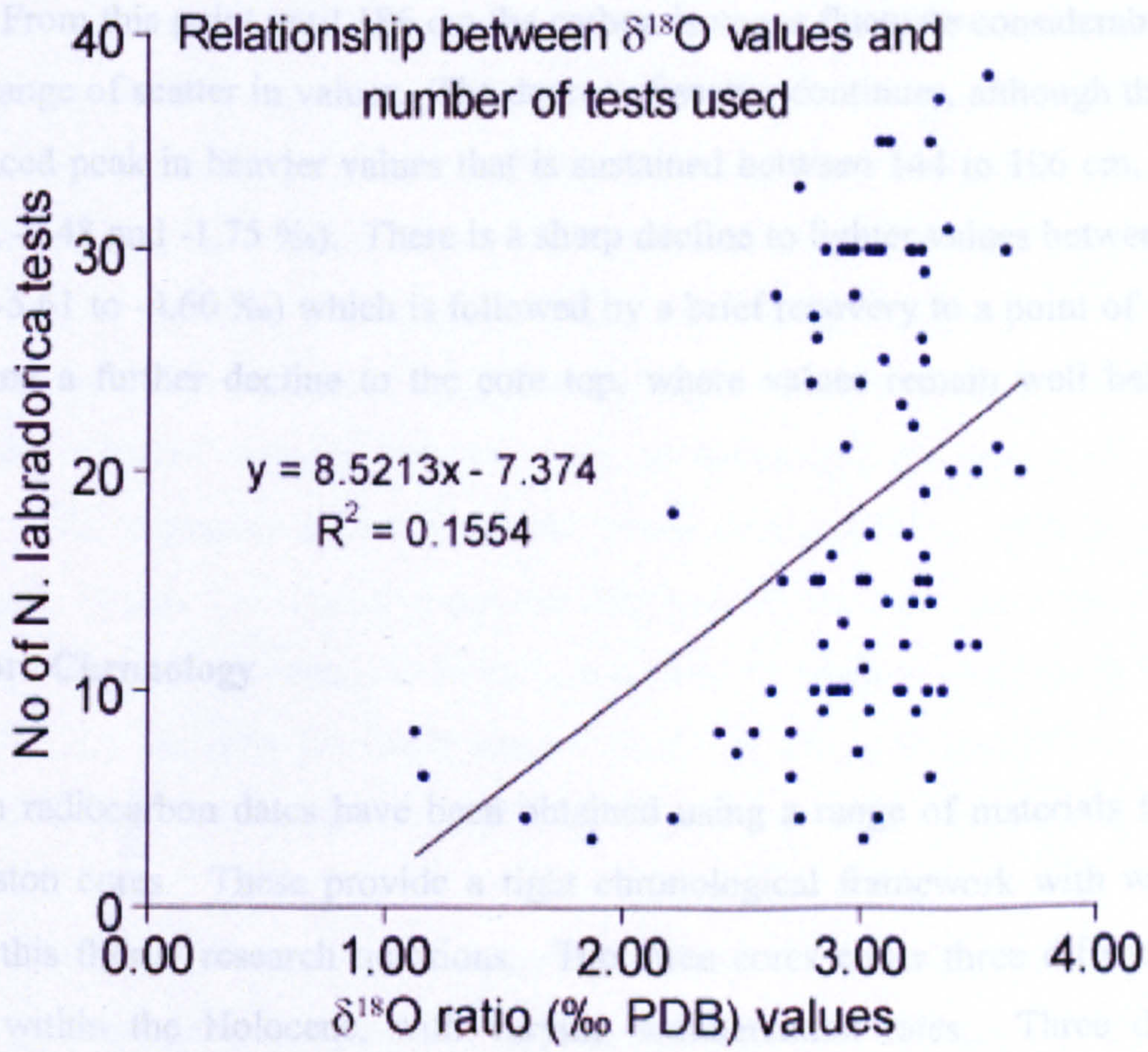

4.4.3.3 DA00-03 carbon isotope record

Zone 1 is characterised by an initial heavy peak in the $\delta^{13}C$ ratio. Values increase from the base of the core from -3.18 to -0.86 ‰ at 944 cm. This heavy spike is followed by a decrease in $\delta^{13}C$ values to a low of -4.29 ‰ at 930 cm. From this poit

there is a staggered increase in the ratio to a peak in heavy values at 840 cm of -1.1 ‰. Following this heavy spike the ratios become more widely scatter, with poorer sample resolution, but there is an overall decline in ratios to -4.2 ‰ at 748 cm. From here there is a large jump to a heavier value of around -1 ‰ at the end of the zone.

Zone 2 The inception of this zone starts with a light spike in the carbon isotope record at 640-610 cm. Following this there is a significant increase to heavier, sustained values of over -1.5 ‰ until 540 cm. From this stage in the zone there is a staggered and rapid decline in isotope ratios to a significant core low at 432 cm of -5.5 ‰. There is a recovery to heavier values at the end of the zone at 448 cm.

Zone 3 The record in this zone starts with an increase in heavier isotope ratios at around 370 cm. Following this there is a sharp decline in values to a light signal of -4.9 ‰. From this point until 186 cm the carbon isotopes fluctuate considerably, with a wide range of scatter in values. The degree of scatter continues, although there is a pronounced peak in heavier values that is sustained between 144 to 106 cm. (values between -2.48 and -1.75 ‰). There is a sharp decline to lighter values between 80 to 40 cm (-5.61 to -4.60 ‰) which is followed by a brief recovery to a point of average value, and a further decline to the core top, where values remain well below the average.

4.5.1 Core Chronology

Eighteen radiocarbon dates have been obtained using a range of materials from all three piston cores. These provide a tight chronological framework with which to address this thesis' research questions. The three cores cover three different time periods within the Holocene, with varying sedimentation rates. Three different institutions, Aarhus University, Denmark, Kiel University, Germany, and the NERC facility at East Kilbride UK have processed the radiocarbon samples. The NERC dates were prepared to graphite in the UK and then sent to the Center for Accelerator Mass Spectrometry, Lawrence Livermore National Laboratory, University of California for ^{14}C analysis The radiocarbon calibration program CALIB 4.3 (Stuiver and Reimer, 1993 and 1998) was used to calibrate all of the core dates to years BP

(relative to 1950 AD). The dates have been corrected for the 'Marine Reservoir Effect' (see chapter 3) and are expressed at the ±2 σ level. The age models show that the piston core retrieval procedures have meant the loss of a top section of all the cores to some degree from 20 to 200 cm. Confidence in all three age models produced is high, with high R-squared values, well-spaced dating intervals, low error ranges and no date inversions.

4.5.2 Core DA00-06: Chronology

The radiocarbon dating results for core DA00-06 are shown in Figure 4.19, giving details of the uncalibrated dates and error values. Difficulties were encountered with obtaining an adequate core chronology with core DA00-06 due to a paucity of suitable dateable material. The condition of the tests of the calcareous forams within the core was both poor, and not available for the most part in high enough concentrations for AMS radiocarbon dating. This has meant that a true bottom core date (960 cm) was unavailable. However, an intact bivalve shell was used to obtain a date as near as possible at 891 cm. X-radiograph analysis of the core showed a distinct change in the sediment composition in the top metre at 98 cm. Dating this change in sediment structure was important to understand the timing of apparent changes in the deposition environment and mechanisms operating. With no dateable foram tests, another intact bivalve derived date was obtained as near as possible at a depth of 159 cm. These shells were extracted from the sediment well away from the core liner edge, meaning the shells were deposited in situ, with limited risk of them having been displaced during coring.

The dates for these two depths of 8321 cal yr BP for 891 cm and 7791 cal yr BP for 159 cm revealed an extremely high sedimentation rate of 1.38 cm yr^{-1} and with a foraminiferal sampling interval of 8 cm, further dating points would be better employed elsewhere. Dating the core top was imperative in order to determine whether core retrieval had meant the loss of vast amounts of sediment, or that there had been hiatuses of sedimentation, or that a significant change in sedimentation rate had taken place in the upper section of the core. Standard AMS dating of foram tests

was not possible as a minimum weight of 10 mg is needed for this procedure, and calcareous forams in a suitable state of preservation were sparse in the sediment available. In order to pick enough tests, the dated interval would have been spread too wide, and chronological resolution would have been lost. An increased volume of sediment from the very top part of the core was taken from the archive section of the core, and enough mixed foram tests were picked for a different dating procedure. This was carried out at Kiel University, and was a direct result of the multidisciplinary nature of the investigative partners involved in the research project as a whole. This procedure needs a much smaller amount of material, which was ideal for this situation. The smaller amount of material needed is due to the fact that the radiation emitted from the sample is measure for a much longer time. A date of 1047 cal yr BP was obtained at 5 cm. This means that for the top 159 cm of the core there is staggering decline (of nearly 100-fold) in sedimentation rate to 2.23 cm per 100 years.

Despite there being only 3 dates available for this core, two distinct and differing periods of sedimentation are clearly defined in the age model illustrated in Figure 4.20. The intercept on the age axis (0 cm depth) gives a core top age of 940 yrs cal BP. The foraminiferal sample depths have been converted to ages and can be seen in Column 2 in Appendices 4, 10 and 11.

DA00-06	Material	**Depth (m)**	^{14}C age (yrs)	^{14}C age (yrs) mar. res. cor.	**Age (cal yrBP)**	2 sigma range	
Lab Code							
KIA-17925	Forams	**0.05**	1500	1100	**1047**	943	1160
AAR-6837	Shell	**1.57**	7350	6950	**7791**	7663	7937
AAR-6839	Shell	**8.91**	7843	7443	**8321**	8154	8416

Figure 4.19: Table of radiocarbon dating results for core DA00-06. Depths are given in metres. Uncalibrated dates (corrected and uncorrected for marine reservoir correction) are given in radiocarbon years. Dates have been calibrated using the radiocarbon calibration program CALIB 4.3 (Stuiver and Reimer, 1993 and 1998) and are given in calibrated years BP.

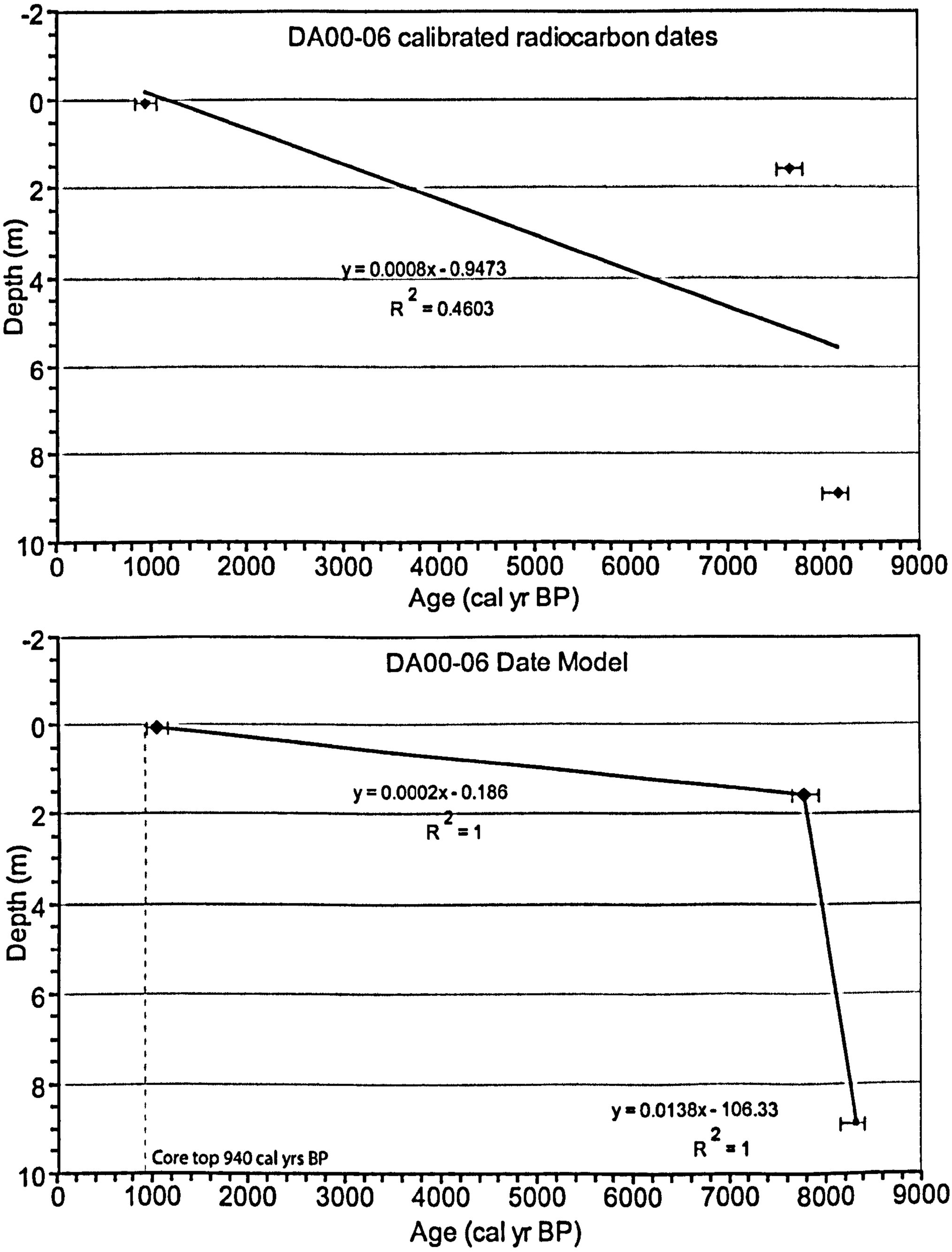

Figure 4.20 Age model for core DA00-06. Upper graph shows marine reservoir corrected, calibrated radiocarbon dates from 3 depths, based on data shown in Figure 4.19. The trendline shows a poor fit between the 3 dates. Lower graph shows the age model interpretation of the dates, with trendlines fitted between the upper and lower sections of the core in response to the likely differing sedimentation rates.

4.5.3 Core DA00-05: Chronology

7 radiocarbon dates based on marine plant macrofossil remains have been obtained for this core. The samples upon which these dates are based were all processed at Aarhus University, and the excellent availability of material resulted in regularly spaced dating intervals and a well-balanced age model. Details of the radiocarbon results are shown in Figure 4.21. The bottom of the core at 10.27 m is dated as near as possible with a date taken from 10.17m. The bottom core date is 6738 cal yr BP, with a top date (at 0.5 m) of 1263 cal yr BP. If the age model is averaged over all 7 dates, the R-squared value is extremely high at 0.982 (Figure 4.22 upper graph). The intercept on the age axis (0 cm depth) gives a core top age of 1200 yrs cal BP. Assuming constant sedimentation, this implies a loss of approximately 2.20 m. Using this trend line gives an average core sedimentation rate of 5.66 cm yr^{-1}.

However, although the trend line fits will with the lower 3 dates at 10.17 m, 8.12 m, and 5.92 m, the line is not as successful at intercepting with the remaining 4 dates. In order to counter this, the age model has been revised by averaging between the upper and lower date sets. Figure 4.22 (lower graph) shows this revised model, and it shows that the trend line fits well with the group of upper core dates.

DA00-05	Material	Depth (m)	^{14}C age (yrs)	^{14}C age (yrs) mar. res. cor.	Age (cal yr BP)	2 sigma range	
Lab Code							
AAR-7509	Plant	**0.5**	1705	1305	**1263**	1109	1393
AAR-7510-b	Plant	**1.06**	2004	1604	**1550**	1391	1727
AAR-7511-b	Plant	**2.62**	3200	2800	**2985**	2735	3327
AAR-6838	Plant	**3.27**	3155	3555	**3438**	3163	3716
AAR-6835	Plant	**5.92**	4189	3789	**4263**	3966	4529
AAR-6840	Plant	**8.12**	4926	5326	**5668**	5558	5883
AAR-6836	Plant	**10.17**	6253	5853	**6704**	6378	7035

Figure 4.21: Table of radiocarbon dating results for core DA00-05. Depths are given in metres. Uncalibrated dates (corrected and uncorrected for marine reservoir correction) are given in radiocarbon years. The dating material is marine in origin. Dates have been calibrated using the radiocarbon calibration program CALIB 4.3 (Stuiver and Reimer, 1993 and 1998) and are given in calibrated years BP.

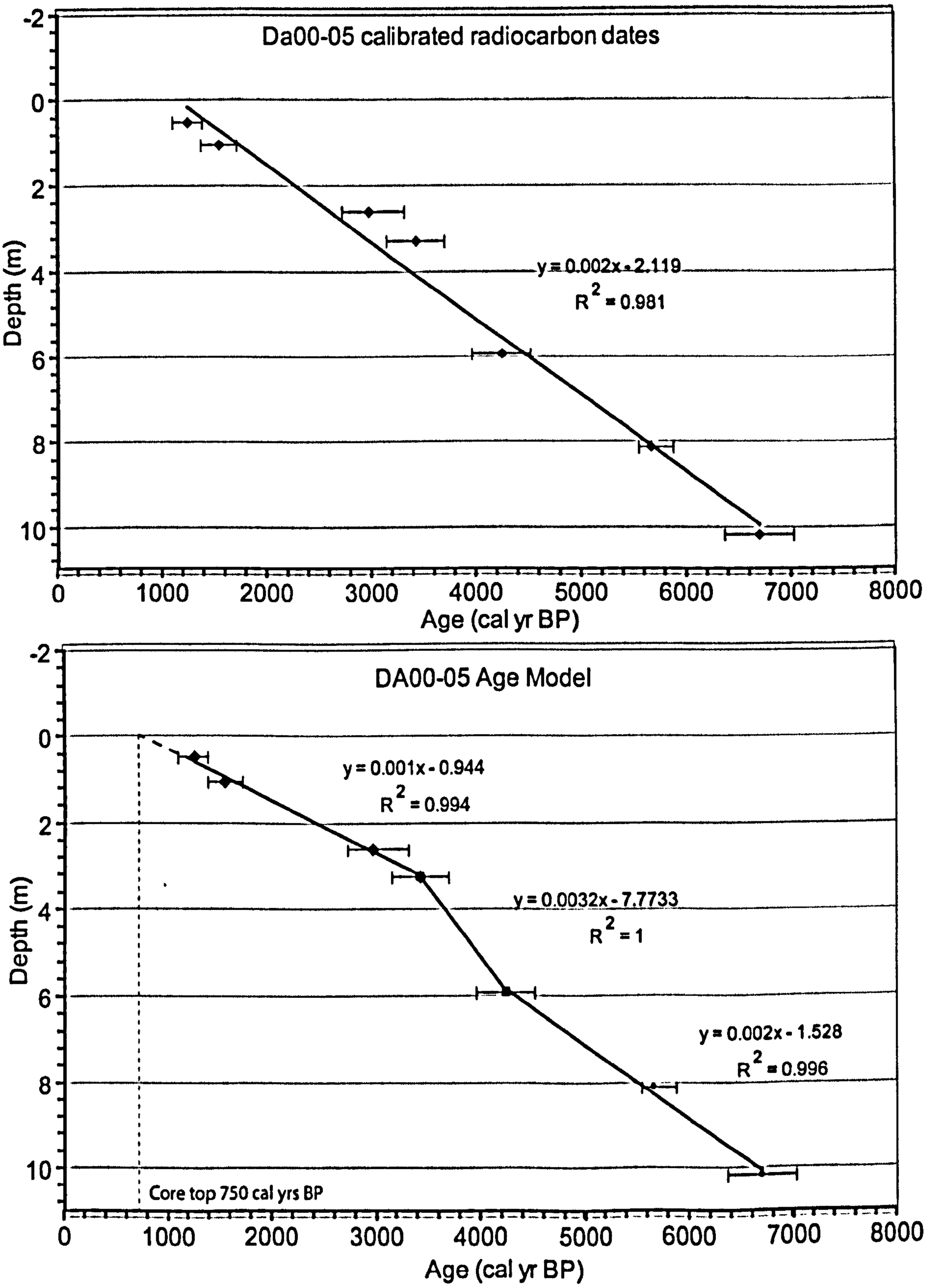

Figure 4.22 Age model for core DA00-05. Upper graph shows marine reservoir corrected, calibrated radiocarbon dates from 7 depths, based on data shown in Figure 4.21. The trendline applied implies the loss of substantial amounts of core material (.2m). Lower graph shows the age model interpretation of the dates, with trendlines fitted between the upper , mid and lower sections of the core in response to the likely differing sedimentation rates in this fjord environment.

The R-squared value of the lower dates is only marginally decreased to 0.9816, but the value of the upper 4 dates is increased to 0.9944. This means that the new

intercept and core top date can be interpreted to be 750 yrs cal BP, with a loss less than 1 m due to coring processes. The revised sedimentation rate for the lower part of the core is (from 10.17 m to 3.27 m) is almost a centimetre per year lower at 4.78 cm yr^{-1}. The upper section of the core (3.27 m to 0.5 m) has a sedimentation rate 1.5 times greater at 7.85 cm yr^{-1}. The foraminiferal sample depths have been converted to ages and can be seen in Appendices 8,9,10.

4.5.4 Core DA00-03: Chronology

Core DA00-03 has the greatest coverage of radiocarbon dates, with 8 dates based on a range of material, including foraminifera (mixed species sample), and shells, both fragments and intact specimens. The full range of dates, raw, and calibrated and sample depths and materials are given in Figure 4.23, and the calibrated radiocarbon dates and the interpreted age model for the core are shown in figure 4.24. The bottom of the core is dated from a sample taken from the core catcher at a depth of 1020 cm, at 3208 cal yrs BP. The nearest date to the top of the core is taken at 128 cm and yields a date of 947 cal yr BP. Assuming a linear rate of sedimentation of 0.39cm yr^{-1} the top of the core can be dated at 500 yr cal BP (when the trend line intercepts with the x-axis at 0 cm depth) with a loss of 2m of top core sediment.

DA00-03	Material	**Depth (m)**	^{14}C age (yrs)	^{14}C age (yrs) mar. res. cor.	**Age (cal yr BP)**	2 sigma range	
Lab Code							
CAMS-91944	Bivalve	**1.28**	1415	1015	**947**	898	1045
AAR-7508	shell	**2.39**	1594	1194	**1162**	1052	1248
CAMS-91935	Bivalve	**4.04**	1940	1540	**1501**	1389	1570
CAMS-86752	Forams	**5**	2065	1665	**1623**	1528	1725
CAMS-82824	Gastropod	**6.42**	2445	2045	**2090**	1980	2173
AAR-6833	Shell	**7.38**	2738	2338	**2425**	2319	2663
AAR-6834	Shell	**9.82**	3245	2845	**3062**	2918	3205
AA-44949	Forams	**10.2**	3351	2951	**3208**	3075	3327

Figure 4.23: Table of radiocarbon dating results for core DA00-03. Depths are given in metres. Uncalibrated dates (corrected and uncorrected for marine reservoir correction) are given in radiocarbon years. Foraminiferal dates are measured on mixed benthic species. Dates have been calibrated using the radiocarbon calibration program CALIB 4.3 (Stuiver and Reimer, 1993 and 1998) and are given in calibrated years BP.

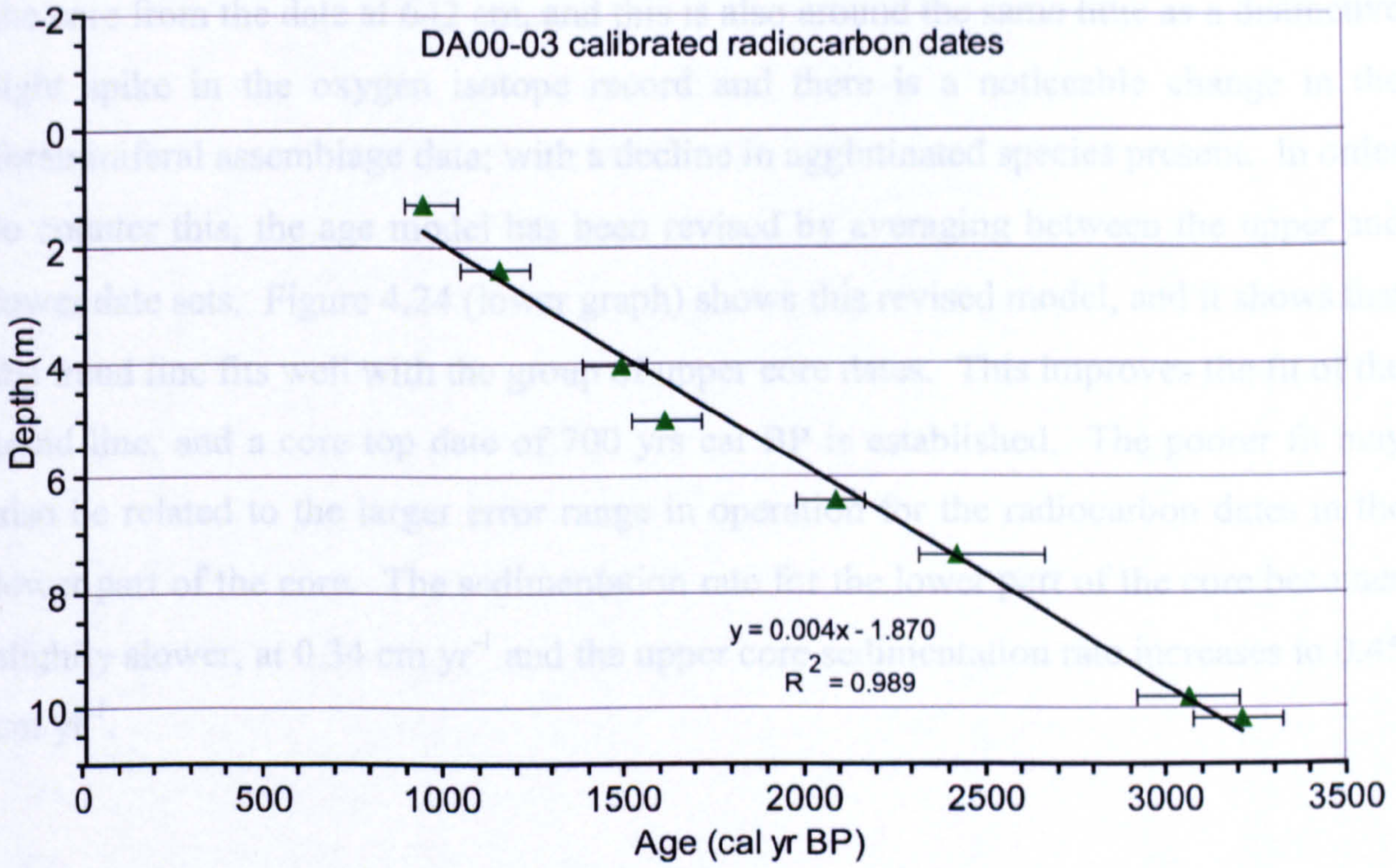

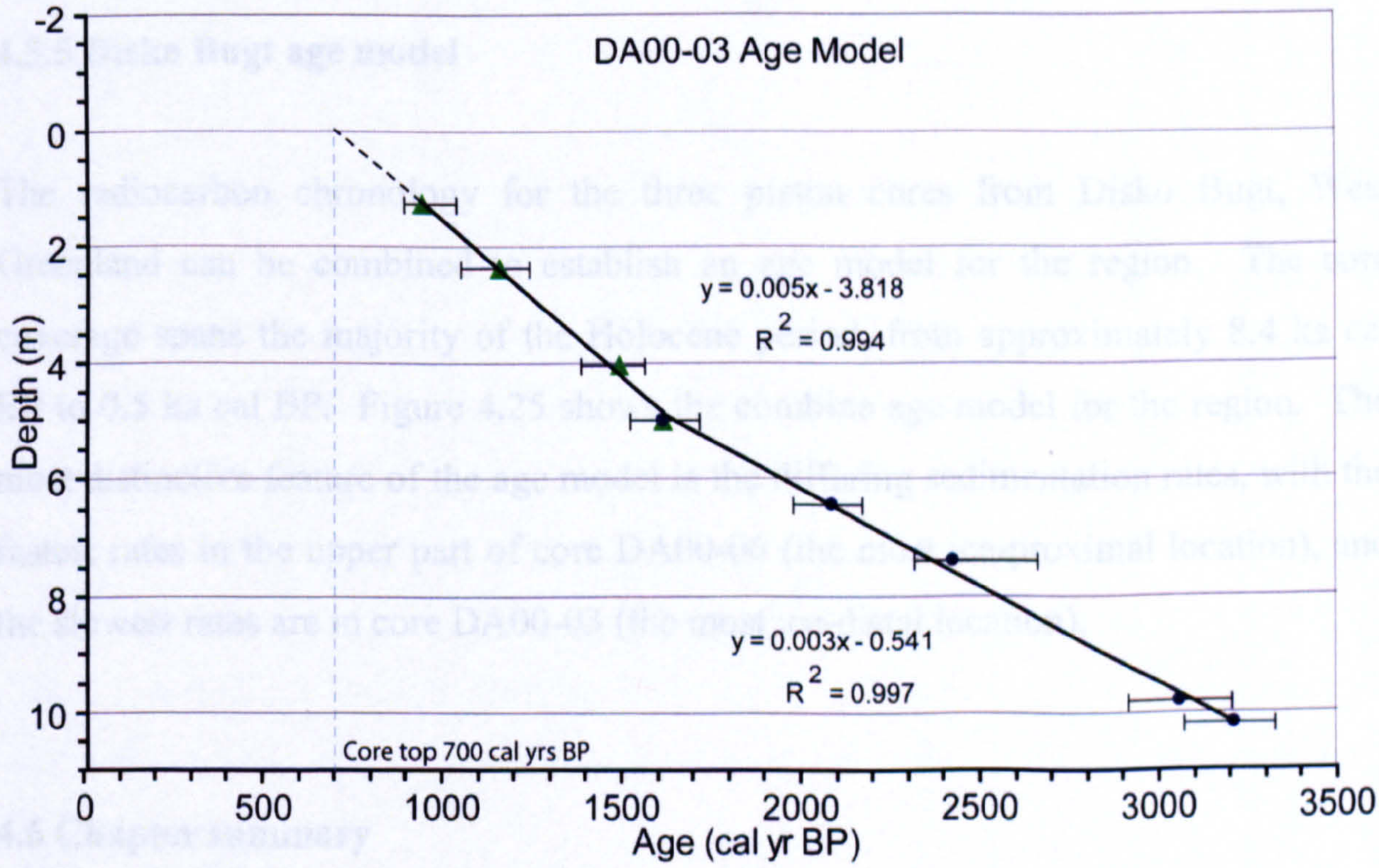

Figure 4.24 Age model for core DA00-03. Upper graph shows marine reservoir corrected, calibrated radiocarbon dates from 8 depths, based on data shown in Figure 4.23. The trendline applied implies the loss of substantial amounts of core material (.2m). Lower graph shows the age model interpretation of the dates, with trendlines fitted between the upper , and lower sections of the core in response to the likely differing sedimentation rates in this ice distal environment.

The R-squared value of the calibrated radiocarbon dates shows a high degree of correlation (0.99). However, the fit is much poorer through the dates at 404 cm, 500

cm and 642 cm. There appears to be a steepening of the dates in the upper section of the core from the date at 642 cm, and this is also around the same time as a distinctive light spike in the oxygen isotope record and there is a noticeable change in the foraminiferal assemblage data; with a decline in agglutinated species present. In order to counter this, the age model has been revised by averaging between the upper and lower date sets. Figure 4.24 (lower graph) shows this revised model, and it shows that the trend line fits well with the group of upper core dates. This improves the fit of the trend line, and a core top date of 700 yrs cal BP is established. The poorer fit may also be related to the larger error range in operation for the radiocarbon dates in the lower part of the core. The sedimentation rate for the lower part of the core becomes slightly slower, at 0.34 cm yr^{-1} and the upper core sedimentation rate increases to 0.45 cm yr^{-1}.

4.5.5 Disko Bugt age model

The radiocarbon chronology for the three piston cores from Disko Bugt, West Greenland can be combined to establish an age model for the region. The core coverage spans the majority of the Holocene period, from approximately 8.4 ka cal BP to 0.5 ka cal BP. Figure 4.25 shows the combine age model for the region. The most distinctive feature of the age model is the differing sedimentation rates, with the fastest rates in the upper part of core DA00-06 (the most ice-proximal location), and the slowest rates are in core DA00-03 (the most ice-distal location).

4.6 Chapter summary

This chapter has presented the foraminiferal, sedimentological (IRD), isotopic and radiocarbon findings of this thesis. In core DA00-06, foraminiferal assemblages show distinct variations in species related either ice proximal or ice distal environments, and three differing zones of assemblages through the core. The most distinctive change in foraminiferal data in this core see a dramatic shift from ice proximal species to more ice-distal or tolerant species.

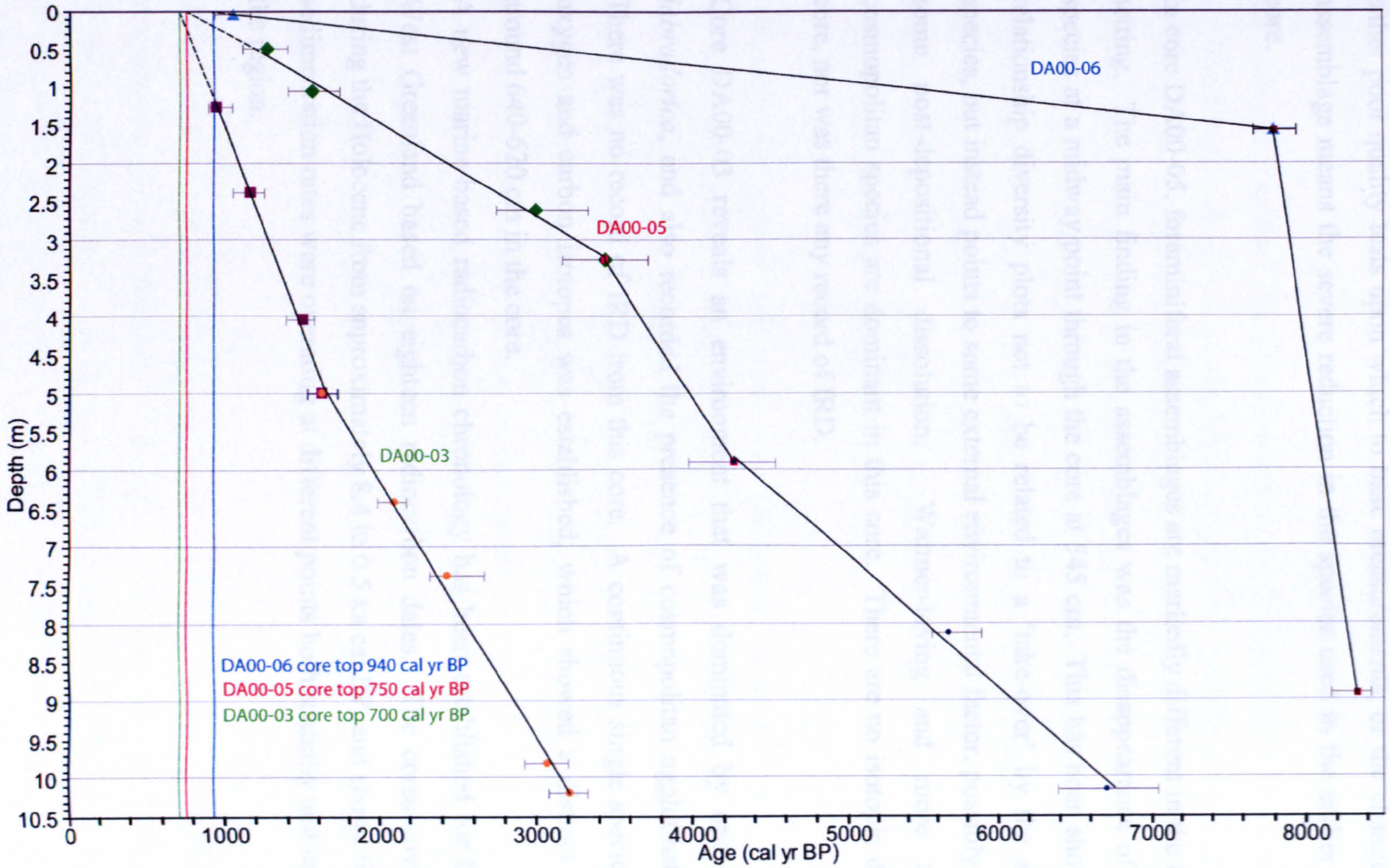

Figure 4.25: Age model for Disko Bugt, West Greenland. Dates are based on 18 marine reservoir corrected, calibrated radiocarbon dates measured on the 3 piston cores. DA00-06 (labelled in blue); DA00-05 (labelled in red); DA00-03 (labelled in green). Dates have been calibrated using the radiocarbon calibration program CALIB 4.3 (Stuiver and Reimer, 1993 and 1998) and are given in calibrated years BP Core top ages are extrapolated and given the same colour code. The age model covers the majority of the Holocene period, from 8.4 ka cal BP to 0.5 ka cal BP.

This coincides with dramatic changes in the record of ice-rafted debris, which shows that at the same time (around 100 cm depth in the core) there is a massive influx of IRD, of mixed sizes. The isotope record around this point in the core is poor, with either poor quality tests upon which to base measurements, or the change in species assemblage means the severe reduction in the species used in the earlier part of the core.

In core DA00-05, foraminiferal assemblages are markedly different in the fjord mouth setting. The main finding in the assemblages was the disappearance of calcareous species at a midway point through the core at 545 cm. This has been shown through relationship diversity plots not to be related to a 'take-over' by the agglutinated species, but instead points to some external environmental factor, possibly controlling some post-depositional dissolution. Warmer-loving and more tolerant or cosmopolitan species are dominant in this core. There are no isotopic data for this core, nor was there any record of IRD.

Core DA00-03 reveals an environment that was dominated by one species, *N. labradorica*, and also recorded the presence of cosmopolitan agglutinated species. There was no record of IRD from this core. A continuous single species record of oxygen and carbon isotopes was established, which showed a distinct light spike around 640-620 cm in the core.

A new marine-based radiocarbon chronology has been established for Disko Bugt, West Greenland based on eighteen radiocarbon dates. The cores cover a period during the Holocene from approximately 8.4 to 0.5 ka cal BP, and shows that different sedimentation rates were operating at different points both spatially and temporally in the region.

Chapter 5: Palaeoenvironmental interpretation in Disko Bugt

5.1 Introduction

This chapter discusses the palaeoenvironmental interpretations of cores DA00-06, DA00-05 and DA00-03. Core site locations are shown in Figure 5.1, and sample site locations used for modern comparative assemblage data are shown in Figure 5.2. A detailed consideration of the environmental requirements of key species present in West Greenland sediments is developed primarily with reference to the longest core record, DA00-06. Key species are determined by significant presence in the core, and whether there is substantial indication of their diagnostic ability (from published sources and contemporary data). Interpretation is based upon classification of foraminifera into Arctic/Atlantic indicator species.

The basis for inference of water mass characteristics relating to specific taxa is derived from Chapter 2 which discusses the regional oceanography, in particular the two constituent water masses of the West Greenland Current (WGC) and the Arctic water mass. Species are found to be diagnostic of either the cold, less saline Arctic water, East Greenland Current (EGC) component, or cold, low salinity meltwater, or the warmer, more saline Atlantic sourced water derived from the Irminger Current (IC). Figure 5.3 summarises the diagnostic environments for the indicator taxa. These inferences, based upon published data from numerous studies in high latitudes, are then applied to the subsequent cores, as the key indicator species are present in all three cores.

15 indicator species are used, although more species than this are identified in the core assemblages. From examination of the relevant literature, the remaining species are found to be cosmopolitan in their distribution, and cannot be ascribed to specific environmental characteristics. Discussion of faunal preservation issues arising in cores DA00-06 and DA00-05 is developed towards the end of the chapter. Assemblage interpretation is aided by reference to ongoing parallel research as part of the wider ARCICE project.

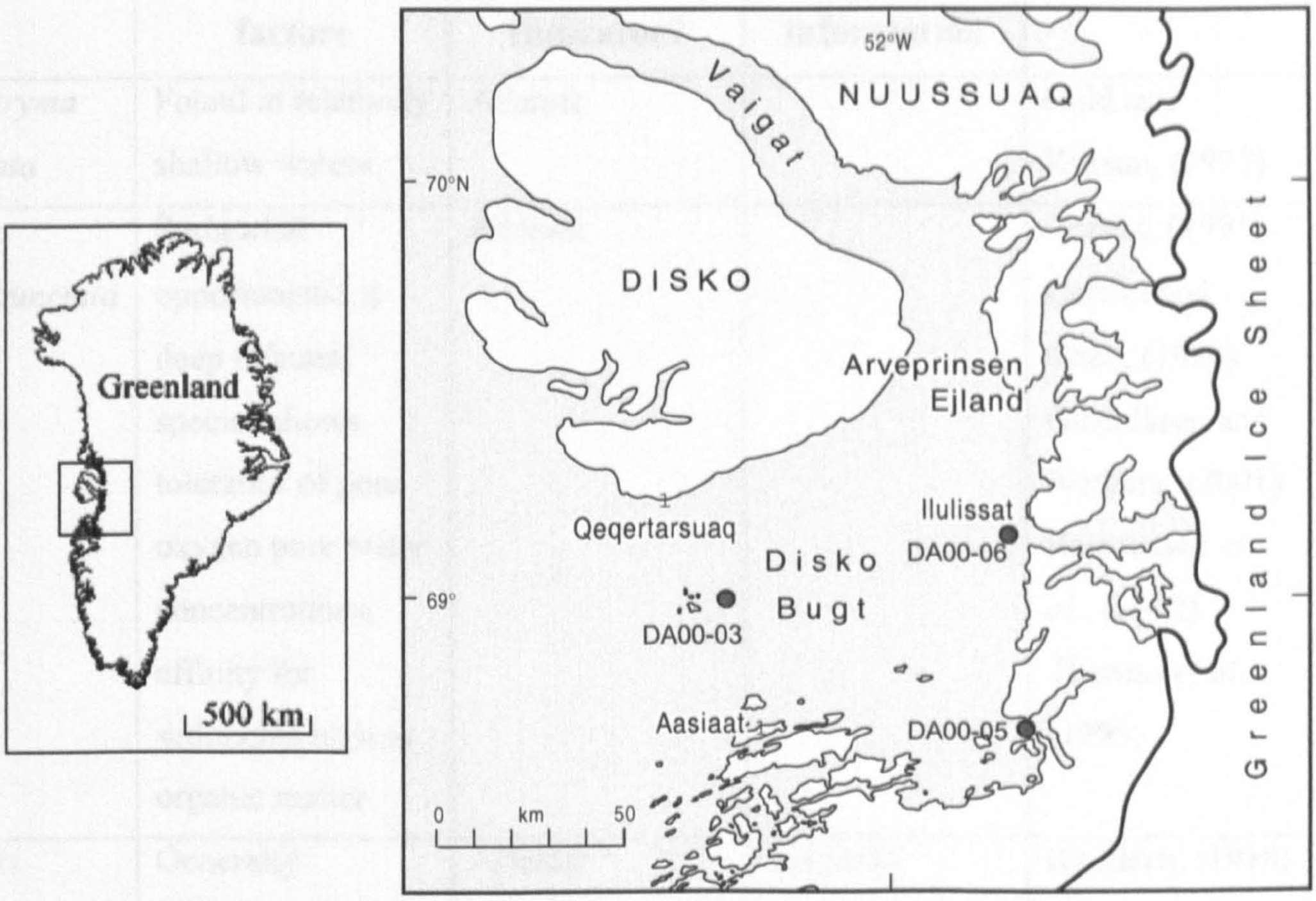

Figure 5.1: The location of the three piston cores in Disko Bugt used within this thesis.

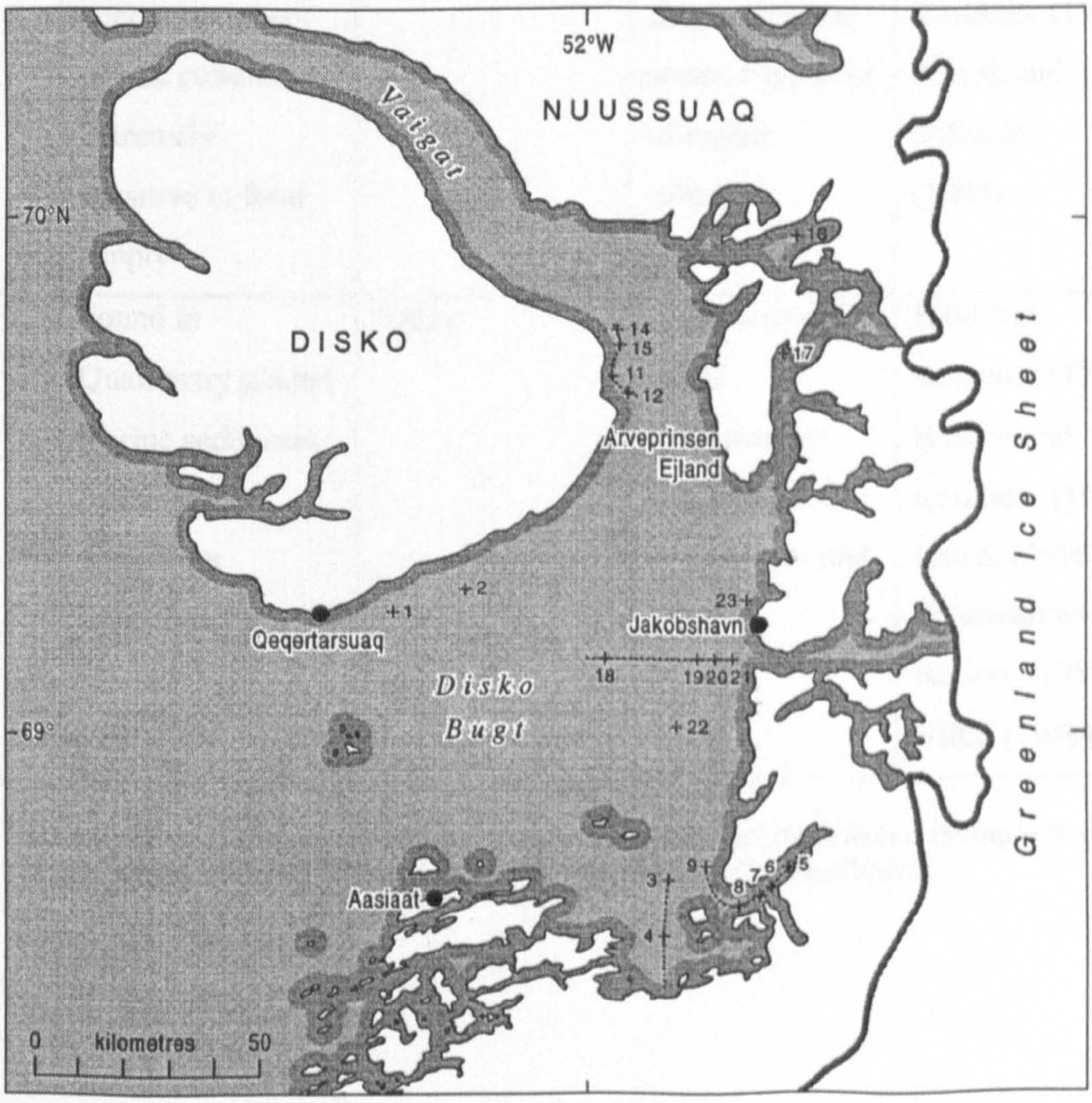

Figure 5.2: Map of surface sample site locations (R/V Porsild 1999 cruise) in Disko Bugt, taken by Kuijpers and Lloyd for modern comparative assemblages. Sites are marked with a cross; the dashed line represents the line of survey taken by the vessel.

Species	Distribution factors	Arctic/Atlantic Indicator?	Other T and S information	References
Adercotryma glomerata	Found in relatively shallow waters	Atlantic		Hald and Korsun, (1997)
Bolivina pseudopunctata	Somewhat opportunistic, a deep infaunal species shows tolerance of poor oxygen pore water concentrations, affinity for sediments high in organic matter	Atlantic		Corliss, (1991) Corliss and Chen, (1988) Gustafsson and Norberg, (2001) Rasmussen *et al.*, (2002) Thomas *et al.*, (1995)
Buccella tenerrima	Generally associated with open water post-glacial conditions, extremely sensitive to food supply	Atlantic	Typically associated with deeper Atlantic water, indicative of higher salinities	Knudsen, (1988) Madsen and Knudsen, (1994) Polyak and Solheim, (1994)
Cassidulina reniforme	Found in Quaternary glacial marine sediments (often with *Elphidium excavatum)*	Arctic	(more precisely distal glaciomarine conditions)/low temperature and salinity	Hald and Korsun, (1997) Hansen and Knudsen, (1995) Lloyd, (1996) Osterman and Nelson, (1989) Vilks, (1989)

Figure 5.3: Summary table of diagnostic conditions of foraminifera associated with differing water mass components in Disko Bugt and the West Greenland Current (WGC)

Cassidulina teretis	Widely distributed throughout both Arctic and Boreal seas. Low levels in Disko Bugt may be due to relatively shallow water depths, or it is out-competed in the area by other species	Atlantic	But related to deeper Atlantic sourced water	Mackensen and Hald, (1988) Wollenberg and Mackensen, (1998a)
Cribostomoides crassimargo	Difficulty in relating this species to particular environmental controlling factors, but common in Disko Bugt modern assemblages	Atlantic	Warmer conditions	Hald and Korsun, (1997) Jennings and Helgadottir, (1994) Lloyd, (*in prep.*)
Cuneata arctica	Cold loving fauna (found in close association with *Spiroplectammina biformis*)	Arctic	Related to colder, less saline or Arctic sourced waters produced from enhanced seasonal melting, transitional/mixed water	Jennings *et al.*, (2001) Madsen and Knudsen, (1994) Silis, (1993)

Figure 5.3 (continued): Summary table of diagnostic conditions of foraminifera associated with differing water mass components in Disko Bugt and the West Greenland Current (WGC)

Elphidium excavatum	Indicator of proximal glaciomarine and/or postglacial conditions dominated by sediment-loaded cold meltwater (often found in association with *Cassidulina reniforme)*	Arctic	Low temperature and salinity meltwater	Hald and Korsun, (1997) Landvik *et al.*, (1995) Nagy, (1984) Osterman, (1984) Osterman and Nelson, (1989) Vilks *et al.*, (1989)
Islandiella norcrossi	May reflect lengthened ice-free season/retreat of sea-ice margin	Atlantic	Representative of water masses of relatively higher salinity and temperature	Duplessy *et al.*, (2001) Hald and Korsun, (1997) Mudie *et al.*, (1984) Vilks, (1980)
Melonis zaandamae	Frequently found on Labrador Shelf, and East Greenland, related to increased productivity	Atlantic	Related to warm and saline water, usually much deeper than found in Disko Bugt	Osterman, (1984) Osterman and Nelson, (1989) Silis, (1993) Vilks and Deonarine, (1988)

Figure 5.3: (continued): Summary table of diagnostic conditions of foraminifera associated with differing water mass components in Disko Bugt and the West Greenland Current (WGC)

Nonionellina labradorica	Relatively well mixed open water conditions (deeper and outer parts of fjords). Associated with higher primary productivity, and sensitive to food supply	Atlantic	Indicative of deeper, stable Atlantic sourced water masses (e.g. found in East Greenland and Arctic Canada),	Hald and Korsun, (1997) Hansen and Knudsen, (1995) Jennings *et al.*, (2001) Mudie *et al.*, (1984) Polyak and Mikhailov, (1996)
Reophax gracilis	Relatively common in Disko Bugt waters, seems to be tolerant of a range of environmental conditions	Cosmopolitan	Is not associated with a specific water mass, found in range of waters in high latitudes	Hald and Korsun, (1997) Hald and Steinsund, (1992) Hansen and Knudsen, (1995) Osterman and Nelson, (1989)
Saccammina diflugiformis	Common in modern Disko Bugt assemblages, and related to more Boreal conditions	Atlantic		Bilodeau *et al.*, (1994) Hald and Korsun, (1997) Jennings and Helgadottir, (1994) Vilks, (1980)

Figure 5.3: (continued): Summary table of diagnostic conditions of foraminifera associated with differing water mass components in Disko Bugt and the West Greenland Current (WGC)

Spiroplectammina biformis	Species adaptive to shallow, nearshore waters	Arctic		Jennings and Helgadottir, (1994) Korsun and Hald, (2000) Madsen and Knudsen, (1994) Schafer and Cole, (1986) Vilks, (1969)
Stainforthia feylingi	Opportunistic, thriving in areas of very harsh, limiting ecological conditions typified by episodic/poor food supply and anoxic conditions	Arctic	Low salinity meltwater	Alve, (1994) Bernhard and Alve, (1996) Jennings *et al.*, (1998) Jennings *et al.*, (2001) Knudsen and Seidenkrantz, (1994) Rasmussen *et al.*, (2002) Silis, (1993)

Figure 5.3: (continued): Summary table of diagnostic conditions of foraminifera associated with differing water mass components in Disko Bugt and the West Greenland Current (WGC)

5.2.1 DA00-06 Introduction

The proximity of core DA00-06 to the mouth of Jakobshavns Isfjord (Figure 5.1) makes it ideal for establishing the interactive history of terrestrial, glacial and marine events since the LGM. Interpretation in this section is based upon the foraminiferal

assemblages, isotope stratigraphies and ice rafted debris records described in Chapter 5, and draws upon concurrent sedimentological data produced by Morros (unpublished data and Lloyd *et al.*, submitted), and information relating to present day foraminiferal assemblages in Disko Bugt (Lloyd, *in prep.*; Lloyd *et al.*, submitted). Reference is made to both the initial foraminiferal assemblage diagrams described in Chapter 4, as well as figures of key indicator species.

5.2.2 Interpretation of DA00-06 Zone 1

Zone 1 from the base of the core shows that from *c.* 8.3 ka cal BP the area was strongly influenced by Arctic sourced waters (Figure 5.4 and Figure 5.5). The faunal assemblage is dominated by three calcareous species, all indicative of distinct environmental circumstances. *Elphidium excavatum* is well established as an indicator of proximal glaciomarine marine conditions (Hald and Korsun, 1997; Osterman, 1984; Osterman and Nelson, 1989; Vilks, 1989), and *Elphidium excavatum* dominated assemblages have been used to indicate postglacial conditions dominated by sediment-loaded cold meltwater (e.g. Landvik *et al.*, 1995; Nagy, 1984). *Cassidulina reniforme* is also representative of cold polar waters, but is more precisely indicative of distal glaciomarine conditions (Osterman and Nelson, 1989). Their co-dominance in Quaternary glacial marine sediments has benn well documented in eastern Arctic Canada, and Svalbard, as well as parts of Northwest Europe (Hald and Korsun, 1997; Hansen and Knudsen, 1995; Lloyd, 1996; Osterman and Nelson, 1989; Vilks, 1989).

The third dominant species is *Stainforthia feylingi*, frequently identified taxonomically as *Fursenkoina fusiformis* (Jennings *et al.*, 2001), and previously recorded as *Stainforthia schreibersiana* (Knudsen and Seindenkrantz, 1994). This species is opportunistic, thriving in areas of extremely harsh, limiting ecological conditions typified by episodic/poor food supply and anoxic conditions (Alve, 1994; Bernhard and Alve, 1996; Knudsen and Seidenkrantz, 1994; Rassmussen *et al.*, 2002).

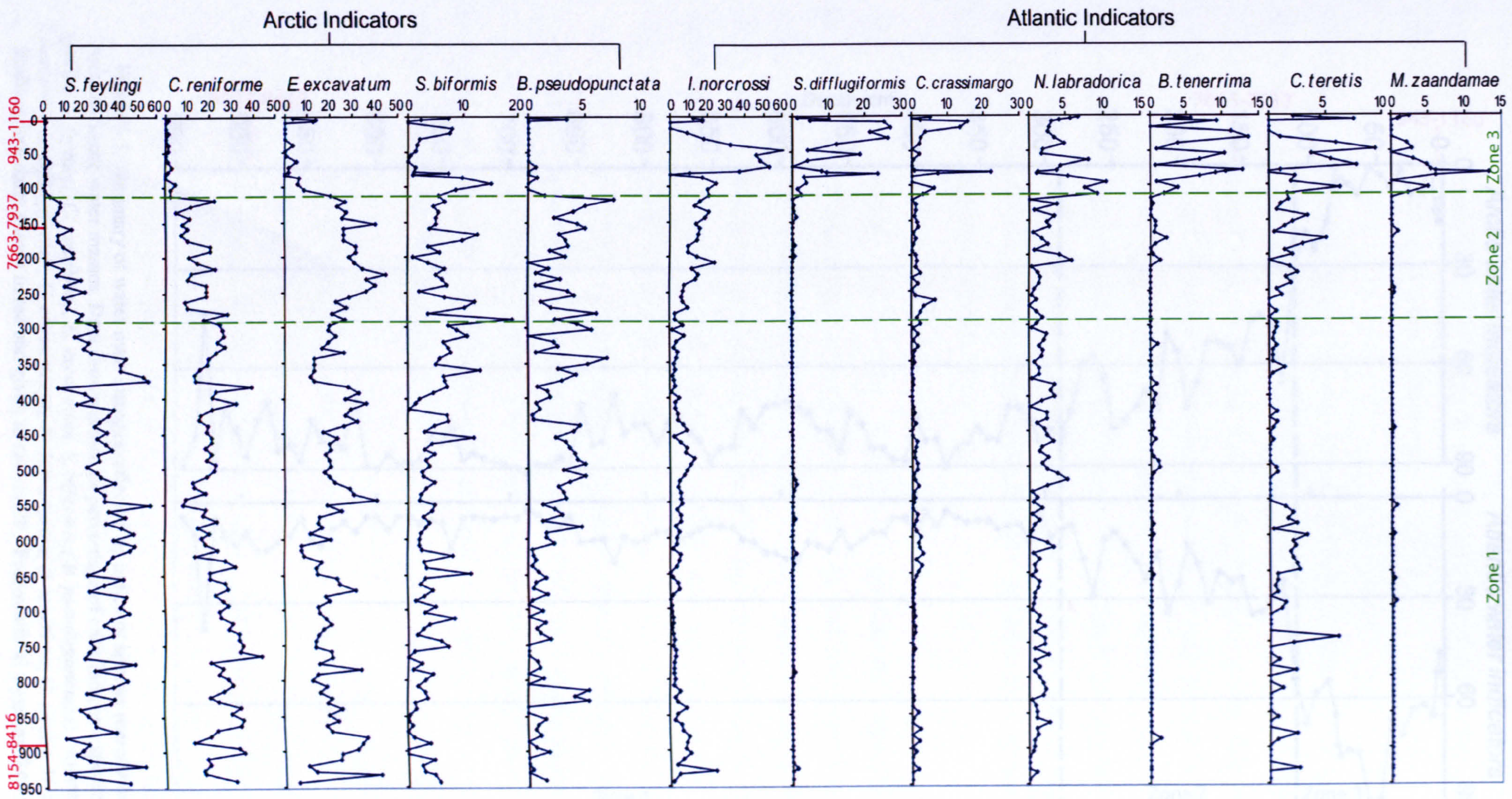

Figure 5.4: Individual percentage assemblage data for indicator species in core DA00-06. Radiocarbon dates are given in red in cal yrs BP. Foraminiferal zones are marked in green based on cluster analysis.

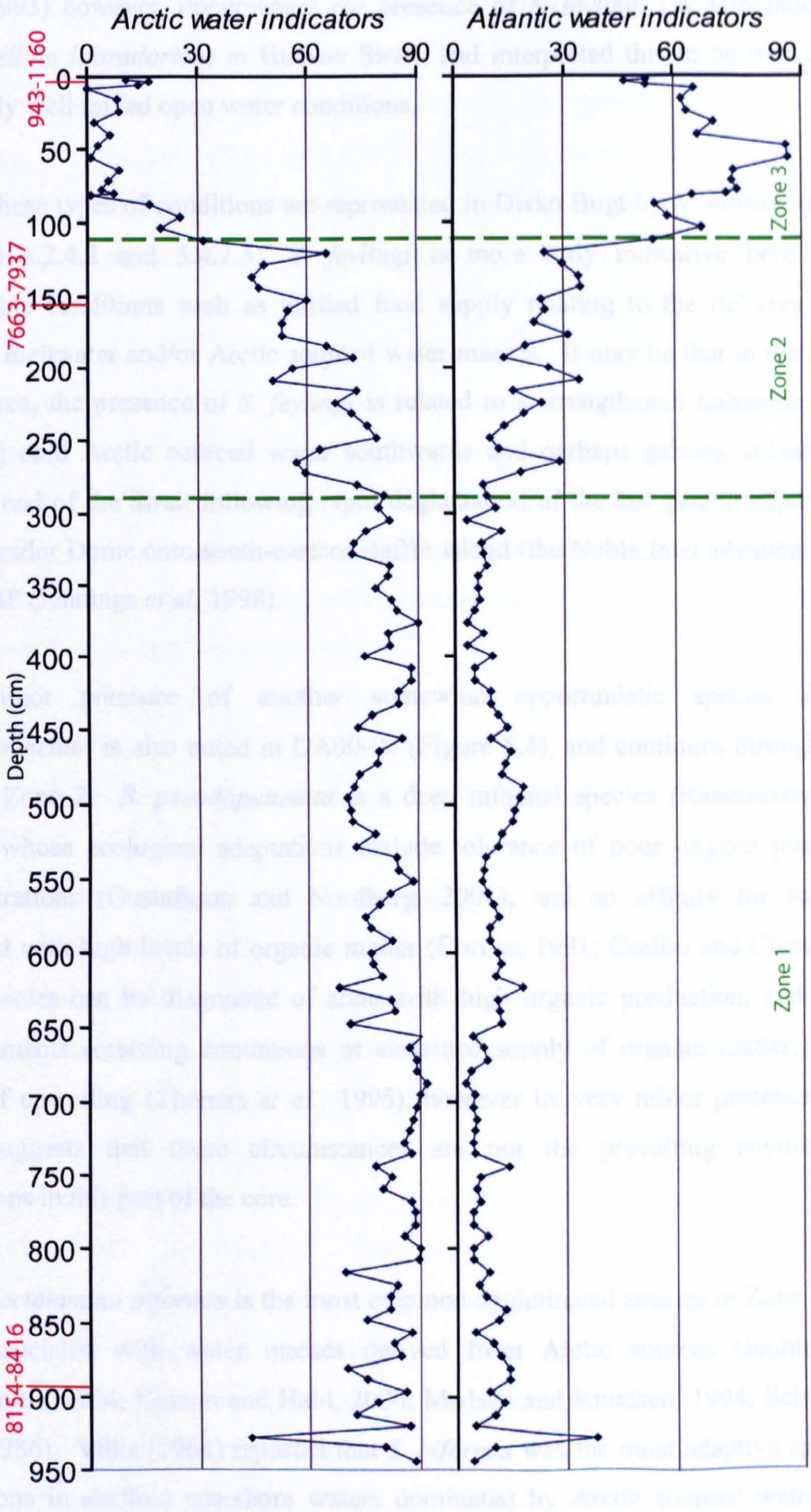

Figure 5.5: Summary of water mass changes reflected by indicator species representative of Arctic/Atlantic water masses. Data shown is sum of percentage of each indicator species. Arctic species: *S. feylingi, C. reniforme, E. excavatum, S. biformis,(B. pseudopunctata).* Atlantic species: *I. norcrossi, S. difflugiformis, C. crassimargo, N. labradorica, B. tenerima, C. teretis, M. zaandamae.* Radiocarbon dates shown in red and given in cal yrs BP. Foraminiferal zones marked in green.

Silis (1993) however, documented the presence of *S. feylingi* (in association with *Nonionellina labradorica*) in Hudson Strait, and interpreted this to be indicative of relatively well mixed open water conditions.

While these types of conditions are represented in Disko Bugt by *N. labradorica* (see sections 5.2.4.2 and 5.4.2.3), *S. feylingi* is more truly indicative here of less favourable conditions such as limited food supply relating to the delivery of low salinity meltwater and/or Arctic sourced water masses. It may be that in the Hudson Strait area, the presence of *S. feylingi* is related to a strengthened Labrador Current carrying cold Arctic sourced water southwards and perhaps gaining access to the eastern end of the Strait following rapid deglaciation of the last glacial expansion of the Labrador Dome onto south-eastern Baffin Island (the Noble Inlet advance) 8.9-8.4 ka cal BP (Jennings *et al.* 1998).

The minor presence of another somewhat opportunistic species *Bolivina pseudopunctata* is also noted in DA00-06 (Figure 5.4), and continues through to the end of Zone 2. *B. pseudopunctata* is a deep infaunal species (Rassmussen *et al.*, 2002), whose ecological adaptations include tolerance of poor oxygen pore water concentrations (Gustafsson and Nordberg, 2001), and an affinity for sediments supplied with high levels of organic matter (Corliss, 1991; Corliss and Chen, 1988). This species can be diagnostic of areas with high organic production, and bathyal environments receiving continuous or sustained supply of organic matter, such as areas of upwelling (Thomas *et al.*, 1995), however its very minor presence in this zone suggests that these circumstances are not the prevailing environmental conditions in this part of the core.

Spiroplectammina biformis is the most common agglutinated species in Zone 1 and is also associated with water masses derived from Arctic sources (Jennings and Helgadottir, 1994; Korsun and Hald, 2000; Madsen and Knudsen, 1994; Schafer and Cole, 1986). Vilks (1964) reported that *S. biformis* was the most adaptive species to conditions in shallow nearshore waters dominated by Arctic sourced water in the Canadian Arctic. Minor amounts of *N. labradorica* and *Islandiella norcrossi* (Hald and Korsun, 1997) indicated that the supply of Atlantic sourced water to the area was limited. Both *N. labradorica* and *I. norcrossi* are generally associated with water

masses of Atlantic water origin (Hald and Korsun, 1997; Mudie *et al.*, 1984; Vilks, 1980) (but see further discussion of their occurrences in sections 5.2.4.2; 5.2.4.3 and 5.4.2.3 below). The low frequencies of *I. norcrossi* do fluctuate in Zone 1, with two maximum peaks at 944-850 cm and 525-425 cm, suggesting that the weak influence of Atlantic water has small episodes of intensification, or that meltwater flux from Jakobshavns Isbrae was not constant, allowing weak West Greenland Current incursion.

In summary therefore, the Zone 1 assemblage is almost wholly dominated by ice proximal and cold/Arctic water loving fauna (Figure 5.4 and 5.5), as well as an opportunistic coloniser *S. feylingi*, which thrives in harsh limiting conditions, typically with low primary productivity levels. This assemblage indicates that from *c.* 8.3 ka cal BP, the area was under the influence of an Arctic sourced water mass, with a greatly reduced warm WGC component.

5.2.3.1 Interpretation of DA00-06 Zone 2

The faunal assemblage in Zone 2 suggests that the water masses in front of Jakobshavns Isbrae were undergoing a transitional period. There is clear evidence of amelioration in conditions, with marginal strengthening of the relatively warm West Greenland Current. While the fauna are still dominated by cold Arctic water species and show glaciomarine species (*S. biformis, C. reniforme* and *E. excavatum*), there is a noticeable decrease in *C. reniforme* (the cold meltwater/Arctic water species) and the opportunistic *S. feylingi*. At the same time there is an increase in the Atlantic indicator species *I. norcrossi,* and the agglutinated *Adercotryma glomerata* (not shown in Figure 5.4 but can be seen in Figure 4.1 in chapter 4), a species commonly associated with Atlantic sourced waters (Hald and Korsun, 1997), and commonly found in the modern day assemblages . Figure 5.6 (Lloyd *et al.*, submitted) shows these modern assemblages, taken from sample sites in Disko Bugt, the locations are marked in Figure 5.2.

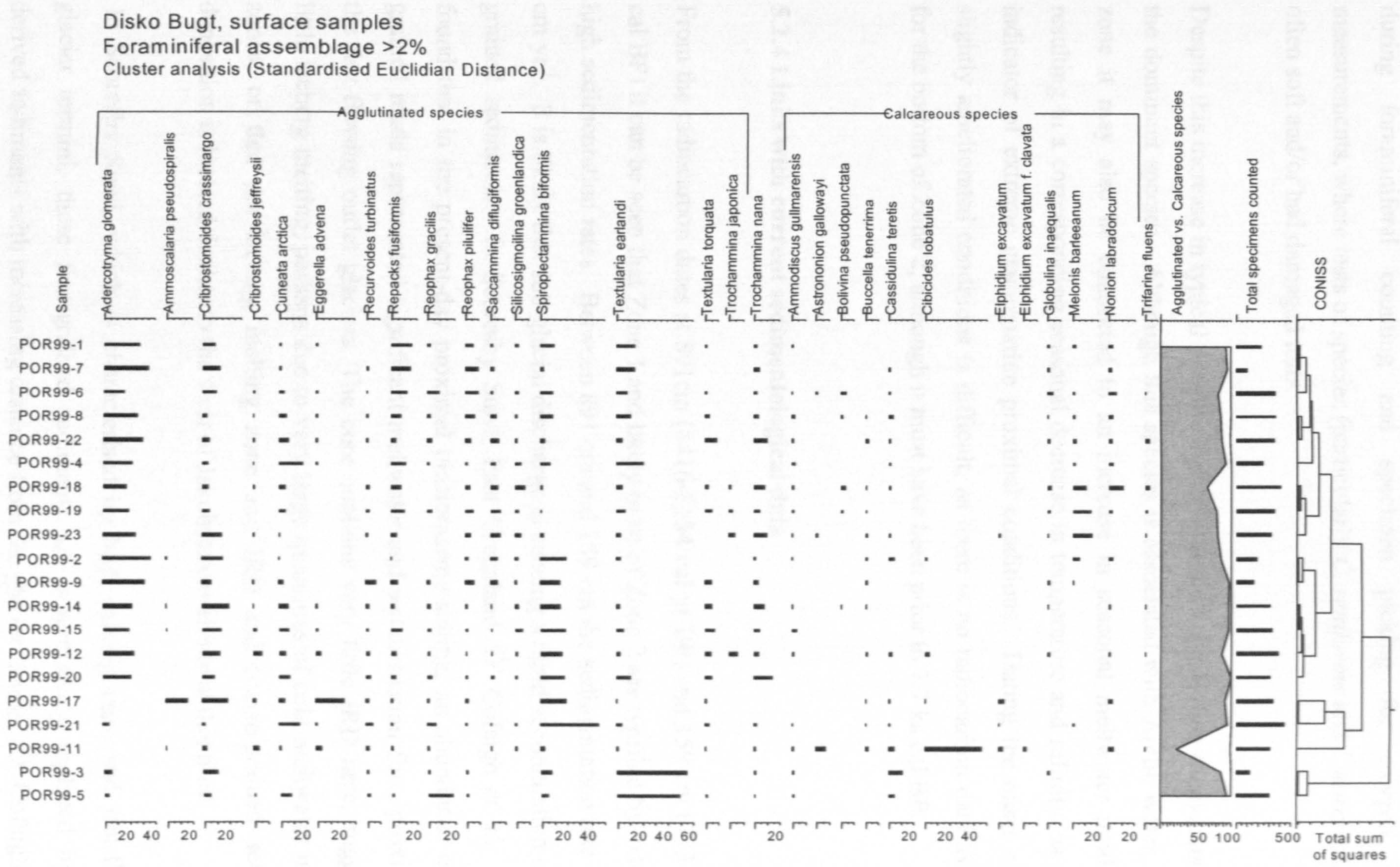

Figure 5.6: Modern assemblage distributions of Disko Bugt foraminifera (codes refer to Porsild 1999 CTD cast sites and surface sampling locations shown in Figure 5.2)

At the same time there is an increase in the organic walled test linings, indicating poor preservation and dissolution of the calcareous tests. Evidence of this was observed during foraminiferal counting and specimen picking for oxygen isotope measurements, where tests of species (particularly *C. reniforme* and *I. norcrossi*) were often soft and/or had damaged tests.

Despite this increase in typical Atlantic Water indicators, *Elphidium excavatum* is still the dominant species. Although this species is associated with Arctic water, in this zone it may also be connected to an increase in seasonal meltwater production, resulting in a corresponding seasonal decrease in temperature and salinity, as it is an indicator of extreme glaciomarine proximal conditions. Dating the onset of these slightly ameliorated conditions is difficult, as there is no radiocarbon date available for the bottom of Zone 2, although it must have been prior to 7.7 ka cal BP.

5.2.4 Links with current sedimentological data

From the radiocarbon dates at 891cm (8416-8154 cal yr BP) and 159 cm (7937-7663 cal BP) it can be seen that Zone 1 and likely most of Zone 2 are typified by extremely high sedimentation rates. Between 891 cm and 159 cm the sedimentation rate is 1.38 cm yr^{-1}. It is likely that sub-glacial discharge is causing a rapid accumulation of fine-grained sediments. In Scoresby Sund, East Greenland, Ó' Cofaigh *et al.*, (2001) found that in the present-day proximal glaciomarine setting, an abundance of fine-grained muds represented significant meltwater and sedimentation flux, proximal to the fast-flowing outlet glaciers. The core contains very little IRD here, suggesting little iceberg melting, perhaps due to very large quantities of cold meltwater in these zones, or that the iceberg melting zone and IRD and coarse-grained sediment deposition is located further to the west of Jakobshavns Isbrae at this time.

In Scoresby Sund, which is characterised by high calving rates and fast-flowing glacier termini, these fine-grained sediments are progressively replaced by IRD derived sediments with increasing distance from the glacier termini (Ó' Cofaigh *et al.*, 2001). Sedimentological data produced by Morros (Lloyd *et al.* submitted) (Figure 5.7) show that Zone 2 is dominated by fine-grained sediments, with generally less

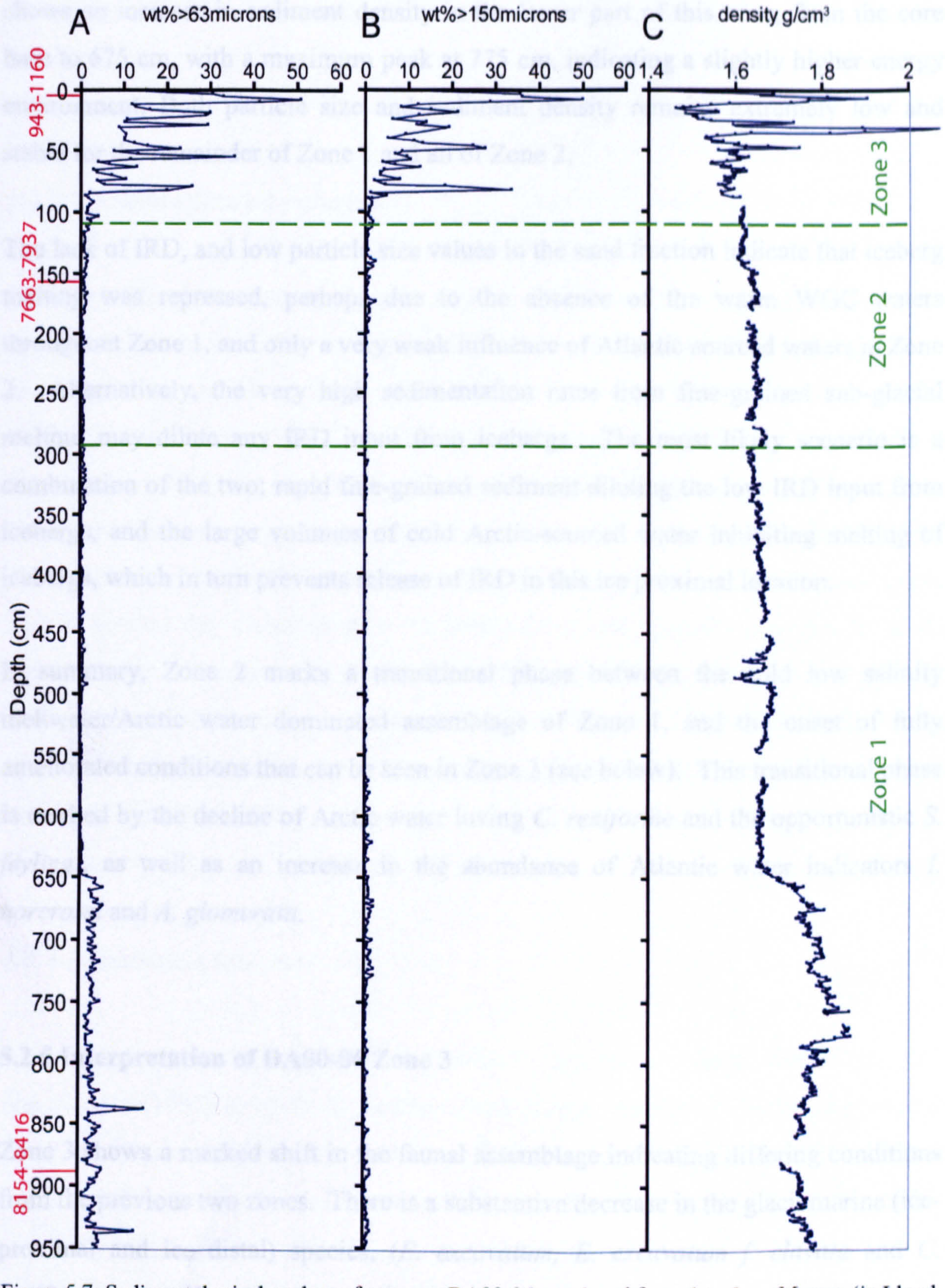

Figure 5.7: Sedimentological analyses from core DA00-06, produced from data from Morros (in Lloyd *et al.*, submitted). A: Particle size data for sediment fraction >63 microns, B: particle size data for sediment fraction >150 microns, C: Sediment density data in grams per cubic cm. Gaps in density data are due to no data being recorded at these depths, and no interpolation between points. Radiocarbon dates are shown in red and are given in cal yrs BP. Foraminiferal zones are shown in green.

than 5% sand fraction in the lower part of the zone, reducing further to <1% above 650 cm (Lloyd *et al.* submitted). This is also shown from a lack of clasts >2 mm in the IRD record (see Chapter 4). The sedimentological data (Lloyd *et al.* submitted)

shows an increase in sediment density in the lower part of this zone, from the core base to 675 cm, with a maximum peak at 775 cm, indicating a slightly higher energy environment. Both particle size and sediment density remains extremely low and stable for the remainder of Zone 1 and all of Zone 2.

The lack of IRD, and low particle size values in the sand fraction indicate that iceberg melting was repressed, perhaps due to the absence of the warm WGC waters throughout Zone 1, and only a very weak influence of Atlantic sourced waters in Zone 2. Alternatively, the very high sedimentation rates from fine-grained sub-glacial meltout may dilute any IRD input from icebergs. The most likely scenario is a combination of the two; rapid fine-grained sediment diluting the low IRD input from icebergs, and the large volumes of cold Arctic-sourced water inhibiting melting of icebergs, which in turn prevents release of IRD in this ice proximal location.

In summary, Zone 2 marks a transitional phase between the cold low salinity meltwater/Arctic water dominated assemblage of Zone 1, and the onset of fully ameliorated conditions that can be seen in Zone 3 (see below). This transitional phase is marked by the decline of Arctic water loving *C. reniforme* and the opportunistic *S. feylingi*, as well as an increase in the abundance of Atlantic water indicators *I. norcrossi* and *A. glomerata*.

5.2.5 Interpretation of DA00-06 Zone 3

Zone 3 shows a marked shift in the faunal assemblage indicating differing conditions from the previous two zones. There is a substantive decrease in the glaciomarine (ice-proximal and ice distal) species, (*E. excavatum, E. excavatum f. clavata* and *C. reniforme*) as well as almost complete disappearance of the opportunistic *S. feylingi*. At the same time, there is a large increase in the species representative of Atlantic-sourced waters; *I. norcrossi* (the most dominant species in this zone), *N. labradorica* and *A. glomerata*. With nearly total decline of cold-water taxa, this allows the establishment of other species of Atlantic origin and warmer water mass conditions, such as *Cribostomoides crassimargo, Saccammina diflugiformis, Bucella tenerrima, Cassidulina teretis,* and *Melonis zaandamae*. The following sections relating to Zone

3 in this core discuss detailed environmental parameters relating to specific indicator species.

5.2.4.2 Nonionellina labradorica

N. labradorica has been interpreted as being indicative of a range of environments and water masses by different authors (e.g. Hald and Korsun, 1997; Jennings *et al.*, 2001; Jennings and Helgadottir, 1994; Schafer and Cole, 1982; Scott *et al.*, 1984; Vilks and Deonarine, 1988). For this thesis I have assumed that *N. labradorica* is diagnostic of relatively warm and stable Atlantic sourced water masses (i.e. the West Greenland Current), supported by the interpretive work of Hald and Korsun (1997), Hansen and Knudsen (1995), Jennings *et al.*, (2001) and Vilks and Deonarine (1988), and its present day distribution in the Disko Bugt area (Lloyd, *in prep.*), in which Atlantic sourced water masses associated with the WGC are dominant. Further discussion relating to the range of associated environmental parameters and water mass associations is developed more fully in section 5.5 as this is the most dominant species in core DA00-03.

5.2.4.3 Islandiella norcrossi

I. norcrossi was found to be associated with "Transformed Atlantic Water" by Hald and Korsun (1997) in fjords of Svalbard, and is representative of water masses with relatively higher salinity and temperature (Mudie *et al.*, 1984; Vilks, 1980). Further specific information concerning controlling environmental parameters is somewhat clouded by likely issues of taxonomic misidentification in other studies (Andrews *et al.*, 1994). For example, Hunt and Corliss (1993) found large tests of *I. norcrossi* difficult to distinguish from *I. helenae*, and therefore did not separate the species, instead grouping them together under *I. helenae*. Unfortunately, Vilks and Deonarine (1988) identify *I. helenae* as a cold and relatively low salinity shelf species, likely to be associated with the Arctic water component of the Labrador Current, and so care must be taken when referring to previously published assemblage interpretations.

In south-central Hudson Bay, the establishment of post-glacial conditions was inferred from a calcareous-dominated assemblage, with species including *N. labradorica* and *I. norcrossi* (Jennings *et al.*, 2001; Silis, 1993), very similar to that seen in Zone 3 of this core from Disko Bugt. The presence of *I. norcrossi/helenae* in sediments relating to the Holocene thermal optimum in the Barents Sea by Duplessy *et al.* (2001) was thought to reflect a lengthened ice-free season, and a retreat of the sea-ice margin.

5.2.4.3 Adercotryma glomerata and Spiroplectamina diflugiformis

A. glomerata and also *S. diflugiformis* (referred to as *Reophax atlantica* by Jennings and Helgadottir, 1994 and Hald and Korsun, 1997), are interpreted in Disko Bugt to be indicative of Atlantic sourced waters, although in sub-Arctic locations in northwest Europe they can be interpreted as transitional species or related to chilled Atlantic waters with a sub-Arctic component (Alve and Nagy, 1986; Hansen and Knudsen, 1994). These slightly contrasting environmental interpretations may well be related to preservation interpretations, or methods of processing sediment samples, as drying and dry picking samples often leads to arenaceous test destruction.

However, in high latitudes, *A. glomerata* and *S. diflugiformis* are clearly associated with Atlantic sourced waters (Bilodeau *et al.* 1994; Hald and Korsun, 1997; Jennings and Helgadottir, 1994; Vilks, 1980), and these interpretations are relied upon here. This interpretation is also clearly supported by contemporary data from Disko Bugt (Lloyd, in prep.), showing high concentrations of *A. glomerata* and *S. diflugiformis* in samples strongly influenced by the present day warm West Greenland Current (see Figure 5.4).

5.2.4.5 Bucella species

Bucella sp. in general, are associated with open water post-glacial conditions, although often in deeper water or slope sediments (Madsen and Knudsen, 1994). Knudsen (1988) found the presence of *Buccella sp.* to be indicative of higher salinities

and deeper, sub littoral environments. The presence of *Bucella sp.* have been interpreted by Polyak and Solheim (1996) to be indicative of periods of higher seasonal productivity in the Barents Sea, and, like *N. labradorica,* are known to be extremely sensitive to food supply (Polyak and Solheim, 1996), and is used in this thesis as being diagnostic of Atlantic sourced water.

5.2.4.6 Cassidulina species

Cassidulina sp. are widely distributed throughout both Arctic and sub-Arctic seas (Mackensen and Hald, 1988; Wollenburg and Mackensen, 1998a; 1998b). Vilks (1989) characterised *C. teretis* as being representative of Labrador Sea waters. *C. teretis* is also well established in deeper waters of Atlantic origin. Jennings and Weiner (1996) found that *C. teretis* occured in chilled Atlantic water at depths usually greater that 100m, but also as shallow as 20 m, and down to depths of 1100 m (Steinsund and Hald, 1994). Mackensen and Hald (1988) described it in their modern samples taken from the Norwegian continental slope under the influence of Atlantic water. It is also found in the Barents Sea at depth in troughs on the shelf (Polyak and Solheim, 1994). It has been found in similar in environments on the shelf and slope of Baffin Island (Osterman and Nelson, 1989; Vilks, 1989).

The weak (or lack of) presence of this species in the Disko Bugt may then be a function of water depth. as opposed to specific water mass characteristics; or, it could just be that it was being out-competed in the area by other species. As discussed by Andrews *et al.,* (1994) care must be taken with the interpretation of this species as it shows considerable taxonomic similarities with other species, such as *Cassidulina laevigata, I. norcrossi* and *I. helenae*, and these authors are convinced that there may be a significant degree of taxonomic mis-representation in similar studies.

5.2.4.7 Melonis zaandamae

M. zaandamae has previously been used to infer boreal or sub-Arctic conditions in Scandinavian palaeoenvironmental studies (Feyling-Hanssen, 1980). However, other

work (Jansen *et al.*, 1983; Mackensen *et al.*, 1985; Sjerup *et al.*, 1981) found that in the Norwegian Sea and surrounding areas, sediment type was a key controlling factor in its distribution. These studies showed that this species can also display a preference for rapid pelitic sedimentation associated with winnowing caused by an increase in bottom water current regimes, and that there is a significant correlation between the occurrence of *M. zandamae* and fine-grained sediments with a high organic content. Osterman and Nelson (1989) however, found that this species could thrive in both this type of sediment, as well as being dominant in environments with a high sand content.

Silis (1993) related the presence of *M. zaandamae* in Eastern Basin, Hudson Strait to the influx of warmer, more saline Labrador Sea waters with increased productivity typical of postglacial conditions. Vilks and Deonarine (1989) identify *M. zaandamae* as being restricted to the warmer and more saline offshore and slope water components of the Labrador Current. The widespread extent of *M. zaandamae* in eastern Canadian sedimentary environments (Osterman, 1984; Osterman and Nelson, 1989) throughout ameliorated postglacial conditions is not seen in DA00-06, or in the other cores (DA00-03 and DA00-05). This is somewhat surprising, as it could have been assumed that this species should have been a key indicator for the presence of the WGC in Disko Bugt.

There are a number of possible reasons for this. Firstly, the lack of dominance of this species in the area is likely to be due in part to a function of water depth. Depths in the eastern part of Hudson strait are up to 900 m (Jennings *et al.*, 1998). However, in surface foraminiferal assemblages taken in Disko Bugt in the same locality as DA00-06 with water depths shallower than 350 m, *M. zaandamae* accounts for up to 20% of the assemblage (Lloyd, *in prep.*). Secondly, it may well be that post-depositional dissolution of calcareous tests is limiting a truly representative picture of the past distribution of this (as well as other) calcareous species in the core.

5.2.4.8 Cuneata arctica

Although not directly associated with the warmer more saline Atlantic sourced waters, *Cuneata arctica* also increases in Zone 3. In recent shelf sediments in Scoresby Sund in East Greenland, Madsen and Knudsen (1994) reported that *C. arctica* (called *R. arctica*) was recorded in association with *S. biformis*, and they linked *C. arctica* with the "Fjord water layer". This layer is characterised by considerable seasonal and annual fluctuations in temperature and salinity related to significant summer glacier meltwater input into Scoresby Sund.

In Hudson Strait, present day assemblages are dominated by *C. arctica* (called *R. arctica*) and *S. biformis*, as well as *S. feylingi* and *N. labradorica* (Jennings *et al.*, 2001), relating to the relatively well mixed open water conditions existing at present, with little glaciomarine influence. *C. arctica* is also found in the contemporary samples analysed in Disko Bugt. However, *N. labradorica* is relatively rare (see Figure 5.6), (Lloyd, *in prep.*)). At first sight this might seem to be surprising given the dominance of the West Greenland Current as the basal water mass throughout Disko Bugt, but it is likely to be due to the relatively shallow sample locations of this study.

It is interesting to note the very low abundances of species such as *S. feylingi, C. reniforme,* and *E. excavatum* in the contemporary data (Figure 5.6). This is due to the limited influence of relatively cold Arctic sourced waters in Disko Bugt at the present day. The conditions in Hudson Strait and the eastern parts of the Canadian Archipelago are influenced by the southward flowing colder and less saline Arctic component of the Labrador Current. Lloyd *et al.* (submitted) categorised *C. arctica* as a cold loving fauna, relating it to Arctic sourced waters and found in close association with *S. biformis* in a short gravity core located further west from the DA00-06 core site (See Figures 5.1 and 5.2).

In DA00-06, *C. arctica* displays a similar distribution to both *A. glomerata*, and *S. biformis*. However, it is not one of the most dominant species in the core (<15% at its greatest extent), and as with the East Greenland studies (Jennings and Helgadottir, 1994; Madsen and Knudsen, 1994) *C. arctica* in this core is likely to be related to the

less saline and colder waters produced from enhanced seasonal melting which will in turn have been influenced by the re-instigation of an Atlantic water mass in the eastern part of Disko Bugt in front of Jakobshavns Isbrae.

5.2.4.9 Links to the sedimentological data

The shift from the core assemblage being dominated by primarily Arctic water indicator species to mainly Atlantic sourced species in Zone 3 is matched by dramatic changes in the sedimentological data (see Figure 5.7). The considerable increases in the three clast fractions in the IRD record previously described in Chapter 4, indicates warming and ameliorated conditions created by the strong presence of WGC waters allowing the rapid melting of sediment loaded icebergs in front of Jakobshavns Isfjord. In the particle size data also shown in Figure 5.6 (Morros, *unpublished data*) there is a corresponding increase in the >63 and >150 micron categories, and sediment density increases, reflecting perhaps a change in sediment type, or source. The onset of these changes is not precisely dated, but occurred some time after 7.7 ka cal BP.

The top of the core and the faunal zone is dated at around 1 ka cal BP, indicating that these changes were accompanied by a tremendous decrease in sedimentation rate from approximately 14 mm/yr to 1 mm/yr. The other most notable change in this zone in the core is the considerable increase in the abundance of organic test linings, relating to increased dissolution. Within this zone it is interesting to note that there is an intensification of these ameliorated conditions around 50-80 cm (Figure 5.2). It can clearly be seen that at this point there is a degree of intensification of particularly calcareous species representative of Atlantic sourced waters, with a peak of *B. tenerrima, C. teretis, I. norcrossi* and *M. zaandamae*, which is accompanied by a distinct lack of organic walled foraminiferal test linings.

This phase in the core can be approximately dated to 4.6-4.0 ka cal BP, prior to the onset of the Neoglacial, which is well documented in West Greenland (Kelly, 1985; Weidick *et al.*, 1990). This represents a period of increased intensity in the West Greenland Current flow, or perhaps an increase in the warmer water Irminger Current component of the WGC. It may be linked to the Holocene optimum prior to the

Neoglacial period. After this short-lived phase, this zone returns to the conditions initiated at the beginning of the zone.

5.2.5 Summary interpretation of DA00-06

By combining the main individual agglutinated and benthic species representative of the two contrasting water mass sources (Figure 5.3 and Figure 5.4), it can clearly be seen that during Zone 1, Arctic sourced waters are overwhelmingly dominant in DA00-06, followed by a transitional period through Zone 2 which develops into an almost fully Atlantic sourced water mass dominated assemblage at some point after 7.7 ka cal BP, indicating a strong WGC had been established by this point.

Although this core is limited by the chronology available, using the age model developed for DA00-06 in Chapter 4 gives an estimate for the onset of this zonal pattern of between 6.1 and 5.7 ka cal BP. This timing is in agreement with evidence from a range of sources in coastal West Greenland and Baffin Bay (e.g. mollusc, dinocyst and foraminferal studies) which provide information on the initiation of the WGC in this area (e.g. Bennike *et al.*, 1994; Donner and Jungner, 1975; Kelly, 1979 and 1985; Osterman and Nelson, 1989, Feyling-Hanssen and Funder, 1990; Funder and Weidick, 1991; Ingolfsson *et al.*, 1990; Levac, 2001), although there has been evidence of a weak WGC in northern Baffin Bay as early as 9 ka cal BP (Osterman and Nelson, 1989). This will be discussed in Chapter 6. Further discussion relating to the WGC strength, initiation and relationship with the post-glacial history of West Greenland will also be developed within Chapter 6.

5.3.1 DA00-05 Introduction

DA00-05 is located in the southeast of Disko Bugt at the mouth of Kangersuneq Fjord (Figure 5.1). It is ideally located to investigate the oceanographic evolution of Disko Bugt away from the considerable influence of Jakobshavns Isbrae. The local signature of Jakobshavns Isbrae may dilute or drown out the regional oceanographic signal at DA00-06. The duration of the core record (approximately 6.7 ka) allows a

detailed interpretation of changing water mass characteristics following the Holocene thermal optimum (~ 9-6 ka) which has been well-documented from a range of studies throughout the high latitudes (e.g. de Vernal *et al.*, 1993; Koç *et al.*, 1993; Sarnthein *et al.*, 1995; Veum *et al.*, 1992).

Interpretation is based upon zonal and sub-zonal faunal assemblage data presented in Chapter 4, and is discussed in relation to existing sedimentological and present day foraminiferal assemblage data (Morros, unpublished data in Lloyd *et al.*, submitted and Lloyd *in prep.*). Agglutinated faunal indicator species are plotted separately to remove the bias created by the dissolution effects seen in Zone 2 (Figure 5.8). No X-radiograph photographs or stable isotope measurements are available for this core.

5.3.2 Interpretation of DA00-05 Zone 1

Zone 1 extends from the base of the core to 545 cm and is further sub-divided into three sub-zones (a, b and c). It is characterised by a mixed benthic foraminiferal assemblage, dominated by *I. norcrossi* and has relatively high species diversity and foraminiferal abundance indicating the presence of stable saline Atlantic sourced waters. Figure 5.9 shows that Atlantic water indicators mainly influence this zone, with a weak influence from colder Arctic sourced water. The most dominant agglutinated species is *Reophax gracilis* which, although has not been specifically related to either Arctic or Atlantic water mass characteristics, is present in other assemblages documented in high latitude studies (Hald and Korsun, 1997; Hald and Steinsund, 1992; Hansen and Knudsen, 1995; Osterman and Nelson, 1989), and more importantly is present in the modern foraminiferal assemblages of Disko Bugt (Figure 5.6) (Lloyd *in prep.*).

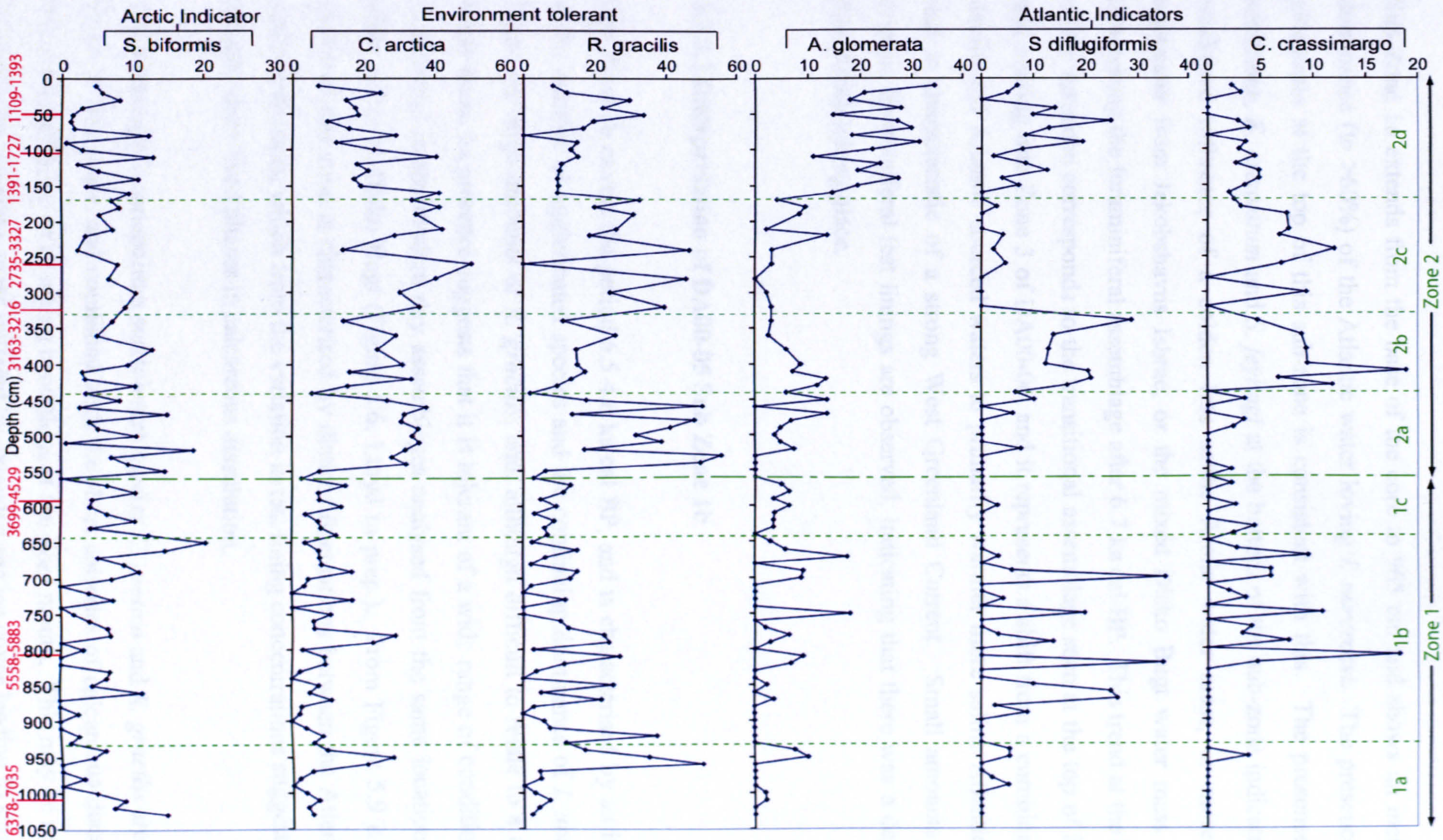

Figure 5.8: Individual percentage assemblage data for (agglutinated) indicator species in core DA00-05. Radiocarbon dates are given in red in cal yrs BP. Foraminiferal zones are marked in green based on cluster analysis.

5.3.2.1 Interpretation of DA00-05 Sub Zone 1a

Sub Zone 1a extends from the base of the core to 965 cm and shows an increasing dominance (to >60%) of the Atlantic water loving *I. norcrossi.* The presence of *A. glomerata* at the top of this sub-zone is consistent with this. The presence of *C. reniforme, E. excavatum* and *S. feylingi* at the bottom of the sub-zone indicate that a weakened influence of a colder, less saline Arctic water mass, or more likely meltwater from Jakobshavns Isbrae, or the mixed Disko Bugt water mass is still influencing the foraminiferal assemblage after 6.7 ka cal BP. This trend at the bottom of the sub-zone corresponds to the transitional assemblage seen at the top of Zone 2, and moving into Zone 3 of DA00-06, and it represents a shift from a combination of Arctic and Atlantic sourced waters to primarily warmer more saline Atlantic water that is characteristic of a strong West Greenland Current. Small amounts of the organic foraminiferal test linings are observed, indicating that there was a degree of dissolution taking place.

5.3.2.2 Interpretation of DA00-05 Sub Zone 1b

Sub Zone 1b covers the period 6.5-4.6 ka cal BP, and is characterised by an increase in the number of agglutinated species and the continuing dominance of *I. norcrossi.* There are large amounts of *R. gracilis*, and, although difficult to relate to a specific water mass, its presence suggests that it is tolerant of a wide range of conditions as it is observed in the modern day assemblages analysed from the same location and at other points in Disko Bugt (Figure 5.6, Lloyd in prep.). From Figure 5.9 it can be seen that this zone is characterised by distinct fluctuations between the Atlantic and Arctic indicators, which from the variation in test lining concentrations suggests a link to rapid short lived phases in calcareous dissolution.

The seemingly cosmopolitan and tolerant species *C. arctica* and *R. gracilis* are able to thrive at this point, and combined with the short episodes of calcareous dissolution, this is an indication of changing conditions at the fjord mouth. This may be related to stagnation of the water mass initiated by extended sea ice cover leading to stagnation, and/or a strong pycnocline (a depth in the water column where there is an abrupt

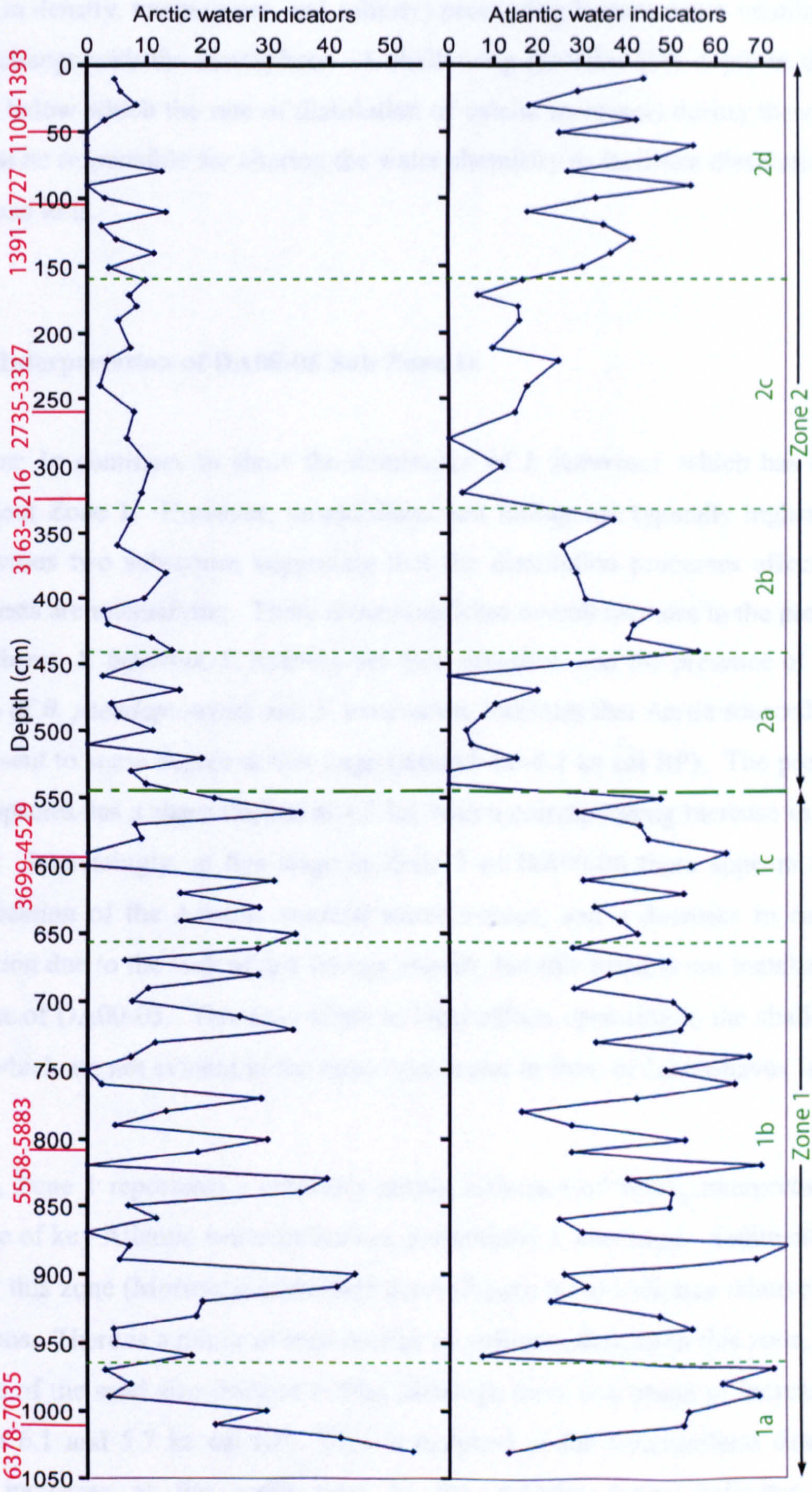

Figure 5.9: Summary of water mass changes reflected by indicator species representative of Arctic/Atlantic water masses in core DA00-05. Data shown is sum of percentage of each indicator species. Arctic species: *S. feylingi, C. reniforme, E. excavatum, S. biformis, S. concava.* Atlantic species: *A. glomerata, I. norcrossi, S. diflugiformis, C. crassimargo, N. labradorica, B. tenerima, C. teretis, M. zaandamae.* Radiocarbon dates shown in red (cal yrs BP). Foraminiferal zones in green.

change in density, temperature, and salinity) preventing bottom water ventilation and CO_2 exchange with the atmosphere. A shallowing lysocline (the depth in the water column below which the rate of dissolution of calcite increases) during these periods may also be responsible for altering the water chemistry to facilitate dissolution of the calcareous tests.

5.3.2.3 Interpretation of DA00-05 Sub Zone 1c

Sub Zone 1c continues to show the dominance of *I. norcrossi,* which has occurred throughout Zone 1. However, foraminiferal test linings are typically higher than in the previous two sub-zones suggesting that the dissolution processes affecting less robust tests are intensifying. There is no significant overall increase in the presence of *C. reniforme, S. biformis, S. feylingi,* but their presence, and the presence of between 15-20% of *B. pseudopunctata* and *E. excavatum,* indicates that Arctic sourced water is still present to some degree at this stage (around 4.6-4.1 ka cal BP). The presence of Arctic species has a sharp decline at 4.3 ka, with a corresponding increase in Atlantic species. Interestingly, at this stage in Zone 3 of DA00-06 there appears to be an intensification of the Atlantic sourced water masses, and a decrease in calcareous dissolution due to the lack of test linings present, but this trend is not matched in this sub-zone of DA00-05. This may relate to local effects operating in the shallow fjord water, which are not evident in the more open water in front of Jakobshavns Isbrae.

Overall, Zone 1 represents a relatively strong influence of WGC, interpreted by the presence of key Atlantic water indicators, particularly *I. norcrossi.* Sedimentological data for this zone (Morros, unpublished data) (Figure 5.10) indicates relatively stable conditions. There is a minor overall decline in sediment density in this zone, and low amounts of the sand size fraction (<5%), although there is a phase of increased sand between 6.1 and 5.7 ka cal BP. This is matched in the foraminiferal data, which shows increases at the same time in the Atlantic water indicator species.

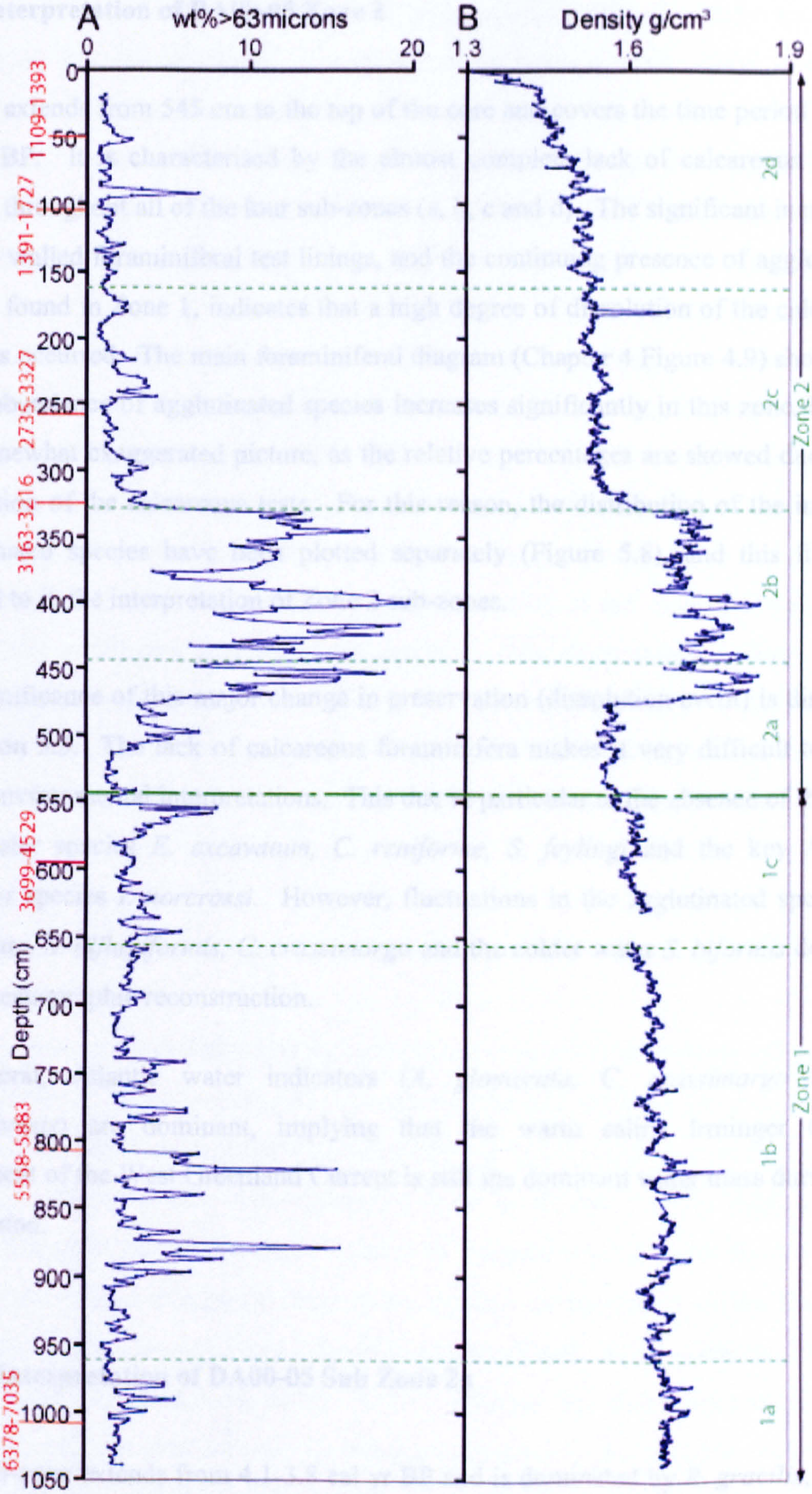

Figure 5.10: Sedimentological analyses from core DA00-05, produced from data from Morros (in Lloyd *et al.*, submitted). A: Particle size data for sediment fraction >63 microns (sand size fraction) B: Sediment density data in grams per cubic cm. Gaps in density data are due to no data being recorded at these depths, and no interpolation between points. Radiocarbon dates are shown in red and are given in cal yrs BP. Foraminiferal zones are shown in green.

5.3.3 Interpretation of DA00-05 Zone 2

Zone 2 extends from 545 cm to the top of the core and covers the time period 4.1-1.3 ka cal BP. It is characterised by the almost complete lack of calcareous species present throughout all of the four sub-zones (a, b, c and d). The significant increase in organic walled foraminiferal test linings, and the continuing presence of agglutinated species found in Zone 1, indicates that a high degree of dissolution of the calcareous tests has occurred. The main foraminiferal diagram (Chapter 4 Figure 4.9) shows that the % abundance of agglutinated species increases significantly in this zone, but this is a somewhat exaggerated picture, as the relative percentages are skewed due to the dissolution of the calcareous tests. For this reason, the distribution of the indicator agglutinated species have been plotted separately (Figure 5.8), and this figure is referred to in the interpretation of Zone 2 sub-zones.

The significance of this major change in preservation (dissolution event) is discussed in section 5.5. The lack of calcareous foraminifera makes it very difficult to make palaeoenvironmental interpretations. This due in particular to the absence of the main cold water species *E. excavatum, C. reniforme, S. feylingi* and the key Atlantic indicator species *I. norcrossi.* However, fluctuations in the agglutinated species *A. glomerata, S. diflugiformis, C. crassimargo* and the colder water *S. biformis* do allow palaeoceanographic reconstruction.

In general, Atlantic water indicators (*A. glomerata, C. crassimargo* and *S. diflugiformis*) are dominant, implying that the warm saline Irminger Current component of the West Greenland Current is still the dominant water mass during this time period.

5.3.3.1 Interpretation of DA00-05 Sub Zone 2a

This sub-zone extends from 4.1-3.8 cal yr BP and is dominated by *R. gracilis*, and *C. arctica.* In the modern surface assemblages (Figure 5. 6), the presence of *R. gracilis* is rare, (its presence is generally negatively correlated with *A. glomerata*) indicating that it is not directly related to a strong WGC influence (Lloyd, in prep). However, it

is important to note that it is not taken to be representative of Arctic water mass conditions, but rather that it is quick to colonize areas where there is no clear dominance of a particular water mass. Indeed, Figure 5.8 shows that specific Arctic and Atlantic water mass indicators are not dominant in this sub-zone (10-15% each), although *A. glomerata,* indicative of warmer, more saline waters does increase towards the top of the sub-zone.

C. arctica is present in the modern assemblages in Disko Bugt, as well as forming part of modern day assemblages in East Greenland (Madsen and Knudsen, 1994) and Hudson Strait (Jennings *et al.,* 2001; Silis, 1993). In East Greenland this species is related to the "Fjord water layer" which reflects the significant variations in temperature and salinity created by seasonal meltwater influx. In East Canada, the presence of *C. arctica* is thought to be representative of the relatively well-mixed-open water conditions existing at present, with little glaciomarine influence. The presence of this species in these differing environmental conditions suggests that *C. arctica* is not sensitive to water mass changes, and Figure 5.8 shows that throughout Zone 1 and most of Zone 2 the occurrence of this species is relatively constant.

5.3.3.2 Interpretation of DA00-05 Sub Zone 2b

This sub-zone is characterized by an increase in the Atlantic water mass indicators, *C. crassimargo, S. diflugiformis* and *A. glomerata* (the latter at the bottom only). Vilks and Deonarine (1989) identified *C. crassimargo* as being representative of the colder, less saline shelf waters. In Kangersuneq Fjord in southeast Disko Bugt however, based on modern assemblage data (Figure 5.6) the presence of *C. crassimargo* is more likely to be related to Atlantic sourced waters, and the occurrence of the species on the Labrador shelf may be more a function of water depth, as the cores were taken in much deeper water, around 580m. *C. crassimargo* has often been identified as *Alveolophragmium crassimargo* in previously published work (Hald and Korsun, 1997). Jennings and Helgadottir (1994) did not find this species in any significant concentration or in tandem with any other species to establish preferential ecological requirements, whilst Hald and Korsun (1997) found similar difficulty in relating this

species in Svalbard fjords to any specific environmental parameter, as it had a patchy distribution in both inner and outer parts of fjords.

Frequencies of *C. arctica* remain constant, but the salinity and temperature tolerant *R. gracilis* decreases significantly throughout this sub-zone, suggesting that it is displaced by the warmer-loving Atlantic indicators. This sub-zone corresponds to an approximate time between 3.8-3.4 cal BP. Unpublished data from Morros indicates significant changes in the sedimentological record, with an increase in sediment density, and a gain in the sand size fraction to 15-20%. The increase in foraminifera (agglutinated), which are associated with warmer more saline waters suggests a stronger WGC, but the sedimentological record indicates increased seasonal sediment/meltwater flux input, and higher amounts of meltwater/Arctic species may therefore be expected.

High amounts of fine-grained sediment suspended in the fjord water are clearly visible during present day summer conditions at the mouth of the fjord, and the modern assemblages are dominated by agglutinated species, with a basal WGC water mass that has been identified in CTD casts (see Chapter 2 section 2.6.5). This indicates a degree of calcareous dissolution associated with prevailing conditions today. Foraminiferal evidence to determine whether the sediment input can be related to increases in colder, lower salinity meltwater in this zone (between 3.8 and 3.4 ka cal BP), is limited, as the key indicator species for this scenario would be the calcareous *C. reniforme/E. excavatum*, and the presence of these is unknown due to the likely dissolution processes occurring in Zone 2.

It may be that localised changes in the fjord hydrological system have allowed relatively warm species indicators to thrive, relating to warmer terrestrial conditions. This would account for the increase in sediment as a result of increased meltwater, which becomes more mixed with the underlying WGC water. The increase in sediment itself may also be a determining factor in the presence of the agglutinated warm indicators. At the same time, the increased sediment could be derived from extended sea ice. If there were a decrease in local precipitation, and increased wind stress, sediment would be transported further down fjord. Seasonal melting of the sea ice would allow input of a higher amount of food supply. The Atlantic indicator

species response to this environmental determining factor may then outweigh a salinity or temperature signal.

5.3.3.3 Interpretation of DA00-05 Sub Zone 2c

Zone 2c, between 3.4 and 2.0 ka cal BP, sees a return to the conditions of sub-zone 2a, with a decline in agglutinated species associated with the warmer more saline Atlantic sourced water masses. Arctic water indicators remain stable (although there is only *S. biformis* to draw inferences from), and the sub-zone assemblage suggests that the Atlantic indicators are competing with the species that are more tolerant of large fluctuations in salinity and temperature (*C. arctica* and *R. gracilis*). The minor amount of *C. crassimargo* suggests that this species is more tolerant than *A. glomerata* and *S. diflugiformis* of fluctuating conditions. These conditions may suggest that there was a dilution of the effect of the warm WGC waters by the overlying colder, low salinity meltwater layer, to give a deeper, well mixed layer similar to the "Fjord water layer" observed by Hansen and Knudsen (1995) in Scoresby Sund in East Greenland. Sedimentological data show stable conditions and that fine-grained sediments were dominant, with low quantities of sand.

5.3.3.4 Interpretation of DA00-05 Sub Zone 2d

This sub-zone extends from 2.0 ka cal BP to the core top which ends at 1.3 ka cal BP. Conditions during this time are likely to have been similar to those occurring in sub-zone 2b. There are decreased amounts of *C. arctica* and *R. gracilis*, which is complemented by an increase in the species associated with a dominantly warm WGC, i.e. *A. glomerata* and *S. diflugiformis*. Unlike sub-zone 2b however there is a shallow water associated species *Textularia torquata*, which is observed in small amounts in the Kangerssuneq fjord mouth modern assemblages. The dominance of *A. glomerata* and *C. crassimargo* is also seen in the present day surface assemblages in this area suggesting conditions similar to a relatively strong WGC.

Sediment density shows a steady gradual decrease to the core top indicating an increase in the quantity of pore water in the sediment. There is no significant change in the particle size data, but magnetic susceptibility is at its highest in the entire core in this sub-zone, indicating an influx of material which may be related to variations in local atmospheric conditions, e.g. an intensification of seaward wind stress. Increased winds and air temperatures may alter localised vegetation cover, and influence routes of sediment input to the fjord.

Throughout Zone 2 it appears that the assemblage is recording a fluctuation between species indicative of the warmer more saline Atlantic water mass associated with a warm and strong WGC, and species which are tolerant of large variations in salinity and temperature. The salinity and temperature fluctuations identified by variations in the foraminiferal fauna may be related to changes in meltwater and sediment supply from local fjord and terrestrial sources, as well as local atmospheric conditions arising from the proximal location of DA00-05 to the terrestrial environment. Dissolution processes operating on the calcareous foraminifera in the upper half of the core through Zone 2 limits interpretation relating to the Arctic water indicators. However the fluctuations seen through Zone 2 may also be tentatively linked to changes in the warm signal of the WGC. Hypothetically, a displacement of the IC component of the WGC to the south and west would allow a strengthening of the EGC branch, allowing the influx of relatively colder, lower salinity waters to the area.

5.3.4 Summary interpretation of DA00-05

In summary, core DA00-05 displays a faunal assemblage typical of relatively warm, saline Atlantic dominated water. The presence of a fully developed WGC system by the timescale covered in this core (around 6.7 ka cal BP) is supported by molluscan colonization patterns (Donner and Jungner, 1975; Funder and Weidick, 1991) as well as reinforcing foraminiferal, dinocyst and terrestrial data from coastal locations in West Greenland and Baffin Bay (e.g. Kelly, 1979 and 1985; Osterman and Nelson, 1989, Feyling-Hanssen and Funder, 1990; Ingolfsson *et al.*, 1990; Bennike *et al.*, 1994; Levac, 2001). In Zone 1, a mixed agglutinated and calcareous assemblage records the presence of a strong warm WGC, accompanied by a weak Arctic water

signal, similar to conditions interpreted by modern day surface assemblages (Lloyd in prep). In zone 2, calcareous fauna are subject to intensive dissolution processes, which will be discussed further in section 5.5. The remaining agglutinated foraminiferal assemblage suggests periods of stable WGC circulation, which were interrupted by changes in relative salinity and temperature perhaps arising from variations in meltwater supply or the separate components of the WGC.

5.4.1 Introduction to DA00-03

The core site and high sedimentation rates of DA00-03 in the deep trough in the outer part of Disko Bugt (see Fig 5.1 core location map) is well placed in the path of the flow of the West Greenland Current coming into Disko Bugt. This makes it suitable for investigation of high resolution changes in the strength of the WGC and its constituent water masses, as well as the interaction between the oceanographic regime in coastal West Greenland and the wider oceanography of Baffin Bay and the Labrador Sea.

The distal location of Jakobshavns Isbrae and its possible overwhelming meltwater influence, suggest that changes in species assemblage will be directly related to changes in the WGC entering Disko Bugt. These changes are likely to be linked to variations in the strength of the two component water currents of the WGC. The core depth, 900m, was significantly greater than at the other sites, and this accounts for the absence of the shallower water loving *A. glomerata*. Where species counts are very low, agglutinated fauna tend to be the dominant species. Interpretation is based primarily on foraminiferal assemblages outlined in Chapter 4, with reference to modern assemblage and sedimentological data (Morros, unpublished data; Lloyd, in prep. and Lloyd *et al.*, submitted). Individual assemblage data for indicator species is given in Figure 5.11, and summary of water mass changes reflected by these indicators is shown in Figure 5.12.

5.4.2 Interpretation of DA00-03 Zone 1

The duration of this zone extends from 3.2 ka cal BP at the base of the core to 2.3 ka cal BP. It consists of 3 subzones (a, b and c), which are zoned according to variations in agglutinated and calcareous species fluctuations outlined in Chapter 4. There are large fluctuations between Arctic and Atlantic indicator species through the zone, as well as significant amounts of the widely tolerant *C. arctica* and *R. gracilis*. The zone is also characterized by relatively lower amounts of organic walled test linings. Arctic species dominance is greater at the bottom of the zone, and Atlantic species at the top.

5.4.2.1 Interpretation of DA00-03 Sub Zone 1a

This sub-zone extends from the base of the core at 3.2 to 2.9 ka cal BP (Figure 5.11). It is characterised by relatively high levels of the Atlantic water mass indicator *N. labradorica*. Also significant are low frequencies of *I. norcrossi*, an indicator of warmer water mass conditions, together with a short lived episode of dominance by the species *C. arctica* and *R. gracilis* which are known to be tolerant to wide variations in temperature and salinity. Foraminiferal abundance fluctuates as the frequency of these latter taxa varies; perhaps reflecting stressed environmental conditions not suited to these Atlantic indicator species, which show preference for relatively warm and saline stable bottom water conditions.

5.4.2.2 Nonionellina labradorica

N. labradorica (frequently identified as *Nonion labradoricum*, Feyling-Hansen, 1990a, 1990b) is indicative of deeper, stable Atlantic sourced water masses in both East Greenland and eastern Arctic Canada. Despite being lower than the abundance expected at individual sites in these locations, somewhat conflictingly, this species has been described as an Arctic species by Scott *et al.* (1984) from its occurrence on the Labrador and Nova Scotian shelves and by Schafer and Cole (1982) from its occurrence on the continental slope and rise to the east of Newfoundland.

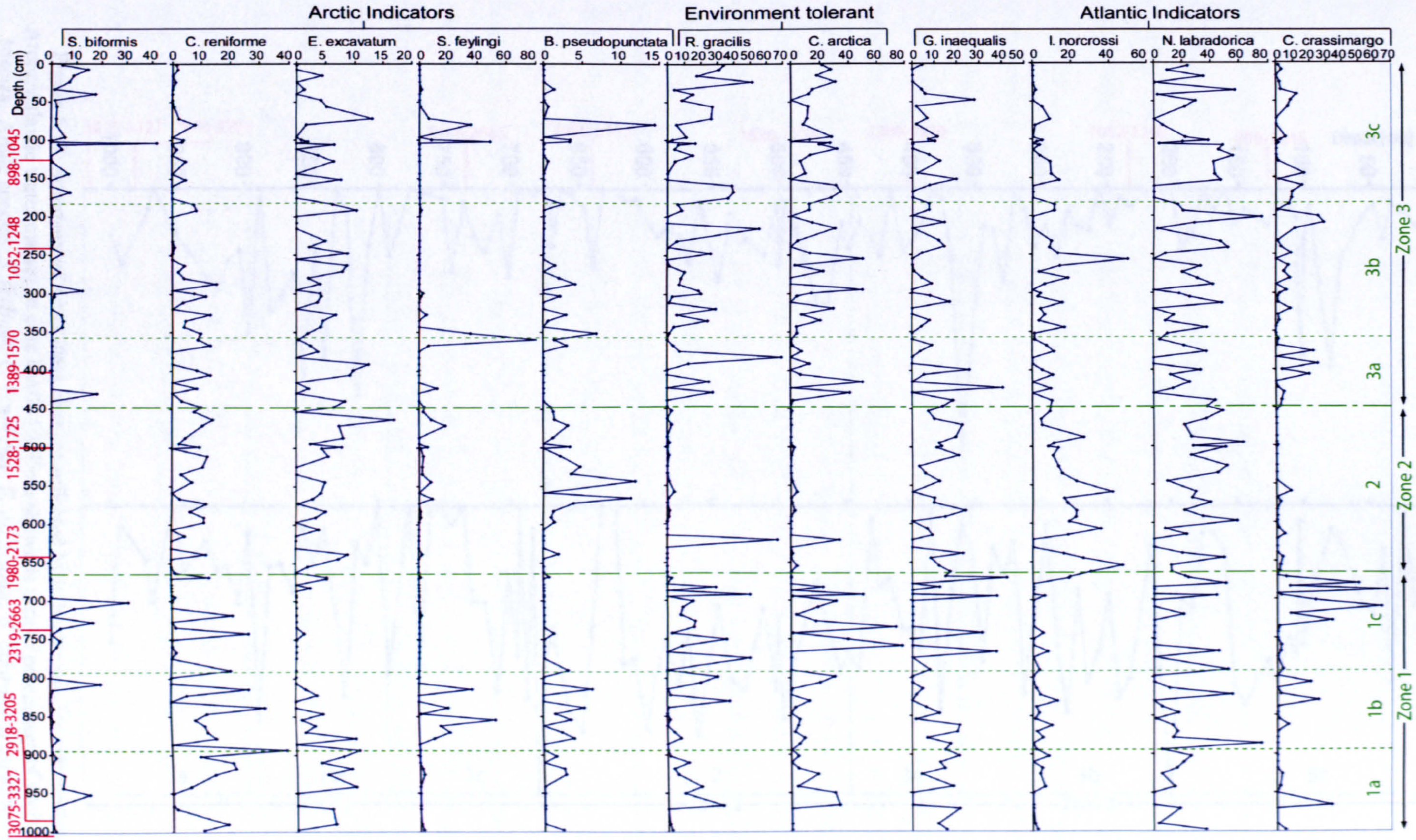

Figure 5.11: Individual percentage assemblage data for indicator species in core DA00-03. Radiocarbon dates are given in red in cal yrs BP. Foraminiferal zones are marked in green based on cluster analysis.

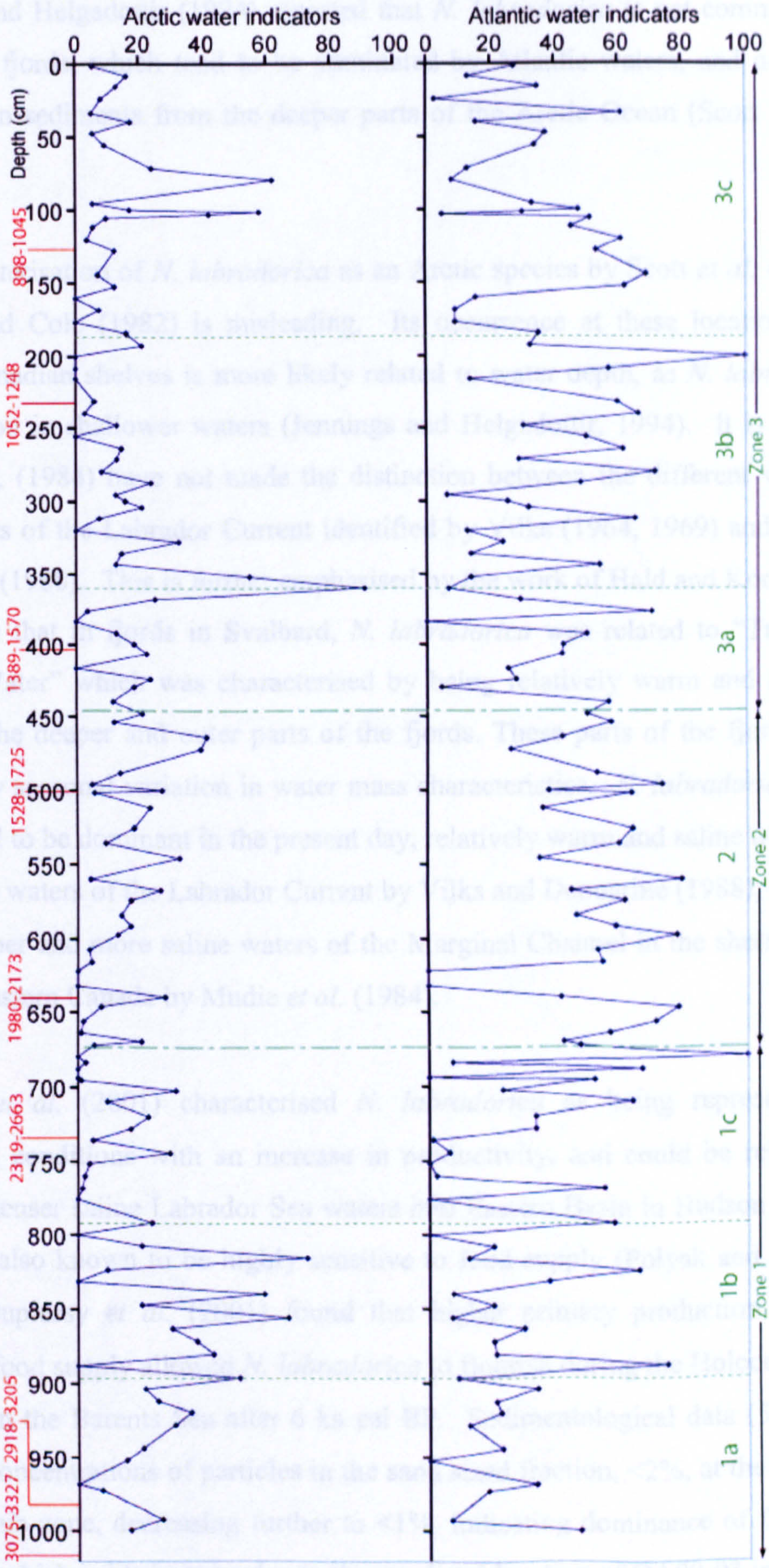

Figure 5.12: Summary of water mass changes reflected by indicator species representative of Arctic/Atlantic water masses in core DA00-03. Data shown is sum of percentage of each indicator species. Arctic species: *S. feylingi, C. reniforme, E. excavatum, S. biformis, B pseudopunctata..* Atlantic species: *I. norcrossi, C. crassimargo, N. labradorica, G. inaequalis (S. diflugiformis & C. teretis* data also included, although not shown in individual species figure). Radiocarbon dates shown in red (cal yrs BP). Foraminiferal zones in green.

Jennings and Helgadottir (1994) reported that *N. labradorica* is not common in east Greenland fjords, which tend to be dominated by Atlantic waters, and neither is it dominant in sediments from the deeper parts of the Arctic Ocean (Scott and Vilks, 1991).

The characterisation of *N. labradorica* as an Arctic species by Scott *et al.* (1984) and Schafer and Cole (1982) is misleading. Its occurrence at these locations off the eastern Canadian shelves is more likely related to water depth, as *N. labradorica* is not common in shallower waters (Jennings and Helgadottir, 1994). It is likely that Scott *et al.* (1984) have not made the distinction between the different water mass components of the Labrador Current identified by Vilks (1964, 1969) and Vilks and Deonarine (1988). This is further emphasised by the work of Hald and Korsun (1997) who found that in fjords in Svalbard, *N. labradorica* was related to "Transformed Atlantic Water" which was characterised by being relatively warm and saline, and occupied the deeper and outer parts of the fjords. These parts of the fjords are less affected by seasonal variation in water mass characteristics. *N. labradorica* has also been found to be dominant in the present day, relatively warm and saline offshore and shelf slope waters of the Labrador Current by Vilks and Deonarine (1988), and related to the deeper and more saline waters of the Marginal Channel in the shelf sediments of north-eastern Canada by Mudie *et al.* (1984).

Jennings *et al.* (2001) characterised *N. labradorica* as being representative of postglacial conditions with an increase in productivity, and could be related to an influx of denser saline Labrador Sea waters into Eastern Basin in Hudson Bay. This species is also known to be highly sensitive to food supply (Polyak and Mikhailov, 1996). Duplessy *et al.* (2001) found that higher primary production leading to increased food supply allowed *N. labradorica* to flourish during the Holocene thermal optimum in the Barents Sea after 6 ka cal BP. Sedimentological data (5.13) shows very low concentrations of particles in the sand sized fraction, <2%, at the base of the core and sub-zone, decreasing further to <1%, indicating dominance of fine grained sediments which is likely to be due to the ice-distal location of DA00-03 in relation to the suspended meltwater sediment from Jakobshavns Isfjord. Based on this information, *N. labradorica* is used as an indicator species for the relatively warm and saline WGC in this thesis.

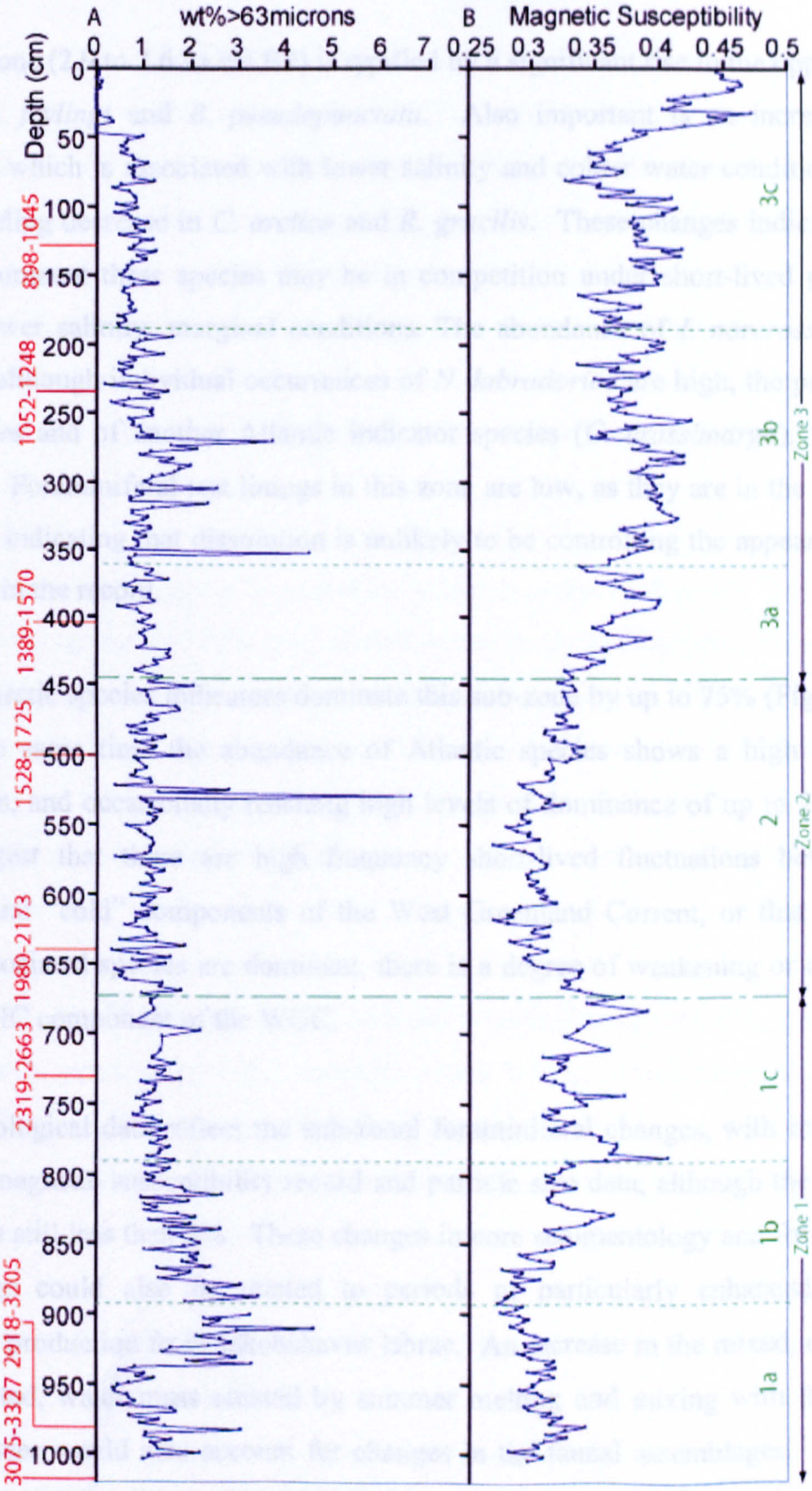

Figure 5.13 Sedimentological analyses from core DA00-03, produced from data from Morros (in Lloyd *et al.*, submitted). A: Particle size data for sediment fraction >63 microns (sand size fraction) B: Magnetic Susceptibility (χ_m). Radiocarbon dates are shown in red and are given in cal yrs BP. Foraminiferal zones are shown in green.

5.4.2.3 Interpretation of DA00-03 Sub Zone 1b

This subzone (2.9 to 2.6 ka cal BP) is typified by a significant rise in the opportunistic species *S. feylingi* and *B. pseudopunctata.* Also important is an increase in *C. reniforme* which is associated with lower salinity and colder water conditions, and a corresponding decrease in *C. arctica* and *R. gracilis.* These changes indicate that in this environment these species may be in competition under short-lived periods of colder, lower salinity, marginal conditions. The abundance of *I. norcrossi* remains low, and although individual occurrences of *N. labradorica* are high, the presence of this species and of another Atlantic indicator species (*C. crassimargo*), is seen to fluctuate. Foraminiferal test linings in this zone are low, as they are in the preceding sub-zone, indicating that dissolution is unlikely to be controlling the appearance of *I. norcrossi* in the record.

In total, Arctic species indicators dominate this sub-zone by up to 75% (Figure 5.12), but at the same time the abundance of Atlantic species shows a high degree of fluctuation, and occasionally reaching high levels of dominance of up to 75%. This may suggest that there are high frequency short-lived fluctuations between the "warm" and "cold" components of the West Greenland Current, or that when the Arctic associated species are dominant, there is a degree of weakening or dilution of the warm IC component of the WGC.

Sedimentological data reflect the sub-zonal foraminiferal changes, with increases in both the magnetic susceptibility record and particle size data, although the wt %>63 microns is still less than 5%. These changes in core sedimentology and foraminiferal assemblage could also be related to periods of particularly enhanced seasonal meltwater production from Jakobshavns Isbrae. An increase in the mixed, colder and more diluted, water mass created by summer melting and mixing with the bottom water masses would also account for changes in the faunal assemblages. However, the greater water depth at this core site, and the distance from Jakobshavns Isbrae makes this unlikely. The changes in the assemblages are more likely to be related to variations in the strengths of the components of the West Greenland Current.

5.4.2.4 Interpretation of DA00-03 Sub Zone 1c

This sub-zone (2.6-2.3 ka cal BP) is characterised by a decline in the number of Arctic associated species, and an increase in the Atlantic associated *C. crassimargo*. There is a dominance of *C. arctica* and *R. gracilis*, which, when considered with the very low levels of foraminifera, and increasing foraminiferal test linings towards the top of the zone, suggests that conditions were highly unstable, fluctuating considerably, and therefore favouring these more tolerant and/or opportunistic species. There is no significant change in the sedimentological record for this sub-zone and overall it appears that this sub-zone represents a period of intensification of the trends seen in sub-zone 1a.

In summary, Zone 1 spans a period of approximately 1000 years, during which species characteristic of Arctic and Atlantic water mass characteristics fluctuate. Low periods of foraminiferal abundance do not favour the presence of indicator species of either group, and there is a high degree of variance between periods of dominance of one group over another. There is also variation between these periods of dominance, and periods of low foraminiferal abundance. These may be related to one of the following:

a) stable conditions with Atlantic sourced foraminifera representing strong WGC
b) stable conditions with relatively more Arctic foraminifera showing the influence of the stronger EGC component of the WGC
c) unstable, fluctuating conditions giving rise to opportunistic/widely tolerant species, common between periods of change between a) and b)

The relatively high sedimentation rate may also account for the generally lower foraminiferal abundances in the core.

5.4.3 Interpretation of DA00-03 Zone 2

Zone 2 (2.3-1.7 ka cal BP) is characterised by a significant dominance of calcareous species, and higher foraminiferal abundance compared to Zones 1 and 3. Arctic

indicator species are low, with only minor amounts of *C. reniforme* and *S. feylingi* increasing towards the top. The calcareous species *I. norcrossi* and *N. labradorica* associated with the relatively warmer more saline Atlantic sourced waters dominate, with abundances between 20% and 60%. The amount of organic-walled test linings remains relatively constant, indicating that, despite a degree of dissolution, abundances are still high enough to record a water mass signal. Particle size data show low amounts of sand, and magnetic susceptibility gradually increasing towards the top of the zone. Overall, abundances of Atlantic-sourced water indicator species are high, but decrease towards the top of the zone. This suggests a generally stable period of around 1500 years where a strong WGC is influencing this outer location in Disko Bugt.

5.4.4 Interpretation of DA00-03 Zone 3

Zone 3 sees a return to the fluctuating pattern between periods of high Atlantic and Arctic species. Amounts of the sand size fraction in the sediments remains relatively unchanged from previous zones, but magnetic susceptibility increases towards the core top. In general the assemblages are dominated by *N. labradorica*. This Zone is again broken down into sub-zones (a, b and c) due to variations in the species assemblage.

5.4.4.1 Interpretation of DA00-03 Sub Zone 3a

Sub Zone 3a, (1.7-1.5 ka cal BP) is characterised by very low foraminiferal abundances and a subsequent dominance by the ecologically insensitive *C. arctica* and *R. gracilis*. The significant Atlantic indicators present are *C. crassimargo* and *N. labradorica* with low amounts of *I. norcrossi*. This assemblage indicates the presence of a warm WGC, but the lowered overall abundances and relative abundance of *C. arctica* and *R. gracilis* suggests some instability in conditions with perhaps a dilution of the relatively warm more saline water. However, this is not enough to lead to an increase in Arctic fauna.

5.4.4.2 Interpretation of DA00-03 Sub Zone 3b

This sub-zone continues the above trend in a similar way from 1.5 to 1.0 ka cal BP. An increase in *I. norcrossi* and *N. labradorica* leads to an overall relative increase in total Atlantic indicator species. This suggests an increasing stability in the water masses reaching the area, and is supported by higher foraminiferal abundances and lower amounts of *C. arctica* and *R. gracilis*. Sedimentological data show little deviations from the patterns previously established. Interestingly, this sub-zone is also characterized by the highest levels of foraminiferal test linings seen in the core, but there appears to be no relationship between this and the degree of preservation seen in the calcareous tests counted, as specimens were extremely robust. A small bloom of *S. feylingi* (usually associated with colder low salinity water, or reduced food supply or higher anoxic bottom water conditions) can be seen at the bottom of the sub-zone at around 1.4 ka cal BP, and demonstrates that changes in environmental conditions in the water masses can operate on very short timescales.

5.4.4.3 Interpretation of DA00-03 Sub Zone 3c

The final sub-zone in core DA00-03 extends from 1.0 ka cal BP to the core top, which is estimated around 0.5 ka cal BP. Amounts of both Atlantic and Arctic indicator species fluctuate considerably. At the base of the sub-zone, the calcareous species associated with relatively warmer more saline Atlantic sourced water masses are absent, with only agglutinated species, typically *C. arctica* and *R. gracilis* present. It is important to emphasize here however, that at this point in the zone the species abundances are extremely low, less than 50 per sample, and that the overall trend in the zone is for higher abundances, with a considerable dominance of *N. labradorica*, which is associated with a warm stable WGC.

The fluctuations seen in previous sub-zones are absent. The abundance of *N.* labradorica causes a reduction in all the other species, including *I. Norcrossi,* which decreases in this zone and is no longer present at all by the core top. A further small bloom of *S. feylingi* appears at around 0.7 ka cal BP. The sub-zone is further typified by the lack of test linings, and a weak presence of Arctic water associated species.

This stable period of *N. labradorica* dominance, and decline of Arctic species may be evidence for a weak Medieval Warm Period (MWP) between 1.0 and 0.7 ka cal BP, which is ended abruptly after 0.7 ka cal BP by the spike in *S. feylingi*. This may represent the onset of distinct Little Ice Age (LIA) conditions, and although Arctic species do not remain high after this, it can be seen that there is a gradual cooling as there is a decline in the warmer-loving Atlantic water associated fauna to the core top. At the same time there is an increase in the lower salinity and temperature tolerant *C. arctica* and *R. gracilis*, and a slight increase in the Arctic associated *S. biformis*. These possible scenarios will be discussed in Chapter 6.

5.4.5 Summary interpretation of DA00-03

In summary, DA00-03 presents detailed information about palaeoenvironmental conditions during the last 3ka of the Holocene in the outer part of Disko Bugt. A fluctuating assemblage through Zone 1 from 3.2 to 2.3 ka cal BP, indicates the presence of a warm West Greenland Current which is periodically either diluted by varying amounts of meltwater from Jakobshavns Isfjord, or due to changes in the relative dominance of the IC and EGC contributions to the WGC. There is no evidence for phases of specific Arctic water incursion, and this relates well to evidence for warm WGC at this time (Donner and Jungner, 1975; Funder and Weidick, 1990; Levac, 2001; Osterman and Nelson, 1989).

Zone 2 (2.3-1.7 ka cal BP) indicates an increasing degree of stability of the water masses entering the outer Disko Bugt area, with a distinct lack of agglutinated foraminifera.

Zone 3 (1.7 ka cal BP) sees a return to more variable conditions, with a possible perturbation of the warmth of the WGC by seasonal changes in the amount of well-mixed lower temperature and salinity water derived from meltwater input from the distal Jakobshavns Isfjord or increases in the EGC contribution to the WGC. There is some evidence that the high-resolution record from DA00-03 is recording a palaeoceanographic signal of late Holocene events such as the Medieval Warm Period (MWP) and the Little Ice Age (LIA).

5.5. Faunal preservation and interpretation of dissolution processes

Dissolution, resulting in poor preservation of calcareous tests is well documented in high latitude regions (Asku, 1983; Hald and Steinsund, 1992; Jennings and Helgadottir, 1994), and is often represented in palaeoenvironmental studies by the presence of, or increase in, the organic-walled test linings, and a reduction or even absence of calcareous fauna in an assemblage. Figure 5.14 illustrates the effect of dissolution on calcareous tests.

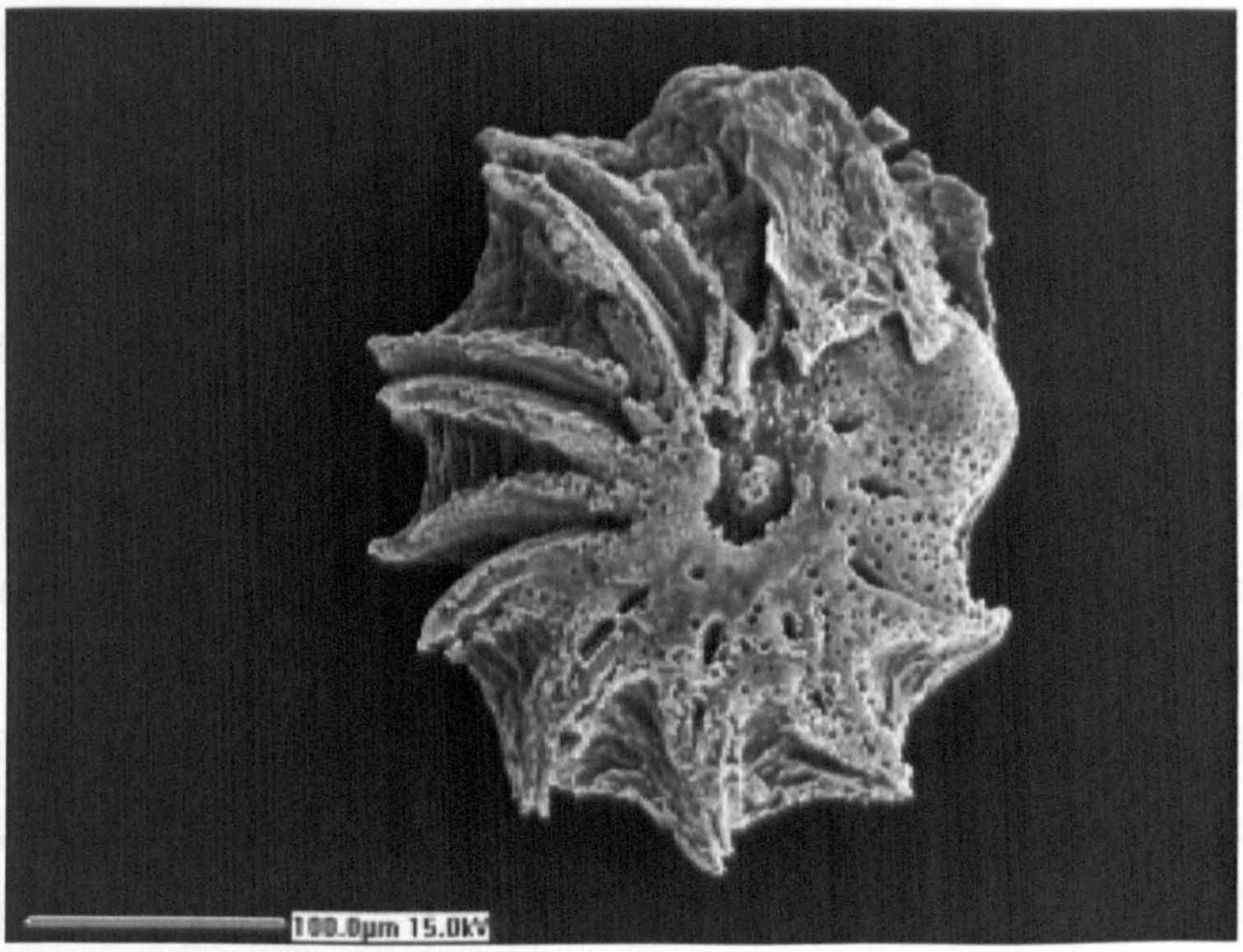

Figure 5.14: Post depositional dissolution of the calcareous foraminifera *Elphidium excavatum* from DA00-06.

Calcareous dissolution is usually associated with dense, cold, low salinity Arctic bottom waters. These water masses are enriched with CO_2, as lower temperatures increase the solubility of CO_2 and create a depletion in the carbonate ion concentration. This means that the threshold of calcium carbonate is below that required by calcareous forms to precipitate their tests. At the same time, lower salinity environments have a decreased calcium ion concentration and carbonate alkalinity (Greiner, 1974). This means therefore, that the overlying water mass greatly influences the distribution of agglutinated and calcareous benthic species. Low values of calcium carbonate are often found corresponding to low ratios of calcareous/agglutinated foraminifera, planktic/benthic foraminifera, high ratios of

living/dead foraminifera, corroded calcareous foraminifera, and high numbers of exposed organic linings of foraminifera (Steinsund and Hald, 1994).

This type of dissolution process is so well defined in fjords of East Greenland that it allowed Jennings and Weiner (1996) to construct a dissolution gradient for modern benthic assemblages which describes change from Polar (or Arctic) Waters at one end of the gradient with approx. 100% calcium carbonate dissolution, and at the other end of the gradient, Atlantic Intermediate Water with around 90% calcium carbonate preservation and a subsequent dominance of agglutinated species. They infer that Polar Water is indicative of naturally lower productivity.

Early workers (Marlowe and Vilks, 1963; Phleger, 1952; Vilks, 1964) in the Canadian Archipelago drew attention to local variations in the abundance of benthic foraminifera. In the western area, agglutinated species are dominant, whilst calcareous forms dominate in the eastern Archipelago. These distinctions were attributed by Vilks (1964) to the presence of two distinct water masses. A surface layer descending to around 200 m composed of low salinity and low temperature water of Arctic origin overlay a water mass of warmer, more saline water of Atlantic origin. The agglutinated species dominated in water depths shallower than the 200 m interface, typically in environments with restricted water turbidity and circulation and phytoplankton activity (Vilks, 1969). At sites in the same area, Hunt and Corliss' (1993) data suggest that calcareous foraminiferal distribution is likely to be controlled to a large extent by the availability of Atlantic sourced water.

Contrary to this well-established and relatively widespread phenomenon in the high latitudes, the dissolution trend in this study appears to be reversed. The dominance of Arctic sourced waters in the early part of core DA00-06 in Zone 1 reveals high levels of calcareous preservation, and no organic test linings, a fundamental source of evidence for periods of calcium carbonate dissolution. Preservation is clearly at its poorest during periods dominated by warm WGC waters, derived from Atlantic sources i.e. the Irminger Current. Andrews *et al.*, (1991) intriguingly reported that agglutinated foraminiferal dominated the stratigraphic record of the past 7-5 ka on the outer parts of the Baffin Shelf. Although the inner shelf areas would at this time have been overwhelmingly under the influence of the colder low salinity Labrador Current,

the outer parts of the shelf may have come into contact with the remnant WGC that would still be present on the eastern Canadian coastal area, and well-established at this time on the West Greenland coast (Donner and Jungner, 1975; Funder and Weidick, 1991; Lloyd *et al., submitted*).

Various authors have associated this agglutinated dominance with increased postglacial carbonate dissolution (e.g. Osterman and Nelson, 1989), likely due to the activity of the Labrador Current, but interpretations are somewhat vague. While de Vernal *et al,*. (1992) found evidence that Arctic derived bottom waters resulted in a degree of calcium carbonate dissolution in the Davis Strait; they also found evidence for dissolution in relation to Atlantic sourced water masses like the pattern found in Disko Bugt. These authors associate greater productivity to the Atlantic sourced water, which creates an increased carbon flux allowing organic matter to oxidise in sediments. The products of oxidation of organic material include CO_2, and increased dissolved CO_2 would encourage calcium carbonate dissolution.

This scenario of increased productivity relating to Atlantic water flux leading to oxidation of organic material fits well with the pattern found in Disko Bugt during times of enhanced or strong WGC flux to the area. During the periods when the bay was dominated by cold low salinity water and preservation of calcareous test was very high, large amounts of meltwater from Jakobshavns Isbrae (with a correspondingly low CO_2 content) may have been available in the form of meltwater. Arctic waters in comparison are poorly oxygenated, and have a much higher dissolved CO_2 content. These scenarios may well explain the unusual reversed dissolution effect demonstrated in core DA00-06.

The dissolution scenario in DA00-05 also deviates from the generally accepted pattern, and this is likely to be related to the shallow fjord mouth setting. Here the environment and oceanography seems to be conducive to calcareous dissolution taking place but for different reasons. The palaeo-setting of the core site at the mouth of a relatively shallow fjord, at a distal location from direct ice/meltwater input is very different from the ice proximal setting of DA00-06. In the lower half of the core in Zone 1, the assemblages indicate the presence of relatively warm saline Atlantic sourced water. As in core DA00-06, there is a degree of dissolution at this time,

which has been related to the WGC water, and is evidenced from the fluctuations in foraminiferal test linings, and the changes in agglutinated and calcareous abundances. However, it is suggested here that these changes and short lived dissolution events are related to changing hydrographic conditions in the fjord, rather than activity of the WGC, perhaps due to extended sea ice cover, allowing stratification of the water masses to take place.

This stratification scenario increases intensely from the start of Zone 2, which coincides with the onset of Neoglacial conditions in this area (Weidick *et al,* 1990). The high degree of stratification creates the severe dissolution effect, perhaps by a shallowing of the lysocline. During these processes in this period from *c.* 4 ka cal BP onwards, evidence of fluctuations in the strength of the WGC, or changes in the meltwater flux to produce faunal changes in the agglutinated species can still be seen.

5.6.1 Introduction to stable isotope interpretations

Stable isotope measurements made on benthic foraminiferal tests have been obtained for cores DA00-06 and DA00-03. The $\delta^{18}O$ and $\delta^{13}C$ records reveal information about prevailing palaeoceanographic conditions in addition to the foraminiferal assemblage interpretations. As a consequence of dissolution processes operating in DA00-06 the record is not comprehensive of the entire core, and due to the greatly different sedimentation rates between Zones 1 and 2, and Zone 3, the sampling resolution is poor through Zone 3. However, inferences relating to bottom water conditions can be made and compared to the assemblage interpretations. Composite isotope values are used in DA00-06, and in DA00-03 the single isotope values from *N. labradorica* are discussed.

5.6.2 Stable isotope interpretations DA00-06

The individual species records of oxygen and carbon isotope variations presented in Chapter 4 show generally good interspecies trend agreement. In this section, 'stacked' records of isotope measurements made on the species *C. reniforme, I.*

norcrossi and *N. labradorica* are presented which provides composite values (Figure 5.15). Composite values are given in Appendix 7. The stacking is based upon a simple arithmetic mean of data from the three species, which are shown in Chapter 4 Figure 4.7 p95. This creates a smoother curve reducing possible errors arising from measurement processes, marginal test numbers or poor test preservation. Interpretations are based upon the stratigraphically-constrained foraminiferal zone boundaries that have been discussed previously. Due to the vastly changing sedimentation rate, the sampling resolution in Zone 3 is too poor to make any firm interpretations, and discussion is therefore limited to Zones 1 and 2, which covers the time period 8.4-7.8 ka cal BP. It is not possible to determine the degree of isotopic disequilibrium of any of the three species used as data regarding $\delta^{18}O$ seawater variations is unavailable, and changes in isotope values are therefore discussed both relatively and qualitatively. The three species used are all infaunal, and it must be noted that changes in the $\delta^{18}O$ values may also be affected by conditions in the interstitial pore water as well as being directly related to the overlying water masses.

Significant variations can be seen in the both the $\delta^{18}O$ record and $\delta^{13}C$ record of DA00-06 (figure 5.15). In Zone 1 (8.4-7.9 ka cal BP), $\delta^{18}O$ values are relatively light (around 1.75‰) at the start of the zone, indicating that there is significant meltwater input. This decline to lower values perhaps signifies a halt in meltwater production from Jakobshavns Isbrae. A similar but more muted trend can be seen in the carbon record at this point, *c.* 8.3 ka cal BP, there is a peak in both records. This is followed by heavier values in the oxygen record, signifying a vast reduction in meltwater production in Disko Bugt. This may be related to stagnation of the ice stream as it reaches a topographic pinning point, or a response to changes in precipitation or cooling of atmospheric temperature. Carbon values are also heavier, although the decrease is not as pronounced. Heavy values continue until *c.* 8.1 ka cal BP, when there is a large light spike in both the isotope records, although the carbon record seems to be recording a change in conditions prior to the oxygen spike. The $\delta^{18}O$ values fall as low as 1.5‰, and $\delta^{13}C$ values are typically around –3.0‰.

Further amounts of meltwater flux from Jakobshavns Isbrae can be interpreted from the $\delta^{18}O$ record following the extreme light peak, at the end of Zone 1 and moving into Zone 2.

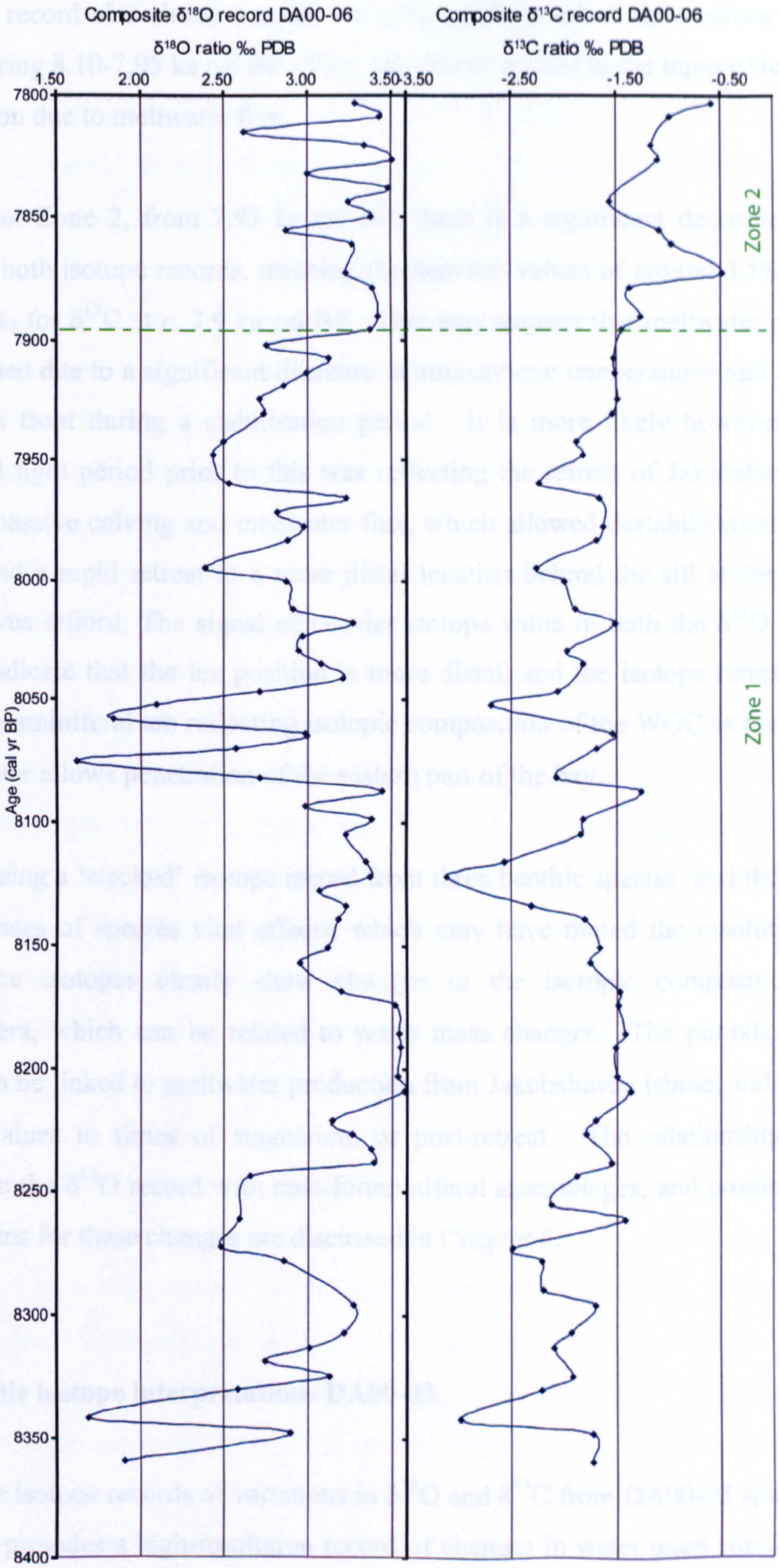

Figure 5.15: 'Stacked' isotope records (oxygen and carbon) for core DA00-06. Values are based on a simple arithmetic mean from 3 species presented earlier in Chapter 4. Zone boundaries are based on cluster analysis performed on foraminiferal assemblages from the core. A smoothed curve has been used between the data points.

The $\delta^{13}C$ record also shows a relatively prolonged period of light values (around -2.0‰) during 8.10-7.95 ka cal BP. This can also be related to the input of terrestrially light carbon due to meltwater flux.

Throughout Zone 2, from 7.95 ka cal BP, there is a significant decrease to heavy values in both isotope records, reaching the heaviest values of around 3.5‰ for $\delta^{18}O$ and –1.0‰ for $\delta^{13}C$ at *c.* 7.9 ka cal BP. This may suggest that meltwater production has declined due to a significant decrease in atmospheric temperatures and stagnation of the ice front during a stabilisation period. It is more likely however, that the prolonged light period prior to this was reflecting the retreat of Jakobshavns Isbrae through massive calving and meltwater flux, which allowed destabilisation of the ice stream, and a rapid retreat to a more distal location behind the sill at the mouth of Jakobshavns Isfjord. The signal of heavier isotope value in both the $\delta^{18}O$ and δ^{13} C records indicate that the ice position is more distal, and the isotope ratios from the benthic foraminiferal are reflecting isotopic composition of the WGC as the reduction in meltwater allows penetration of the eastern part of the bay.

Despite using a 'stacked' isotope record from three benthic species, and the unknown consequences of species vital effects, which may have muted the resolution of the record, the isotopes clearly show changes in the isotopic composition of the foraminifera, which can be related to water mass changes. The periods of lighter values can be linked to meltwater production from Jakobshavns Isbrae, and periods of heavier values to times of stagnation, or post-retreat. The relationship of these changes in the $\delta^{18}O$ record with core foraminiferal assemblages, and possible driving mechanisms for these changes are discussed in Chapter 6.

5.6.3 Stable isotope interpretations DA00-03

The stable isotope records of variations in $\delta^{18}O$ and $\delta^{13}C$ from DA00-03 spans the last 3 ka, and provides a high-resolution record of changes in water mass conditions, and productivity in the western part of Disko Bugt. These records are shown in Figure 5.16 together with the relative % abundance of *N. labradorica* which is often an indicator of productivity. This core site location is at a water depth of 750 m, and its

significant distance from Jakobshavns Isbrae increases the possibility that changes in the isotopic ratios of the foraminifera are likely to be recording oceanographic changes on a wider scale. Lighter $\delta^{13}C$ values in benthic foraminifera may relate to increases in surface productivity with the influx or increase in proportion of warmer more saline Atlantic waters.

The $\delta^{18}O$ record for DA00-03 indicates relatively stable bottom water mass conditions for the duration of the core record. Values are typically around 3‰, which are similar to the values for DA00-06 following the retreat of Jakobshavns Isbrae from Isfjeldsbanken. Zone 2 is characterised by an extremely light excursion from the record at 2.1 ka cal BP. This indicates either a distinctive increase in meltwater flux from Jakobshavns Isbrae, which creates a lighter signal when mixed with the WGC to give the Disko Bugt water mass, or suggests a greater component of EGC sourced water in the WGC. The latter scenario is more likely, as the core site water depth is too great, and location from the Jakobshavns meltwater source too distal for the mixed layer to descend. Ice core records (GISP2) indicate a peak of warmth at *c.* 2 ka, and this may be responsible for a rapid increase in meltwater flux from the Arctic, which is translated to a greater EGC component of colder, less saline water in the WGC. This would also account for the enhanced $\delta^{13}C$ depletion seen following the light spike and high abundances of *N. labradorica*, as this is indicative of enhanced nutrient concentrations and productivity which would arise from greater meltwater input of isotopically lighter carbon.

It is important to note that as *N. labradorica* is also used as an Atlantic water/warmer WGC indicator, that a similar effect, in terms of increases in its abundance, may be seen with a greater proportion of Irminger Current sourced water in the WGC. This situation, where different factors contrive to produce a similar end effect is know as equifinality, and it is likely that in Disko Bugt, the location of the cores, water depth and post-depositional preservation factors may well impact upon the "response" that can be seen in the indicator species. In general, abundances of *N. labradorica* are well correlated with periods of enhanced $\delta^{13}C$ depletion. Disparity between the $\delta^{13}C$ record and the $\delta^{18}O$ record may well be a function of differential depth or microhabitat effects of the foraminifera, as well as changing carbonate ion

concentration or vital effects, which are poorly known for benthic species, and natural conditions (Rohling and Cooke, 1999).

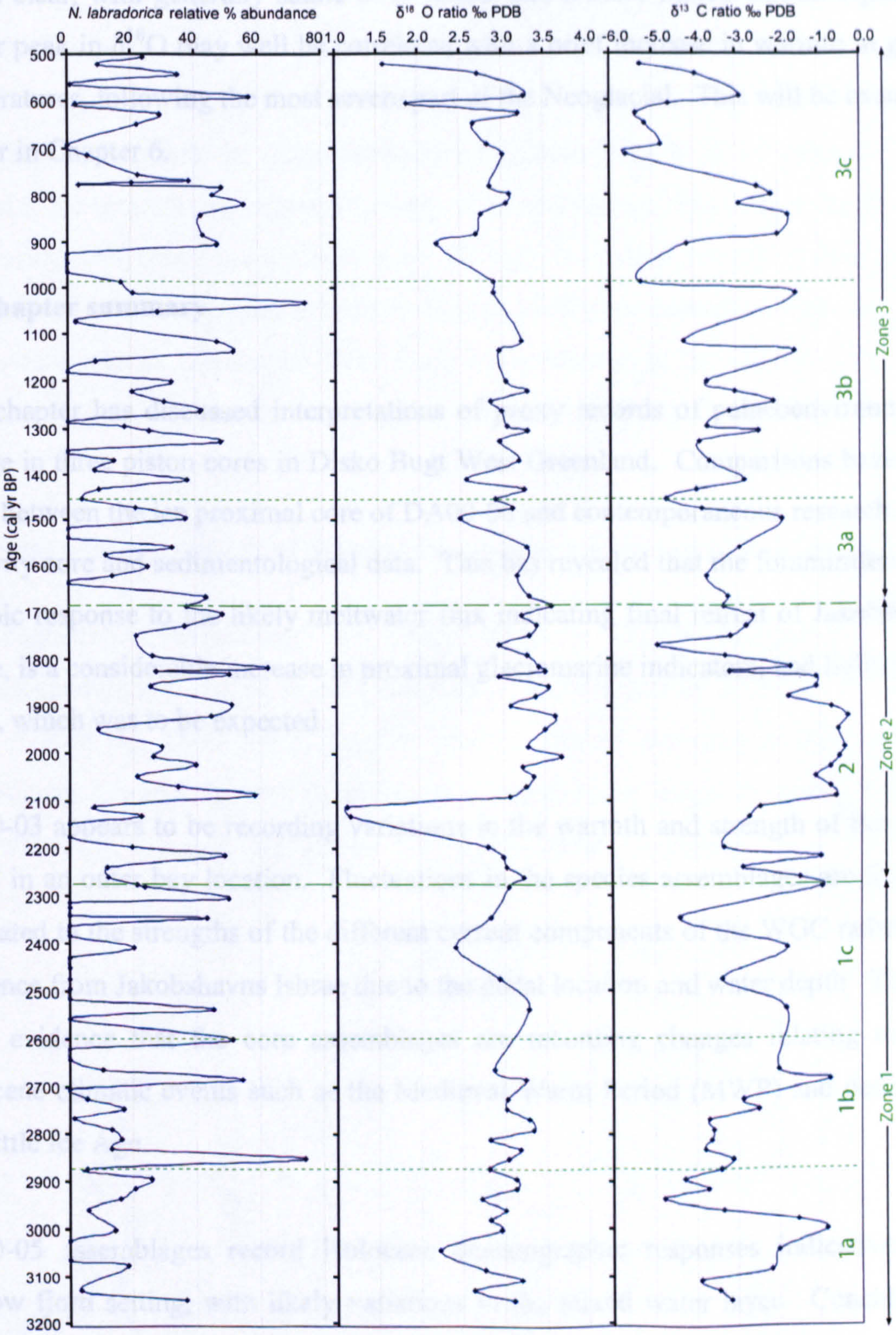

Figure 5.16: Core DA00-03 isotope interpretations and foraminiferal productivity indicator species. *N. labradorica* relative % abundances; Oxygen isotope record; carbon isotope record, all plotted with age (cal yr BP). Zone boundaries are based on cluster analysis performed on foraminiferal assemblages from the core. A smoothed curve has been used between the data points.

In summary, the stable isotope records from DA00-06 and DA00-03 show relative changes in bottom water mass conditions. In DA00-06, the isotopic response is

directly related to the meltwater flux from Jakobshavns Isbrae, which influences the isotopic concentration of the Disko Bugt mixed water layer. In DA00-03 the situation is less clear, with generally stable $\delta^{18}O$ ratios, and a more mixed carbon signal. A lighter peak in $\delta^{18}O$ may well be correlated with a brief increase in warmth in global temperatures, following the most severe part of the Neoglacial. This will be examined further in Chapter 6.

5.7 Chapter summary

This chapter has discussed interpretations of proxy records of palaeoenvironmental change in three piston cores in Disko Bugt West Greenland. Comparisons have been made between the ice proximal core of DA00-06 and contemporaneous research using a gravity core and sedimentological data. This has revealed that the foraminiferal and isotopic response to the likely meltwater flux indicating final retreat of Jakobshavns Isbrae, is a considerable increase in proximal glaciomarine indicators, and lighter $\delta^{18}O$ ratios, which was to be expected.

DA00-03 appears to be recording variations in the warmth and strength of the stable WGC in an outer bay location. Fluctuations in the species assemblages are likely to be related to the strengths of the different current components of the WGC rather than influence from Jakobshavns Isbrae due to the distal location and water depth. There is some evidence that the core assemblages are recording changes relating to late-Holocene climatic events such as the Medieval Warm Period (MWP) and descent to the Little Ice Age.

DA00-05 assemblages record Holocene oceanographic responses indicative of a shallow fjord setting, with likely variations in the mixed water layer. Considerable dissolution processes appear to be operating in both DA00-05 and DA00-06, but the conditions creating these scenarios are likely to be very different and relate to water depth and core location. This again raises the possibility of equifinality: that different operating processes or driving mechanisms can lead to the same signal being present in a palaeoenvironmental proxy record.

Chapter 6: Late Quaternary palaeoceanography in West Greenland

6.1 Introduction

This chapter discusses the deglacial history of Disko Bugt in West Greenland, and evaluates the relationship between the retreat of Jakobshavns Isbrae from Disko Bugt and post-glacial water mass circulation. A high resolution record of mid to late-Holocene palaeoceanography is developed, and driving mechanisms for change in the palaeoceanographic history of Disko Bugt are evaluated in the context of existing palaeoenvironmental records on a range of temporal and spatial scales.

6.2.1 Deglacial chronology of Jakobshavns Isbrae ice stream within Disko Bugt

The deglaciation chronology of Disko Bugt is clearly represented in the palaeoeceanographic record of core DA00-06. A short gravity (POR18) core to the west of core site DA00-06 is used to provide further evidence of the retreat of Jakobshavns Isbrae (Figure 6.1), as this core record has a longer timespan (Lloyd *et al.*, submitted). Figure 6.2 shows the foraminiferal assemblage data from core POR18.

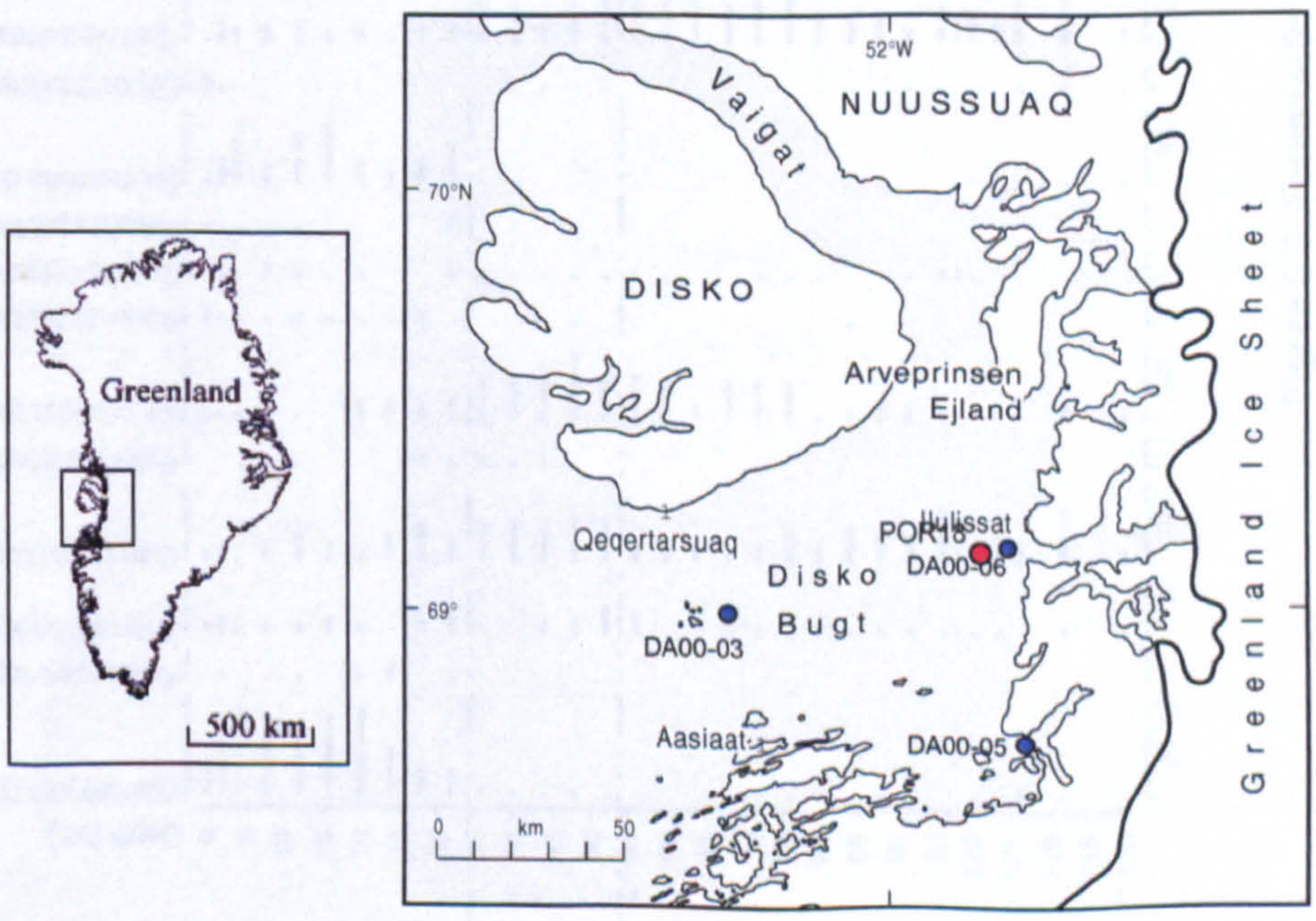

Figure 6.1: Core location map showing piston cores DA00-03 to DA00-06 (blue dots), and the short gravity core POR18 (marked with a red dot) site located west of DA00-06 in front of Jakobshavns Isbrae.

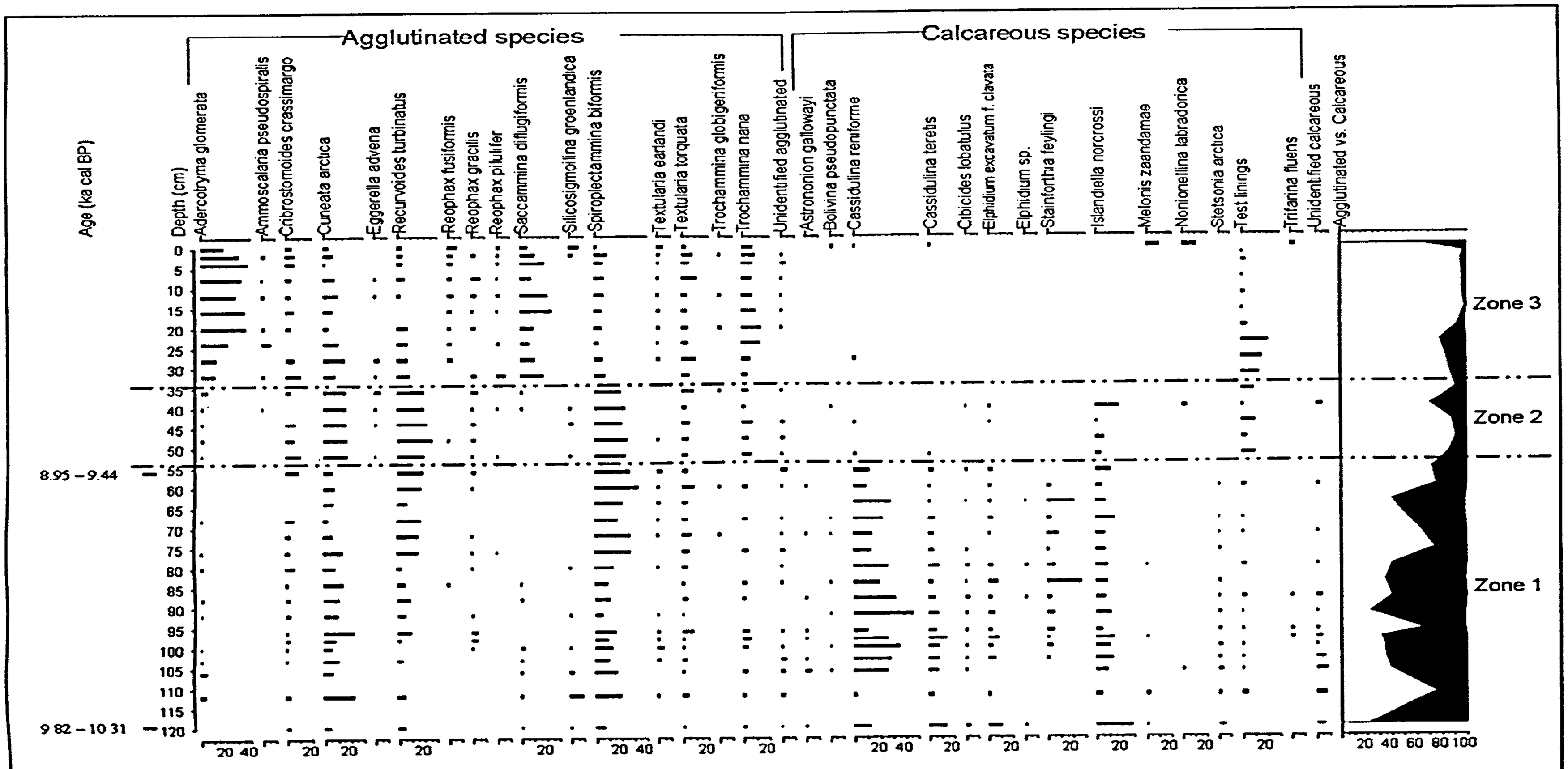

Figure 6.2: Foraminiferal assemblage data for POR18 (adapted from Lloyd *et al.*, submitted)

6.2.2 Comparisons between DA00-06 and POR18

Both DA00-06 and POR18 show similar trends in faunal and sedimentological characteristics:

- A lowermost zone dominated by cold Arctic foraminifera, rare at the present day in Disko Bugt with relatively low coarse sediment content;
- a middle transitional zone with a mixture of arctic and sub-arctic/Atlantic water foraminifera still with relatively low content of coarse grained material; then
- an upper zone dominated by sub-arctic/Atlantic water fauna with significant increase in sand fraction and large clasts up to several centimetres in diameter (IRD). This clearly relates to the deglaciation chronology of Disko Bugt and, more specifically, to the retreat of the Jakobshavns Isbrae ice stream and incursion of warmer WGC waters into Disko Bugt.

As has been previously established, DA00-06 contains a very high resolution record of Holocene palaeoeceanographic change. POR18 has slightly lower resolution, but a longer duration of record. Using these two cores, it is possible to track deglaciation and the influx of WGC across eastern Disko Bugt.

The chronology for POR18 provides the first direct evidence from offshore, near central Disko Bugt for deglaciation of the main area of the bay giving a limiting date of 9.82 – 10.31 ka cal BP. POR18 was recovered from the margins of one of the two deep water channels crossing Disko Bugt interpreted by Long and Roberts (2003), as the route-way for the ice stream. The basal date therefore provides a minimum date for the time of the retreat of the ice stream back towards Jakobshavns Isfjord. This date fits well with the minimum ages for deglaciation from terrestrial sites around the margins of Disko Bugt (Figure 6.3).

Figure 6.3: Minimum radiocarbon dates for terrestrial deglaciation (Long *et al.*, 2003) given in mean cal kyr BP. (Data are from Rasch, 1997 supplemented with data from Bennike, 2000; Long and Roberts 2002; Long *et al.*, 1999, 2003).

Various hypotheses have been proposed for the nature of the deglaciation of Disko Bugt. Long and Roberts (2003), suggest initial deglaciation was relatively rapid, with no significant still stands until the shallower waters of the eastern bay were reached. This interpretation is based on dated organic accumulations in lake basins above the marine limit from the outer margins of Disko Bugt, and similar data from inner margins, as well as dates on marine molluscs from various locations. Several authors have suggested a more punctuated deglaciation. Weidick (1996) suggests the bedrock high between Aasiaat and Qeqertarsuaq acted as a pinning point during ice retreat, while Rasch (2000) suggests a still stand or readvance at approximately 11 ka cal BP based on changes in the marine limit near Aasiaat. The direct evidence from POR18 shows the Jakobshavns Isbrae ice stream had retreated at least to the east of the core

site by *c.* 10.2 ka cal BP, which does not rule out the Rasch still-stand prior to this. However, there is no evidence for a significant still stand or readvance within central or western Disko Bugt once initial deglaciation took place, supporting the Long and Roberts interpretation of rapid deglaciation, and the Rasch standstill is not ruled out either.

After this initial rapid retreat the ice stream almost certainly paused for several thousand years between the POR18 core site and the Jakobshavns Isfjord threshold (Isfjeldsbanken, a shallow ridge immediately south of Ilulissat blocking the fjord with a depth varying from 50 – 200m). From *c.* 10.2 - 9.2 ka cal BP the presence in POR18 of low numbers of *I. norcrossi* and *R. turbinatus* suggest some influence of WGC waters, however the fauna is dominated by cold glaciomarine species suggesting proximity to the calving/melting ice front. The initial deglaciation of Disko Bugt took place before a strong influx of WGC began. The high meltwater flux from the ice margin would have displaced the WGC westwards, in effect diluting its influence within Disko Bugt. The still-stand position of the ice stream until *c.* 9.2 ka cal BP may well be represented by a number of arcuate ridges which were identified during a high resolution 'Chirp' seismic survey carried out in the 2000 Porsild fieldwork season at a location just west of DA00-06 (Dix, unpublished data).

After *c.* 9.2 ka cal BP (zone 2 in POR18) there is a gradual reduction of glaciomarine and cold water fauna (*C. reniforme* and *E. excavatum f. clavata*). The warmer indicating *I. norcrossi* is maintained and test linings become common reflecting an increase in the influence of the WGC in Disko Bugt. This warmer current influence is due, either to a strengthening of the WGC flow into Disko Bugt or to a reduction in the dilution effect of the meltwater flux from the Jakobshavns Isbrae ice stream due, in turn, to continued retreat of the calving margin.

A third option is a combination of the two, a stronger WGC causing ice stream retreat. Present day conditions with a strong WGC influence were reached sometime after *c.* 9.2 ka cal BP, early in zone 3. The data from POR18 show that the grounded ice stream had retreated to the east of the site by *c.* 10.2 ka cal BP, and remained relatively close until *c.* 9.2 ka cal BP, producing large quantities of meltwater and sediment to explain the Arctic water fauna and relatively high sedimentation rates.

After *c.* 9.2 ka cal BP the calving front retreated further eastwards and by at least *c.* 8.3 ka cal BP was in a position to the east of DA00-06, most likely grounded on Isfjeldsbanken at the mouth of Jakobshavns Isfjord. As DA00-06 did not sample the full sedimentary sequence, the basal age is an underestimate of the date of retreat, indeed it seems likely that once the ice stream retreated from a position to the east of POR18 after *c.* 9.2 ka cal BP it retreated to Isfjeldsbanken very rapidly. This can be inferred from the slow sedimentation rate present in the lower two Zones of DA00-06, implying that the ice was distal to this location.

6.2.3 DA00-06 summary of core changes

A summary of the record of core changes in DA00-06 is shown in Figure 6.5. Figure 6.4 summarises the main features shown in zones 1 and 2 (defined by assemblage changes in Chapter 4). The ice stream must have been grounded close to DA00-06 during zone 1, from before *c.* 8.3 ka cal BP to approximately *c.* 7.9 ka cal BP. The calving ice stream must have been present to supply the large quantities of sediment (sedimentation rate of 13.8 mm/yr) and a significant meltwater flux to support the glaciomarine and Arctic water fauna during DA00-06 Zone 1. The fauna from POR18 show the presence of the WGC in Disko Bugt at this time, so the ice stream meltwater must have been deflecting/diluting the influence of the WGC at the DA00-06 core site.

The low levels of IRD present during this period may relate to reduced melting of the calving icebergs due to the dominance of cold meltwater close to the calving front, periods of prolonged sea-ice cover, or due to dilution of the coarse IRD by the rapid fine grained sedimentation produced from the basal ice melt (13 mm/yr, over 20 times greater than the lower section of POR18). In DA00-06, the overall decrease in Arctic/meltwater indicator species, and rise in Atlantic species related to the warm WGC, indicate the reduced influence of Jakobshavns Isbrae from *c.* 8.3 ka cal BP. Minor fluctuations in the amounts of Atlantic and Arctic water fauna from *c.* 8.3 to 7.9 ka cal BP can be interpreted as a response to local meltwater flux from Jakobshavns Isbrae during this grounding period, and a possible response to the larger driving mechanism of changing global temperature.

Event (cal yr BP)	Interpretation
1 (8.25-8.10)	8.2 event. Heavy benthic $\delta^{18}O$ values suggesting cold conditions, with significantly reduced meltwater flux. The record shows a distinct double peak in heavy values, matched by peaks in Arctic species, and lowered amounts of Atlantic species.
2 (8.08-8.04)	Significant light meltwater spike in benthic $\delta^{18}O$ record. The meltwater spike is associated with a slight decrease in Arctic species and an increase in Atlantic species, indicating a degree of incursion by the WGC, possibly initiated by recovery of atmospheric temperature seen as a light spike in the GISP2 record.
3 (8.01-7.96)	Lighter benthic $\delta^{18}O$ values indicate further significant meltwater flux. Low amounts of Atlantic species suggest volumes of meltwater have a considerable dilution effect or deflection of the warm WGC. Warming peaks in the ice core record suggest that increases in meltwater production are related to rising temperatures.
4 (7.93-7.80)	Heavier $\delta^{18}O$ values indicate reduced meltwater flux and stable conditions. Rapic decline in Arctic species signal a rapid retreat of the ice stream from Isfjeldsbanken and increasing influence of a warm stable WGC.

Figure 6.4: Summary table of palaeoenvironmental changes in DA00-06 during the deglaciation of Jakobshavns Isbrae. Numbered events relate to events depicted in Figure 6.4.

6.2.4 Jakobshavns Isbrae: response to the "8.2" event

The foraminiferal record from DA00-06 indicates that the ice stream retreat halted for approximately 400 years, grounded on the Isfjeldbanken at the mouth of the Isfjord. The timing of this stagnation of retreat correlates with a spatially widespread cooling phenomenon. The high resolution nature of the palaeoeceanographic record from DA00-06 allows a detailed examination of ice stream response to this early Holocene cold pulse, widely referred to as the "8.2 event", which is recorded in the oxygen isotope records from Greenland ice core proxies (Alley *et al.*, 1997). This distinctive Holocene climatic event lasted approximately 200 years; between 8.3-8.1 ka cal BP (labelled on Figure 6.5) in the Greenland ice cores (Alley *et al.*, 1997), and displayed half the amplitude of the Younger Dryas cold period (Fairbanks, 1990).

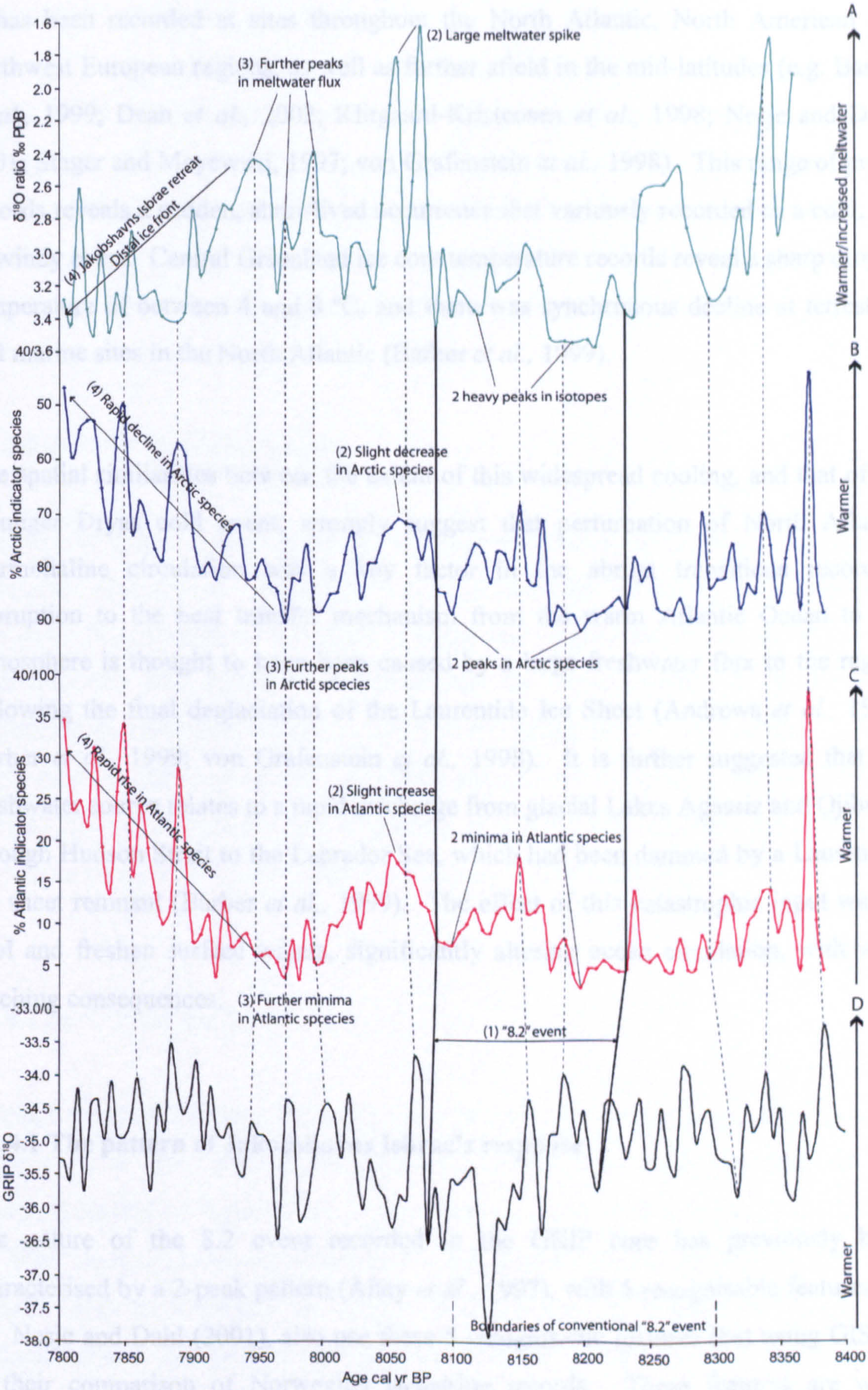

Figure 6.5: Palaeoceanographic change in core DA00-06 during final deglaciation of Jakobshavns Isbrae. **A**: Benthic $\delta^{18}O$ ratio composite record. **B**: % assemblage Arctic indicator species (*S. feylingi, C. reniforme, E. excavatum, S. biformis,B. pseudopunctata).* **C**: % assemblage Atlantic indicator species (*I. norcrossi, S. difflugiformis, C. crassimargo, N. labradorica, B. tenerima, C. teretis, M. zaandamae).* **D**: GRIP ice core $\delta^{18}O$ record. Numbered events (1, 2, 3, 4) link to table in Figure 6.4.

It has been recorded at sites throughout the North Atlantic, North American and northwest European regions, as well as further afield in the mid-latitudes (e.g. Barber *et al.*, 1999; Dean *et al.*, 2002; Klitgaard-Kristensen *et al.*, 1998; Nesje and Dahl, 2001; Stager and Mayewski, 1997; von Grafenstein *et al.*, 1998). This range of proxy records reveals a sudden, short-lived occurrence that variously recorded as a cold, dry or windy event. Central Greenland ice core temperature records reveal a sharp drop in temperature of between 4 and 8 °C, and there was synchronous decline at terrestrial and marine sites in the North Atlantic (Barber *et al.*, 1999).

The spatial similarities between the extent of this widespread cooling, and that of the Younger Dryas cold event, strongly suggest that perturbation of North Atlantic thermohaline circulation was a key factor in the abrupt transitions recorded. Disruption to the heat transfer mechanism from the warm Atlantic Ocean to the atmosphere is thought to have been caused by a large freshwater flux to the region following the final deglaciation of the Laurentide Ice Sheet (Andrews *et al.*, 1999; Barber *et al.*, 1999; von Grafenstein *et al.*, 1998). It is further suggested that the freshwater source relates to a rapid discharge from glacial Lakes Agassiz and Ojibway, through Hudson Strait to the Labrador Sea, which had been dammed by a Laurentide ice sheet remnant (Barber *et al.*, 1999). The effect of this catastrophic input was to cool and freshen surface waters, significantly altering ocean circulation, with wide reaching consequences.

6.2.4.1 The pattern of Jakobshavns Isbrae's response

The nature of the 8.2 event recorded in the GRIP core has previously been characterised by a 2-peak pattern (Alley *et al.*, 1997), with 5 recognisable features (a-e). Nesje and Dahl (2001), also use these 5 recognisable features (but using GISP2) in their comparison of Norwegian lacustrine records. These features are well-reproduced in the foraminferal assemblage data, and the benthic $\delta^{18}O$ record (Figure 6.6). from Disko Bugt.

6.2.4.2 Part "a" in the 8.2 event

At this point it is relatively warm in ice core, and a degree of meltwater flux is indicated by the benthic $\delta^{18}O$ record. Although amounts of Atlantic species are generally low, there is a marginal increase in their abundance at this point. Arctic/ice proximal species are relatively high, indicating the nearness of the calving front of the ice stream, however it can be seen that there is a minor decline in abundance.

6.2.4.3 Part "b" in the 8.2 event

The ice core record shows the first of a 2-peak reduction in $\delta^{18}O$ values, indicating a significant cold period. Benthic $\delta^{18}O$ values are also consistent with a reduced meltwater flux, relating to a decline or stagnation of the rate of ice stream retreat. This indicates that Jakobshavns Isbrae, and the West Greenland Ice Sheet, is responding directly to a decline in atmospheric temperature. The extreme low of warm Atlantic indicator species, and high peak of Arctic species indicate that the West Greenland Current is either very weak, or it is not able to penetrate east into the bay due to an increase in depth of the Disko Bugt mixed water layer.

6.2.4.4 Part "c" in the 8.2 event

A minor recovery can be seen in the GRIP record, and this temperature increase is likely to be the driving mechanism for an increase in meltwater flux from the ice stream, indicated by lighter $\delta^{18}O$ values. Despite an obvious increase in meltwater, the West Greenland Current signal is stronger, shown by a rise in Atlantic indicator species. This suggests that the WGC is vigorous enough to penetrate beneath the meltwater and mixed water layer. This could be due to an increase in the Irminger Current component of the WGC. On a larger scale, amounts of Arctic meltwater flux to the East Greenland Current would be generally decrease during this event, and this reduction in EGC component of the WGC could be responsible for the relative increase in warmth and salinity.

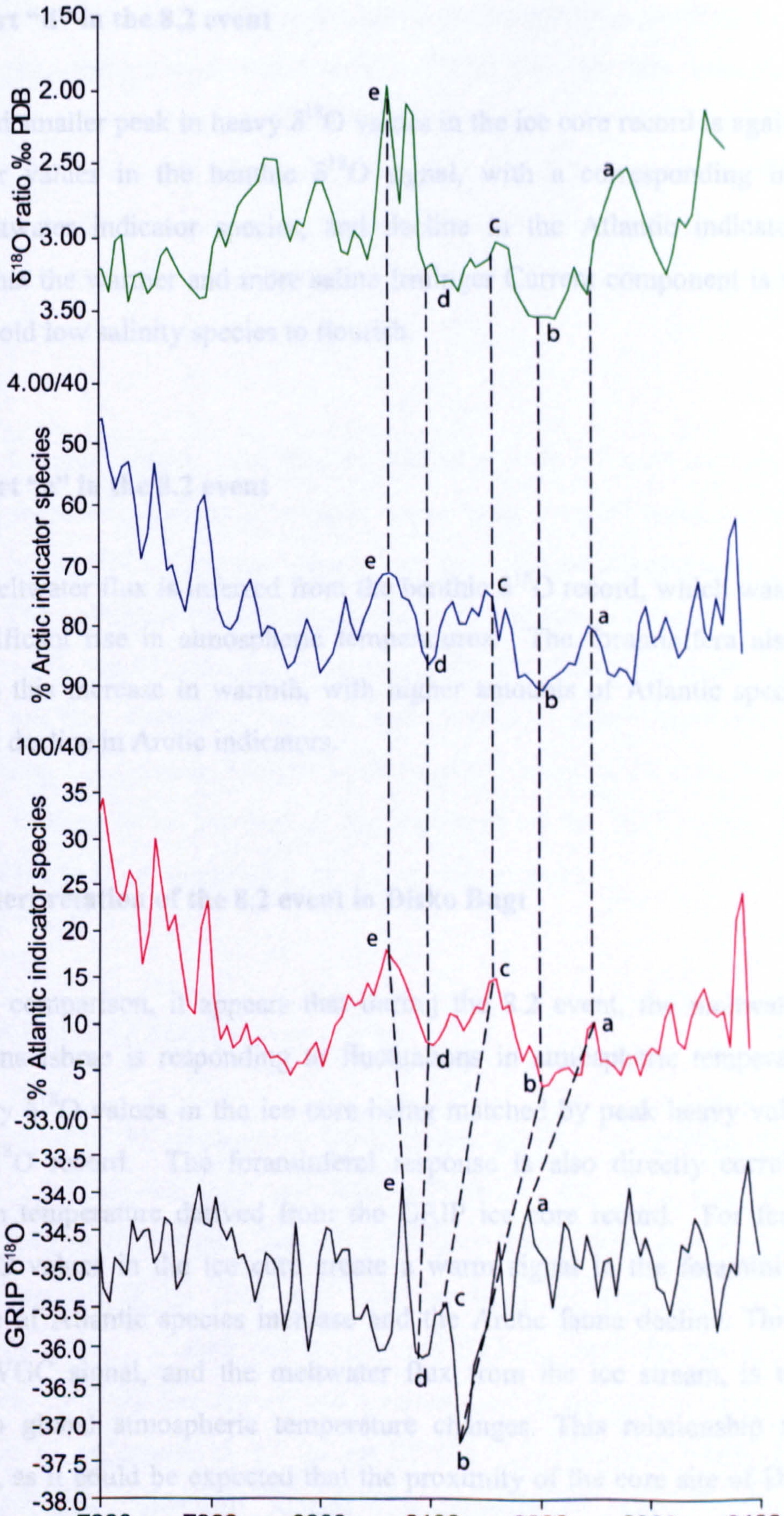

Figure 6.6: Diagram of the nature of the 8.2 event recorded in core DA00-06 in Disko Bugt. 5 recognisable features (a-e) are marked, and these features are matched to the GRIP ice core record. Note in particular the 2-peak pattern minima of (d) and (b) in the benthic isotope record, and "warm" Atlantic indicator record. This is matched by highs in the Arctic indicator record.

6.2.4.5 Part "d" in the 8.2 event

The second smaller peak in heavy $\delta^{18}O$ values in the ice core record is again matched by heavier values in the benthic $\delta^{18}O$ signal, with a corresponding increase in Arctic/meltwater indicator species, and decline in the Atlantic indicators. This suggests that the warmer and more saline Irminger Current component is weakened, allowing cold low salinity species to flourish.

6.2.4.6 Part "e" in the 8.2 event

A large meltwater flux is inferred from the benthic $\delta^{18}O$ record, which was prompted by a significant rise in atmospheric temperatures. The foraminifera also respond directly to this increase in warmth, with higher amounts of Atlantic species, and a significant decline in Arctic indicators.

6.2.4.7 Interpretation of the 8.2 event in Disko Bugt

From this comparison, it appears that during the 8.2 event, the meltwater flux of Jakobshavns Isbrae is responding to fluctuations in atmospheric temperature, with peak heavy $\delta^{18}O$ values in the ice core being matched by peak heavy values in the benthic $\delta^{18}O$ record. The foraminferal response is also directly correlated with changes in temperature derived from the GRIP ice core record. For features a-e, heavy $\delta^{18}O$ values in the ice core create a warm signal in the foraminifera. The abundance of Atlantic species increase and the Arctic fauna decline. This suggests that the WGC signal, and the meltwater flux from the ice stream, is responding directly to global atmospheric temperature changes. This relationship may seem surprising, as it could be expected that the proximity of the core site of DA00-06 to the mouth of Jakobshavns Isfjord would be almost wholly dominated by Arctic/meltwater dominated species, which would drown out any signal of a warm WGC.

The benthic isotope signal and the foraminiferal assemblages continue to be closely correlated with the ice core record until *c.* 7.9 ka BP. By this time, rising global atmospheric temperatures have led to significant meltwater flux from Jakobshavns Isbrae. At 7.9 ka cal BP, temperatures reach a post-8.2 event maximum, and it is likely that this pattern was enough to destabilise the grounded ice stream from its position at Isfjeldsbanken, and initiate a rapid draw down of the Greenland Ice Sheet through the deep trough.

Evidence for this comes from the dramatically reduced sedimentation rate and significant increase in sub-arctic/Atlantic water fauna over the transition from zone 2 to zone 3 in DA00-06 marking a major change in the oceanographic regime at the core site. The sedimentation rate is reduced by two orders of magnitude (13.8 mm/yr to 0.24 mm/yr), the large quantities of fine grained sediment produced by the basal meltwater are now trapped within the deep waters of Jakobshavns Isfjord east of Isfjeldsbanken. The retreat of the ice front would also reduce the influence of diluting meltwater leading to an increase in the influence of the WGC along the eastern margins of Disko Bugt identified in the foraminiferal fauna.

6.2.5 Final retreat of Jakobshavns Isbrae

The final retreat of the Jakobshavns Isbrae to the east of Isfjeldsbanken into the main Jakobshavns Isfjord took place soon after *c.* 7.9 ka cal BP. Supporting evidence for the timing of this final retreat into the main fjord comes from two sources, mollusc data from eastern Disko Bugt, and new lacustrine evidence from just south of Jakobshavns Isfjord. Donner and Jungner (1975) have dated the first appearance of boreal molluscs along the eastern and southern coastal margin of Disko Bugt. The oldest dates group around *c.* 7.5 ka cal BP (eg. *Mytilus edulis* 6790±160 ^{14}C BP, *Macoma balthica* 6680±160 ^{14}C BP, *Mya truncata* 7210±170 ^{14}C BP, *Chlamys islandica* 5930±130 ^{14}C BP, *Zirphaea crispata* 5040±140 ^{14}C BP). Once the ice stream had retreated inside the main fjord system the reduced meltwater flux allowed the WGC to penetrate the shallow waters and fjords of eastern Disko Bugt leading to colonisation of warmer water mollusc fauna. The second line of evidence comes from

Long *et al.* (in prep.), through dating of the organic accumulation of lake sediments within the LGM limit of the Jakobshavns Isbrae ice stream just to the south of the main fjord. A date on organic accumulation of *c.* 7.9 ka cal BP dates the down draw of the icestream associated with its retreat into Jakobshavns Isfjord.

6.2.6 'Fjord Stade' moraine

A prominent feature in the deglacial chronology of West Greenland is the 'Fjord Stade' moraine. This is a series of moraines correlated over wide areas of West Greenland that are thought to represent a still stand/minor readvance at *c.* 9.3 ka cal BP related to either regional climate deterioration or a topographic control on ice sheet retreat (Ten Brink and Weidick, 1974; Warren and Hulton, 1990; Weidick, 1968). Evidence for the 'Fjord Stade' in Disko Bugt is limited to a moraine at Orpissooq in the southeast of the bay with an age estimated > *c.* 8.9 ka cal BP (Donner and Jungner, 1975; Weidick, 1972). Long and Roberts (2002) re-evaluated the age of the Orpissooq moraine to between *c.* 8.4 and 7.7 ka cal BP, about a thousand years younger than previously thought.

The data from core DA00-06, and POR18 suggests there was a still stand in the ice retreat across Disko Bugt in the shallower eastern margins of the bay. The dating resolution of DA00-06 is not good enough to accurately date this event, but as previously discussed it is likely to have taken place between *c.* 10.2 and *c.* 9.2 ka cal BP (fauna from POR18 suggests close proximity of the grounded ice front). This evidence suggests the event described as the 'Fjord Stade' further south in Greenland may correlate to a still stand in a position beyond the present day coastline. The moraine at Orpissooq may well represent a later event in the deglacial chronology of Disko Bugt.

6.3.1 The WGC in Disko Bugt during deglaciation

There is evidence from a range of sources (eg. mollusc, dinocyst and foraminifera data) from coastal locations in West Greenland and Baffin Bay providing information on the initiation and strength of the relatively warm WGC after the last glacial (Donner and Jungner, 1975; Kelly, 1979 and 1985; Osterman and Nelson, 1989; Feyling-Hanssen and Funder, 1990; Ingolfsson *et al.*, 1990; Funder and Weidick, 1991; Bennike *et al.*, 1994; Levac, 2001). The earliest age for initiation of the WGC is 9.73 - 10.58 ka cal BP (Feyling-Hanssen and Funder, 1990), based on mollusc data from the Thule area of NW Greenland. This early initiation is supported by the influx of relatively warm water dinocysts indicating conditions similar to present in the North Water Polynya (northern Baffin Bay) by *c.* 9.8 ka cal BP (Levac *et al.* 2001). Evidence for this early initiation is rather limited further south, though there is a weak signal of WGC influence in Disko Bugt at this time (zone 1 in POR18). A stronger EGC component of the WGC displacing the IC component westwards might explain the limited evidence of warmer conditions in central West Greenland at this time.

Funder and Weidick (1991) document a slightly later date based on the occurrence of a boreal assemblage of molluscs from a number of sites in central West Greenland (65°30'N to 68°30'N) indicating the presence of the WGC and oceanic conditions 1-3°C warmer than present during the period 9.2 - 5.64 ka cal BP. This agrees with foraminiferal data from the Baffin Island continental shelf identifying influx of Atlantic waters from *c.* 9 ka cal BP (Osterman and Nelson, 1989) likely relating to a stronger WGC strengthening the anti-clockwise gyres in Davis Strait and Baffin Bay. This is supported by the evidence from POR18 suggesting an increase in the influence of the WGC in Disko Bugt at this time, and perhaps even encouraging retreat of the Jakobshavns Isbrae ice stream through increased basal melting.

There was clearly a delay in the influx of WGC into eastern part of Disko Bugt after its initiation along the west coast of Greenland from *c.* 9.2 ka cal BP. As previously discussed the colonisation of a large number of boreal molluscs dated to *c.* 7.5 ka cal BP by Donner and Jungner (1975) suggests the delay was due to the meltwater flux produced by the Jakobshavns Isbrae ice stream. It was only once the ice stream had

retreated inside the present day fjord that the WGC could reach the present coastal areas and fjords of eastern Disko Bugt, and the atmospheric temperature variations during the 8.2 event could be recorded in the foraminiferal assemblages. The date for this retreat from DA00-06, *c.* 7.8 ka cal BP, is close to the date for colonisation of boreal molluscs of *c.* 7.5 ka cal BP.

6.3.2 Larger scale links to the inception of WGC

At a larger regional scale, Rahman and de Vernal (1994) reported that the northeastern Labrador Sea remained cold until 8400 ^{14}C BP corresponding to *c.* 9.4 ka cal BP. They suggest establishment of a stronger WGC immediately after this time, which is in support of the observations reported from Baffin Bay (Osterman and Nelson, 1989). The Labrador Sea paleoceanographic scenario thus provides further evidence for cold conditions favouring a relatively stable Jakobshavns Isbræ ice stream position close to the POR18 position until *c.* 9.2 ka cal BP. After a phase of retreat, the ice stream grounded close to DA00-06, where it stayed from before *c.* 8.3 ka cal BP to approximately 7.8 ka cal BP. This stage can be correlated with marked cooling and lowered surface water salinity on the continental margin off Nova Scotia (Keigwin and Jones 1995), which is further evidence that Disko Bugt hydrographic changes and Jakobshavns Isbrae ice stream movements can be linked to large-scale oceanographic changes in the Labrador Sea region.

6.4 Summary of deglaciation of Jakobshavns Isbrae and early WGC activity

Core DA00-06, was collected from the former trough of the Jakobshavns Isbrae ice stream in Disko Bugt, and used to constrain the deglacial chronology and palaeoceanography of Disko Bugt during the early Holocene. From POR18 (Lloyd *et al.*, submitted), it can be seen that the main part of Disko Bugt was deglaciated by *c.* 10.2 ka cal BP. By this time the Jakobshavns Isbrae ice stream had retreated rapidly to a position near the eastern margins of the bay. This initial deglaciation took place before a strong influence of the WGC can be identified in the area. An increase in the strength of the WGC after *c.* 9.2 ka cal BP was accompanied by a retreat of the

Jakobshavns Isbrae ice stream further eastwards, most likely to Isfjeldsbanken immediately west of Jakobshavns Isfjord. The large volumes of meltwater produced by the melting ice stream, diluted/deflected the warmer waters of the WGC away from the eastern coastal areas of Disko Bugt, until *c.* 7.9 ka cal BP when the ice stream finally retreated inside the present day fjord system. Despite this dilution effect, variations have still been recorded in the strength of the WGC during the marked widespread Holocene cooling episode known as the 8.2 event. The final retreat into the fjord system allowed the warmer WGC to fully penetrate to the eastern margins of Disko Bugt supporting the boreal mollusc and foraminiferal faunas associated with its Atlantic sourced waters.

6.5.1.1 Mid to late-Holocene modes of palaeoceanographic change and driving mechanisms in West Greenland: Scenarios for change

Ocean circulation responds to driving mechanisms on a range of temporal and spatial scales. Comparisons between the ice core records of Northern Hemisphere atmospheric temperatures and the West Greenland Current signal recorded in the foraminifera are made. This reveals that following the rapid retreat of Jakobshavns Isbrae, and increasing distance of the proximal calving front, the WGC signal can be "in-phase" and "out of phase" with changes in ice core temperature. This suggests that the response of the warm, saline WGC is more complicated than the direct relationship with atmospheric temperature seen during the 8.2 event. It also suggests that the presence or strength of the WGC may be affected by other local and region components of the ocean-atmosphere climate system. Three scenarios have therefore been developed to explain the variations in the modes of the Holocene palaeoceanographic record in Disko Bugt, West Greenland.

6.5.1.2 Scenario 1: Atmospheric warming is associated with a warmer/strong WGC signal

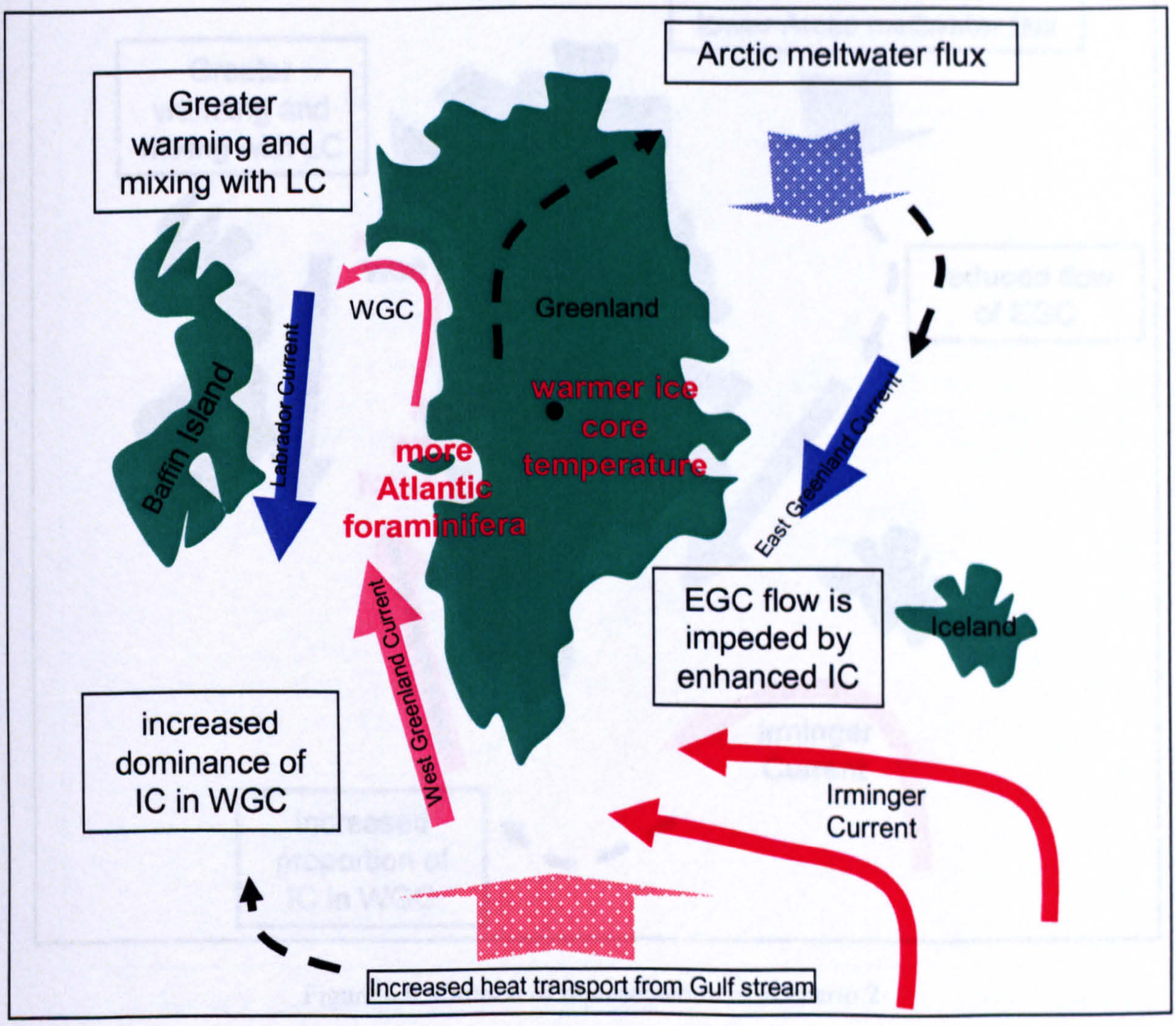

Figure 6.7: Cartoon representation of Scenario 1

Lighter $\delta^{18}O$ values recorded in the ice core record (GISP2) indicate global atmospheric warming. Increased heating at mid latitudes drives a stronger Gulf Stream leading to greater warming in the North Atlantic. A resulting warmer and stronger Irminger Current (branch of the Gulf Stream) will become a proportionally more significant component in the West Greenland Current (WGC). The increased warmth and salinity of the WGC allows the development of warmer loving Atlantic/Boreal foraminfera to dominate in Disko Bugt. (In the reverse scenario, atmospheric cooling would lead to a weaker IC component of the WGC, resulting in a decrease in the Atlantic fauna).

6.5.1.3 Scenario 2: Atmospheric cooling is associated with a warmer strong WGC signal

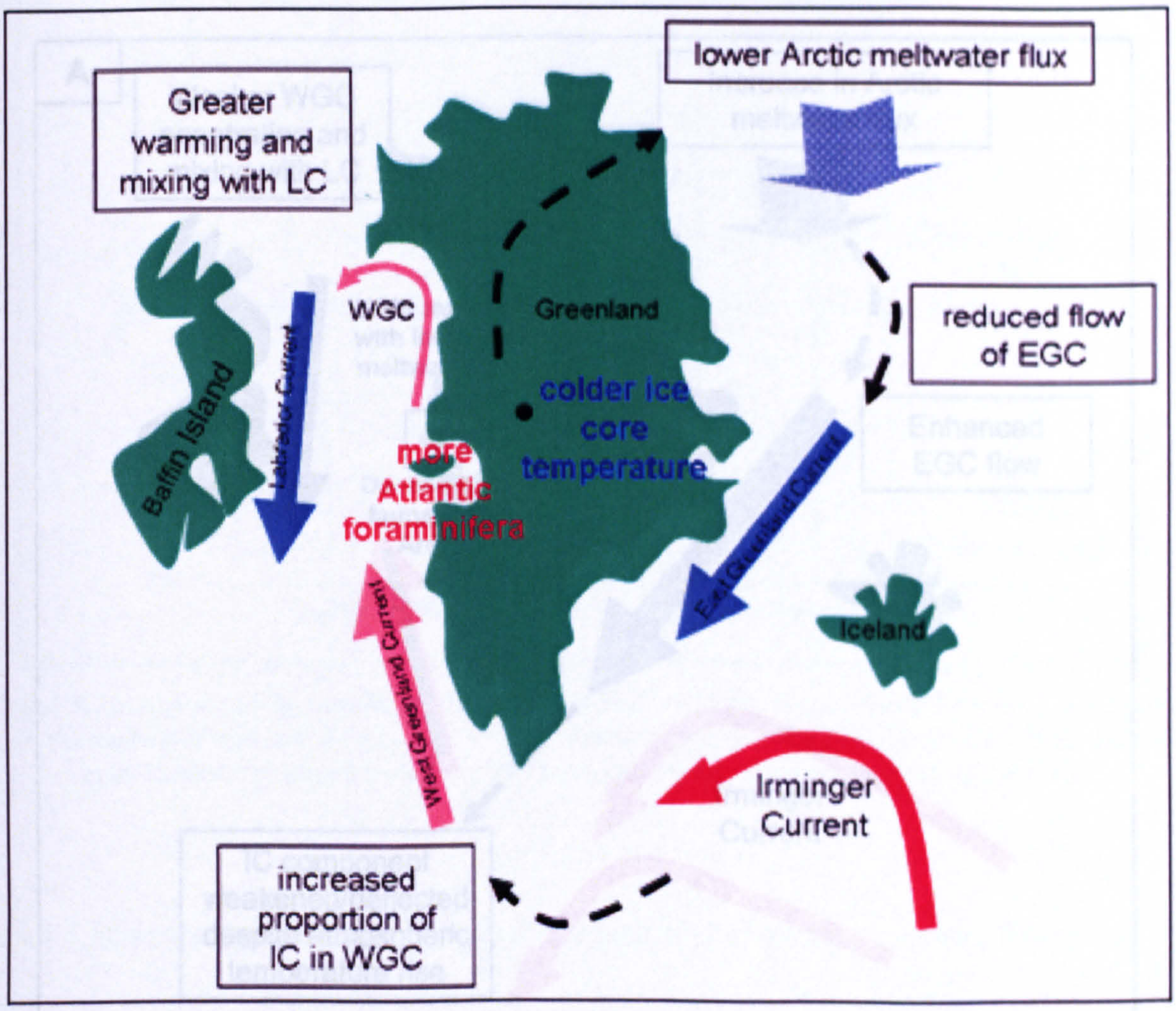

Figure 6.8: Cartoon of representation of Scenario 2

Heavy $\delta^{18}O$ values recorded in the ice core record (GISP2) indicate global atmospheric cooling. During colder periods, there is a decreased Arctic meltwater input into the Nordic Seas, which leads to a reduced flux of cooler low salinity East Greenland Current (EGC) water. This allows an increased proportion of Irminger Current (IC) water in the West Greenland Current (WGC). The result is an increase in the proportion of warmer, more saline waters entering Disko Bugt, which is recorded in the foraminiferal assemblage as an increase in Atlantic water associated species.

6.5.1.4 Scenario 3: Atmospheric warming is associated with a cooler/weakened WGC signal

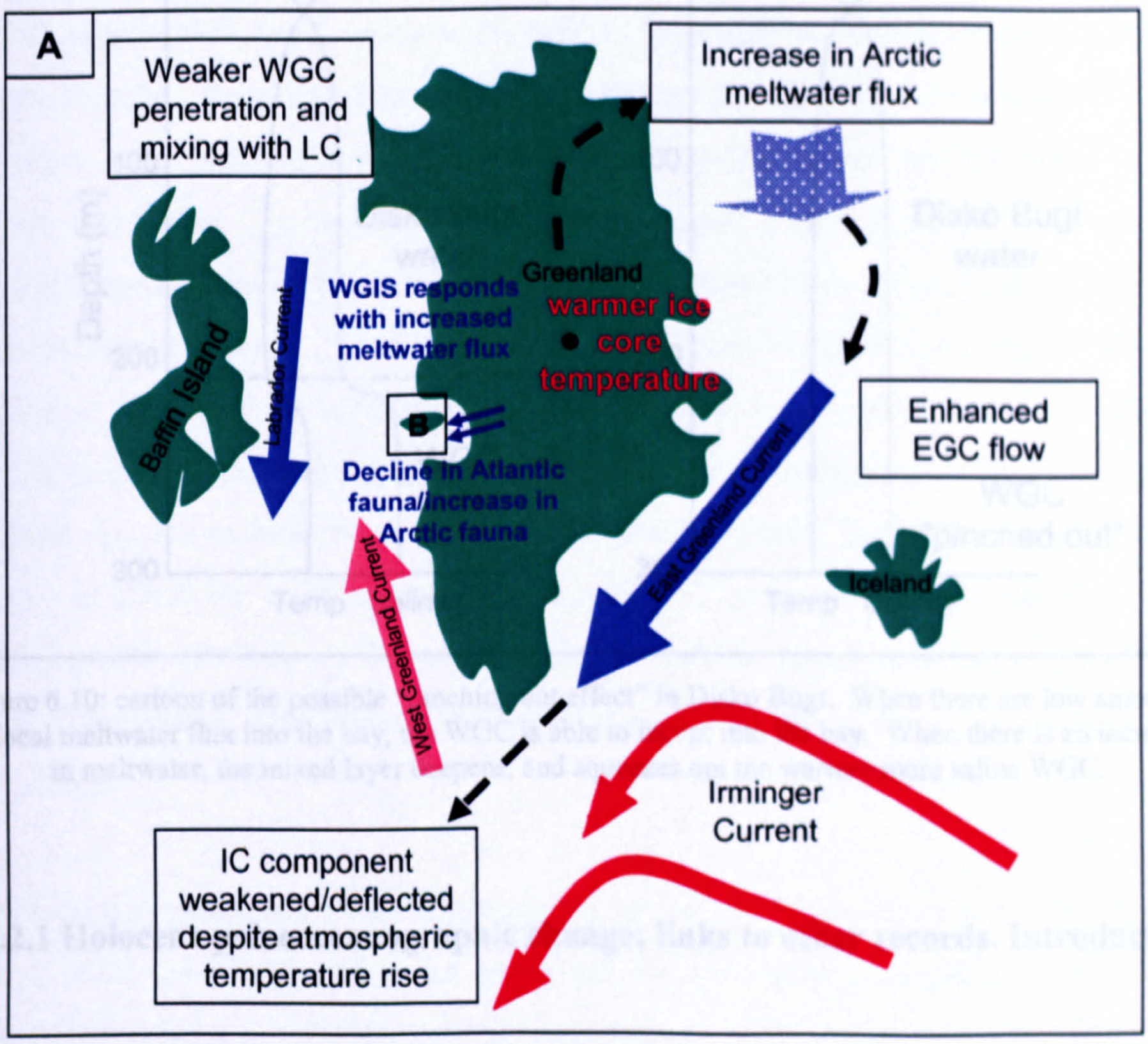

Figure 6.9: Cartoon representation of Scenario 3. B marked above links to figure 6.10; the "pinching out" effect in Disko Bugt.

Lighter $\delta^{18}O$ values recorded in the ice core record (GISP2) indicate global atmospheric warming. During warmer periods, there is an increased flux of Arctic meltwater into the Nordic Seas, which increases the strength of EGC leading to a more dominant EGC component of the WGC. At the same time, localised increases in meltwater flux from outlets of the West Greenland Ice Sheet (WGIS) increase the depth of the cooler lower salinity mixed water layer in Disko Bugt. This leads to a cooling effect of the WGC and an increase in Arctic fauna. In relatively shallow settings this may also lead to a "pinching out" effect (Figure 6.10) of the warmer more saline WGC water mass, allowing more Arctic foraminifera fauna, or species with a greater tolerance to temperature and salinity variations to be represented.

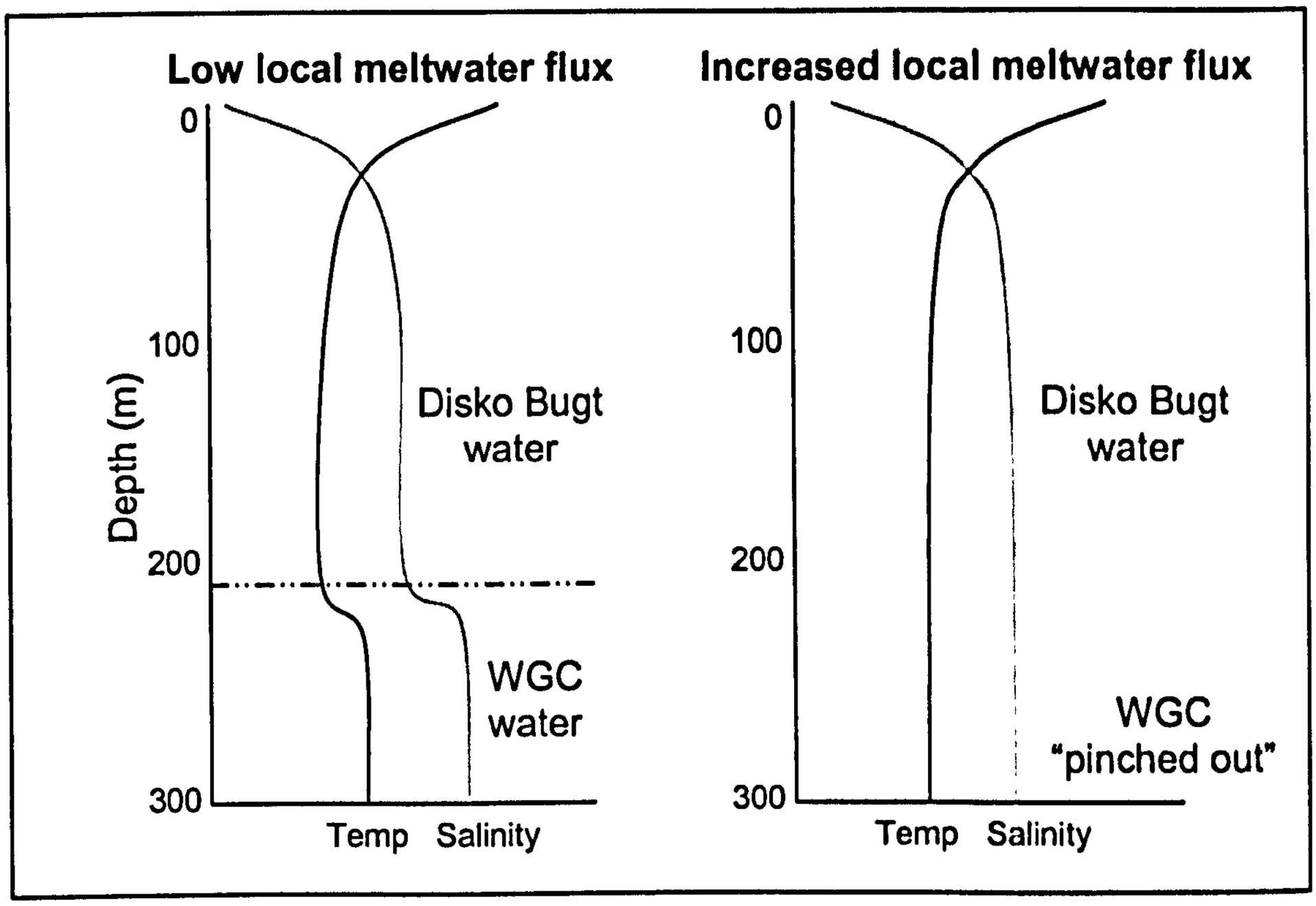

Figure 6.10: cartoon of the possible "pinching out effect" in Disko Bugt. When there are low amounts of local meltwater flux into the bay, the WGC is able to incept into the bay. When there is an increase in meltwater, the mixed layer deepens, and squeezes out the warmer more saline WGC.

6.5.2.1 Holocene palaeoceanographic change; links to other records. Introduction

The tight chronological control in both DA00-05 and DA00-03 allows a detailed examination of palaeoceanographic change in West Greenland, and enables close comparison to other proxy records, such as the GISP2 derived temperature record. Timings of change in the West Greenland records are compared to other marine evidence from East Greenland, the waters of North Iceland and the Labrador Sea area. Although dating control is poorer in DA00-06, inferences can still be made about the strength of the WGC following deglaciation.

6.5.2.2 Palaeoceanographic change in DA00-06, and links to other records

In core DA00-06 in front of Jakobshavns Isfjord, warmer saline loving fauna are present since the incursion of the WGC following final deglaciation around 7.9 ka cal BP. Sampling resolution becomes much weaker following the end of zone 2, and

inferences about high resolution changes at this site are more difficult to make. However, it can clearly be seen from the foraminiferal diagram presented in (Chapter 4, section 4.2.1) that there is a period of maximum warmth between *c.* 7.5 and 5.7 ka cal BP, represented by *M. zaandamae,* and *N. labradorica,* with the highest amounts of test linings. This period is likely to represent the maximum Holocene climatic optimum, and strongest WGC circulation in West Greenland, its inception having started well before this (see the discussion in Chapter 6 section 6.2.5). The ice core records show that the Holocene climatic optimum lasted from approximately 8 to 4 ka cal BP (Dansgaard *et al.,* 1994, Johnsen *et al.,* 2001)), but from foraminiferal data in this thesis, and other marine records in West Greenland, and eastern Arctic Canadian, as well as comparisons to East Greenland and the North Iceland shelf (see below), its duration appears to have been shorter in West Greenland. Following the maximum warmth in DA00-06, there appears to be a period of minimum warmth, between *c.* 5.7 and 3.3 ka cal BP. The resolution of the core is poorer here, but the record of DA00-05 in Kangersuneq also records this cooling phase in the WGC, on a much higher resolution.

Funder and Weidick (1991) document warm loving boreal molluscs in coastal sites in central West Greenland until *c.* 5.6 ka cal BP, with a cluster of *Zirphea crispata* beds in a sheltered inner coastal site in Disko Bugt data 5.2-4.9 ka cal BP, and suggest that this is the maximum Holocene thermal optimum. It is likely that localised atmospheric warming in sheltered waters at the site in Disko Bugt explains the abundance of these warmer loving molluscs. Further evidence of terrestrial warming during the Holocene comes from lacustrine palynological investigations in Disko Bugt (Fredskild, 1988). The taxa show that thermal optimum conditions were reached by 7.5 ka cal BP. Combined with crustacean assemblage data, the lake records show that by 7.5 ka cal BP, high Arctic crustacean species were extinct, and were replaced by more thermophilous species. These warmer conditions are estimated to have lasted until *c.* 4.2 ka cal BP. On the eastern Baffin continental shelf, the warming event identified by Osterman and Nelson (1989) at *c.* 8.5 ka cal BP by the presence of *m. zaandamae* and *N. labradorica,* was over by *c.* 6 ka cal BP.

Along the North Iceland margin, Andrews *et al.*, (2003) found evidence for the thermal maximum *c.* 8-6 ka cal BP from increases in coarse sediments, and lower benthic $\delta^{18}O$. They relate this to changes in variations in deep convection in the Greenland and Iceland Seas. Timing for the end of the Holocene thermal optimum in the marine records therefore appears to be earlier than terrestrial, (ice core and lacustrine) records.

6.5.2.3 Palaeoceaongraphic change in DA00-05, and links to other records

Core DA00-05 extends from *c.* 6.7 ka cal BP. Figure 6.11 highlights significant changes in the foraminiferal assemblages, which are summarised below in Figure 6.12.

Event (ka cal yr BP)	Palaeoceanographic conditions
1 (6.4-6.0)	Atlantic foraminifera decline, high amounts of species indicative of fluctuating or poorer conditions
2 (5.6-5.2)	Further decline in Atlantic fauna, high amounts of species tolerant to changing conditions, low amounts of Arctic specific fauna. Indicates increasing cooling trend
3 (4.7-4.4)	Distinct colder ice core temperatures and very low Atlantic foraminifera. The much colder period is represented by a rise in the Arctic water indicator, and relatively high amounts of species tolerant to poorer conditions with lowered or fluctuating temperature and salinity
4 (4.4-3.9)	Despite a recovery in ice core record, fauna continue to show declining conditions, with continuing lows of Atlantic species, and increases in the tolerant fauna
5 (3.4-2.2)	Faunal assemblages show prolonged period of cool/weak WGC, with very low levels (<10%) of Atlantic species, and up to 60% of species relating to faunal tolerant of poorer conditions
6 (2.0-1.4)	A significant rise in Atlantic species indicates amelioration of water mass conditions. It is accompanied by a relative rise in ice core temperatures. A decline in the arctic indicator is accompanied by a decline in the species that are related to poorer or cooler conditions.

Figure 6.12: Summary of distinct changes in palaeoceanographic conditions in Disko Bugt from DA00-05. Numbered events relate to events marked with a black line in Figure 6.11, and are referred to in the text.

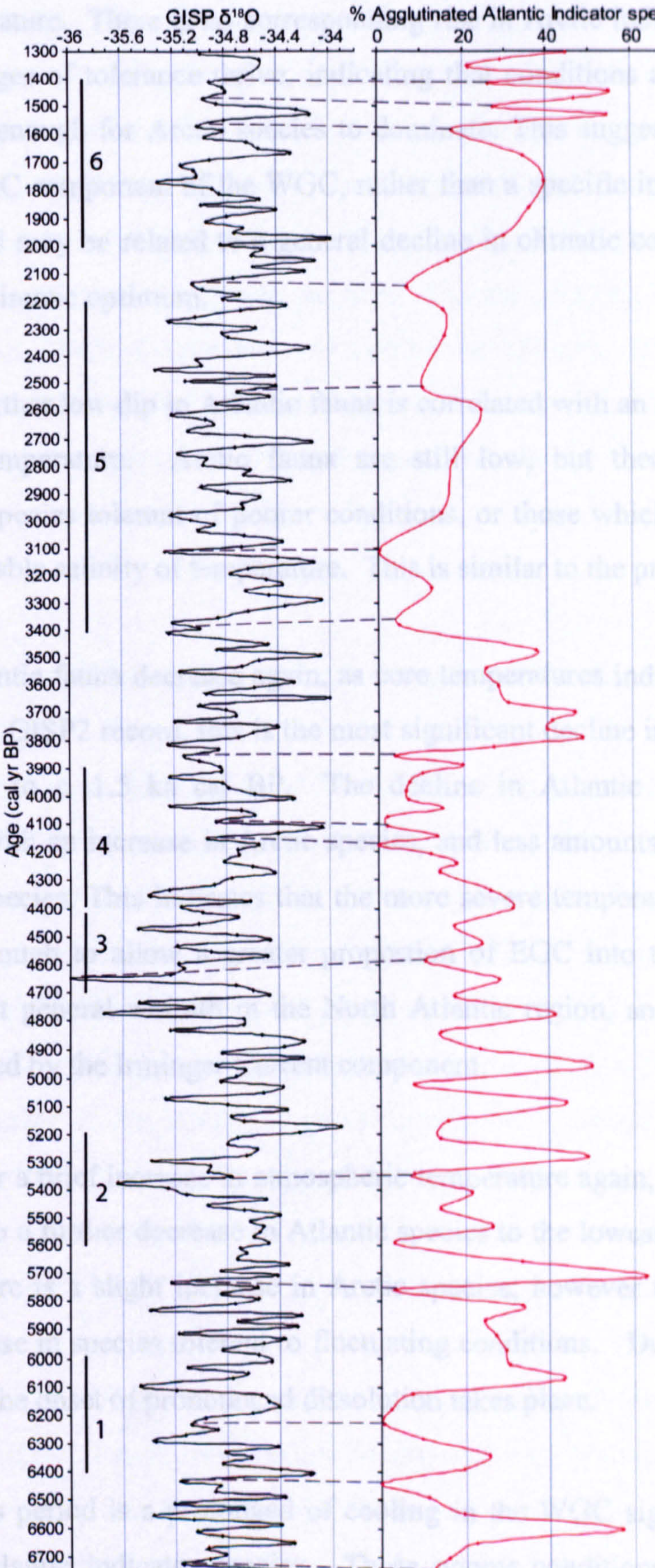

Figure 6.11: Summary of palaeoceanographic change represented by foraminiferal faunal changes in agglutinated Atlantic species (*A. glomerata, S. diflugiformis, C. crassimargo*) for core DA00-05. Points of correlation between temperature minima in the GISP2 ice core records and low amounts of Atlantic water mass indicator species are marked with a dashed link. Black bars 1-6 mark periods of distinct palaeoenvironmental conditions that are summarised in Figure 6.10, and referred to in the section text.

Event 1) A trough in Atlantic indicator species corresponds with 2 minor troughs in ice core temperature. There is no corresponding rise in Arctic indicators, but species with wider ranges of tolerance thrive, indicating that conditions are not favourable, but not severe enough for Arctic species to dominate. This suggests a weakening or cooling of the IC component of the WGC, rather than a specific increase in the EGC component, and may be related to a general decline in climatic conditions following the Holocene climatic optimum.

Event 2) A further low dip in Atlantic fauna is correlated with an episode of lowered atmospheric temperature. Arctic fauna are still low, but there is a significant abundance of species tolerant of poorer conditions, or those which show affinity for water with variable salinity of temperature. This is similar to the previous event (1).

Event 3) Atlantic fauna decrease again, as core temperatures indicate a further cold episode. In the GISP2 record, this is the most significant decline in temperature from 6.7 ka cal BP to *c.* 1.5 ka cal BP. The decline in Atlantic fauna is this time accompanied with an increase in Arctic species, and less amounts of the water mass "indifferent" species. This indicates that the more severe temperature decline during this time is enough to allow a greater proportion of EGC into the WGC, or more likely to inhibit general warmth in the North Atlantic region, and reduced the heat transfer provided by the Irminger Current component.

Event 4) After a brief increase in atmospheric temperature again, the ice core record can be linked to a further decrease in Atlantic species to the lowest levels observed in this core. There is a slight increase in Arctic species; however the main change is related to the rise in species tolerant to fluctuating conditions. During this period, at 4.1 ka cal BP, the onset of pronounced dissolution takes place.

Event 5) This period is a prolonged of cooling in the WGC signal, with very low amounts of Atlantic indicator species. These poorer conditions see a rise in the tolerant fauna, but no corresponding rise in the Arctic associated indicators. There are generally fluctuating temperatures derived from the ice core record at this time, so there is no direct correlation for this peak. This period may relate to a decrease in the

warmth of the IC component of the WGC, as a result of the general decline in warmth during the neoglacial.

Event 6) This period is significantly different from the previously established pattern of decreased warmth of the WGC, with intervals of more ameliorated conditions. The Atlantic indicators show a distinctive rise in abundance, and both Arctic species, and fauna indicative of poorer conditions, decline. The ice core record indicates a brief but significant decline in temperature, followed by a recovery. This brief decline is not distinctive in the faunal assemblages however, and may point to local factors such as local sea ice cover, or local atmospheric conditions such as changes in wind stress drowning out a more regional signal.

6.5.2.4 Overview of palaeoceanographic cooling trends in DA00-05

The foraminiferal assemblages in DA00-05 show fluctuations in the warmth and strength of the WGC from *c.* 6.4 ka cal BP, moving generally to a cooler signal of the WGC. This is earlier than in DA00-06. However, this is likely to be a combination of poorer dating control in the top 150 cm of DA00-06, and lower sample resolution. Cooler phases of the WGC in DA00-05 (*c.* 6.4 to 6.0, 5.6 to 5.2, 4.7 to 4.4, 4.4 to 3.9 and 3.4 to 2.2 cal yr BP), identified by decreases in the Atlantic species, and rises in the species tolerant of fluctuating or poorer conditions, intersperse with the warm Atlantic water WGC signal. The assemblages are not replaced by Arctic species, although this is somewhat difficult to gauge, given the alteration to fjord hydrological circumstances, which led to the dissolution conditions. (The major species such as *s. feylingi, B. pseudopunctata,* and *C. reniforme* that would be representative of increasingly cooler or fluctuating unstable conditions are not present in the record, due to the post depositional dissolution). Despite this, the agglutinated record is still able to suggest that the foraminiferal fauna are sensitive responders to minor fluctuations in the strength of the WGC.

6.5.2.5 Palaeoceanographic trends 9-6 ka cal BP

Reconstructed conditions on the North Icelandic shelf indicate higher than present day temperatures between 9 and 6 ka cal BP, representing a Holocene climatic optimum. Eiriksson *et al.* (2000b) attribute these to a relative strengthening of the palaeo-Irminger Current, which fits well with the record of changing palaeoceanographic circulation of the WGC in Disko Bugt. In the northwest Atlantic and Denmark Strait (Balsam, 1981; Kellogg, 1984), the Iceland Sea (Koc Karpuz and Schrader, 1990), and the North Icelandic shelf (Eiriksson *et al.* 2000b), a general decrease in sea surface temperatures is documented from benthic and planktic foraminiferal faunal changes temperature following the Holocene climatic optimum (9-6 ka cal BP) in these regions. On the East Greenland shelf, Jennings *et al.* (2002) report a shift to colder, lower salinity 'polar' conditions around 5 ka cal BP, with several oscillations, similar to the pattern seen in the Disko Bugt record from DA00-05.

In the Kangerdlugssuaq Trough, on the southeast Greenland shelf, Williams *et al.* (1995a) use sedimentological proxies to infer general cooling from *c.* 6 ka cal BP. These studies suggest changes in the East Greenland Current are linked to severe increases in sea ice over the East Greenland shelf. The onset of cooling in the North Icelandic shelf is also related to this increased influence of the East Greenland Current (Eiriksson *et al.*, 2000). These conditions translate well to the inferred changes in the foraminiferal fauna in Disko Bugt through its connectivity to the WGC.

6.5.2.6 Palaeoceanographic trends 6-4.7 ka cal BP

Jennings *et al.*, (2002) find evidence for Neoglacial cooling in East Greenland waters around 4.7 ka cal BP, and on Baffin Island, nearshore molluscan assemblages have been identified which indicate cooling begins around 5 ka cal BP. In the terrestrial record from Baffin Island, records show a delay of climatic deterioration until as late as 3 ka cal yr BP (Osterman and Nelson, 1989), and this pattern of an early oceanographic signal, followed by a later terrestrial signal is also duplicated in west Greenland, as Fredskild (1984) found evidence of terrestrial warming in lakes until *c.* 4.2 ka cal BP, which declined and culminated in an inland ice margin advance.

6.5.2.7 Palaeoceanographic trends from 4.7-2.2ka cal BP

The core record from DA00-05 suggests an intensification of cooling or weakening in the WGC between *c.* 4.7 and 2.2 ka cal BP. This increased phase of cooling may well have initiated changes in local fjord hydrology in Kangersuneq, and by *c.* 4.1 ka cal BP, conditions had declined enough to significantly alter post-depositional preservation processes, until the present day.

At *c.* 3.8 ka cal BP in the DA00-05 record, there is no record of the further *c.* 3.8/3.7 ka cal BP cold peak which is seen in the East Greenland sites. In fact there is a slight increase in Atlantic indicator species, around 450 cm, which includes a significant amount of calcareous fauna (*I. norcrossi,* in particular), which can be seen in the foraminiferal assemblage diagram for DA00-05 presented in Chapter 4 (section 4.3.1). Although the calcareous species appear only once, the agglutinated indicators suggest this slight warmth lasted until 3.4 ka cal BP. This does not seem to be linked to records from the East Greenland (Jiang *et al.,* 2002), where diatom assemblage changes suggest cold points (temporal) in sea surface temperatures at 4.1 and 3.7 ka cal BP, and further cooling from 3.6 to 3.2 ka cal BP.

6.5.3 Palaeoceanography and controlling factors for dissolution in DA00-05

McGowan *et al.,* (2003) found an enhanced phase of effective precipitation until 4.7 ka cal BP from a limnological study in southwest Greenland. Reducing seasonal fjord meltwater due to declining summer insolation at 60°N (Berger and Loutre, 1991), and reduced atmospheric moisture, may have initially allowed the slight rise in Atlantic species recorded at around 4.3 ka cal BP in DA00-05, allowing a brief stable incursive period of WGC water.

Less mixing of water masses in the fjord due to reduced seasonal melting, combined with likely prolonged seasonal pack ice cover due to lower temperatures and general cooling may have been conducive to creating the following dissolution scenario: Intensification of stratification processes through the increasing seasonal ice cover that would be expected at this time, may lead to the development of cold dense saline

bottom waters for most of the year. The sea ice diatom record from Kangersuneq at this time also indicates a short cold spell (K.G. Jensen, *unpublished data*).

The absence of calcareous foraminiferal taxa due to post-depostional dissolution is likely to be related to the development of these colder heavier bottom waters. The stratification process may lead to the development of a strong pycnocline. This would prevent bottom water ventilation, leading to lowered dissolved oxygen levels and higher CO_2 concentrations from organic decay of the sediments. Atmospheric CO_2 exchange would be inhibited by stratification, and the fjord bottom water conditions would become very corrosive to calcareous foraminifera.

Osterman and Nelson (1989) found evidence of an interglacial dissolution event from 6-0 ka cal BP, following the Holocene climatic optimum on the eastern Baffin continental shelf, with an increased transfer in Arctic Water through the Queen Elizabeth Islands in the eastern Canadian Arctic, leading to the re-establishment of the Baffin Current (cold dense and saline). Asku (1983) has identified a similar dissolution scenario from 8 ka cal BP in central Baffin Bay. These dissolution events are related to the CO_2 concentration of the waters, which are controlled by temperature and the age of the water mass. Older water (Baffin Bay Deep Water) has a higher amount of dissolved CO_2, which favours dissolution of calcareous tests. In Disko Bugt, WGC water is older than cold shallow water from meltwater, and is likely to have higher levels of CO_2. This would also contribute to the changing hydrological conditions in the fjord.

A significant peak in carbonate flux at c. 4.2 ka cal BP heralds the mid-Holocene shift in Arctic sea ice on the East Greenland shelf, which is contemporaneous with the change in preservation conditions in Kangersuneq, Disko Bugt. Jennings *et al.* (2002) suggest that this event is linked to sea surface cooling associated with the flux of polar water and sea ice to the East Greenland Current. It marks the distinctive onset of Neoglacial conditions in the East Greenland shelf, and provides an excellent link to the decline seen in the warm signal of the WGC in Disko Bugt at this time. Further peaks are observed in their record at 3.8 and 2.4 ka cal BP, which are not seen in the Kangersuneq record. Similarly, Jiang *et al.* (2002) record a short-lived cooling in sea surface temperatures inferred from diatoms at 4.1 ka cal BP, and again at 3.7 ka cal

BP. This line of evidence is backed by the ice core record from DYE-3, which documents decreasing atmospheric temperature (Dahl-Jensen *et al.*, 1998). Contrary to the DYE-3 ice core, the GISP2 ice core record indicates slightly increased atmospheric temperatures from 4 ka cal BP (Figure 6.10 and Alley *et al.*, 1999).

6.5.4 Link between atmospheric conditions and cold phase in Disko Bugt

The disparity between the ice core records and the palaeoceanographic records from Disko Bugt may stem from their location and localised atmospheric conditions at ice core sites. The higher altitude and central location of the GISP2 ice core in relation to DYE-3 is affected by both the Iceland Low to the southeast, and Davis Strait/Baffin Bay storms from the Baffin Bay Trough to the southwest and west (Barlow *et al.*, 1997). The North Atlantic Oscillation influences the GISP2 isotopic signal through the "seesaw" in winter temperatures between West Greenland and northern Europe.

The Baffin Bay Trough is a westward extension of the Iceland Low, and during enhanced positive phases of NAO, when the Icelandic Low is centred high, a westward displacement of the Baffin Bay Trough gives rise to colder, dryer conditions over West Greenland (Barlow *et al.*, 1997; Dawson *et al.*, 2003). During enhanced NAO phases or extremes of the seesaw, inferred temperature excursions from the deuterium ice core record correspond to a similar shift in the West Greenland side of the seesaw (Barlow *et al.*, 1997). This change in atmospheric conditions may explain the significant cold phase in Disko Bugt, and be the driving mechanism for changing fjord conditions in Kangersuneq. Both Dawson *et al.* (2003) and Jones *et al.* (1997) demonstrate the GISP2 ice core record shows good correlation to synoptic scale climatology.

From other lines of proxy evidence from Kangersuneq fjord, there is a marked increase in coarser grained sediment at this time (Morros, *unpublished data*), and a decline in sea-ice diatoms (K.G. Jensen, pers. comm., 2003). This suggests that there may be some short-lived local response of the flora and fauna in the Kangersuneq fjord. This may be explained by a change of source of sediment input, or localised atmospheric conditions such as increased wind stresses. These may have been enough

to ameliorate conditions in the water masses in the fjord to allow a brief period of mixing; enough to disturb the stratified conditions, altering the lysocline depth and leading to a brief re-oxygenation of the bottom waters. This effect however, may well be a local response to a regional forcing, for example a reduction in the positive NAO phase seen earlier in the record. A weakly positive or enhanced negative NAO phase in West Greenland would see increased moisture supply to West Greenland and "warmer" winters (Jones *et al.*, 1997).

The prolonged cool period in DA00-05 (3.4-2.2 ka cal BP) is analogous with several other proxy records for palaeoenvironmental change. Extreme phases of winter aridity have been recorded in terrestrial sites around Kangerlussuaq in West Greenland, prior to 3.5 ka cal BP, and around 3.25 and 2.8 ka cal BP (Willemse *et al.*, 2003). These can be attributed to shifts in the air masses over the Greenland Ice Sheet and West Greenland, as a result of increased phases of enhanced NAO. West Greenland pollen assemblages indicate a decline in frequencies of exotic North American taxa transported by southwesterly winds, indicating a shift to colder, dryer northerly winds dominating over the region (Fredskild, 1984), and similar pollen evidence comes from east-central Baffin Island (Short *et al.*, 1985). A reduction in marine aerosols in the Devon Ice Cap in the eastern Canadian Arctic after 3.5 ka suggests prolonged sea ice cover in the region, reducing seasonally open water conditions (Levac *et al.*, 2001). Eiriksson *et al.* (2000) find evidence of increased ice rafting and a marked cooling of surface water around 3 ka cal BP, and Bond *et al.* (1997) document a North Atlantic IRD event linked to decreased solar insolation around 2.8 ka cal BP (van Geel *et al.*, 1999).

A reduction in solar insolation beyond a critical threshold has been held responsible for the onset of Neoglacial conditions in East Greenland, the eastern Canadian Arctic, and the Nordic Seas (e.g. Andrews *et al.*, 1997; Koc and Jansen, 1994; Williams *et al.*, 1995b). This reduction together with enhanced NAO conditions may have led to a southward displacement of the Arctic Fronts and southerly advance of the Arctic drift ice limits along East Greenland (Jennings *et al.*, 2002). A similar scenario has already been suggested for the Nordic Seas area (Koc *et al.*, 1993; Koc and Jansen, 1994). The effects of enhanced positive NAO may also account for the glacial activity in Iceland during this time. Gudmundsson, (1997) describes generally increasing glacier

expansion in North Iceland *c.* 6-5 ka cal BP, and Kirkbride and Dugmore (2001) further constrain the timing of the most significant glacier expanses to between 4.7 and 4.2 ka cal BP.

6.5.5 Palaeoceanographic trends from 2.2 ka cal BP onwards

From *c.* 2.2 ka cal BP to 1.4 ka cal BP there is a distinctive warming trend seen in the agglutinated Atlantic indicator species. This is not matched by particular warming in the ice core record, which shows only a peak and then swift decline *c.* 2 ka cal BP. However, Andrews and Giraudeau (2003) find evidence for warming around 2 ka cal BP from coccolith evidence on the inner North Iceland shelf, and surface warming in the Norwegian Seas from foraminiferal evidence (Risebrobakken *et al.*, 2003). This is attributed to both reduced discharge from the Russian High Arctic rivers, and increasing strength of the Irminger Current supplying Atlantic water to the area. A true picture of the WGC signal in relation to atmospheric temperatures may well be being obscured by the stratification scenario during the most severe cooling of the Neoglacial.

Conditions in Kangersuneq Fjord seem to relate to the general onset of cooler climatic conditions related to the Neoglacial. The intensity of these inferred cooler phases of the WGC increases through the core, towards the timing of the onset of widespread Neoglacial cooling (*c.* 4 ka cal BP). These cooler/fluctuating conditions imply that the strength and warmth of the WGC is not constant during the end of the Holocene climatic optimum, and indeed may support evidence for an early palaeoceanographic descent to Neoglacial conditions, prior to declining terrestrial atmospheric conditions.

6.6.1 DA00-03: late-Holocene palaeoceanography

The outer bay location of DA00-03 has the shortest duration of record. However, resolution is extremely high, and distinctive trends (1-6) can be seen in Figure 6.13. A description of the inferred palaeoceanographic conditions is given in Figure 6.13 It is proposed that these relate to strengthening and weakening of the warm WGC signal.

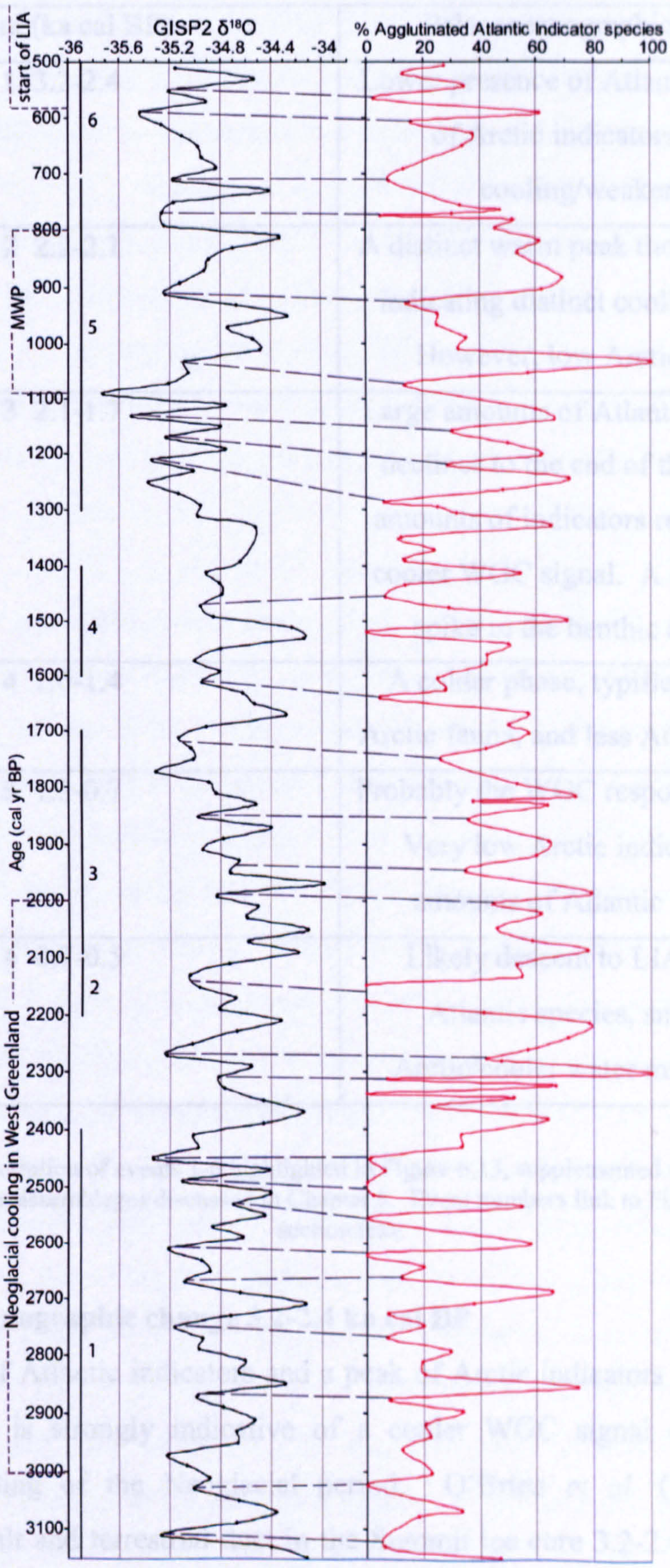

Figure 6.13: Summary of palaeoceanographic change represented by foraminiferal faunal changes in Atlantic species (*I. norcrossi, C. crassimargo, N. labradorica, G. inaequalis, S. diflugiformis & C. teretis*) for core DA00-03, plotted with bidecadal oxygen isotope record from GISP2 ice core. Points of correlation between temperature minima in the GISP2 ice core records and low amounts of Atlantic water mass indicator species are marked with a dashed link. Black bars 1-6 mark periods of distinct palaeoenvironmental conditions that are summarised in Figure 6.14, and referred to in the section text Classical events are labelled along the time axis: LIA= Little Ice Age; MWP= Mediaeval Warm Period.

Event (ka cal BP)	Palaeoceanographic conditions
1 3.2-2.4	Lower presence of Atlantic species, peak of Arctic indicators, indicates cooling/weaker WGC
2 2.2-2.1	A distinct warm peak then a sharp trough indicating distinct cooling/freshening. However, low Arctic indicators.
3 2.1-1.7	Large amounts of Atlantic species which declines to the end of the phase. Low amounts of indicators representative of cooler WGC signal. A distinctive light spike in the benthic d18O record
4 1.6-1.4	A colder phase, typified by a peak of Arctic fauna, and less Atlantic indicators.
5 1.3-0.7	Probably the WGC response to the MWP. Very low Arctic indicators, higher amounts of Atlantic foraminiera.
6 0.7-0.5	Likely descent to LIA, decreasing Atlantic species, small peak of Arctic/cooler water mass indicators.

Figure 6.14: Description of events 1-6 highlighted in Figure 6.13, supplemented with interpretative summaries based on assemblages discussed in Chapter 5. Event numbers link to Figure 6.13, and to the section text.

6.6.2 Palaeoceanographic change 3.2-2.4 ka cal BP

Low amounts of Atlantic indicators and a peak of Arctic indicators between 3.2 and 2.4 ka cal BP is strongly indicative of a cooler WGC signal during the most distinctive cooling of the Neoglacial period. O'Brien *et al.* (1995) document increased sea salt and terrestrial dust in the Summit ice core 3.2-2.4 ka cal BP, and during the LIA. They attribute these increases to either an intensification of the meridonal air flow, or expansion of the north polar vortex. Weidick *et al.* (1990; 1994, and Kelly, (1980) advocate readvance of glaciers on the West Greenland Ice Margin beginning around 3.5 ka cal BP which brought them to their current positions. This concurs with the most intense cooling seen in the WGC signal in DA00-05 and in

DA00-03. The cooling signal in the WGC seen at this point in DA00-03 may well be related to both decreasing temperature and salinity from enhanced meltwater flux from the distal Jakobshavns Isbrae, and to a freshening and intensification of the EGC component of the WGC. Jennings *et al.* (2002) document a freshening of the EGC which became more pronounced after 2 ka cal BP, and link it with a widespread increase in sea ice conditions in the (East) Greenland region. In south Greenland, between 3 and 2 ka cal BP, Kaplan *et al.*, (2002) used lake sediment records to infer the most widespread effects of Neoglacial cooling that were likely to have had far-felt effects throughout the Labrador sea and Greenland area, including Baffin Bay.

A positive NAO index encourages strong winds which increase ice export through the Fram and Denmark Straits (Jennings *et al.*, 2002), which is translated into a cooling and freshening of the EGC. The effect of an EGC component increase and dilution/deflection of the IC component finds two recent modern analogue situations. Observed sea surface salinities (SSS) in the Labrador Sea (55W-40W, 45N-55N) surface salinities during the last 50 years show a distinct freshening, particularly in the coastal waters (Hakkinen, 2002). Values in the highest salinity range, typically generated by the influence of the North Atlantic Current (a branch of which is the Irminger Current) indicate weakened transport of warmer more saline Atlantic water. This can be interpreted as weakened transport of saline waters to the area.

The well-documented Great Salinity Anomaly (GSA) of the 1970's, was widespread through the North Atlantic region (Dickson *et al.*, 1988) and is generally thought to be related to a significant increase in sea ice flux. However, it occurred during NAO negative years. This points towards the issue of equifinality, whereby different forcing mechanisms can produce the same signals in proxy records. Indeed in general, the correlation between ice flux and NAO negative phases is much poorer (Kwok and Rothrock, 1999).

6.6.3 Palaeoceanographic change 2.2-1.4 ka cal BP

The slight differences between the Kangersuneq record and the outer Disko Bugt core record between *c.* 2.2 and 1.5 ka cal BP may be explained by localised atmospheric

conditions, where relatively lower air temperatures in the coastal fjord setting may have inhibited meltwater flux, giving rise to an apparent peak in the agglutinated Atlantic indicators. In the deeper water depth setting of DA00-03, bottom water conditions of the WGC will not have been as distinctly affected by this. Instead the DA00-03 core record shows good agreement with the East Greenland record of peak warmth at *c.* 2 ka cal BP, followed by cooling and freshening of the EGC. Reduced solar activity (O'Brien *et al.*, 1995), as well as the increased winter storminess relating to enhanced NAO conditions recorded in the GISP2 ice core (Dawson *et al.*, 2003), may have been a possible forcing or amplifying mechanism of this cooling. This could have enabled increased build up of sea ice, and delayed retreat of the seasonal pack ice on the East Greenland margin. Migration of the Arctic atmospheric and oceanic Fronts will lead to increased extent and duration of sea ice in East Greenland and the Greenland Sea. This leads to a southward displacement of the EGC, which deflects the IC component of the WGC, which is represented by an increase in colder lower salinity loving (Arctic) foraminifera in Disko Bugt during phases of increased positive NAO.

A contrasting signal is seen during this period (at 2.2-1.7 ka cal BP). Increased sea surface temperatures have been inferred from sea ice diatom studies (K.G. Jensen, *unpublished data*) during the period *c.* 2.1 to 1.5 ka cal BP, and further evidence of sea surface warming in South Greenland is inferred from foraminiferal fjord assemblages (Lassen *et al., in press*). The forcing mechanism ascribed by these researchers is thought to be related to enhanced mixing of the water column, rather than a weakening of the EGC component of the WGC (K.G. Jensen, *unpublished data*). This is difficult to confirm. Disparity between the sea ice diatoms showing increasing SST's, while bottom water conditions at the same site (DA00-03) are implying freshening and cooling are difficult to explain. Localised increases in atmospheric heating of the surface seasonal meltwater layer in Disko Bugt may account for the apparent lack of connectivity between the palaeoceanographic signals here.

A cooling in the record from DA00-03 between 1.6 and 1.4 ka cal BP is also recorded on the northern Icelandic shelf by Eiriksson *et al.* (2000a). A shift in the Polar front across the area is thought to explain changes in benthic foraminfera faunal abundance

and increased IRD. Colder conditions are also indicated in the diatom record from the same area by Jiang *et al,* (2002).

6.6.4 Palaeoceanographic change 1.3-0.7 ka cal BP

The distinct rise in abundances of the Atlantic indicator species from *c.* 1.3 to 0.7 ka cal BP is almost certainly related to the climatic amelioration known throughout the North Atlantic as the Medieval Warm Period (MWP). Increased SST's in the north Icelandic region are observed at the same time (Jiang *et al.*, 2002). Foraminiferal and lithofacies evidence from fjord settings in eastern Greenland indicate much warmer and stable climatic conditions, with Atlantic Intermediate Water at the sea bed, and decreased sea ice incidence during the summer (Jennings and Weiner, 1996). Recent evidence from marine cores from fjords in South Greenland implies that wind stresses over South Greenland may have been increasing during the MWP (Lassen et al., 1999). This culminated at the transition to the Little Ice Age (LIA) at the time when the Western Settlement of the Norse at Godthaab District is thought to have failed (Buckland *et al.*, 1996).

6.6.5 Palaeoceanographic change post 0.7 ka cal BP

The Little Ice Age cooling is not well represented in the core record from DA00-03, due to the loss of core sediment through piston coring processes. However, it can clearly be seen that there is a distinct decline in Atlantic indicator species, and a rise in Arctic indicator species. The rise in Arctic indicators as opposed to a general lack thereof implies that this cooling is significantly more intense than at other points during the core record following the maximum cooling during the Neoglacial. There is evidence relating to the advance of Jakobshavns Isbrae's margin during this time (Ingolfsson, 1990; Kelly, 1985; Weidick, 1990). However it is unclear from the core record whether the cooling seen in the foraminiferal fauna is related to increased flux of meltwater from the east, or related to an intensification of the EGC component of the WGC. This is because there is likely to be a 'signal trapping' of the expected IRD flux from Jakobshavns Isbrae behind the bedrock sill at the mouth of Isfjeldsbanken,

(the sediment produced by IRD is deposited in-situ behind the sill) and from the X-ray analysis, no IRD flux can be seen. Glacier advances and cooling in Iceland and Europe during the latter part of the LIA are shown to coincide with a solar activity minimum (Beer *et al.*, 2000), which may be a possible driving mechanism.

6.7.1 Chapter summary: Driving mechanisms

Possible driving mechanisms for changes in the components of the West Greenland Current have been addressed. From analysis of foraminiferal and isotope data from DA00-06, changes in the West Greenland Current from *c.* 8.4 to 7.9 ka cal BP are related directly to global atmospheric temperatures. A decline in ice core temperature is reflected in the decline of warmer more saline Atlantic foraminifera, related to a weakening of the Irminger Current component of the WGC. With a temperature increase, there is a corresponding rise in the warm current indicator species. The rise in temperature initiates an increase in meltwater flux from Jakobshavns Isbrae during its standstill position on the Isfjeldsbanken. Despite the large volumes of meltwater and sediment produced, the warm water signal is still evident. This suggests that at this time and place on the west coast of Greenland, a situation similar to that outlined in Scenario 1 is operating.

In DA00-05, linkage with the ice core record is more loosely correlated. It appears for the most part, a similar situation to that outlined in Scenario 1 is in force, where changes in atmospheric temperatures are mirrored in the strength/warmth of the WGC signal inferred from the foraminiferal assemblages. However, cooling in the WGC current appears to take place earlier in the ocean than in the ice core records, and there are a number of possible reasons for this. The cooling signal in the atmospheric temperatures may actually be being forced by oceanographic changes taking place first. The WGC signals interpreted from the core may be misleading given the total calcareous dissolution following *c.* 4 ka cal BP. The disparity may also be explained by processes similar to that outlined in Scenario 3, whereby atmospheric warming increases meltwater and sea ice flux from the Arctic through the Fram and Denmark Straits to the EGC. Decreased salinity and cooler water mass temperatures would be

translated to a cooler/weaker WGC signal, which although may not be enough to directly encourage increases in specific Arctic water foraminiferal indicators, may well explain the relatively high instability of oceanographic conditions inferred from the species tolerant to large fluctuations in salinity and temperature.

6.7.2 Chapter summary: West Greenland climate and links to the NAO

The variability/oscillatory nature of the NAO *is* likely to be a long term feature of the North Atlantic climate system (Cook *et al.*, 1998; Cronin *et al.*, 2003; Nesje *et al.*, 2000). Moreover, instrumental temperature records over the last century show significant correlation of coastal temperature anomalies during autumn and winter at western and coastal sites with the NAO (Box, 2002). There appears to be an increasing trend in palaeoclimatic studies to ascribe NAO forcing mechanisms (enhanced negative or positive phases) to account for changes in proxy records on a range of temporal and spatial scales. It is of course likely that NAO variations affect atmospheric and oceanographic circulation in the North Atlantic regions due to displacement of the Arctic front. Enhanced positive phases are well known for creating anomalously atmospheric high temperatures in Europe, as far northeast as Siberia, and much lower temperatures in West Greenland (Nesje *et al.*, 2000; Rogers, 1997; White, *et al.*, 1997).

Greenland is influenced by both the Icelandic Low to the southeast and Davis Strait/Baffin Bay storms to the southwest and west, and the NAO creates a "seesaw" in winter temperatures between West Greenland and Northern Europe (Barlow *et al.*, 1997; Dawson *et al.*, 2003). Enhanced positive phases of NAO intensifies the seesaw in terms of atmospheric temperature, but may also influence sea surface temperatures (SSTs), geostrophic wind strength, and sea ice cover extending beyond the winter season (Andrews and Giraudeau, 2003; Barlow *et al.*, 1993; Jiang *et al.*, 2002; Schulz and Paul, 2002). Correlation in excursion directions of temperature records derived from GISP2, and East Greenland and Iceland temperature records may be associated with different positions of the Baffin trough in winter (Dahl-Jensen *et al.*, 1998; Dawson *et al.*, 2003) sea surface temperatures (SSTs), atmospheric pressures,

geostrophic wind strength, and sea ice extents beyond the winter season (Barlow *et al.*, 1993).

6.7.3 Chapter summary: Dominant operating Scenario

In terms of scenarios, or explanations regarding forcing mechanisms for controlling the strength of the WGC signal, evidence from the three piston cores, in particular DA00-05 and DA00-03 suggest that during the mid to late Holocene, Scenario 1 is operating. Colder ice core temperatures tend to be related to decreased incidences of Atlantic indicator species. Stratification processes relating to Neoglacial cooling and alteration of the fjord hydrographic conditions is likely to explain the severe dissolution scenario from 4.1 ka cal BP. During the Neoglacial, changes in the foraminiferal assemblages appear to be responding directly to increases in intensity of the East Greenland Current component of the West Greenland Current. There is good evidence that the Disko Bugt record has recorded the Medieval Warm Period, and the descent to the Little Ice Age. This implies that the 'dampening effect' of the seesaw mechanism thought to exist in the GISP2 ice core (Dawson *et al.*,2003), is not apparent in the palaeoceanographic record.

Chapter 7: Conclusions

7.1 Introduction

This chapter discusses the thesis results in relation to the original thesis aims, and assesses the limitations to this work. Future avenues of research arising from the original findings in this thesis are then discussed. This thesis has focussed on the nature of the relationship between the deglacial history and water mass changes of Disko Bugt in West Greenland, and has increased the spatial and temporal resolution of marine multi-proxy data in the region. With the material available, the research has been able to address the oceanographic component of the Durham University based ARCICE project by identifying rapid instabilities in the record of final deglaciation of Jakobshavns Isbrae, and producing high resolution records of mid-to late-Holocene palaeoceanographic circulation. The importance of Jakobshavns Isbrae as a sediment and meltwater flux source from the Greenland Ice Sheet during post-glacial times has been assessed, and a tight radiocarbon chronology for marine palaeoenvironmental change has been developed for West Greenland, which has not previously been attempted. Direct comparisons to Greenland ice core records have been made (GISP2 and GRIP), and these show that despite limitations in sample material, the paleoceanographic response of the WGC can be directly related to changes in atmospheric temperature, as well as more regional atmospheric forcings.

7.2 Thesis aims and results

The overall aim of this research was:

To develop a high resolution record of Holocene modes of palaeoceanography, focussing on the dynamics of deglaciation; Holocene rapid instabilities and the role of Jakobshavns Isbrae using foraminiferal, sedimentological and oxygen isotope data from three piston core locations in Disko Bugt.

7.2.1 Objective 1

To determine the deglacial history of Disko Bugt, West Greenland, and water mass interaction relating to the West Greenland Current (WGC), using marine records from three piston cores.

The longest piston core record from Disko Bugt used during this research extends only for the past *c.* 8.4 ka, and so knowledge relating to the timing of ice retreat from the western margins of Disko Bugt is limited. Information from contemporaneous work suggests that ice in Disko Bugt had retreated from the western part of the bay by *c.* 10.2 ka cal BP. The foraminiferal and isotope evidence in this thesis, derived from marine sediments in front of Jakobshavns Isbrae, suggest that once the main part of Disko Bugt was deglaciated, *c.* 10.2 ka cal BP, the ice stream reached a still stand position at Isfjeldsbanken. Large volumes of meltwater during this time prevented the incursion of warm, saline West Greenland Current waters into the eastern part of the bay.

The timing of this retreat and then halt, coincides with the widespread "8.2" event and it appears that this short cold phase may be responsible for prolonging the still stand episode. The record from DA00-06 reveals that from this still stand position, Jakobshavns Isbrae responded to increased atmospheric temperature by producing large volumes of meltwater. During colder episodes in the 8.2 event, meltwater flux was reduced significantly enough to allow a weak incursion at depth of the WGC. This reduced amount of meltwater decreases the depth of the colder, fresher "mixed layer" in Disko Bugt.

Following rapid temperature increase, a final, longer meltwater release occurred until *c.* 7.9 ka cal BP, which marked the final retreat of Jakobshavns Isbrae through a deep trough behind the Isfjeldsbanken in a draw down effect. This is recorded in the foraminiferal record by rapidly increasing amounts of Atlantic water indicator species, as the WGC was able to reach the eastern parts of the bay, and is likely to have been linked to intensification of the Irminger Current branch of the West Greenland Current.

During the 8.2 event, evidence from the benthic oxygen isotope record reveals that the meltwater flux from Jakobshavns Isbrae is responding directly to fluctuations in global atmospheric temperature, with significant increases in meltwater recorded at the front of Jakobshavns Isfjord in Disko Bugt corresponding to warmer peaks during this rapid event in the ice core record. It was expected that large meltwater fluxes to the area may have drowned out or diluted the warm WGC signal, and this is true to a certain extent. However, despite a weaker signal that may be seen at a site further west of the core location (POR18), foraminiferal assemblages are clearly recording changes in the strength of the West Greenland Current.

From comparisons to the ice core records, the WGC during this time seems to be responding directly to changes in atmospheric temperature, with decreases in fauna indicative of warmer, more saline, Atlantic-sourced water, declining during cold episodes in the ice core record. This strongly suggests that the strength of the West Greenland Current is affected by changes in the strength of the Irminger Current component of the WGC. It is proposed that Scenario 1, discussed in Chapter 6, is the operating mechanism for driving palaeoceanographic circulation change. The weakening in the Irminger Current/Atlantic-sourced water is likely to be related to the perturbation of the thermohaline circulation by the massive influx of meltwater through Hudson Strait to the Labrador Sea, which marked the final deglaciation of the Laurentide Ice Sheet following the 8.2 event.

7.2.2 Objective 2

To test the hypothesis that Jakobshavns Isbrae has experienced a punctuated discharge history during the Holocene.

The coring locations of DA00-06, DA00-05 and DA00-03 were chosen to evaluate the nature of Jakobshavns Isbrae's role in providing sediment and meltwater flux to Disko Bugt and coastal West Greenland. From isotopic and foraminiferal evidence, punctuated discharge of the ice stream was evident during the '8.2 event'. The stability provided to the ice stream by grounding at Isfjeldsbanken allowed a meltwater flux response to changes in atmospheric temperature. Increased discharge

was evident during relatively higher temperatures, and was significantly reduced during the two 'cold peaks'. Further information regarding testing the hypothesis that discharge was punctuated during the Holocene is limited. This is because once the ice stream had retreated behind the bedrock sill, into the deep trough; the majority of sediment discharge would have been trapped, as it is during the present day. The distal location of DA00-03 and deeper water depths make it unlikely that changes in indicator species record fluctuations in meltwater, rather they are responding to variations in the intensity of the EGC.

7.2.3 Objective 3

To establish a high resolution record of Holocene water mass changes within Disko Bugt from faunal and isotopic records.

A high resolution record of Holocene water mass circulation has been produced from Disko Bugt. Comparisons to ice core records and evidence from other sites in the North Atlantic region suggest that palaeoceanographic circulation in Disko Bugt has responded to both local and regional forcing mechanisms, such as atmospheric perturbations by enhanced (positive or negative) phases of NAO-like conditions, global atmospheric temperatures, and local climatic conditions (especially in the shallow and sheltered fjord setting of Kangersuneq).

It is clear that foraminiferal benthic assemblages can be related to the warmth and strength of the WGC. The results suggest that there is a distinct connectivity between water masses in Disko Bugt, and changes in the palaeoceographic strength of the WGC component currents, in particular the East Greenland Current. This is predominantly seen in the record from core DA00-03, where changes in the EGC relating to sea ice incidence, and Arctic meltwater flux during the late-Holocene are transposed to the WGC signal. There is good evidence of the intensive cooling seen during the latter part of the Neoglacial in both DA00-05, and DA00-03, and the record from DA00-05 suggests that the oceanographic response to the end of the Holocene thermal optimum pre-empted terrestrial cooling.

7.2.4 Objective 4

To develop a tight chronology for these palaeoenvironmental records through radiocarbon dating to give reliable age-depth models.

Good dating control has been achieved in cores DA00-05 and DA00-3 from a range of material. The lack of date inversions give confidence in the age-depth model developed for the Holocene in Disko Bugt. Continuously high sedimentation rates are inferred from both these cores. Preservation issues and lack of dateable material has somewhat limited the radiocarbon chronology from DA00-06, which is precisely where accurate dating was required to constrain timings of deglacial activity of Jakobshavns Isbrae. Despite the poorer dating control, proxy evidence from foraminiferal assemblages, sedimentological data and comparisons to the terrestrial record of deglaciation suggests that the age-model developed for this core is consistent with the current understanding of palaeoenvironmental change in the region.

7.2.5 Objective 5

To compare these results to established global climate records such as GRIP, and GISP2, as well as to previous work from the North Atlantic region.

Comparisions of the foraminiferal and isotopic records with the ice core records indicate that in general, warmer ice core temperatures create a warm WGC signal and *vice versa* (Scenario 1). In DA00-06 this is particularly seen during the still stand position of Jakobshavns Isbrae at Isfjeldsbanken, where meltwater flux can be related directly to changes in temperature during the '8.2 event'. In core DA00-05, this trend is not as clear; this is thought to be an effect of the stratification processes operating through the Neoglacial period. There is good correlation between the high resolution late-Holocene record of DA00-03 in the outer part of the bay, and changes in the EGC seen on the north Icelandic shelf and the East Greenland margin. Variations in the strength of the WGC seen in DA00-05 and the upper section of DA00-06 fit well with the marine records from West Greenland (molluscan data) as well as foraminiferal evidence from the Labrador Sea and Baffin Bay area. During the late-Holocene, it is

more difficult to draw regional comparisons to these sites, as there is limited published data from records spanning this time.

7.3.1 Limitations to research

This research has limitations to the findings. Limiting factors can be related to:

- processes operating in Disko Bugt itself - (dissolution and the dominance of Jakobshavns Isbrae, signal trapping and equifinality),
- methodological aspects (core sample location, lack of integration of seismic modelling, and isotope sample limitations), as well as
- more regional issues (relatively poor comparative data available from Baffin Bay and West Greenland sites during the late-Holocene).

7.3.2 Limitations in Disko Bugt: Dissolution

The dissolution processes operating in Disko Bugt, relating to the warm WGC current inferred from DA00-06 have hampered detailed interpretation about specific species associations with the WGC, and reconstructions of fjord processes from DA00-05. In eastern Disko Bugt, preservation is clearly at its poorest during periods dominated by warm WGC waters, associated with greater productivity of the Atlantic-sourced water. This study has argued that an enhanced WGC creates an increased carbon flux allowing organic matter to oxidise in sediments. The products of oxidation of organic material include CO_2, and increased dissolved CO_2 would encourage calcium carbonate dissolution.

Inferred stratification processes operating in the fjord mouth of Kangersuneq have limited the interpretation of water mass changes, as there are only continuous *agglutinated* foraminiferal assemblages able to record fluctuations in the strength of the WGC during the widespread Neoglacial period. It is suggested that these stratification processes were developed through the increasing seasonal ice cover prior

to the widespread onset of Neoglacial times, which led to the development of cold dense saline bottom waters for most of the year. The subsequent development of strong pycnocline prevented bottom water ventilation, leading to lowered dissolved oxygen levels and higher CO_2 concentrations from organic decay of the sediments. Atmospheric CO_2 exchange may well have been inhibited by stratification, and extended pack ice cover. The resulting fjord bottom water conditions became very corrosive to calcareous foraminifera.

7.3.3 Limitations in Disko Bugt: Chronology

The development of age depth models in Disko Bugt has generally been very successful, and good inferences have been made regarding the timing of fluctuations in the strength of the WGC, which are compared to other established proxy records. However, dating control is weaker when addressing questions about the timing of the re-instigation of the WGC circulation following the deglaciation of Disko Bugt, and also regarding the timing and duration of the final retreat of Jakobshavns Isbrae. Only three radiocarbon dates have been generated from DA00-06. This is mainly a function of low test counts, and poor preservation of calcareous faunal in the top part of the core. There is no date spanning the inferred "8.2 event" which occurs throughout zones 1 and 2 in the core, and dating the phase of intense IRD deposition was not achieved.

7.3.4 Limitations in Disko Bugt: Core locations and sedimentology

The core sample locations have been ideal for generating a palaeoceanographic record of mid to late-Holocene changes in the WGC, however, none of the piston cores penetrated the full sequence, and chronology is therefore based on minimum ages. This research was designed to capture rapid instabilities and records of high resolution records of change through coring in areas with high sedimentation rates. It appears that this aim was almost too successful, with extremely high sedimentation rates apparent; the much shorter duration of the core records was not anticipated, and the influence of Jakobshavns Isbrae in delivering fine-grained sediment to the bay is over

whelming. The expected presence of IRD (clasts greater than 2 mm) in the cores is absent. Initially it had been hoped that the presence of IRD could be related to episodes of punctuated discharge of Jakobshavns Isbrae. It seems likely that the lack of IRD in other cores (DA00-03 in particular) is due to the sediment signal trapping at Isfjeldsbanken. The shallow sill traps icebergs in the Isfjord, which appear to rain out most of their debris behind the sill until they have melted and are shallow enough to pass over the bedrock obstacle.

These high sedimentation rates, and lack of distinction in the sediment architecture, have been one of the limiting factors in the successful development of a seismic model. There are indications however, that the tentative identification of arcuate ridges in front of Jakobshavns Isbrae may be evidence of a punctuated retreat prior to the ice stream halt at Isfjeldsbanken around 8.3 ka cal BP. Ongoing research may be able to develop an initial model of sediment architecture for stages of ice retreat through the bay through the use of palaeomagnetic proxies (J. Dix, pers. comm., 2002). This process allows the recognition (and correlation) of different sediment signals from different types of sediment measured throughout the cores, to the high resolution seismic data produced during the surveying in Disko Bugt. The varying sediment layers recorded in the seismic data can be correlated to the differing signals given off by the sediments in the cores.

7.3.5 Limitations in Disko Bugt: Isotopes

Despite evidence from the oxygen isotope records that Jakobshavns Isbrae is likely to have responded directly to changes in atmospheric temperature in varying its amounts of meltwater flux, overall results from the isotopes have been disappointing. The discontinuous nature of the calcareous fauna due to dissolution and low test abundance in DA00-06, and lack of isotope data for DA00-05, has not allowed firm conclusions to be drawn about changes in bottom water conditions during the Holocene climatic optimum, and Neoglacial periods. The likely infaunal effects and quantitative unknowns regarding species variations and vital effects of the taxa used in this thesis have limited interpretation regarding past records of productivity and changing isotopic signals of variations in the strength of the WGC.

However, this is the first attempt to produce a benthic isotope record from this region, and from species that have never before been used. The degree of correlation between the high resolution oxygen isotope record and the ice core data during the "8.2" event is the first to show a correlation between oceanographic activity on the west coast of Greenland with atmospheric changes (from ice core data).

This compilation of a 'stacked' isotope signal from Disko Bugt West Greenland is the first proxy to corroborate the (low resolution) macrofaunal evidence for meltwater fluxes, fluctuations of the West Greenland Current, and ultimately to show that there is a distinct and discernable relationship between terrestrial processes and records, and oceanographic patterns in Disko Bugt West Greenland.

7.3.6 Limitations in Disko Bugt: Equifinality

Concerns have been raised in this thesis about the possibility of equifinality operating in the apparent signals in the palaeoenvironmental records developed for Disko Bugt. This theory concerns the process by which different operating mechanisms can give rise to the same observed pattern. For example, dissolution processes active in Kangersuneq fjord during the Neoglacial have virtually eliminated any evidence of calcareous species, which are representative of cooler conditions, or a much weaker/diluted WGC signal. Without comparisons to other proxy records, the DA00-05 data may well be interpreted as displaying a relatively strong WGC signal through the relative increased abundances of the agglutinated foraminifera, and very minor amounts of species present that are specifically associated with cooler conditions. The scenarios presented in Chapter 6 also highlight the possibility that warmer atmospheric temperatures could equally give rise to a "cold" WGC signal, as well as a warm signal. This is because on a larger scale, increases in atmospheric temperature are likely to increase Arctic melting, and intensify the East Greenland Current component of the West Greenland component, diluting the Irminger Current part. Using all the lines of available evidence from this study, this scenario seems less likely, as atmospheric temperature rises can be correlated to intensification of the Irminger Current branch, and subsequent warming of the WGC.

7.4 Regional issues

There is a considerable amount of proxy evidence available from the Baffin Bay region, Labrador Sea and eastern Arctic Canada relating to palaeoceanography and glaciomarine interactions during the Last Glacial Maximum and transition to the present interglacial (e.g. Andrews *et al.*, 1991, 1994, 1995; Hillaire-Marcel *et al.*, 1993; Hiscott *et al.*, 2001; Jennings *et al.*, 2001; Silis, 1993; Vilks, 1980, 1981). However, higher resolution records spanning the Holocene with which to compare the results of this thesis are somewhat limited. Marine evidence of palaeoceanographic change from sites in West Greenland is also limited, particularly by the dating control, resolution and material used (e.g. Bennike *et al.*, 1994; Donner and Jungner, 1975; Feyling-Hanssen and Funder, 1990; Funder and Weidick, 1991).

There is also a significant amount of contemporary observational data available regarding the warmth and strength of the WGC in recent times (e.g. Buch, 1993, 2000; Buch and Nielsen, 2001; Buch and Stein, 1987, 1989; Stein, 1991, 1993; Stein and Buch, 1985; Stein and Wegner, 1990). Despite this, it is difficult to validate the three hypothesis controlling palaeoceanographic regimes during the Holocene which have been proposed in this thesis, without corroboration of these observational data with published knowledge of contemporary floral and faunal assemblages and distributions. Ideally these contemporary observational data could be used to create a regional model of operating mechanisms (such as enhanced phases of positive or negative NAO) for controlling changes in the WGC, and this atmosphere-ocean "transfer function" could be applied to palaeoceanographic records such as these produced from Disko Bugt.

7.5.1 Future research

The original work produced in this thesis shows that there is considerable scope for the pursuit of further research in this location. No coring outside of Disko Bugt has been attempted in West Greenland. It is likely that to remove the overwhelming influence and "noise" from Jakobshavns Isbrae in terms of sediment delivery, an increased westward coring location would be required. An ideal location for the

procurement of longer core records, (but still with relatively high sedimentation rates to allow high resolution data to be produced) could be the large offshore sediment fan at the mouth of Disko Bugt on the shelf margin. A coring site such as this would enable longer core records of palaeoceanographic circulation to be developed and it is suggested that the deeper water depth at a shelf location would also enable a proxy record of changes in sea surface temperatures to be made from planktic foraminifera.

7.5.2 Future research: Coring locations

It is likely that an alternative coring location such as this would allow further determination of palaeoceanographic modes of circulation, and controlling operating mechanisms of the glacial and deglacial history of West Greenland. Questions can then be addressed about the extent of the West Greenland Ice Sheet during the Last Glacial Maximum, and subsequent timing of the destabilisation and retreat of the marine based portion of the West Greenland Ice Sheet, which this thesis cannot answer. Timing of the break up of the West Greenland Ice Sheet has only been tentatively estimated by Funder and Hansen, (1996) and requires further constraining in order to develop and extend the palaeoenvironmental history of West Greenland.

7.5.3 Future research: Alternate proxy methods

Due to the controlling mechanisms on dissolution relating to the warm West Greenland current, an alternative proxy method is proposed for this further research. The recent use of biomarker alkenones in marine sediments from the Nordic Seas has allowed identification of changes in temperature and salinity in the East Greenland Current (J. Bendle, pers. comm., 2003). The recent application of this technique involves the use of C_{37} alkenones as biomarkers for some types of algae. The sedimentary abundance of these alkenones have been related in the Nordic seas to two types of water masses, Arctic and Atlantic, and present day observations of these organic compounds have been used as a modern analogue to reconstruct variations in the position of the Arctic Front (Rosell-Mele *et al.*, 1998). The biomarker technique has also been successfully employed to determine how the Indian Ocean has

responded to a freshwater flux in the surface waters of the North Atlantic, in terms of changes in oxygen concentration of bottom waters (Shulte *et al.*, 1999). This relatively new technique has been used to infer climatic changes in terms of sea surface temperatures and changes in the atmospheric North East Trade Winds system, in the upwelling region off Cap Blanc, northwest Africa, over the last 70 ka (Sicre *et al.*, 2001). Application of this proxy method, in combination with further foraminiferal analyses (planktic and benthic), to sediments retrieved from the West Greenland Shelf, would be invaluable for determining high resolution changes in sea surface temperature, water mass variations and ocean-atmospheric interaction since the Late Glacial Maximum.

Intrinsically linked to the benthic record of water mass changes (in terms of information about productivity, seasonal pack ice duration and stratification processes), proxy records from sea ice diatoms will prove invaluable for reconstructing models of palaeoceanographic changes through the water column. It is anticipated that the data from this thesis will be used in conjunction with contemporaneous parallel research relating to palaeo-pack ice records currently being developed (K.G. Jensen, pers. comm., 2003).

7.5.4 Future research: Localised hydrographics and sampling resolution

The development of an in-depth hydrographic study of annual CTD profiles from Disko Bugt would allow quantitative replication of seasonal changes in the WGC. This could create a transferable model which could then be applied to palaeo-core records from the marine environment. At the same time, in order for the potential for benthic isotopic ratio records to be fully exploited in this region, data needs to be generated relating to contemporary isotopic equilibrium values of infaunal species which dominate in Disko Bugt.

This study has highlighted the differing rates of sedimentation that are operating within the three different environmental settings of ice-proximal, ice-distal, and a fjord setting. This was not known prior to the instigation of the sampling strategy of the three piston cores. With this in mind, it can be seen that by increasing the

resolution of sampling, especially in the upper section of core DA00-06, it would be possible to increase the confidence in comparison of benthic foraminiferal and isotopic records with ice core data, and produce an even greater high-resolution data set for palaeoceanographic changes during the Holocene in West Greenland.

Future research directions such as these would be ideal next steps in developing the findings of this thesis. These proposals may produce a more spatially and temporally comprehensive record of palaeoceanographic change, and ice margin instabilities in West Greenland since the Late Glacial Maximum.

7.6 Thesis conclusions

This research is an original contribution to the growing body of knowledge about palaeoenvironmental change in West Greenland. This thesis has furthered the understanding of modes of Holocene palaeoceanographic circulation in Disko Bugt and West Greenland, and linked them to likely operating mechanisms of change. Information about past variations in the strength of the dominant water current in West Greenland (the West Greenland Current), has been successfully reconstructed through the application of foraminiferal analysis and isotope techniques. New data relating to the timing of final retreat of Jakobshavns Isbrae, the most important ice stream draining the West Greenland Ice Sheet, has been determined through evidence of meltwater and sediment fluxes from the calving margin. The high resolution records produced in this thesis clearly document the rapid instability and subsequent retreat of the ice stream to be related to the rapid atmospheric warming following the well-documented "8.2 event".

Mid-Holocene climatic changes are recorded in a fjord mouth setting of Kangersuneq. Despite considerable dissolution processes operating in the fjord (which are in fact a product of climatic change themselves), a high resolution record of variable and declining warmth of the WGC is recorded from *c.* 6.3 ka cal BP, prior to the onset of full Neoglacial conditions around 4.1 ka cal BP. The maximum cooling during the Neoglacial period is clearly seen from *c.* 3.2 to 2.2 ka cal BP in DA00-05 and DA00-03. A distinct warming of the WGC takes place around 2.2 ka cal BP, which can be

linked to an increased component of Irminger Current water, which is also seen in the records from East Greenland as well as the Nordic Seas. The foraminiferal assemblages from DA00-03 show evidence of a distinct climatic amelioration which is associated with the Medieval Warm Period. There is some evidence towards the top of DA00-03 for a deterioration of oceanographic conditions which is linked to the onset of the Little Ice Age.

References

Abdalati, W., Krabill, W.B. (1999). Calculation of ice velocities in the Jakobshavns Isbrae area using airborne laser altimetry. *Remote Sensing Environments* **67**, 194-204.

Adkins, J. F., Boyle, E.A., Keigwin, L., Cortijo, E. (1997). Variability of the North Atlantic thermohaline circulation during the last interglacial period. *Nature* **390**, 154-156.

Ahrens, M. J., Graf, G., Altenbach, A.V. (1997). Spatial and temporal distribution patterns of benthic foraminifera in the Northeast Water Polynya, Greenland. *Journal of Marine Systems* **10**, 445-465.

Aksenov, Y., Coward, A.C. (2001). The Arctic Ocean Circulation as simulated in a very high-resolution global ocean model (OCCAM). *Annals of Glaciology* **33**, 567-576.

Aksu, A. E. (1983). Holocene and Pleistocene dissolution cycles in deep-sea cores of Baffin Bay and Davis Strait: Palaeoceanographic implications. *Marine geology* **53**, 331-348.

Aksu, A. E., Mudie, P.J. (1985). Late Quaternary stratigraphy and paleoecology of northwest Labrador Sea. *Marine Micropaleontology* **9**, 537-557.

Alley, R. B. (1998). Palaeoclimatology: icing the North Atlantic. *Nature* **392**, 335-337.

Alley, R. B. (2000). The Younger Dryas cold interval as viewed from central Greenland. *Quaternary Science Reviews* **19**, 213-226.

Alley, R. B., et al. (1995). Changes in continental and sea-salt atmospheric loadings in central Greenland during the most recent glaciation: model-based estimates. *Palaeoclimatology* **41**, 503-514.

Alley, R. B., Mayewski, P.A., Saltzman, E.S. (1999). Increasing North Atlantic climate variability recorded in a Central Greenland ice core. *Polar Geography* **23**, 119-131.

Alley, R. B., Taylor, K.C., Clark, P.U., Mayewski, P.A. Sowers, T., Stuiver, M. (1997). Holocene climatic instability: a prominent, widespread event 8200 yr ago. *Geology* **25**, 483-486.

Alve, E. (1994). Opportunistic features of foraminifer *Stainforthia fusiformis* (Williamson): evidence from the Frierfjord, Norway.

Alve, E., Bernhard, J.M. (1996). Vertical migratory response of benthic foraminifera to controlled oxygen concentrations in an experimental mesocosm. *Marine Ecology Progressive Series* **116**, 137-151.

Alve, E., Nagy, J. (1986). Estuarine foraminferal distribution in Sandebukta, A branch of the Oslo Fjord. *Journal of Foraminiferal Research* **16**, 1-4.

Anderson, N. J., Bennike, O., Christoffersen, K., Jeppesen, E., Markager, S., Miller, G., Renberg, I. (1999). Limnological and palaeolimnological studies of lakes in south-western Greenland. *Geology of Greenland Survey Bulletin* **183**, 68-74.

Anderson, N. J., Harriman, R., Ryves, D.B., Patrick, S.T. (2001). Dominant factors controlling variability in the ionic composition of West Greenland lakes. *Arctic, Antarctic and Alpine Research* **33**, 418-425.

Andresen, C. S., Björck, S., Bennike, O., Heinmeier, J., Kromer, B. (2000). What do □^{14}C changes across the Gerzensee oscillation/GI-1b event imply for deglacial oscillations? *Journal of Quaternary Science* **15**, 203-214.

Andrews, J. T. (1998a). Abrupt changes (Heinrich events) in late Quaternary North Atlantic marine environments: a history and review of data and concepts. *Journal of Quaternary Science* **13**, 3-16.

Andrews, J. T., Caseldine, C., Weiner, N.J., Hatton, J. (2001a). Late Holocene (ca. 4ka) Marine and terrestrial environmental change in Reykjarfjordur, north Iceland: climate and/or settlement. *Journal of Quaternary Science* **16**, 133-143.

Andrews, J. T., Cooper, T.A., Jennings, A.E., Stein, A.B., Erlenkeuser, H. (1998b). Late Quaternary iceberg-rafted detritus events in the Denmark Strait-Southeast Greenland continental slope (~65N) related to North Atlantic Heinrich events? *Marine geology* **149**, 211-228.

Andrews, J. T., Erlenkeuser, H., Evans, L.W., Briggs, W.M., Jull, A.J.T. (1991). Meltwater and deglaciation, SE Baffin shelf (NE margin Laurentide ice sheet) between 13.5 and 7ka: from O and C stable isotopic data. *Paleoceanaography* **6**, 621-637.

Andrews, J. T., Giraudeau, J. (2003a). Multi-proxy records showing significant Holocene environmental variability: The inner N. Iceland shelf (Húnaflói). *Quaternary Science Reviews* **2**, 175-193.

Andrews, J. T., Helgadottir, G., Geirsdottir, A., Jennings, A.E. (2001b). Multicentury-scale records of carbonate (hydrographic?) variability on the northern Iceland margin over the last 5000 years. *Quaternary Research* **56**, 199-206.

Andrews, J. T., Jennings, A.E., Cooper.T, Williams. K.M. and Mienert, J. (1996). Late Quaternary sedimentation along a fjord to shelf (trough) transect, East Greenland (ca. 68°N). In: *Late Quaternary Palaeoceanography of North Atlantic Margins* (Eds Andrews, J. T., Austen, W., Bergsten, H. and Jennings, A. E.). *Geological Society of London Special Publication* **111**, 153-166.

Andrews, J. T., Jennings, A.E., Smith, L.M., Preston, R., Cooper.T. (1997). Spatial and temporal patterns of iceberg rafting (IRD)along the East Greenland margin, ca.68oN, over the last 14 cal. ka. *Journal of Quaternary Science* **12**, 1-13.

Andrews, J. T., Keigwen, L., Hall, F., Jennings, A.E. (1999). Abrupt deglaciation events and Holocene palaeoceanography from high-resolution cores, Cartwright Saddle, Labrador Shelf, Canada. *Journal of Quaternary Science* **14**, 383-397.

Andrews, J. T., Kristjansdottir, G.B., Koc, N., Hardadottir, J., Stoner, J.S., Mann, M.E. (2003b). Decadal to millennial-scale periodicities in North Iceland shelf sediments over the last 12 000 cal yr: Long term North Atlantic oceanographic variability and solar forcing. *Earth and Planetary Science Letters* **210**, 453-465.

Andrews, J. T., MacLean, B., Kerwin, M., Manley, W., Jennings, A.E., Hall, F. (1995). Final stages in the collapse of the Laurentide Ice Sheet, Hudson Strait, Canada, NWT: 14C AMS dates, seismic stratigraphy, and magnetic susceptibility logs. *Quaternary Science Reviews* **4**, 983-1004.

Andrews, J. T., Matsch, C.L. (1983). Glacial marine sediment and sedimentation: an annotated bibliography. Norwich: Geo Books.

Andrews, J. T., Tedesco, K., Briggs, W.M., Evans, L.W. (1994). Sediments, sedimentation rates and environments, southeast Baffin Shelf and northwest Labrador Sea, 8-26 ka. *Canadian Journal of Earth Sciences* **31**, 90-103.

Appenzeller, A., Schwander, J., Sommer, S., Stocker, T.F. (1998a). The North Atlantic Oscillation and its imprint on precipitation and ice accumulation in Greenland. *Geophysical Research Letters* **25**, 1939-1942.

Appenzeller, A., Stocker, T.F., Anklin, M. (1998b). North Atlantic Oscillation dynamics recorded in Greenland Ice cores. *Science* **282**, 446-449.

Austin, W. E. N., Evans, J.R. (2000). Benthic foraminifera and grain size variability at intermediate water depths in the Northeast Atlantic during the late Pliocene-early Pleistocene. *Marine geology* **170**, 423-441.

Azetsu-Scott, K., Tan, F.C. (1997). Oxygen isotope studies from Iceland to an East Greenland fjord: behaviour of glacial meltwater plume. *Marine Chemistry* **56**, 239-251.

Bacon, S. (1998). Decadal variability in the outflow from the Nordic Seas to the deep Atlantic Ocean. *Nature* **394**, 871-874.

Balsam, W. (1981). Late Quaternary sedimentation in the western North Atlantic: stratigraphy and paleoceanography. *Palaeogeography, Palaeoclimatology. Palaeoecology* **35**, 215-240.

Bamber, J. L., Hardy, R.J., Huybrechts, P., Joughin, I. (2000a). A comparison of balance velocities, measured velocities and thermomechanically modelled velocities for the Greenland ice sheet. *Annals of Glaciology* **30**, 211-216.

Bamber, J. L., Hardy, R.J., Joughin, I. (2000b). An analysis of balance velocities over the Greenland ice sheet and comparison with synthetic aperture radar interferometry. *Journal of Glaciology* **46**, 67-74.

Bandy, O. L. (1964). General correlation of foraminiferal structure with environment. In *Introduction to Paleoecology*, (ed. J. Imbrie, Newell, N.D.), pp.234, London: John Wiley and Sons.

Barber, D. C., Dyke, A., Hillaire-Marcel, C., Jennings, A.E., Andrews, J.T., Kerwin, M.W., Bilodeau, G., McNeely, R., Southon, J., Morehead, M.D., Gagnon, J.-M. (1999). Forcing of the cold event 8,200 years ago by catastrophic drainage of Laurentide lakes. *Nature* **400**, 344-34?

Barber, D. G., Hanesiak, J.M., Chan, W., Piwowar, J. (2001). Sea-Ice and Meteorological Conditions in Northern Baffin Bay and the North Water Polynya between 1979 and 1996. *ATMOSPHERE-OCEAN* **39**, 343-359.

Barlow, L. K., Groote, P.M., White, J.W.C., Barry, R.G., Rogers, J.C. (1993). The North Atlantic oscillation signature in deuterium and deuterium excess signals in the Greenland Ice Sheet Project 2 ice core. *Geophysical Research Letters* **20**, 2901-2904.

Barlow, L. K., Rogers, J.C., Serreze, M.C., Barry, R.G. (1997). Aspects of climate variability in the North Atlantic sector: discussion and relation to the Greenland Ice Sheet Project 2 high resolution isotopic signal. *Journal of Geophysical Research* **102**, 26333-26344.

Beer, J., Mende, W., Stellmacher, R. (2000). The role of the sun in climate forcing. *Quaternary Science Reviews* **19**, 403-415.

Belkin, I. M., Malmberg. S-A., Levitus, S., Antony, J. (1998). Great Salinity Anomalies in the North Atlantic. *Progress in Oceanography* **41**, 1-68.

Bennike, O., Bjorck, S. (2002). Chronology of the last recession of the Greenland Ice Sheet. *Journal of Quaternary Science* **17**, 211-219.

Bennike, O., Hansen, K.B. Knudsen, K.L., Penney, D.N., Rasmussen, K.L. (1994). Quaternary marine stratigraphy and geochronology in central West Greenland. *Boreas* **23**, 194-215.

Berger, A., Loutre, M.F. (1991). Insolation values for the climate of the last 10 million years. *Quaternary Science Reviews* **10**, 297-317.

Bergsten, H. (1994). Recent benthic foraminifera of a transect from the North Pole to the Yermak Plateau, eastern central Arctic Ocean. *Marine geology* **119**, 251-267.

Bernhard, J. M., Alve, E. (1996). Survival, ATP pool, and ultrastructural characterization of benthic foraminifera from Drammensfjord (Norway): response to anoxia. *Marine Micropaleontology* **28**, 5-17.

Bianchi, G. G., McCavè, I.N. (1999). Holocene periodicity in North Atlantic climate and deep-ocean flow south of Iceland. *Nature* **397**, 515-517.

Bigg, G. R. (1999). An estimate of the flux of iceberg calving from Greenland. *Arctic, Antarctic and Alpine Research* **31**, 174-178.

Broecker, W. (1997). Future directions of paleoclimate research. *Quaternary Science Reviews* **16**, 821-825.

Buch, E. (1984). Variations in temperature and salinity of West Greenland waters, 1970-82. *NAFO scientific Council Studies* **7**, 39-44.

Buch, E. (1993). The North Atlantic Water component of the West Greenland Current. *Contribution to Council Meeting of the Hydrographic Committee of the International Council for the Exploration of the Sea (ICES)* **C.M1993/**, 1-17.

Buch, E. (2000). Air-sea-ice conditions off Southwest Greenland, 1981-1997. *Journal of the Northwest Atlantic Fisheries Science* **26**, 123-136.

Buch, E., Nielsen, M.H. (2001). Oceanographic investigations off West Greenland. *North Atlantic Fisheries Organisation. Scientific Council meeting* **N4618 Doc02/17**, 1-17.

Buch, E., Stein, M. (1987). Time series of temperature and salinity at the Fylla Bank Section, West Greenland. *Contribution to Council Meeting of the Hydrographic Committee of the International Council for the Exploration of the Sea (ICES)*, 1-22.

Buch, E., Stein, M. (1989). Environmental conditions off West Greenland, 1980-1985. *Journal of the Northwest Atlantic Fisheries Science* **9**, 81-89.

Buckland, P. C., Mayewski, P.A., McGovern, T.H., Ogilvie, A.E.J., Sadler, J.P., Skidmore, P., Amorosi, T., Barlow, L.K., Dugmore, A.J. (1996). Bioarchaeological and climatological evidence for the fate of Norse farmers in medieval Greenland. *Antiquity* **70**, 88-96.

Carbonnell, M., Bauer, A. (1968). Exploitation des couvertures photographiques aeriennes repetees du front des glaciers velant dans Disko Bugt et Umanak Fjord, juin-juillet 1964; 1, nouvelles mesures photogrammetriques de la vitesse superficielle des glaciers du Groenland; 2, acceleration de l'ecoulement des glaciers groenlandais vers leur front et determination de leur debit solide. *Meddelelser om Gronland* **173**, pp78.

Chalmers, J. A., Pulvertaft, T.C.R., Marcussen, C., Pedersen, A.K. (1999). New insight into the structure of the Nuussuaq Basin. *Marine and Petroleum Geology* **16**, 197-224.

Chapman, M. R., Shackleton, N.J. (1998). Millennial-scale fluctuations in North Atlantic heat flux during the last 150 000 years. *Earth and Planetary Science Letters* **159**, 57-70.

Chapman, M. R., Shackleton, N.J. (2000). Evidence of 550-year and 1000-year cyclicities in North Atlantic circulation patterns during the Holocene. *Holocene* **10**, 287-291.

Charles, C. (1998). The ends of an era. *Nature* **394**, 422-423.

Christiansen, H. H., Murray, A.S., Mejdahl, V., Humlum, O. (1999). Luminescence dating of Holocene geomorphic activity on Ammassalik Island, SE Greenland. *Quaternary Geochronology* **18**, 191-205.

Clarke, R. A., Gascard, J. (1983). The formation of Labrador Sea Water, part I. Large scale processes. *Journal of Physical Oceanography* **13**, 1764-1778.

Clarke, T. S., Echelmeyer, K. (1996). Seismic-reflection evidence for a deep subglacial trough beneath Jakobshavns Isbrae, West Greenland. *Journal of Glaciology* 14, 219-232.

Clausen, H. B., Steffensen, J.P., Kipfstuhl, J and others. (1997). A comparison of the volcanic records over the past 4000 years from the Greenland Ice Core Project and Dye-3 Greenland ice cores. *Journal of Geophysical Research* **102**, 299-307.

Cook, E. R., D'Arrogo, R.D., Briffa, K.R. (1998). A reconstruction of the North American Oscillation using tree-ring chronologies from North America and Europe. *Holocene* **8**, 9-17.

Corliss, B. H. (1985). Microhabitats of benthic Foraminifera within deep-sea sediments. *Nature* **314**, 435-438.

Corliss, B. H. (1991). Morphology and microhabitat preferences of benthic foraminifera from the northwest Atlantic Ocean. *Marine Micropaleontology* **17**, 195-236.

Corliss, B. H., Chen, C. (1988). Morphotype patterns of Norwegian Sea deep benthic foraminifera and ecological implications. *Geology* **16**, 716-719.

Cowan, E. A., Seramur, K.C., Cai, J., Powell, R.D. (1999). Cyclic sedimentation produced by fluctuations in meltwater discharge, tides and marine productivity in an Alaskan fjord. *Sedimentology* **46**, 1109-1126.

Cremer, H., Melles, M., Wagner, B. (2001). Holocene climate changes reflected in a diatom succession from Basaltso, East Greenland. *Canadian Journal of Botany* **79**, 649-656.

Cronin, T. M., Schwede, S., Willard, D.A., Dwyer, G.S., Kamiya, T. (2003). Medieval Warm Period, Little Ice Age and 20th century temperature variability from Chesapeake Bay. *Global and Planetary Change* **36**, 17-29.

Cuffey, K. M., Marshall, S.J. (2000). Substantial contribution to sea-level rise during the last interglacial from the Greenland ice sheet. *Nature* **404**.

Culver, S. J., Buzas, M.A. (2000). Global latitudinal species diversity gradient in deep-sea benthic foraminifera. *Deep-Sea Research (part I)* **47**, 259-275.

Dahl-Jensen, D., Mosegaard, K., Gundestrup, N., Clow, G.D., Johnsen, S.J., Hansen, A.W., Balling, N. (1998). Past temperatures directly from the Greenland ice sheet. *Science* **282**, 268-271.

Dahl, S. O., Nesje, A. (1996). A new approach to calculating Holocene winter precipitation by combining glacier equilibrium-line altitudes and pine-tree limits: a case study from Hardangerjokulen, central southern Norway. *Holocene* **6**, 381-398.

Dansgaard, W., et al. (1984). North Atlantic climatic oscillations revealed by deep Greenland ice cores. In *Climate processes and climate sensitivity*, vol. Geophysical Monograph 29 (ed. J. E. Hansen), pp. 288-298: American Geophysical Union.

Dansgaard, W., Johnsen, S.J., Clausen, H.B., Dahl-Jensen, D., Gundestrup, N.S., Hammer, C.U., Hvidberg, C.S., Steffensen, J.P., Sveinbjornsdottir, A.E., Jouzel, J. and Bond, G.C. (1993). Evidence for general instability of past climate from a 250 kyr ice-core record. *Nature* **364**, 218-220.

Dansgaard, W., White, J.W.C., Johnsen, S.J. (1989). The abrupt termination of the Younger Dryas climate event. *Nature* **339**, 532-533.

Darby, M., Willmott, A.J., Mysak, L.A. (1994). Nonlinear steady-state model of the North Water Polynya. *Journal of Physical Oceanography* **24**, 1011-1020.

Dawson, A. G., Noone, S., Hickey, K., Holt, T., Wadhams, P., Foster I., Elliott, L., Mayewski, P., Lockett, P. (2003). Late-Holocene North Atlantic climate 'seesaws', storminess changes and Greenland ice sheet (GISP2) palaeoclimates. *Holocene* **13**, 381-392.

de Vernal, A., Bilodeau, G., Hillaire-Marcel, C., Kassou, N. (1992). Quantitative assessment of carbonate dissolution in marine sediments from foraminiferal test linings vs. shell ratios: Davis Strait, northwest North Atlantic. *Geology* **20**, 527-530.

de Vernal, A., Guiot, J., Turon, J-L. (1993). Late and postglacial paleoenvironments of the Gulf of St. Lawrence; marine and terrestrial palynological evidence Geographie Physique et Quaternaire. *Geographie Physique et Quaternaire* **47**, 167-180.

de Vernal, A., Miller, G.H., Hillaire-Marcel, C. (1991). Paleoenvironments of the last interglacial in northwest North Atlantic region and adjacent mainland Canada. *Quaternary International* **10-12**, 95-106.

Dean, W. E., Forester, R.M., Bradbury, J.P. (2002). Early Holocene change in atmospheric circulation in the Northern great plains: An upstream view of the 8.2 ka cold event. *Quaternary Science Reviews* **21**, 1763-1775.

Denmark. (1977). Referat af den Kongelige Grønladske Handels Fiskerimode, mandag den 18 April 1977. *Den Kongelige Grønlandske Handel* **(mimeograph)**.

Deser, C., Holland, M., Reverdin, G., Timlin M. (2002). Decadal variations in Labrador Sea Ice cover and North Atlantic sea surface temperatures. *Journal of Geophysical Research C: Oceans* **107**, 1-13.

Desloges, J. R., Christiansen, C., Rasch, M., Øhlenschlager, R., Gilbert, R., Nielsen, N. (2002). Holocene glacimarine sedimentary environments in fjords of Disko Bugt, West Greenland. *Quaternary Science Reviews* **21**, 947-963.

Dickson, R. R., Meincke, J., Malmberg, S.A., Lee, A.J. (1988). The "Great Salinity Anomaly" in the northern North Atlantic. *Progress in Oceanography* **20**, 103-151.

Dixon, K. W., Lanzante, J.R. (1999). Global mean surface air temperature and North Atlantic overturning in a suite of coupled GCM climate change experiments. *Geophysical Research Letters* **26**, 1885-1888.

Dokken, T. M., Jansen, E. (1999). Rapid changes in the mechanism of ocean convection during the last glacial period. *Nature* **401**, 458-461.

Domack, E. W., Mayewski, P.A. (1999). Bi-polar ocean linkages: Evidence from late-Holocene Antarctic marine and Greenland ice-core records. *Holocene* **9**, 247-251.

Donner, J., Jungner, H. (1975). Radiocarbon dating of shells from marine deposits in the Disko Bugt area, West Greenland. *Boreas* **4**, 25-45.

Dorn, W., Dethloff, K., Rinke, E., Roeckner, E. (2003). Competition of NAO regime changes and increasing greenhouse gases and aerosols with respect to Arctic climate change. *Climate Dynamics* **21**, 447-458.

Dowdeswell, J. A., Elverhøi, A., Andrews, J.T., Hebbeln, D. (1999). Asynchronous deposition of ice-rafted layers in the Nordic seas and North Atlantic. *Nature* **400**, 348-351.

Dowdeswell, J. A., Elverhøi, A., Spielhagen, R. (1998). Glacimarine sedimentary processes and facies on the polar North Atlantic margins. *Quaternary Science Reviews* **17**, 243-272.

Dowdeswell, J. A., Mackensen, A., Marienfield, P., Whittington, R.J., Jennings, A.E., Andrews, J.T. (2000). An origin for laminated glacimarine sediments through sea-ice build-up and suppressed iceberg rafting. *Sedimentology* **47**, 557-576.

Dowdeswell, J. A., Villinger, H., Whittington, R.J., Marienfield, P. (1993). Iceberg scouring in Scoresby Sund and on the East Greenland continental shelf. *Marine geology* **111**, 37-53.

Drewry, D. (1986). Glacial Geologic Processes: Arnold.

Dunbar, M. J. (1989). West Greenland Story: climatic, ecological and economic change. In *Proceedings of the sixteenth Stanstead seminar "High Latitude Climate Processes, with Special Emphasis on Large Scale Air-Sea-Ice interactions"*, vol. CRG Report No. 89-12 (ed. L. A. Mysak), pp. 105-114. Climate Research Group: McGill University, Montreal, Quebec.

Dunbar, M. J., Thompson, D.H. (1979). West Greenland salmon and climatic change. *Meddeleser om Grønland* **202**, 19 pp.

Duplessy, J.-C. (1999). Climate and the Gulf Stream. *Nature* **402**, 593-594/595.

Duplessy, J.-C., Duprat, J., Van Weering, T.C.E., Labeyrie, L., Arnold, M., Paterne, M. (1992). Changes in surface salinity of the North Atlantic Ocean during the last deglaciation. *Nature* **358**, 485-488.

Duplessy, J.-C., Ivanova, E., Murdmaa, I., Paterne, M., Labeyrie, L. (2001). Holocene paleoceanography of the northern Barents Sea and variations of the northward heat transport by the Atlantic Ocean. *Boreas* **30**, 2-16.

Dyke, A. S., Savelle, J.M. (2000). Holocene driftwood incursion to Southwest Victoria Island, Canadian arctic archipelago, and its significance to palaeoceanography and archaeology. *Quaternary Research* **54**, 113-120.

Echelmeyer, K., Clarke, T. S. & Harrison, W. D. (1991). Surficial glaciology of Jakobshavns Isbrae, West Greenland: part I. Surface morphology. *Journal of Glaciology* **127**, 368-382.

Eddy, J. A. (1976). The Maunder minimum. *Science* **192**, 1189-1202.

Eden, C., Böning, C. (2002). Sources of eddy kinetic energy in the Labrador Sea. *Journal of Physical Oceanography* **32**, 3346-3363.

Eiríksson, J., Knudsen, K.L., Haflidason, H., Heinemeier, J. (2000a). Chronology of late Holocene climatic events in the northern North Atlantic based on AMS ^{14}C dates and tephra markers from the volcano Hekla, Iceland. *Journal of Quaternary Science* **16**, 573-580.

Eiriksson, J., Knudsen, K.L., Haflidason, H., Henriksen, P. (2000b). Late-glacial and Holocene palaeoceanography of the North Icelandic shelf. *Journal of Quaternary Science* **15**, 23-34.

Elberling, B., Knudsen, K.L., Kristensen, P.H., Asmund, G. (2003). Applying foraminiferal stratigraphy as a biomarker for heavy metal contamination and mining impact in a fiord in West Greenland. *Marine Environmental Research* **55**, 235-256.

Elverhøi, A., Liestøl, Nagy, J. (1980). Glacial erosion, sedimentation and microfauna in the inner part of Kongsfjorden, Spitsbergen. *Norsk Polarinstitute Skrifter* **132**, 33-61.

Eyles, C. H., Eyles, N., Miall, A.D. (1985). Models of glaciomarine sedimentation and their application to the interpretation of ancient glacial sequences. *Palaeogeography, Palaeoclimatology, Palaeoecology* **51**, 15-84.

Fairbanks R. G. (1989). A 17,000-year glacio-eustatic sea level record: influence of glacial melting rates on the Younger Dryas event and deep-ocean circulation. *Nature* **342**, 637- 642

Fairbanks, R. G. (1990). The age and origin of the 'Younger Dryas climate event' in Greenland ice cores. *Paleoceanography* **5**, 937-948.

Fastook, J. L., Brecher, H.H., Hughes, T.J. (1995). Derived bedrock elevations, strain rates and stresses from measured surface elevations and velocities: Jakobshavns Isbrae, Greenland. *Journal of Glaciology* **137**, 161-173.

Feyling-Hanssen, R. W. (1980). Micro biostratigraphy of young Cenozoic marine deposits of the Qivituq Peninsula, Baffin Island. *Marine Micropaleontology* **5**, 153-184.

Feyling-Hanssen, R. W. (1990a). A remarkable foraminiferal assemblage from the Quaternary of northeast Greenland. *Bulletin of the Geological Society of Denmark* **38**, 101-107.

Feyling-Hanssen, R. W. (1990b). Foraminiferal stratigraphy in the Plio-Pleistocene Kap København Formation, North Greenland. *Meddelelser om Grønland, Geoscience* **24**, 3-32.

Feyling-Hanssen, R. W., Funder, S. (1990). Fauna and flora: Late Quaternary stratigraphy and glaciology in the Thule area, Northwest Greenland. *Meddelelser om Grønland* **22**, 19-22.

Finkel, R. C., and Nishiizumi, K. (1997). Beryllium 10 concentrations in the Greenland Ice Sheet Project 2 ice core from 3-40 ka. *Journal of Geophysical Research* **102**, 26699-26706.

Fleming, K., Johnston, P., Zwartz, D. Yokoyama, Y., Lambeck, K., Chappell, J. (1998). Refining the eustatic sea-level curve since the Last Glacial Maximum using far- and intermediate-field sites. *Earth and Planetary Science Letters* **163**, 327-342.

Foged, N. (1953). Diatoms from West Greenland. *Meddeleser om Grønland* **147**, 1-86.

Foged, N. (1955). Diatoms from Peary Land, North Greenland. *Meddelelser om Grønland* **128**, 1-90.

Foged, N. (1958). The diatoms in the basalt area and adjoining areas of Archean rock in West Greenland. *Meddeleser om Grønland* **156**, 1-145.

Foged, N. (1972). The diatoms in four postglacial deposits at Godthåbsfjord, West Greenland. *Meddeleser om Grønland* **194**, 1-66.

Foged, N. (1977). The diatoms in four postglacial deposits at Godthåbsfjord, West Greenland. *Meddelelser om Grønland* **199**, pp 72.

Fredskild, B. (1984). Holocene palaeo- winds and climatic changes in West Greenland as indicated by long-distance transported and local pollen in lake sediments. In *Climatic changes on a yearly to millennial basis*, vol. Proc. 2nd Nordic symposium, Stockholm, 1983 (ed. N.-A. Morner), pp. 163-171: Reidel.

Fredskild, B. (1988). Planteresterne. In *Boplads i Dybfrost*, vol. 11-12 (ed. B. Gronnow, and Meldegaard, M.), pp. 429-431.

Fredskild, B. (2000). The Holocene vegetational changes on Qeqertarsuatsiaq, a West Greenland island. *Geografisk Tidsskrift* **100**, 7-14.

Frew, R. D., Dennis, P.F., Heywood, K.J., Meredith, M.P., Boswell, S.M. (2000). The oxygen isotope composition of water masses in the northern North Atlantic. *Deep-Sea Research I* **47**, 2265-2286.

Fronval, T., Jansen, E. (1996). Rapid changes in ocean circulation and heat flux in the Nordic seas during the Last Interglacial period. *Nature* **383**, 806-810.

Funder, S. (1989). Quaternary geology of the ice-free areas and adjacent shelves of Greenland. In *Quaternary Geology of Canada and Greenland*, (ed. R. J. Fulton), pp. 741-792: Geological Survey of Canada.

Funder, S., Hansen, L. (1996). The Greenland icesheet - a model for its culmination and decay during and after the Last Glacial Maximum. *Bulletin of the Geological Society of Denmark* **42**, 137-152.

Funder, S., Simonarson, L.A. (1984). Bio- and aminostratigraphy of some Quaternary marine deposits in West Greenland. *Canadian Journal of Earth Sciences* **21**, 843-852.

Funder, S., Weidick, A. (1991). Holocene boreal molluscs in Greenland-palaeoceanographic interpretations. *Palaeogeography, Palaeoclimatology, Palaeoecology* **85**, 123-135.

Gabel-Jøorgensen, C. C. A., Egedal, J. (1940). Tidal observations made at Nanortalik and Julianehaab in 1932-1934. København: C.A. Reitzels.

Gilbert, R., Rasch, M., Neilsen, N., Desloges, J.R. (1998). Contrasting glacimarine sedimentary environments of two Arctic fjords on Disko, West Greenland. *Marine geology* **147**, 63-83.

Gooday, A. J. (1986). Meiofaunal foraminireans from the bathyal Porcupine Seabight (north-east Atlantic): size structure, standing stock, taxonomic composition, species diversity and vertical distribution in the sediment. *Deep-Sea Research* **33**, 1345-1373.

Gooday, A. J. (1988). A response by benthic foraminifera to the deposition of phytodetritus in the deep sea. *Nature* **332**, 70-73.

Gooday, A. J., Lambshead, P.J.D. (1989). The impact of seasonally deposited phytodetritus on benthic foraminifera populations in the bathyal northeast Atlantic: the species response. *Marine Ecology Progressive Series* **58**, 53-67.

Gregory, J. M., Oerlemans, J. (1998). Simulated future sea-level rise due to glacier melt based on regionally and seasonally resolved temperature changes. *Nature* **391**, 474-476.

Greiner, G. O. G. (1974). Environmental factors controlling the distribution of recent benthonic foraminifera. *Brevoria* **420**, 1-35.

Grimm, E. C. (1986). TILIA, TILIAGRAPH. *MS-DOS based program for species assemblage data and stratigraphically constrained palaeoenvironmental analysis* **Version 3.1.**

Grimm, E. C. (2001). TGVIEW. *Windows based viewer for MS-DOS programs TILIA, TILIAGRAPH* **version 3.1.4.1.**

GRIP, members. (1993). Climate instability during the last interglacial period recorded in the GRIP ice core. *Nature* **364**, 203-207.

Grootes, P. M., Stuiver, M. (1997). Oxygen 18/16 variability in Greenland snow and ice with 10^{-3} - to 10^{5}-year time resolution. *Journal of Geophysical Research* **102**, 26455-26470.

Grootes, P. M., Stuiver, M., White, J.W.C, Johnsen, S.J. and Jouzel, J. (1993). Comparison of oxygen isotope records from the GISP2 and GRIP Greenland ice cores. *Nature* **339**, 552-554.

Grotzner, A., Latif, M., Timmermann, A., Voss, R. (1999). Interannual to decadal predictability in a coupled ocean-atmosphere general circulation model. *Journal of Climate* **12**, 2607-2624.

Gudina, V. I., Saidova, Kh. M., Troitskaya, T.S. (1968). Ecology and systematics of Islandiellids (foraminifera). *Institute of Geology and Geophysics, Academy of Sciences of the USSR* **182**, 615-616.

Gudmundsson, H. J. (1997). A review of the Holocene environmental history of Iceland. *Quaternary Science Reviews* **16**, 81-92.

Gustafsson, M., Nordberg, K. (2001). Living (stained) benthic foraminiferal response to primary production and hydrography in the deepest part of the Gullmar Fjord, Swedish West coast, with comparisons to Hoglund's 1927 material. *Journal of Foraminiferal Research* **31**, 2-11.

Häkkinen, S. Freshening of the Labrador Sea surface waters in the 1990s: Another great salinity anomaly? *Geophysical Research Letters* **29**, 85-1 - 85-4.

Hald, M., Aspeli, R. (1997). Rapid climatic shifts of the Northern Norwegian Sea during the last deglaciation and the Holocene. *Boreas* **26**, 15-28.

Hald, M., Korsun, S. (1997). Distribution of modern benthic foraminifera from fjords of Svalbard, European Arctic. *Journal of Foraminiferal Research* **27**, 101-122.

Hald, M., Steinsund, P.I. (1992). Distribution of surface sediment benthic foraminifera in the southwestern Barents Sea. *Journal of Foraminiferal Research* **22**, 347-362.

Hald, M., Steinsund, P.I., Dokken, T., Korsun, S., Polyak, L., Aspeli, R. (1994). Recent and Late Quaternary distribution of *Elphidium excavatum* f. *clavata* in Arctic seas. *Cushman Foundation Special Publication* **32**, 141-153.

Hald, M., Vorren, T.O. (1987). Stable isotope stratigraphy and paleoceanography during the last deglaciation on the continental shelf off Troms, northern Norway. *Paleoceanography* **2**, 583-599.

Hambrey, M. J. (1994). Glacial Environments. Published by UCL Press, London. Chapters 3 and 4, pages 93-107.

Hansen, A., Knudsen, K.L. (1995). Recent foraminiferal distribution in Freemansundet and Early Holocene stratigraphy on Edgeøya, Svalbard. *Polar Research* **14**, 215-238.

Hansen, L., Funder, S., Murray, A.S., Mejdahl, V. (1999). Luminescence dating of the last Weichselian Glacier advance in East Greenland. *Quaternary Geochronology* **18**, 179-190.

Hardy, R. J., Bamber, J.L., Orford, S. (2000). The delineation of drainage basins on the Greenland ice sheet for mass-balance analyses using a combined modelling and geographical information system approach. *Hydrological Processes* **14**.

Hay, W. W., DeConto, R.M., Wold, Ch. N. (1997). Climate: Is the past the key to the future? *Geol. Rundsch.* **86**, 471-491.

Hemming, S. R., Vorren, T.O., Kleman, J. (2002). Provinciality of ice rafting in the North Atlantic: application of $^{40}Ar/^{39}Ar$ dating of individual ice rafted hornblende grains. *Quaternary International* **95-96**, 75-85.

Herman, Y., O'Neil, J.R., Drake, C.L. (1972). Micropaleontology and paleotemperatures of postglacial SW Greenland fjord cores. In *Climatic Changes in Arctic Areas during the last ten thousand years*, (ed. H. H. Y. Vasari, S. Hicks), pp. 357-407. Oulou: University of Oulou.

Hesse, R., klauck, I., Khodabakhsh, S., Piper, D. (1999). Continental slope sedimentation adjacent to an ice margin. III. The upper Labrador slope. *Marine geology* **155**, 249-276.

Hillaire-Marcel, C., Bilodeau, G. (2000). Instabilities in the Labrador Sea water mass structure during the last climatic cycle. *Canadian Journal of Earth Sciences* **37**, 795-809.

Hillaire-Marcel, C., de Vernal, A., Bilodeau, G., Wu, G. (1993). Isotope stratigraphy, sedimentation rates, deep circulation, and carbonate events in the Labrador Sea during the last ~200ka. *Canadian Journal of Earth Sciences* **31**, 63-89.

Hiscott, R. N., Asku, A.E., Mudie, P.J., Parsons, D.F. (2001). A 340,000 year record of ice rafting, palaeoclimatic fluctuations, and shelf-crossing glacial advances in the Southwestern Labrador Sea. *Global and Planetary Change* **28**, 227-240.

Hjort, C. (1997). Glaciation, climate history, changing marine levels and the evolution of the Northeast Water Polynya. *Journal of Marine Systems* **10**, 23-33.

Holtzscherer, J.-J., Bauer, A. (1954). Contribution a la conaissance de L'Inlandsis du Groenland. *International Association of Scientific Hydrology* **39**, 244-296.

Hughes, T. (1986). The Jakobshavn Effect. *Geophysical Research Letters* **13**, 46-48.

Hui Jiang, S., M.-S., Knudsen, K.-L., Eiriksson, J. (2002). Late-Holocene summer sea-surface temperatures based on a diatom record from the North Icelandic Shelf. *The Holocene* **12**, 137-147.

Humlum, O. (1985). The glaciation level in West Greenland. *Arctic and Alpine Research* **17**, 311-319.

Humlum, O. (1999). Late-Holocene climate in central West Greenland: meteorological data and rock-glacier isotope evidence. *Holocene* **9**, 581-594.

Hunt, A. S., Corliss, B.H. (1993). Distribution and microhabitats of living (stained) benthic foraminifera from the Canadian Arctic Archipelago. *Marine Micropaleontology* **20**, 321-345.

Hunter, L. E., Powell, R.D., Lawson, D.E. (1996). Morainal-bank sediment budgets and their influence on the stability of tidewater termini of valley glaciers entering Glacier Bay, Alaska, USA. *Annals of Glaciology* **22**, 211-216.

Hurrell, J. W. (1995). Decadal trends in the North Atlantic Oscillation regional temperatures and precipitation. *Science* **269**, 676-679.

Hurrell, J. W. (1996). Influence of variations in extratropical wintertime teleconnections on Northern Hemisphere temperature. *Geophysical Research Letters* **23**, 665-668.

Hurrell, J. W., Van Loon, H. (1997). Decadal variations in climate associated with the North Atlantic Oscillation. *Climate Change* **36**, 301-326.

Huybrechts, P. (2002). Sea-level changes at the LGM from ice-dynamic reconstructions of the Greenland and Antarctic ice sheets during the glacial cycles. *Quaternary Science Reviews* **21**, 203-231.

Igarashi, A., Numanami, H., Tsuchiya, Y., Fukuchi, M. (2001). Bathymetric distribution of fossil foraminifera within marine sediment cores from the eastern part of Lützow-Holm Bay, East Antarctica, and its palaeoceanographic implications. *Marine Micropaleontology* **42**, 125-162.

Ingólfsson, O., Frich, P., Funder, S., Humlum, O. (1990). Palaeoclimatic implications of an early Holocene glacier advance on Disko Island, West Greenland. *Boreas* **19**, 297-311.

Ingram, R. G., Prinsenberg, S. (1998). Coastal oceanography of Hudson Bay and surrounding eastern Canadian arctic waters. In *The Sea*, vol. 11 (ed. A. R. B. Robinson, K.H.), pp. 835-859: John Wiley and Sons, Inc.

Jacobs, J. D., Andrews, J.T., Funder, S. (1985). Environmental background. In *Quaternary Environments: Eastern Canadian Arctic, Baffin Bay and Western Greenland*, (ed. J. T. Andrews), pp. 26-68.

Jansen, E. (1989). The use of stable oxygen and carbon isotope stratigraphy as a dating tool. *Quaternary International* **1**, 151-166.

Jansen, E., Sjerup, H -P., Fjaeran, T., Hald, M., Holte-Dahl, H., Skarbo, O. (1983). Late Weichselian paleoceanography of the southeastern Norwegian Sea. *Norsk Geologisk Tidsskrift* **63**, 117-146.

Jennings, A. E., Helgadottir, G. (1994). Foraminiferal assemblages from the fjords and shelf of Eastern Greenland. *Journal of Foraminiferal Research* **24**, 123-144.

Jennings, A. E., Knudsen, K.L., Hald, M., Hansen, C.V., Andrews, J.T. (2002). A mid-Holocene shift in Arctic sea-ice variability on the East Greenland shelf. *Holocene* **12**, 49-58.

Jennings, A. E., Manley, W.F., MacLean, B., Andrews, J.T. (1998). Marine evidence for the last glacial advance across eastern Hudson Strait, eastern Canadian Arctic. *Journal of Quaternary Science* **13**, 501-514.

Jennings, A. E., Vilks, G., Deonaire, B., Silis, A., Weiner, N. (2001). Foraminiferal biostratigraphy and paleoceanography. *Bulletin of the Geological Survey of Canada* **566**, 127-146.

Jennings, A. E., Weiner, N.J. (1996). Environmental change in Eastern Greenland during the last 1300 years: evidence from foraminiferal and lithofacies in Nansen Fjord, 68°N. *Holocene* **6**, 179-191.

Jensen, H. M., Pedersen, L., Burmeister, A, Hansen, B.W. (1999). Pelagic primary production during summer along 65 to 72°N off West Greenland. *Polar Biology* **21**, 269-278.

Jensen, K. G., Daugbjerg, N., Thomsen, H. A. Diversity and succession of planktonic and sea ice diatoms from Disko Bugt, West Greenland. *Meddelelser om Grønland* **Submitted**.

Jensen, K. G., Kuijpers, A., Koc, N., Heinemeier, J. Diatom evidence of hydrographic changes and sea ice conditions in Igaliku Fjord, South Greenland during the past 1500 years. *The Holocene* **In press**.

Jiang H., S., M.-S., Knudsen K.L., Eiríksson J. (2002). Late-Holocene summer sea-surface temperatures based on a diatom record from the north Icelandic shelf. *Holocene* **12**, 137-147.

Johnsen, S. J., Dahl-Jensen, D., Gunderstrup, N., Steffensen, J.P., Clausen, H.B., Miller, H., Masson-Delmotte, V., Sveinbjörnsdottir, A.E., White, J. (2001). Oxygen isotope and palaeotemperature records from six Greenland ice-core stations: Camp Century, Dye-3, GRIP, GISP-2, Renland and NorthGRIP. *Journal of Quaternary Science* **16**, 299-307.

Johnson, R. G. (1997). Ice age initiation by an ocean-atmospheric circulation change in the Labrador Sea. *Earth and Planetary Science Letters* **148**, 367-379.

Johnson, R. G., Lauritzen, S-E. (1995). Hudson Bay-Hudson Strait jökulhlaups and Heinrich events: a hypothesis. *Palaeogeography, Palaeoclimatology, Palaeoecology* **117**, 123-137.

Jones, P. D., Jonsson, T., Wheeler, D. (1997). Extension to the North Atlantic Oscillation using early instrumental pressure observations from Gibraltar and south-west Iceland. *International Journal of Climatology* **17**, 1433-1450.

Jorissen, F. J., De Stigter, H.C., Widmark, J.G, V. (1995). A conceptual model explaining benthic foraminiferal microhabits. *Marine Micropaleontology* **26**, 3-15.

Joughin, I., Abdalati, W., Fahenstock, M. (2004). Large fluctuations in speed on Greenland's Jakobshavn Isbrae glacier. *Nature* **432**, 608-610.

Joughin, I., Gogineni, P., Fahnestock, M., MacAyeal D., Bamber J.L. (2001). Observation and analysis of ice flow in the largest Greenland ice stream. *Journal of Geophysical Research* **D: Atmospheres 106**, 34021-34034.

Joughin, I. R., Fahnestock, M.A., Bamber, J.L. (2000). Ice flow in the Northeast Greenland ice stream. *Annals of Glaciology* **31**, 141-146.

Joughin, I. R., Fahnestock, M.A., Ekholm, S., Kwok, R. (1997). Balance velocities of the Greenland ice sheet. *Geophysical Research Letters* **24**, 3045-3048.

Kaiho, K. (1994). Benthic foraminiferal dissolved-oxygen index and dissolved oxygen levels in the modern ocean. *Geology* **22**, 719-722.

Kaplan, M. R., Wolfe, A.P., Miller, G.H. (2002). Holocene Environmental Variability in Southern Greenland Inferred from Lake Sediments. *Quaternary Research* **58**, 149-159.

Keigwin, L. D., Jones, G.A. (1995). The marine record of deglaciation from the continental margin off Nova Scotia. *Paleoceanography* **10**, 973-985.

Kellogg, T. B. (1984). Late-glacial - Holocene high-frequency climatic changes in deep- sea cores from the Denmark Strait. In *Climatic changes on a yearly to millennial basis*, vol. Proc. 2nd Nordic symposium, Stockholm, 1983 (ed. N.-A. Morner), pp. 123-133: Reidel.

Kellogg, T. B., Osterman, L.E., Stuiver, M. (1979). Late Quaternary sedimentology and benthic foraminiferal palaeoecology of the Ross Sea, Antarctica. *Journal of Foraminiferal Research* **9**, 322-335.

Kelly, M. (1979). Comments on the implications of new radiocarbon dates from the Holsteinsborg region, central West Greenland. *Gronlands Geologiske Undersogelse* **Rapport 95**, 35-42.

Kelly, M. (1980). The status of the Neoglacial in western Greenland. *Gronlands Geologiske Undersogelse Rapport* **96**, 24.

Kelly, M. (1985). A review of the Quaternary geology of western Greenland. In *Quaternary Environments Eastern Canadian Arctic, Baffin Bay, and Western Greenland*, (ed. J. T. Andrews), pp. 461-501. Boston: Allen and Unwin.

Kelly, M., Funder, S., Houmark-Nielsen, M., Knudsen, K.L., Kronborg, C., Landvik, J., Sorby, L. (1999). Quaternary glaciation and marine environmental history of northwest Greenland: a review and appraisal. *Quaternary Science Reviews* **18**, 373-392.

Kerr, R. A. (1992). Did the Great Salinity Anomaly cool the North Atlantic? *Science* **255**, 1509.

Kerwin, M. (1996). A regional stratigraphic isochron (ca. 8000 14C yr BP) from final deglaciation of Hudson Strait. *Quaternary Research* **46**, 89-98.

Kim, J.-M., Kucera, M. (2000). Benthic foraminifer record of environmental changes in the Yellow Sea (Hwanghae) during the last 15,000 years. *Quaternary Science Reviews* **19**, 1067-1085.

Kirkbride, M. P., Dugmore, A.J. (2001). Can lichenometry be used to date the "Little Ice Age" glacial maximum in Iceland? *Climatic Change* **48**, 151-167.

Kleiber, H. P., Knies, J., Niessen, F. (2000). The Late Weichselian glaciation of the Franz Victoria Trough, Northern Barents Sea: ice sheet extent and timing. *Marine geology* **168**, 25-44.

Klitgaard-Kristensen, D., Sejrup, H.P., Haflidason, H., Johnsen, S., Spuk, M. (1998). A regional 8200 cal. yr BP cooling event in northwest Europe, induced by final stages of the Laurentide ice-sheet deglaciation? *Journal of Quaternary Science* **13**, 165-169.

Knight, P. G., Robinson, Z.P., Waller, R.I., Patterson., C.J., Jones, A.P. (2002). Discharge of debris from ice at the margin of the Greenland ice sheet. *Journal of Glaciology* **48**, 192-198.

Knudsen, K. L. (1988). Marine interglacial deposits in the Cuxhaven area, NW Germany: a comparison of Holsteinian, Eemian and Holocene foraminiferal faunas. *Eiszeitalter und Gegenwart* **38**, 69-77.

Knudsen, K. L., Austin, W. E. N. (1996). ***? In *Late Quaternary Palaeoceanography of the North Atlantic Margins*, vol. 111 (ed. A. J.T. Andrews, W.E.N., Bergsten, H., Jennings, A.E.): Geological Society Special Publications.

Knudsen, K. L., Seidenkrantz, M-S. (1994). *Stainforthia feylingi* new species from arctic to subarctic environments, previously recorded as *Stainforthia schreibersiana* (Czjek). *Cushman Foundation Special Publication* **32**, 5-13.

Koç Karpuz, N., Schrader, H. (1990). Surface sediment diatom distribution and Holocene paleotemperature variations in the Greenland, Iceland and Norwegian seas throughout the last 14 Ka based on diatoms. *Paleoceanaography* **5**, 557-580.

Koç, N., Jansen, E. (1994). Response of the high-latitude Northern Hemisphere to orbital climate forcing: evidence from the Nordic Seas. *Geology* **22**, 523-526.

Koç, N., Jansen, E., Haflidason, H. (1993). Paleoceanographic reconstructions of surface ocean conditions in the Greenland, Iceland and Norwegian Seas though the last 14 Ka based on diatoms. *Quaternary Science Reviews* **12**, 115-140.

Koç, N. a. J., E. (1992). A high-resolution diatom record of the last deglaciation from the SE Norwegian Sea: Documentation of rapid climatic changes. *Paleoceanography* **7**, 499-520.

Koerner R.M., F. D. A. (2002). Ice-core evidence for widespread Arctic glacier retreat in the Last Interglacial and the early Holocene. *Annals of Glaciology* **35**, 19-24.

Korsun, S., Hald, M. (1998). Modern benthic foraminifera off Novaya Zemlya tidewater glaciers, Russian Arctic. *Arctic and Alpine Research* **30**, 61-77.

Korsun, S., Hald, M. (2000). Seasonal dynamics of benthic foraminifera in a glacially fed fjord off Svalbard, European Arctic. *Journal of Foraminiferal Research* **30**, 251-271.

Krabill, W., Abdalati, W., Frederick, E., Manizade, S., Martin, C., Sonntag, J., Swift, R., Thomas, R., Wright, W., Yungel, J. (2000). Greenland ice sheet: high-elevation balance and peripheral thinning. *Science* **289**, 428-430.

Krinner, G., Genthon, C. (1998). GCM simulations of the Last Glacial Maximum surface climate of Greenland and Antarctica. *Climate Dynamics* **14**, 741-758.

Kuijpers, A., Andersen, M.S., Kenyon, N.H., Kunzendorf, H., van Weering, T.C.E. (1998a). Quaternary sedimentation and Norwegian Sea overflow pathways around Bill Bailey Bank, Northeastern Atlantic. *Marine geology* **152**, 101-127.

Kuijpers, A., Lloyd, J.M., Jensen, J.B., Endler, R., Moros, M., Park, L.A., Schulz, B., Gutfelt, J., Laier, T. (2001). Late Quaternary circulation changes and sedimentation in Disko Bugt and adjacent fjords, central West Greenland. *Geology of Greenland Survey Bulletin* **189**, 41-47.

Kuijpers, A., Troelstra, S.R., Prins, M.A., Linthout, K., Akhmetzhanov, A., Bouryak, S., Bachmann, M.F., Lassen, S., Rasmussen, S., Jensen, J.B. (2003). Late Quaternary sedimentary processes and ocean circulation changes at the Southeast Greenland margin. *Marine geology* **195**, 109-129.

Kuijpers, A., Troelstra, S.R., Wisse, M., Heier Nielsen, S., van Weering, T.C.E. (1998b). Norwegian Sea overflow variability and NE Atlantic surface hydrography during the past 150,000 years. *Marine geology* **152**, 75-99.

Kwok, R., Rothrock, D.A. (1999). Variability of Fram Strait ice flux and North Atlantic Oscillation. *Geophysical Research C: Oceans* **104**, 5177-5189.

Lacasse, C. (2001). Influence of climate variability on the atmospheric transport of Icelandic tephra in the subpolar North Atlantic. *Global and Planetary Change* **29**, 31-55.

Landvik, J. Y., Hjort, C., Mangerud, J., Moller, P., Salvigsen, O. (1995). The Quaternary record of eastern Svalbard. *Polar Research* **14**, 95-103.

Larsen, H. C. (1983). Marine geophysical investigations offshore East Greenland. *Rapport - Groenlands Geologiske Undersoegelse* **115**, 93-100.

Lassen, S., Lindgren, H., Heinemeier, J., Jansen, E., Knudsen., K.L., Kuijpers, A., Kunzendorf, H. (2002). Intermediate water signal leads surface water response during Northeast Atlantic deglaciation. *Global and Planetary Change* **32**, 111-125.

Latif, M., Roeckner, E., Mikolajewicz, U., Voss, R. (2000). Tropical stabilization of the thermohaline circulation in a greenhouse warming simulation. *Journal of Climate* **13**, 1809-1813.

Lazier, J. R. N. (1988). Temperature and salinity changes in the deep Labrador Sea, 1962-1986. *Deep-Sea Research* **35**, 1247-1253.

Lehman, S. (1997). Sudden end of an interglacial. *Nature* **390**, 117-118/119?

Lenham, J. W., Bull, J.M., Dix, J.K., Quinn, R.J. (*In press*). Experiences of rapid post-processing of shallow marine high-resolution Chirp seismic reflection data. *n/a.*

Letreguilly, A., Reeh, N., Huybrechts, P. (1991). The Greenland ice sheet through the last glacial-interglacial cycle. *Global and Planetary Change* **4**, 385-394.

Levac, E., de Vernal, Blake, W. Jr. (2001). Sea-surface conditions in northernmost Baffin Bay during the Holocene: Palynological evidence. *Journal of Quaternary Science* **16**, 353-363.

Lewis, E. L., Ponton, D., Legendre, L., LeBlanc, B. (1996). Springtime sensible heat, nutrients, and phytoplankton in the Northwater Polynya, Canadian Arctic. *Continental Shelf Research* **16**, 1775-1792.

Li, B., Yoon, H-I, Park, B-K. (2000). Foraminiferal assemblages and $CaCO_3$ dissolution since the last deglaciation in the Maxwell Bay, King George Island, Antarctica. *Marine geology* **169**, 239-257.

Lloyd, J. M. (in prep). Modern distribution of benthic foraminifera in Disko Bugt, West Greenland: Indicators for the West Greenland Current. *Journal of Foraminiferal Research.*

Lloyd, J.M. (2000). Combined foraminiferal and thecamoebian environmental reconstruction from an isolation basin in NW Scotland: implications for sea-level studies. *Journal of Foraminiferal Research* **30**, 294–305

Lloyd, J. M., Kroon, D., Laban, C., Boulton, G. (1996). Deglaciation history and palaeoceanography of the western Spitsbergen margin since the last glacial maximum. In *Late Quaternary Palaeoceanography of the North Atlantic Margins*, vol. 111 (ed. J. T. Andrews, Austin, W.E.N., Bergsten, H., Jennings, A.E.), pp. 289-301: Geological Society Special Publications.

Lloyd, J. M., Park, L.A., Kuijpers, A., Morros, M. (submitted). Early Holocene palaeoceanography and deglacial chronology of Disko Bugt, West Greenland. *Journal of Quaternary Science.*

Loder, J. W., Petrie, B. (1998). The coastal ocean off northeastern North America: a large-scale view. In *The Sea*, vol. 11 (ed. A. R. Robinson, Brink, K.H.), pp. 105-133. New York: John Wiley and Sons.

Loeblich, A. R., Jr., Tappan, H. (1953). Studies of Arctic foraminifera. *Washington Smithsonian Institute* **121**, 1-142 + 24 plates.

Lohmann, G. P. (1995). A model for variation in the chemistry of planktonic foraminifera due to secondary calcification and selective dissolution. *Paleoceanography* **10**, 445-457.

Long, A. J., Roberts, D.H.R. (2002). A revised chronology for the "Fjord Stage" moraine in Disko Bugt, West Greenland. *Journal of Quaternary Science* **17**, 561-579.

Long, A. J., Roberts, D.H.R. (2003a). Late Weichselian deglacial history of Disko Bugt, West Greenland, and the dynamics of the Jakobshavns Isbrae ice stream. *Boreas* **32**, 208-226.

Long, A. J., Roberts, D.H.R., Rasch, M. (2003b). New observations on the relative sea level and deglacial history of Greenland from Innaarsuit, Disko Bugt. *Quaternary Research* 60, 162-171.

Long, A. J., Roberts, D.H.R., Wright, M.R. (1999). Isolation basin relative stratigraphy and Holocene relative sea-level change on Arveprinsen Ejland, Disko Bugt, West Greenland. *Journal of Quaternary Science* **14**, 323-345.

Lønne, I., Syvitski, J.P. (1997). Effects of the readvance of an ice margin on the seismic character of the underlying sediment. *Marine geology* **143**, 81-102.

Löwemark, L., Werner, F. (2001). Dating errors in high-resolution stratigraphy: a detailed X-ray radiography and AMS-^{14}C study of *Zoophycos* burrows. *Marine geology* 177, 191-198.

Mackensen, A., Futterer, D.K., Grobe, H., Schmiedl, G. (1993). Benthic foraminiferal assemblages from the eastern South Atlantic Polar Front region between 35o and 57oS: distribution, ecology and fossilization potential. *Marine Micropaleontology* **22**, 33-69.

Mackensen, A., Hald, M. (1983). *Cassidulina teretis* Tappan and *C. laevigata* d'Orbigny; their modern and late Quaternary distribution in northern seas. *Journal of Foraminiferal Research* **18**, 16-24.

Mackensen, A., Hald, M. (1988). Cassidulina teretis Tappan and C. laevigata d'Orbigny; their modern and late Quaternary distribution in the northern seas. *Journal of Foraminiferal Research* **18**, 16-24.

Mackensen, A., Schumacher, S., Radke, J., Schmidt, D.N. (2000). Microhabitat preferences and stable carbon isotopes of endobenthic foraminifera: clue to quantitative reconstruction of oceanic new production? *Marine Micropaleontology* 40, 233-258.

Mackensen, A., Sejrup, H.P., Jansen, E. (1985). The distribution of living benthic foraminifera on the continental slope and rise off southwest Norway. *Marine Micropaleontology* 9, 275-306.

Madsen, H. B., Knudsen, K.L. (1994). Recent foraminifera in shelf sediments of the Scoresby Sund fjord, East Greenland. *Boreas* **23**, 495-504.

Mann, M. E., Bradley, R.S., Hughers, M.K. (1998). Global scale temperature patterns and climate forcing over the past six centuries. *Nature* **392, 779-778.**

Marko, J. R., Fissel, D.B., Wadhams, P., Kelly., P.M., Brown, R.D. (1994). Iceberg severity off eastern North America: its relationship to sea ice variability and climate change. *Journal of Climate* **7, 1335-1351.**

Marlowe, J. L., Vilks, G. (1963). Marine geology, eastern part of Prince Gustaf Adolf Sea, district of Franklin. (Polar continental shelf project). *Ottawa, Dept of Mines and technical Surveys* **Geological Survey of Canada, 23.**

Matsumoto, K. (1996). An iceberg drift and decay model to compute the ice-rafted debris and iceberg meltwater flux; application to the interglacial North Atlantic. *Paleoceanography* **11, 729-742.**

Mazaud, A., Vimeux, F., Jouzel, J. (2000). Short fluctuations in Antarctic isotope records: a link with cold events in the North Atlantic? *Earth and Planetary Science Letters* **177, 219-225.**

McCabe, A. M., Clark, P.U. (1998). Ice-sheet variability around the North Atlantic Ocean during the last deglaciation. *Nature* **392, 373-377.**

McConnell, J. R., Arthern, R.J., Mosley-Thompson, E., Davis, C.H., Bales, R.C., Thomas, R., Burkhart, J.F., Kyne, J.D. (2000). Changes in Greenland ice sheet elevation due to snow accumulation variability. *Nature* **406, 877-879.**

McGowan, S., Ryves, D.B., Anderson, N.J. (2003). Holocene records of effective precipitation in West Greenland. *Holocene* **13, 239-249.**

McManus, J. F., Bond, G.C., Oppo, D.W., Keigwin, L.D., Cullen, J.L. (2002). Thermohaline circulation and prolonged interglacial warmth in the North Atlantic. *Quaternary Research* **58, 17-21.**

Meese, D. A., Alley, R.B., Fiacco, R.J., Germani, M.S., Gow, A.J., Grootes, P.M., Illing, M., Mayewski, P.A., Morrison, M.C., Ram, M., Taylor, K.C., Yang, Q. and Zeilinski, G.A. (1994). Preliminary depth-agescale of the GISP2 ice core. *CRREL Special Report* **94.**

Mienert, J., Abrantes, F., Auffret, G., Evans, D., Kenyon, N., Kuijpers, A., Serjup, H.P., van Weering, T. (1998). European North Atlantic Margin (ENAM I): sediment pathways, processes, and fluxes - an introduction. *Marine geology* **152, 3-6.**

Miller, G. H., Mode, W.N., Wolfe, A.P., Sauer, P.E., Bennike, O., Forman, S.L., Short, S.K., Stafford, T.W. Jr. (1999). Stratified interglacial lacustrine sediments from Baffin Island, Arctic Canada: chronology and paleoenvironmental implications. *Quaternary Science Reviews* **18, 789-810.**

Mitrovica, J. X., Tamislea, M.E., Davis, J.L., Milne, G.A. (2001). recent mass balance of polar ice sheets inferred from patterns of global sea-level change. *Nature* **409, 1026-1029.**

Moller, H. S., Rasch, M., Christiansen, C. (2001). Investigation of a modern glacimarine sedimentary environment in the fjord Kuannsuit Sulluat, Disko, West Greenland. *Geografisk Tidsskrift* **101**, 1-10.

Molina, B., Post, A., Carlson, P.R. (1996). 20th-century glacial-marine sedimentation in Vitus Lake, Bering Glacier, Alaska, USA. *Annals of Glaciology* **22**, 205-210.

Moros, M., Kuijpers, A., Snowball, I., Lassen, S., Bäckström, Gingele, F., McManus, J. (2002). Were glacial iceberg surges in the North Atlantic triggered by climate warming? *Marine geology* **192**, 393-417.

Mudie, P. J., Keen, C.E., Hardy, I.A., Vilks, G. (1984). Multivariate analysis and quantitative paleoecology of benthic foraminifera in surface and late Quaternary shelf sediments, northern Canada. *Marine Micropaleontology* **8**, 283-313.

Murray, J. W. (1991). Ecology and Palaeoecology of Benthic Foraminifera. Harlow: Longman Scientific and Technical.

Myers, R. A., Helbig, J., Holland, D. (1989). Seasonal and interannual variability of the Labrador Current and West Greenland Current. In *Proceedings of the sixteenth Stanstead seminar "High Latitude Climate Processes, with Special Emphasis on Large Scale Air-Sea-Ice interactions"*, vol. CRG Report No. 89-12 (ed. L. A. Mysak), pp. 76-82. Climate Research Group: McGill University Montreal, Quebec.

Myers, R. A., Mertz, G. Helbig, J.A. (1990). Long period changes in the salinity of Labrador Sea Water. *Contribution to Statutory Meeting Hydrographic Committee. International Council for the Exploration of the Sea* **ICES C.M.1990/**, 1-8 plus figures.

Mysak, L. A., Manak, D.K. (1989). Arctic sea ice extent and anomalies, 1953-1984. *Atmosphere and Ocean* **27**, 376-405.

Mysak, L. A., Manak, D.K., Marsden, R.F. (1990). Sea-ice anomalies observed in the Greenland and Labrador Seas during 1901-1984 and their relation to an interdecadal Arctic climate cycle. *Climate Dynamics* **5**, 111-133.

Nagy, J. (1984). Quaternary glaciomarine deposits and foraminifera from Edgeoya, Svalbard. *Boreas* **13**, 319-322.

Nesje, A., Dahl, S.O. (2001). The Greenland 8200 cal yr BP event detected in loss-on-ignition profiles in Norwegian lacustrine sediment sequences. *Journal of Quaternary Science* **16**, 155-166.

Nesje, A., Lie, O., Dahl, S.O. (2000). Is the North Atlantic Oscillation reflected in Scandinavian glacier mass balance records? *Journal of Quaternary Science* **15**, 587-601.

Norden Andersen, O. G. (1981). The annual cycle of phytoplankton primary production and hydrography in the Disko Bugt area, West Greenland. *Meddelelser om Grønland, Bioscience* **6**, 3-67.

Novak, B., Pedersen, G.K. (2000). Sedimentology, seismic facies and stratigraphy of a Holocene spit-platform complex interpreted from high-resolution shallow, seismics, Lysegrund, Southern Kattegat, Denmark. *Marine geology* **162**.

Novak, B., Stoker, M.S. (2001). Late Weichselian glacimarine depositional processes in the Southern Skagerrak revealed by high-resolution seismic facies analysis. *Marine geology* 178, 115-133.

O'Brien, S. R., Twickler, M.S., Whitlow, S.I., Mayewski, P.A., Meeker, L.D., Meese, D.A. (1995). Complexity of Holocene climate as reconstructed from a Greenland ice core. *Science* **270**, 1962-1964.

Ó Cofaigh, C., Dowdeswell, J.A. (2001a). Laminated sediments in glacimarine environments: diagnostic criteria for their interpretation. *Quaternary Science Reviews* **20**, 1411-1436.

Ó Cofaigh, C., Dowdeswell, J.A., Grobe, H. (2001b). Holocene glacimarine sedimentation, inner Scoresby Sund, East Greenland: the influence of fast-flowing ice-sheet outlet glaciers. *Marine geology* **175**, 103-129.

Oeschger, H., Dansgaard, W., Langway C.C., Beer J., Siegenthaler, U., Stauffer, B. (1984). Late glacial climate history from ice cores. In *Climate processes and climate sensitivity*, vol. Geophysical Monograph 29 (ed. J. E. Hansen), pp. 299-306: American Geophysical Union.

Ogha, T., Kitazato, H. (1997). Seasonal changes in Bathyal foraminiferal populations in response to the flux of organic matter (Sagami Bay, Japan). *Terra Nova* 9, 33-37.

Øhlenschlager, R. (2000). Recent foraminiferers fordeling og Sen-Holocaeneklimavariationer fra fjordsystemer i det centrale Vestgronland. In *Geological Institute*, (ed., pp. 128. Aarhus: University of Aarhus.

Osterman, L. E. (1984). Benthic foraminiferal zonation of a glacial/interglacial transition from Frobisher Bay, Baffin Island, N.W.T., Canada. In *Benthos '83. 2nd International Symposium on Benthic Foraminifera*, (ed. H. J. Oertli), pp. 471-476. Pau, France.

Osterman, L. E., Nelson, A.R. (1989). Latest Quaternary and Holocene paleoceanography of the eastern Baffin island continental shelf, Canada: benthic foraminiferal evidence. *Canadian Journal of Earth Sciences* **26**, 2236-2248.

Overpeck, J., Case, R., Douglas, M., Finney, B., Gajewski, K., Jacoby, G., Jennings, A., Lamoureux, S., Lasca, A., MacDonald, G., Moore, J., Retelle, M., Smith, S., Wolfe, A., Zeilinski, G., Hughen, K., Hardy, D., Bradley, R. (1997). Arctic environmental change of the last four centuries. *Science* **278**, 1251-1256.

Patience, A. J., Kroon, D. (1991). Oxygen isotope chronostratigraphy. In *Quaternary Dating Methods - a Users Guide. Quaternary Research Association, Technical Guide, No.4*, (ed. P. D. F. P.L. Smart), pp. 199-228: QRA.

Patterson, R. T., Fishbein, E. (1989). Re-examination of the statistical methods used to determine the number of point counts needed for micropalotological quantitative research. *Journal of Paleontology* **63**, 245-248.

Peacock, J. D. (1989). Marine molluscs and Late Quaternary environmental studies with particular reference to the late-glacial period in northwest Europe: a review. *Quaternary Science Reviews* **8**, 179-192.

Pelto, M. S., Hughes, T.J. (1989). Equilibrium state of Jakobshavns Isbrae, West Greenland. *Annals of Glaciology* **12**, 127-131.

Perry, A. (2000). The North Atlantic Oscillation: an enigmatic see-saw. *Progress in Physical Geography* **24**, 289-294.

Phleger. (1952). Foraminifera distribution in some sediment samples from the Canadian and Greenland Arctic. *Cushman Foundation Special Publication* **3**, 80-89.

Polyak, L., Levitan, M., Gataullin, V., Khusid, T., Mikhailov, V., Mukhina, V. (2000). The impact of glaciation, river-discharge and sea-level change on Late Quaternary environments in the southwestern Kara Sea. *International Journal of Earth Sciences* **89**, 550-562.

Polyak, L., Mikhailov, V. (1996). Post-glacial environments of the southeastern Barents Sea: foraminiferal evidence. In *Late Quaternary paleoceanography of the North Atlantic margins*, vol. 111 (ed. A. J.T. Andrews, W.E.N., Bergsten, H., Jennings, A.E.), pp. 323-337: Geological Society Special Publications.

Polyak, L., Solheim, A. (1994). Late- and post-glacial environments in the northern Barents Sea west of Franz Josef Land. *Polar Research* **13**, 97-207.

Powell, R. D., Dawber, M., McInnes, J.N., Pyne, A.R. (1996). Observations of the grounding-line area at a floating glacier terminus. *Annals of Glaciology* **22**, 217-223.

Prell, W. L., Imbrie, J., Martinson, D.G., Morley, J.J., Pisias, N.G., Shackleton, N.J., Streeter, H.F. (1986). Graphic correlation of oxygen isotope stratigraphy application to the Late Quaternary. *Paleoceanaography* **1**, 137-162.

Prins, M. A., De Jong, A.F.M., Weltje, G.J., Troelstra, S.R., Kruk, R.W., Van der Borg, K. (2001). The late quaternary sedimentary record of Reykjanes Ridge, North Atlantic. *Radiocarbon* **43**, 939-947.

Prinsenberg, S. J., Peterson, I.K., Narayanan, S., Umoh, J.U. (1997). Interaction between atmosphere, ice cover and ocean off Labrador and Newfoundland from 1962 to 1992. *Canadian Journal of Fisheries and Aquatic Science* **54**, 30-39.

Pudsey, C. J. (2000). Sedimentation on the continental rise west of the Antarctic Peninsula over the last three glacial cycles. *Marine geology* **167**, 313-338.

Quinn, R., Bull., J.M., Dix, J.K. (1997a). Buried scour marks as indicators of palaeo-current direction at the *Mary Rose* wreck site. *Marine geology* **140**, 405-413.

Quinn, R., Bull., J.M., Dix, J.K. (1997b). Imaging wooden artefacts using Chirp sources. *Archaeological Prospection* **4**, 25-35.

Rahman, A., de Vernal, A. (1994). Surface oceanographic changes in the eastern Labrador Sea: nannofossil record of the last 31,000. *Marine geology* **121**, 247-263.

Rasch, M. (2000). Holocene relative sea level changes in Disko Bugt, West Greenland. *Journal of Coastal Research* **16**, 306-315.

Rasch, M., Jakobsen, B.H., Nielsen, N. (1997a). Geomorphology and sedimentary record of three cuspate forelands as indicators of late Holocene relative sea-level changes, Disko, West Greenland. *Geografisk Tidsskrift* **97**, 33-46.

Rasch, M., Jensen, J. F. (1997b). Ancient Eskimo dwelling sites and Holocene relative sea-level changes in southern Disko Bugt, central West Greenland. *Polar Research* **16**, 101-115.

Rasch, M., Nielsen, N. (1995). Coastal morpho-stratigraphy and Holocene relative sea level changes at Tuapaat, southeastern Disko Island, central West Greenland. *Polar Research* **14**, 277-289.

Rasmussen, K. L., Rahbek, U. (1996). The 14C reservoir effect in Greenland. In *The Paleo-Eskimo Cultures of Greenland. New Perspectives in Greenlandic Archaeology*, vol. no.1/1996 (ed. B. G. J. Pind), pp. 334. Copenhagen: Danish Polar Center.

Rasmussen, T. L., Kiltgaard-Kristensen, D., Knutz, P.C., Kuijpers, A., Lassen, S., Thomsen, E., Troelstra, S.R., Van Weering, T. C. E., Backstrom, D., Heinemeier, J. (2002a). The Faeroe-Shetland Gateway: Late Quaternary water mass exchange between the Nordic seas and the northeastern Atlantic. *Marine geology* **188**, 165-192.

Rasmussen, T. L., Oppo, D.W., Thomsen, E., Lehman, S.J. (2003). Deep sea records from the southeast Labrador Sea: Ocean circulation changes and ice-rafting events during the last 160,000 years. *Paleoceanography* **18**.

Rasmussen, T. L., Thomsen, E., Troelstra, S.R., Kuijpers, A., Prins, M.A. (2002b). Millennial-scale glacial variability versus Holocene stability: changes in planktic and benthic foraminifera faunas and ocean circulation in the North Atlantic during the last 60, 000 years. *Marine Micropaleontology* **47**, 143-176.

Reeh, N. (1984). Reconstruction of the glacial ice covers of Greenland and the Canadian Arctic islands by three-dimensional perfectly plastic ice- sheet modelling. *Annals of Glaciology* **5**, 115-121.

Reeh, N., Mayer, C., Miller, H., Thomsen, H.H., Weidick, A. (1999). Present and past climate controls on fjord glaciations in Greenland: Implications for IRD-deposition in the sea. *Geophysical Research Letters* **26**, 1039-1042.

Renssen, H., Isarin, R.F.B., Vandenberghe, J., Workshop participants. (2001). Rapid climatic warming at the end of the last glacial: new perspectives. *Global and Planetary Change* **30**, 155-165.

Rignot, E., Thomas, R. (2002). Mass balance of polar ice sheets. *Science* **297**, 1502-1506.

Risebrobakken, B., Jansen, E., Andersson, C., Mjelde, E., Hevroy, K. (2003). A high-resolution study of Holocene paleoclimatic and paleoceanographic changes in the Nordic Seas. *Paleoceanography* **18**.

Rogers, J. C. (1997). North Atlantic storm track variability and its association to the North Atlantic Oscillation and climate variability of Northern Europe. *Journal of Climate* **10**, 1635-1647.

Rohling, E. J., De Rijk, S. (1999). Holocene climate optimum and last glacial maximum in the Mediterranean: The marine oxygen isotope record. *Marine Geology* **153**, 57-75.

Rosell-Mele, A., Jansen, E., Weinelt, M., Samthein, M., Koc, N. (1998). Variability of the Arctic front during the last climatic cycle: Application of a novel molecular proxy. *Terra Nova* **10**, 86-89.

Roussel, A. (1941). Farms and Churches in the Medieval Norse Settlements of Greenland.

Rutberg, R. L., Hemming, S.R., Goldstein, S.L. (2000). Reduced North Atlantic Deep Water flux to the glacial Southern Ocean inferred from neodymium isotope ratios. *Nature* **405**, 935-938.

Ryves, D. B., McGowan, S., Anderson, N.J. (2002). Development and evaluation of a diatom-conductivity model from lakes in West Greenland. *Freshwater Biology* **47**, 995-1014.

Sarnthein, M., Jansen, E., Weinelt, M., Arnold, M., Duplessy, J.C., Erlenkeuser, H., Flatøy, A., Johannessen, G., Johannessen, T., Jung, S., Koç, N., Labeyrie, L., Maslin, M., Pflaumann, U., and Schulz, H. (1995). Variations in Atlantic surface ocean paleoceanography, 50°- 80°N: a time-slice record of the last 30 000 years. *Paleoceanaography* **10**, 1063-1094.

Saxov, S. (1958). The uplift of western Greenland; a preliminary note. *Bulletin of the Geological Society of Denmark* **13**, 518-523.

Schafer, C. T., Cole, F.E. (1982). Living benthic foraminifera distributions on the continental slope and rise east of Newfoundland, Canada. *Geological Society of America* **93**, 207-217.

Schafer, C. T., Cole, F.E. (1986). Reconnaissance survey of benthonic foraminifera from Baffin Fjord environments. *Arctic* **39**, 232-239.

Schmittner, A., Saenko, O.A., Weaver, A.J. (in press). Coupling of the hemispheres in observations and simulations of glacial climate change. *Quaternary Science Reviews*.

Schmittner, A., Stocker, T.F. (1999). The stability of the thermohaline circulation in global warming experiments. *Journal of Climate* **12**, 1117-1133.

Schulte, S., Rullkotter, J., Marchal, O., Rostek, F., Bard, E. (1999). Variations of oxygen-minimum and primary productivity recorded in sediments of the Arabian Sea. *Earth and Planetary Science Letters* **173**, 205-221.

Schulz, M. (2002a). On the 1470-year pacing of Dansgaard-Oeschger warm events. *Paleoceanography* **17**, 4[1]-4[10].

Schulz, M., Paul, A. (2002b). Holocene Climate Variability on Centennial-to-Millennial Time Scales: 1. Climate Records from the North-Atlantic Realm. *Climate Development and History of the North Atlantic realm*, 41-54.

Scott, D. B., Cole, F.E., Mudie, P.J., Baki V., Mackinnon, K.D. (1989). Biostratigraphy and late Cenozoic paleoceanography of the Arctic Ocean: foraminiferal, lithostratigraphic, and isotopic evidence. *Geological Society of America* **101**, 260-277.

Scott, D. B., Mudie, P.J., de Vernal, A., Hillaire-Marcel, C., Baki, V., MacKinnon, K.D., F. S. and Medioli, F. S., Mayer, L. (1989). Lithostratigraphy, biostratigraphy, and stable-isotope stratigraphy of cores from ODP Leg 105 site surveys, Labrador Sea and Baffin Bay. In *Proceedings, scientific results, ODP, Leg 105, Baffin Bay and Labrador Sea,* (ed. S. P. Srivastava), pp. 561-582. Michigan University, College Station; UK distributors, IPOD Committee, NERC, Swindon: ODP, Texas &Aamp.

Scott, D. B., Mudie, P.J., Younger, C.D., Vilks, G. (1984). Late Pleistocene - Holocene paleoceanographic trends on the continental margin of eastern Canada: foraminiferal, dinoflagellates and pollen evidence. *Marine Micropalcontology* **9**, 181-218.

Scott, D. B., Vilks, G. (1991a). Benthic foraminifera in the surface sediments of the deep-sea Arctic Ocean. *Journal of Foraminiferal Research* **21**, 20-38.

Scott, D. B., Vilks, G. (1991b). Benthonic foraminifera in the surface sediments of the deep-sea Arctic Ocean. *Journal of Foraminiferal Research* **21**, 20-38.

Seager, R., Naik, N., Clement, A.C., Cane, M.A., Battisti, D.S., Yin, J., Gordon, N. (2002). Is the Gulf Stream responsible for Europe's mild winters? *Quarterly Journal of the Royal Meteorological Society* **128**, 2563-2586.

Seidenkrantz, M.-S. (1995). *Cassidulina teretis* Tappan and *Cassidulina neoteretis* new species (Foraminifera): Stratigraphic markers for deep sea and outer shelf areas. *Journal of Micropalaeontology* **14**, 145-157.

Seidov, D., Haupt, B. (2003). Freshwater teleconnections and ocean thermohaline circulation. *Geophysical Research Letters* **30**, 621-624.

Sejrup, H. P., Fjaeran, T., Hald, M., Beck, L., Hagen, J., Miljeteig, I., Morvik, I., Norvik, O. (1981). Benthonic foraminifera in surface samples from the Norwegian continental margin between 62 degrees N and 65 degrees N. *Journal of Foraminiferal Research* **11**, 277-293.

Sejrup, H. P., Groslashsfjeld, K., Larsen E., Haflidason, H., Flatebo, T., Kristensen, D.K. (2001). Late-glacial to Holocene environmental changes and climate variability: Evidence from Voldafjorden, Western Norway. *Journal of Quaternary Science* **16**, 181-198.

Sen Gupta, B. K. (1999). Modern Foraminifera. Dordrecht: Kluwer Academic Publishers.

Seramur, K. C., Powell, R.D., Carlson, P.R. (1997). Evaluation of conditions along the grounding line of temperate marine glaciers: an example form Muir Inlet, Glacier Bay, Alaska. *Marine geology* **140**, 307-327.

Severinghaus, J. P., Bender, M.L., Sowers, T., Brook, E.J., Alley, R.B. (1998). Timing of abrupt climate change at the end of the Younger Dryas interval from thermally fractionated gases in polar ice. *Nature* **391**, 141-146.

Shabbar, A., Higuchi, K., Skinner, W., Knox, J.L. (1997). The association between the BWA index and winter surface temperature variability over Eastern Canada and West Greenland. *International Journal of Climatology* **17**, 1195-1210.

Shaw, J., Grant, D.R., Guilbault, J-P., Anderson, T.W., Parrott, D.R. (2000). Submarine and onshore end moraines in Southern Newfoundland: Implications for the history of late Wisconsinan ice retreat. *Boreas* **29**, 295-314.

Short, S. K., Mode, W. N., Davis, P.T. (1985). The Holocene record from Baffin Island: modern and fossil pollen studies. In *Quaternary environments: eastern Canadian Arctic, Baffin Bay, and West Greenland*, (ed. J. T. Andrews), pp. 608-642. London: Allen and Unwin.

Sicre, M.-A., Martinez, P., Bertrand, P., Ternois, Y., Paterne, M. (2001). Climatic changes in the upwelling region off Cap Blanc, NW Africa, over the last 70 kyr: A multi-biomarker approach. *Organic Geochemistry* **32**, 981-990.

Siegert, M. J. (2001). Ice Sheets and Late Quaternary Change. Published by John Wiley & Sons, Chichester, 231pp.

Silis, A. B. (1993). Late Quaternary foraminiferal biostratigraphy of Hudson Strait. *Geological Survey of Canada* **3340**, 1-127.

Sjerup, H.-P., Fjaeran, T., Hald, M., Beck, L., Hagen, J., Miljeteig, I., Morvik. I., Norvik, I. (1981). Benthonic foraminifera in surface samples from the Norwegian continental margin between 62oN and 65oN. *Journal of Foraminiferal Research* **11**, 277-295.

Skene, K. I., Piper, D.J.W. (2003). Late Quaternary stratigraphy of Laurentian Fan: a record of events off the eastern Canadian continental margin during the last deglacial period. *Quaternary International* **99-100**, 135-152.

Smith, I. R. (2002). Diatom-based Holocene paleoenvironmental records from continental sites on northeaster Ellesmere Island, high Arctic, Canada. *Journal of Paleolimnology* **27**, 9-28.

Smith, L. M., Andrews, J.T. (2000). Sediment characteristics in iceberg dominated fjords, Kangerlussuaq region, East Greenland. *Sedimentary Geology* **130**, 11-25.

Sohn, H.-G., Jezek, K.C., van der Veen, C.J. (1998). Jakobshavn Glacier, West Greenland: 30 years of spaceborne observations. *Geophysical Research Letters* **25**, 2699-2702.

Spero, H. J., Bijma, J., Lea, D.W. (1997). Effect of seawater carbonate concentration on foraminiferal carbon and oxygen isotopes. *Nature* **390**, 497-500.

Spooner, I., Douglas, M.S.V., Terrusi, L. (2002). Multiproxy evidence of and early Holocene (8.2kyr) climate oscillation in central Nova Scotia, Canada. *Journal of Quaternary Science* **17**, 639-645.

Stager, J. C., Mayewski, P.A. (1997). Abrupt early to mid-Holocene climatic transition registered at the equator and the poles. *Science* **276**, 1834-1836.

Steffen, K. (1985). Warm water cells in the North Water, northern Baffin Bay during winter. *Journal of Geophysical Research* **90**, 9129-9136.

Steig, E. J., Grootes, P.M. and Stuiver, M. (1994). Seasonal precipitation timing and ice core records. *Science* **266**, 1885-1886.

Stein, M. (1991). Recent variations of salt and heat flow in West Greenland waters. *NAFO scientific Council Studies* **15**, 31-34.

Stein, M. (1993). On the consistency of thermal events in the East Greenland/West Greenland Current system and off Labrador. *NAFO scientific Council Studies* **19**, 7-14.

Stein, M. (1999). Climate conditions around Greenland -1997. *NAFO scientific Council Studies* **32**, 69-74.

Stein, M., Buch, E. (1985). 1983: an unusual year off West Greenland? *Archaeologiske. FischerieWisstiung* **36**, 81-95.

Stein, M., Wegner, G. (1990). Recent thermohaline observations on the deep waters off West Greenland. *NAFO scientific Council Studies* **14**, 29-37.

Steinsund, P. I., Hald, M. (1994). Recent calcium carbonate dissolution in the Barents Sea: paleoceanographic applications. *Marine geology* **117**, 303-316.

Stocker, T. F. (2000). Past and future reorganizations in the climate system. *Quaternary Science Reviews* **19**, 301-319.

Stocker, T. F., Schmittner, A. (1997). Influence of CO_2 emission rates on the stability of the thermohaline circulation. *Nature* **388**, 862-865.

Stoner, J. S., Channell, J.E.T., Hillaire-Marcel, C., Kissel, C. (2000). Geomagnetic paleointensity and environmental record form Labrador Sea core MD95-2024: global marine sediment and ice core chronostratigraphy for the last 110 kyr. *Earth and Planetary Science Letters* **183**, 161-177.

Stuiver, M., Reimer, P.J. (1993). Extended 14C database and revised CALIB 3.0 14C age calibration program. *Radiocarbon* **35**, 215-230.

Stuiver, M., Reimer, P.J., Bard, E., Beck, J.W., Burr, G.S., Hughen, K.A., Kromer, B., McCormac, F.G., can der Plicht, J, Spurk, M. (1998). INTERCAL98 radiocarbon age calibration, 24000-0 cal BP. *Radiocarbon* **40**, 1041-1084.

Stuiver, M., Braziunas, T.F., Grootes, P.M. and Zeilinski, G.A. (1997). Is there evidence for solar forcing of climate in the GISP2 oxygen isotope record? *Quaternary Research* **48**, 259-266.

Stuiver, M., Grootes, P.M. and Braziunas, T.F. (1995). The GISP2 d ^{18}O climate record of the past 16,500 years and the role of the sun, ocean and volcanoes. *Quaternary Research* **44**, 341-354.

Sugden, D. E. (1974). Landscapes of glacial erosion in Greenland and their relationship to ice, topography and bedrock conditions. *Institute of British Geographers* **Special Publication**, 177-195.

Sugden, D. E., Shouchez R.A., Tison, J.L., Knight, P.G., Livesey, N., Lorrain, R.D. (1987). Evidence for two zones of debris entrainment beneath the Greenland ice sheet. *Nature* **328**, 238-241.

Syvitski, J. P. M., Andrews, J.T., Dowdeswell, J.A. (1996). Sediment deposition in an iceberg-dominated glacimarine environment, East Greenland: basin fill implications. *Global and Planetary Change* **12**, 251-270.

Syvitski, J. P. M., Stein, A.B., Andrews, J.T., Milliman, J.D. (2001). Icebergs and the sea floor of the East Greenland (Kangerlussuaq) continental margin. *Arctic, Antarctic and Alpine Research* **33**, 52-61.

Taylor, K. C., Lamorey, G.W., Doyle, G.A., Alley, R.B., Grootes, P.M., Mayewski, P.A., White, J.W.C., Barlow, L.K. (1993). The 'flickering switch' of late Pleistocene climate change. *Nature* **361**, 432-436.

Ten Brink, N. W. (1974a). Glacio-isostasy: new data from West Greenland and geophysical implications. *Bulletin of the Geological Society of America* **85**, 251-264.

Ten Brink, N. W. (1975). Holocene history of the Greenland ice sheet based on radiocarbon dated moraines in west Greenland. *Meddelelser om Gronland* **202**, 44.

Ten Brink, N. W., Weidick, A. (1974b). Greenland Ice Sheet History Since the Last Glaciation. *Quaternary Research* **4**, 429-440.

Thomas, E., Booth, C., Massin, M., Shackleton, N. (1995). Northeastern Atlantic benthic foraminifera during the last 45 000 years: changes in productivity seen from the bottom up. *Paleoceanography* **10**, 545-562.

Thomas, R. H., Kuivinen, K., Csatho, B.M., Gogineni, S., Jezek, K.C. (1998). Thickening of the western part of the Greenland ice sheet. *Journal of Glaciology* **44**, 653-658.

Thompson, K. R., Lazier, J.R.N., Taylor, B. (1986). Wind-forced changes in Labrador Current transport. *Journal of Geophysical Research* **91**, 14261-14268.

Ulbrich, U., Christoph, M. (1999). A shift of the NAO and increasing storm track activity over Europe due to anthropogenic greenhouse gas forcing. *Climate Dynamics* **15**, 551-559.

van der Veen, C. J. (2001). Greenland ice sheet response to external forcing. *Journal of Geophysical Research* **D: Atmospheres 106**, 34047-34058.

Van der Zwaan, G. J., Duijnstee, I.A.P., den Dulk, M., Ernst, S.R., Jannink, N.T., Kouwenhoven, T.J. (1999). Benthic foraminifers: proxies or problems? A review of paleoecological concepts. *Earth Science Reviews* **46**, 213-236.

van Geel, B., Raspopov, O.M., Renssen, H., van der Plicht, J., Dergachev, V.A., Meijer, H.A.J. (1999). The role of solar forcing upon climate change. *Quaternary Science Reviews* **18**, 331-338.

Van Loon, H., Rodgers, J.C. (1978). Van Loon, H., and J. C. Rodgers, The seesaw in winter temperatures between
Greenland and northern Europe, Part I: General description. *Monthly Weather Review* **106**, 296-310.

Van Tatenhove, F. G. M., Van der Meer, J. J. M., Huybrechts, P. (1995). Glacial-geological/geomorphological research in West Greenland used to test an ice-sheet model. *Quaternary Research* **44**, 317-327.

Van Tatenhove, F. G. M., Van der Meer, J. J. M., Koster, E. A. (1996). Implications for deglaciation chronology from new AMS age determinations in central West Greenland. *Quaternary Research* **45**, 245-253.

Van Tright, R., Kerstel, E.R.Th., Meijer, H.A.J. and others. (2002). Measuring stable isotopes of hydrogen and oxygen in ice by means of laser spectrometry: The Bolling transition in the Dye-3 (South Greenland) ice core.

Veum, T., Duplessy J.-C., Jansen, E., Arnold M., Beyer, I. (1992). Water mass exchange between the North Atlantic and the Norwegian Sea during the past 28 000 years. *Nature* **356**, 783-785.

Vilks, G. (1964). Foraminiferal Study of East Bay Mackenzie King Island, District of Franklin, Report 64-4. *Report, Bedford Institute of Oceanography* **64**.

Vilks, G. (1969). Recent foraminifera from the Canadian Arctic. *Micropaleontology* **15**, 35-60.

Vilks, G. (1980). Postglacial basin sedimentation on the Labrador Shelf. *Geological Society of Canada, (paper78-28)*, 1-28.

Vilks, G. (1981). Late Glacial-Postglacial foraminiferal boundary in sediments of eastern Canada. *Geoscience Canada* **8**, 48-55.

Vilks, G. (1989). Ecology of recent Foraminifera on the Canadian continental shelf of the Arctic Ocean. In *The Arctic Seas*, pp. 497-569.

Vilks, G., Deonarine, B. (1988). Labrador shelf benthic foraminifera and stable oxygen isotopes of *Cibicides lobatulus* related to the Labrador Current. *Canadian Journal of Earth Sciences* **25**, 1240-1255.

von Grafenstein, U., Johnsen, S., Erlenkeuser, H., Muller, J., Jouzel, J. (1998). The cold event 8200 years ago recorded in oxygen isotope records in Europe and Greenland. *Climate Dynamics* **14**, 78-81.

Waelbroeck, C., Duplessy, J-C., Michel, E., Labeyrie, L., Paillard, D., Duprat, J. (2001). The timing of the last deglaciation in North Atlantic climate records. *Nature* **412**, 724-727.

Wanner, H., Luterbacher, J., Schmutz, C., Stephenson, D.B., Xoplaki, E., Bronnimann, S., Casty, C., Gyalistras, D. (2001). North Atlantic Oscillation - Concepts and studies. *Surveys in Geophysics* **22**, 321-382.

Warren, C. R. (1991). Terminal environment, topographic control and fluctuations of West Greenland glaciers. *Boreas* **20**, 1-15.

Warren, C. R., Hulton, N.R.J. (1990). Topographic control and glaciological controls on Holocene ice-sheet margin dynamics, central West Greenland. *Annals of Glaciology* **14**, 307-310.

Warrick, R., Oerlemans, J. (1990). Sea Level Rise. In *Climate change: the IPCC scientific assessment*, (ed. H. J.T.), pp. 257-281: Cambridge University Press.

Weidick, A. (1968). Observations on some Holocene glacier fluctuations in West Greenland. *Meddelelser om Grønland* **165**, pp 202.

Weidick, A. (1972). Holocene shore-lines and glacial stages in Greenland; an attempt at correlation. *Rapport - Groenlands Geologiske Undersoegelse* **41**, pp 39.

Weidick, A. (1985). Review of glacier changes in West Greenland. *Zeitschrift fur Gletscherkunde und Glazialgeologie* **21**, 301-309.

Weidick, A. (1992). Jakobshavn Isbrae area during the climatic optimum. *Rapport - Groenlands Geologiske Undersoegelse* **155**, 67-72.

Weidick, A. (1993). Neoglacial change of ice cover and the related response of the Earth's crust in West Greenland. *Rapport Gronlands Geologiske Undersogelse* **159**, 121-126.

Weidick, A. (1996). Neoglacial change of ice cover and sea level in Greenland - A classical enigma. In *The Palaeo-Eskimo Cultures of Greenland: New Perspectives in Greenlandic Archaeology*, (ed. B. Gronnow), pp. 257-270. Copenhagen: Danish Polar Center.

Weidick, A., Andreasen, C., Oerter, H., Reeh, N. (1994). Neoglacial glacier changes around Storstrommen, north-east Greenland. *Polarforschung* **64**, 95-108.

Weidick, A., Thorning, L., Oerter, H., Reeh, N., Thomsen, H.H. (1990). The recession of the Inland Ice margin during the Holocene climatic optimum in the Jakobshavns Isfjord area of West Greenland. *Palaeogeography, Palaeoclimatology, Palaeoecology* **82**, 389-399.

White, J. W. C., Jouzel, J., Johnsen, S.J., Stuiver, M., Clausen, H., Barlow, L.K., Fisher, D., Grootes, P. (1997). The climate signal in the stable isotopes of snow from Summit, Greenland: results of comparisons with modern climate observations. *Journal of Geophysical Research* **102**, 26425-26439.

Willemse, N. W., Koster, E.A., Hooggakker, B., van Tatenhove, F.G.M. (2003). A continuous record of Holocene eolian activity in West Greenland. *Holocene* **13**, 322-334.

Willemse, N. W., Tornqvist, T.E. (1999). Holocene century-scale temperature variability from West Greenland lake records. *Geology* **27**, 580-584.

Williams, K. M., Andrews, J.T., Jennings, A.E., Short, S.K., Mode, W.N., Syvitski, J.P.M. (1995b). The Eastern Canadian Arctic at ca. 6 ka: a time of transition. *Geographie Physique et Quaternaire (Canadian Global Change Issue)* **49**, 13-27.

Williams, K. M., Andrews, J.T., Weiner N.J., Mudie, P.J. (1995a). Late Quaternary paleoceanography of the mid- to outer continental shelf, East Greenland. *Arctic & Alpine Research* **27**, 352-363.

Wollenburg, J. E., Kuhnt, W. (2000). The response of benthic foraminifers to carbon flux and primary production in the Arctic Ocean. *Marine Micropaleontology* **40**.

Wollenburg, J. E., Mackensen, A. (1998a). Living benthic foraminifers from the central Arctic Ocean: Faunal composition, standing stock and diversity. *Marine Micropaleontology* **34**, 153-185.

Wollenburg, J. E., Mackensen, A. (1998b). On the vertical distribution of living (Rose Bengal stained) benthic foraminifera in the Arctic Ocean. *Journal of Foraminiferal Research* **28**, 268-285.

Yoder, J. A., Balch, W.M., Ackleson, S.G., Barber, R.T., Flament, P. (1994). A line in the sea. *Nature* **371**, 689-692.

Yoon, H. I., Han, M.W., Park, B-K., Oh, J-K., Chang, S-K. (1997). Glaciomarine sedimentation and palaeo-glacial setting of Maxwell Bay and its tributary embayment, Marian Cove, South Shetland Islands, West Antarctica. *Marine geology* **140**.

Yoon, H. I., Park, B-H., Kim, Y., Kim, D. (2000). Glaciomarine sedimentation and its paleoceanographic implications along the fjord margins in the South Shetland Islands, Antarctica during the last 6000 years. *Palaeogeography, Palaeoclimatology, Palaeoecology* **157**, 189-211.

Zarudzki, E. F. K. (1979). Interpretation of shallow seismic profiles over the continental shelf in West Greenland between latitudes 64 degrees and 69 degrees 30'N. *Rapport - Groenlands Geologiske Undersoegelse* **100**, 58-61.

Zdanowicz, C. M., Fisher, D.A., Clark, I., Lacelle, D. (2002). An ice-marginal d ^{18}O record from Barnes Ice Cap, Baffin Island, Canada. *Annals of Glaciology* **35**, 145-149.

Zeeberg, G. G., Forman, S.L. (2001). Changes in glacier extent on north Novaya Zemlya in the twentieth century. *Holocene* **11**, 161-175.

Zreda, M., England, J., Phillips, F., Elmore, D., Sharma, P. (1999). Unblocking of the Nares Strait by Greenland and Ellesmere ice-sheet retreat 10,000 years ago. *Nature* **398**, 129-142.

Appendix 1
Species list and reference codes

Species	***Varcode***
Adercotryma glomerata (Brady, 1878)	*aderglom*
Ammpdiscus gullmarensis (Höglund, 1947)	*amogull*
Ammoscalaria pseudospiralis (Williamson, 1858)	*amopseudo*
Astrononion gallowayi (Loeblich and Tappan, 1953)	*astrogal*
Bolivina pseudopunctata (Höglund, 1947)	*bolpseudo*
Buccella frigida (Cushman, 1922)	*bucfrige*
Buccella tenerrima (Bandy, 1950)	*buctener*
Cassidulina laevigata (d'Orbigny, 1826)	*caslaevi*
Cassidulina reniforme (Nørvang, 1945)	*casrenif*
Cassidulina teretis (Tappan, 1951)	*casterit*
Chilostomellina fimbriata (Cushman, 1926)	*chilfim*
Cibicides lobatulus (Walker and Jacob, 1798)	*ciblobat*
Cribostomoides crassimargo (Norman, 1892)	*cribcras*
Cribostomoides jeffreysi (Williamson, 1858)	*cribjeff*
Cuneata arctica (Brady, 1881)	*cunart*
Dentalina advena (Cushman, 1923)	*dentadve*
Dentalina baggi (Galloway & Whistler, 1927)	*dentbagi*
Dentalina frobisherensis (Loeblich & Tappan, 1953)	*dentfrob*
Eggerella advena (Cushman, 1922)	*eggadv*
Elphidium asklundi (Brotzen, 1943)	*elphask*
Elphidium bartletti (Cushman, 1933)	*elphbart*
Elphidium excavatum (Terquem, 1987)	*elphex*
Elphidium excavatum f. clavata (Cushman, 1930)	*elphexfc*
Elphidium incertum (Williamson, 1858)	*elph*
Glonia inaequalis (Reuss, 1930)	*globina*
Haynesina orbiculare (Brady, 1881)	*hancsobi*
Islandiella islandica (Nørvang, 1945)	*islanisl*
Islandiella norcrossi (Cushman, 1933)	*islanorc*
Lagena mollis (Cushman, 1944)	*lagmoll*
Melonis zaandamee (Williamson, 1858)	*melobar*
Neoglobigerina pachyderma (Ehrenberg, 1861)	*npachys*
Nonion auricula (Heron-Allen & Earland, 1930)	*nonauric*
Nonion labradoricum/Nonionellina labradorica	*nonilabr*

(Dawson for the latter, 1860)	
Nonion orbiculare (Brady, 1881)	*nonauric*
Pyrgo williansoni (Sylvestri, 1923)	*pyrgowil*
Quinqueloculina stalkeri (Loeblich & Tappan, 1953)	*quinstak*
Recurvoides turbinatus (Brady, 1881)	*recturb*
Reophax fusiformis (Williamson, 1858)	*reofusi*
Reophax gracilis (Kiar)	*reograci*
Reophax guttifer (Brady, 1881)	*reogutt*
Reophax nana (Rhumbler, 1913)	*reonana*
Reophax pilulifer (Brady, 1884)	*reopilu*
Reophax scorpiurus (Montfort, 1808)	*reoscorp*
Reophax sp.	*reosp*
Saccammina diflugiformis (Brady, 1879)	*sacdifli*
Saccammina subfusiformis (Earland, 1933)	*sacsubfu*
Silicosigmoilina groenlandica (Cushman, 1933)	*silicosi*
Spiroplectammina biformis (Parker & Jones, 1865)	*spirobif*
Stainforthia concava (Höglund, 1947)	*staincon*
Stainforthia feylingi (Knudsen & Seidenkrantz, 1994)	*stainfey*
Textularia earlandi (Parker, 1952)	*texear*
Textularia sagittula (Murray, 1971)	*texsagi*
Textularia torquata (Parker, 1952)	*textorq*
Trifarina fluens (Todd, 1947)	*trifluen*
Trochammina japonica (Ishiwada, 1950)	*trochjap*
Trochammina nana (Brady, 1881)	*trochnana*

Appendix 2: Core DA00-06
Calcareous foraminiferal counts

Sample Depth (cm)	Age (cal yr BP)	buctener	casrenif	casterit	dentfrob	elphex	elphexfc	islanorc	melobarl	nonilabr	staincon	stainfey	trifluen	upachys
2	915.6	4	0	2	0	4	1	12	2	7	1	0	4	0
4	1003.2	6	1	5	0	14	0	17	1	6	2	0	1	0
6	1090.8	2	1	8	0	13	0	18	1	4	1	1	5	0
8	1178.4	9	0	0	0	0	0	0	0	3	0	0	3	0
16	1528.7	0	0	0	0	0	0	0	0	3	0	0	3	0
24	1879.0	11	1	0	0	0	0	9	0	3	0	0	1	1
32	2229.4	14	0	1	2	0	0	18	0	3	0	0	3	0
40	2589.7	4	1	6	0	3	1	32	2	5	0	1	10	0
48	2930.1	1	1	9	0	0	0	60	3	2	0	0	2	0
56	3280.4	10	0	4	0	1	0	46	0	2	0	0	0	0
64	3630.7	7	1	5	0	5	0	48	3	8	1	3	2	0
72	3981.1	1	3	8	0	2	0	53	5	4	4	0	2	0
78	4243.3	13	1	1	0	2	0	37	5	4	0	0	3	0
80	4331.4	10	0	0	0	0	0	10	6	1	0	0	1	0
82	4419.0	9	0	0	5	0	0	0	13	1	0	0	1	0
88	4681.7	7	0	2	0	6	0	18	6	5	3	1	3	0
96	5032.1	1	5	2	0	6	0	25	0	10	0	0	0	0
104	5382.4	4	3	6	0	9	0	20	5	8	0	0	3	0
112	5732.7	2	2	2	0	21	1	21	2	9	2	3	0	0
120	6083.1	0	23	2	0	27	0	16	0	0	0	8	0	0
128	6433.4	0	11	1	0	24	2	13	0	4	4	8	0	1
136	6783.8	0	5	1	0	28	2	21	0	1	6	7	0	0

Appendix 2: Core DA00-06
Calcareous foraminiferal counts

Sample Depth (cm)	Age (cal yr BP)	buctener	casrenif	casterit	dentfrob	elphex	elphexfc	islanore	melobarl	nonilabr	staincon	stainfey	trifluen	npachys
144	7134.1	0	11	3	0	26	3	18	0	3	2	5	0	0
152	7484.4	1	8	2	0	40	1	14	0	2	3	7	0	1
160	7791.7	1	10	1	0	26	4	16	0	3	4	14	0	1
168	7797.5	0	7	0	0	27	5	15	1	0	5	7	0	0
176	7803.3	2	10	5	0	26	2	14	0	2	1	7	0	1
184	7809.1	1	21	3	0	32	2	9	0	3	4	9	0	2
192	7814.9	0	20	1	0	31	1	9	0	1	2	15	0	1
200	7820.7	0	11	2	0	29	2	15	0	4	4	15	0	1
208	7826.4	1	14	0	0	31	4	24	0	6	6	1	0	2
216	7832.2	0	23	2	0	34	2	12	0	0	0	10	0	1
224	7838.0	0	11	3	0	45	1	15	0	1	2	6	0	2
232	7843.8	0	10	1	0	36	1	14	0	1	2	19	0	1
240	7849.6	0	19	2	0	40	1	8	0	1	1	10	0	2
248	7855.4	0	19	1	0	36	2	7	0	1	2	22	0	2
256	7861.2	0	18	1	0	29	3	6	0	0	3	9	0	1
264	7867.0	0	9	0	0	23	1	7	0	1	1	13	0	0
272	7872.8	0	10	0	0	28	2	10	0	0	2	12	0	2
280	7878.6	0	28	1	0	21	2	3	0	1	1	20	0	2
288	7884.4	0	17	0	0	27	0	3	0	2	1	17	0	0
296	7890.2	0	25	1	0	20	0	7	0	1	3	27	0	0
304	7895.9	0	26	1	0	20	0	2	0	0	1	27	0	0
312	7901.7	0	27	0	0	23	0	8	0	2	2	16	0	2

Appendix 2: Core DA00-06
Calcareous foraminiferal counts

Sample Depth (cm)	Age (cal yr BP)	buctener	casrenif	casterit	dentfrob	elphex	elphexfc	islanorc	melobarl	nonilabr	staincon	stainfey	trifluen	npachys
320	7907.5	0	24	. 0	0	19	2	4	0	2	2	23	0	3
328	7913.3	1	27	1	0	17	3	2	0	1	2	21	0	3
336	7919.1	0	23	0	0	26	2	4	0	2	1	25	0	3
344	7924.9	0	20	0	0	13	0	3	0	2	1	43	0	2
352	7930.7	0	19	0	0	13	0	2	0	1	3	41	0	3
360	7936.5	0	16	1	0	13	0	3	0	1	1	41	0	3
368	7942.3	0	14	0	0	11	0	1	0	1	0	53	0	2
376	7948.1	0	14	0	0	13	0	2	0	0	1	56	0	1
384	7953.9	1	39	0	0	28	0	3	0	3	2	7	0	2
392	7959.7	0	23	0	0	33	5	1	0	3	1	22	0	0
400	7965.5	1	21	0	0	27	4	5	0	3	1	25	0	2
408	7971.2	0	33	0	0	36	2	3	0	2	0	18	0	2
416	7977.0	0	21	0	0	29	0	3	0	0	1	37	0	1
424	7982.8	0	16	1	0	27	0	4	0	2	0	35	0	1
432	7988.6	0	16	0	0	32	0	4	0	2	0	30	0	1
440	7994.4	0	20	1	0	26	0	7	0	1	2	27	0	1
448	8000.2	0	19	0	0	17	0	9	0	2	1	34	0	2
456	8006.0	0	21	0	0	24	0	2	0	2	0	29	0	2
464	8011.8	1	22	0	0	20	0	6	0	3	1	33	0	1
482	8017.6	0	19	0	0	21	0	9	0	2	1	37	0	2
480	8023.4	0	21	0	0	19	1	8	0	1	1	29	0	1
488	8029.2	0	19	0	0	20	0	13	0	3	1	29	0	1

Appendix 2: Core DA00-06
Calcareous foraminiferal counts

Sample Depth (cm)	Age (cal yr BP)	buctener	casrenif	casterit	dentfrob	elphex	elphexfc	islanorc	melobarl	nonilabr	staincon	stainfey	trifluen	npachys
496	8035.0	1	23	0	0	21	0	11	0	2	2	23	0	2
504	8040.7	1	23	1	0	18	0	9	0	2	1	28	0	1
512	8046.5	0	19	1	0	20	0	7	0	4	1	30	0	2
520	8052.3	0	13	0	0	22	0	5	0	5	2	38	0	0
528	8058.1	0	13	0	0	29	0	4	0	2	2	28	0	2
536	8063.9	0	18	0	0	31	0	6	0	0	0	32	0	4
544	8069.7	0	9	0	0	41	0	5	0	1	0	33	0	2
552	8075.5	0	8	0	0	19	0	6	0	0	0	57	0	1
560	8081.3	0	18	1	0	25	0	3	1	2	0	34	0	1
568	8087.1	0	18	2	0	16	0	5	0	0	1	43	0	0
576	8092.9	0	24	2	0	15	0	5	0	1	0	33	0	3
584	8098.7	0	15	2	0	17	0	3	0	1	1	42	0	2
592	8104.5	0	20	0	0	12	0	5	0	0	2	48	0	1
600	8110.3	0	17	3	0	21	0	4	0	0	0	37	0	1
608	8116.0	0	19	2	0	8	0	3	0	2	3	49	0	1
616	8121.8	0	24	2	0	7	0	1	0	3	2	46	0	1
624	8127.6	0	14	2	0	8	0	6	0	0	1	37	0	2
632	8133.4	0	28	2	0	16	0	5	0	1	2	35	0	1
640	8139.2	0	33	2	0	15	0	3	0	1	1	33	0	1
648	8145.0	0	21	3	0	15	0	0	0	1	0	24	0	0
656	8150.8	0	21	1	0	23	0	2	0	0	1	43	0	0
664	8156.6	0	28	1	0	25	2	4	0	1	0	32	0	1

Appendix 2: Core DA00-06
Calcareous foraminiferal counts

Sample Depth (cm)	Age (cal yr BP)	buctener	casrenif	casterit	dentfrob	elphex	elphexfc	islanorc	melobarl	nonilabr	staincon	stainfey	trifluen	npachys
672	8162.4	0	29	0	0	31	0	5	0	1	0	24	0	1
680	8168.2	0	23	1	0	19	0	1	0	1	1	44	0	2
688	8174.0	0	27	0	0	20	0	0	0	1	0	43	0	2
696	8179.8	0	29	1	0	15	0	1	0	0	0	41	0	2
704	8185.5	0	25	1	0	15	1	1	0	0	0	46	0	2
712	8191.3	0	26	0	0	18	0	1	0	1	0	36	0	2
720	8197.1	0	31	0	0	21	0	1	0	1	0	32	0	0
728	8202.9	0	29	0	0	17	3	1	0	2	0	37	0	2
736	8208.7	0	34	0	0	15	1	1	0	1	0	37	0	1
744	8214.5	0	34	6	0	14	0	2	0	2	0	24	0	0
752	8220.3	0	35	2	0	14	5	1	0	2	0	26	0	4
760	8226.1	0	34	0	0	21	2	2	0	1	1	24	0	4
768	8231.9	0	44	0	0	22	0	3	0	3	1	22	0	3
776	8237.7	0	21	1	0	15	2	2	0	1	0	49	0	2
784	8243.5	0	27	0	0	34	2	2	0	1	0	27	0	0
792	8249.3	0	25	2	0	15	0	2	0	1	0	41	0	2
800	8255.1	0	29	0	0	13	0	2	0	1	0	45	0	3
808	8260.8	0	32	0	0	19	0	2	0	2	1	37	0	3
816	8266.6	0	27	1	0	16	1	5	0	2	5	23	0	3
824	8272.4	0	21	0	0	21	1	3	0	2	2	38	0	2
832	8278.2	0	25	0	0	19	0	4	0	0	1	36	0	1
840	8284.0	0	35	0	0	26	0	9	0	1	2	19	0	1

Sample Depth (cm)	Age (cal yr BP)	buctener	casrenif	casterit	dentfrob	elphex	elphexfc	islanorc	melobarl	nonilabr	staincon	stainfey	trifluen	npachys
848	8289.8	0	31	0	0	20	0	4	0	1	0	24	0	3
856	8295.6	0	36	1	0	24	0	3	0	1	2	27	0	1
864	8301.4	0	35	0	0	19	0	6	0	3	2	28	0	1
872	8307.2	0	25	0	0	21	0	7	0	1	0	38	0	1
880	8313.0	0	21	2	0	37	7	10	0	1	3	11	0	3
888	8318.8	1	13	1	0	34	3	9	0	1	2	24	0	3
896	8324.6	0	34	0	0	32	0	8	0	1	1	20	0	1
904	8330.3	0	36	0	0	25	2	11	0	0	2	17	0	1
912	8336.1	0	19	0	0	25	2	7	0	0	2	23	0	4
920	8341.9	0	20	0	0	10	0	4	0	0	0	54	0	5
928	8347.7	0	17	3	0	14	1	25	0	0	5	10	0	2
934	8353.5	0	18	0	0	42	0	5	0	1	2	15	0	6
944	8359.3	0	32	0	0	6	0	1	0	0	0	45	0	4

Appendix 2: Core DA00-06
Calcareous foraminiferal counts

Appendix 3: Core DA00-06
Agglutinated foraminiferal counts

Sample Depth (cm)	Age (cal yr BP)	aderglom	amopseud	cribcras	cribjeff	cunart	recturb	reofusi	reograci	reopilu	sacdifli	spirobif	texear	trochjap
2	915.6	11	0	5	1	8	3	1	3	0	1	7	3	4
4	1003.2	1	0	0	6	1	0	1	5	0	10	2	0	10
6	1090.8	13	1	3	6	1	3	5	0	1	5	0	0	5
8	1178.4	3	6	16	0	9	0	9	6	3	25	0	0	0
16	1528.7	11	14	14	0	8	5	0	3	5	27	8	0	0
24	1879.0	4	1	4	1	13	6	4	4	0	21	8	1	0
32	2229.4	1	5	2	0	6	3	5	2	2	26	2	1	0
40	2579.7	1	2	2	3	3	2	2	2	0	12	2	1	0
48	2930.1	5	0	0	0	2	0	2	2	0	4	1	0	0
56	3280.4	2	2	2	0	2	1	1	0	1	18	1	0	0
64	3630.7	0	0	0	0	0	0	0	1	0	4	0	0	0
72	3981.1	1	0	0	2	4	0	0	4	0	0	1	0	0
78	4243.3	4	0	1	2	5	3	2	1	1	8	1	0	0
80	4331.4	8	0	22	0	6	2	3	1	2	9	7	1	2
82	4419.0	4	1	7	3	7	0	5	4	2	23	1	0	0
88	4681.7	4	0	0	1	10	2	3	4	0	3	10	3	0
96	5032.1	14	0	0	2	3	0	0	3	0	4	15	2	5
104	5382.4	6	0	6	0	11	0	0	0	1	1	9	1	0
112	5732.7	8	0	3	0	5	1	0	0	2	2	5	0	0
120	6083.1	4	2	0	0	3	0	0	0	0	0	7	0	0
128	6433.4	6	0	1	0	3	2	0	2	1	0	5	0	0
136	6783.8	9	0	1	0	1	4	0	0	0	0	6	0	1
144	7134.1	6	0	1	1	2	1	1	0	0	1	5	3	1

Appendix 3: Core DA00-06
Agglutinated foraminiferal counts

Sample Depth (cm)	Age (cal yr BP)	aderglom	amopseud	cribcras	cribjeff	cunart	recturb	reofusi	reograci	reopilu	sacdifli	spirobif	texear	trochjap
152	7484.4	3	1	1	2	1	1	0	1	0	0	5	0	0
160	7791.7	2	0	2	0	0	2	0	0	1	0	4	1	0
168	7797.5	2	0	0	0	2	3	0	2	0	0	13	0	0
176	7803.3	5	0	1	0	2	2	0	2	0	0	10	0	0
184	7809.1	2	0	0	0	1	2	0	0	0	1	4	0	0
192	7814.9	2	0	0	0	1	2	0	1	0	0	6	3	1
200	7820.7	1	0	1	0	2	2	0	1	0	1	1	2	0
208	7826.4	1	0	1	0	0	0	0	0	0	0	4	1	0
216	7832.2	1	0	1	0	0	0	0	1	0	0	7	1	1
224	7838.0	3	0	3	1	0	0	0	0	0	0	5	0	0
232	7843.8	2	0	0	0	1	1	0	0	0	0	6	0	0
240	7849.6	1	0	2	0	0	1	0	0	0	0	7	3	1
248	7855.4	1	0	0	0	0	0	0	0	0	0	2	0	0
256	7861.2	2	0	1	0	1	3	0	0	0	0	7	0	0
264	7867.0	3	0	7	0	11	2	0	0	0	0	12	5	0
272	7872.8	1	1	3	0	3	1	0	2	0	0	10	0	1
280	7878.6	0	0	2	0	0	1	0	1	0	0	4	0	0
288	7884.4	2	0	1	0	0	2	0	0	0	0	19	3	0
296	7890.2	0	0	2	0	0	0	0	1	0	0	7	0	0
304	7895.9	0	0	0	0	1	2	0	0	0	0	9	1	0
312	7901.7	0	0	2	0	0	1	0	0	0	0	11	4	1
320	7907.5	0	0	0	0	1	0	0	0	0	0	6	1	0

Appendix 3: Core DA00-06
Agglutinated foraminiferal counts

Sample Depth (cm)	Age (cal yr BP)	aderglom	amopseud	cribcras	cribjeff	cunart	recturb	reofusi	reograci	reopilu	sacdifli	spirobif	texear	trochjap
328	7913.3	0	1	2	0	1	1	0	2	0	0	7	3	0
336	7919.1	0	0	1	0	1	1	0	0	0	0	8	0	1
344	7924.9	0	0	0	0	1	1	0	0	0	0	6	0	0
352	7930.7	0	0	1	0	2	1	0	1	0	0	5	0	1
360	7936.5	1	0	0	0	0	0	0	3	0	0	13	0	0
368	7942.3	0	0	0	0	2	0	0	0	0	0	6	1	0
376	7948.1	0	0	0	0	1	0	0	0	0	0	7	0	0
384	7953.9	0	0	0	1	0	0	0	0	0	0	7	2	0
392	7959.7	0	0	0	0	0	0	0	3	0	0	5	0	0
400	7965.5	0	0	0	0	2	1	0	1	0	0	2	2	0
408	7971.2	0	0	0	0	0	0	0	0	0	0	1	1	0
416	7977.0	0	0	0	0	2	0	0	1	0	0	0	0	0
424	7982.8	0	1	1	0	2	0	0	1	0	0	7	1	1
432	7988.6	1	0	0	0	2	0	0	0	0	0	7	1	1
440	7994.4	0	0	1	0	1	0	0	1	0	0	5	0	1
448	8000.2	0	0	0	1	2	2	0	1	0	0	3	0	0
456	8006.0	0	0	0	0	5	0	0	0	0	0	12	0	0
465	8011.8	1	0	1	0	3	0	0	0	0	0	4	0	0
472	8017.6	1	0	1	0	1	0	0	0	0	0	3	0	0
480	8023.4	1	0	1	0	1	3	0	2	0	0	5	0	0
488	8029.2	0	0	1	0	1	0	0	1	0	0	3	0	0
496	8035.0	1	0	1	0	1	0	0	2	0	0	4	0	0

Appendix 3: Core DA00-06
Agglutinated foraminiferal counts

Sample Depth (cm)	Age (cal yr BP)	aderglom	amopseud	cribcras	cribjeff	cunart	recturb	reofusi	reograci	reopilu	sacdifli	spirobif	texear	trochjap
504	8040.7	1	0	1	0	1	0	0	2	0	0	2	1	1
512	8046.5	1	0	0	1	2	2	0	1	0	0	3	0	0
520	8052.3	0	0	1	0	1	0	0	1	0	1	5	0	0
528	8058.1	1	0	2	0	2	0	0	2	0	1	3	1	0
536	8063.9	0	0	0	0	1	0	0	0	0	0	2	0	0
544	8069.7	0	0	1	0	1	0	0	0	0	0	2	1	0
552	8075.5	0	0	0	0	0	0	0	0	0	0	5	0	0
560	8081.3	0	0	0	0	2	0	0	1	0	0	4	1	2
568	8087.1	0	0	1	0	1	1	0	1	0	0	3	1	0
576	8092.9	0	0	1	0	2	2	0	2	0	1	4	0	0
584	8098.7	1	0	0	0	2	0	0	2	0	0	3	0	1
592	8104.5	0	0	1	0	2	0	0	2	0	0	2	0	0
600	8110.3	0	0	2	0	1	2	0	0	0	0	2	1	1
608	8116.0	0	0	2	0	3	2	0	1	0	0	2	0	1
616	8121.8	0	0	2	0	2	0	0	1	0	0	3	2	0
624	8127.6	3	0	3	1	4	2	0	0	0	1	8	2	0
632	8133.4	1	0	1	0	1	1	0	0	0	0	3	0	0
640	8139.2	0	0	3	0	2	0	0	0	0	0	3	1	0
648	8145.0	3	0	2	0	4	3	0	3	0	0	11	7	0
656	8150.8	0	0	1	0	1	0	0	1	0	0	3	0	0
664	8156.6	0	0	0	0	0	0	0	0	0	0	2	0	0
672	8162.4	0	0	0	0	1	0	0	0	0	0	5	0	0

Appendix 3: Core DA00-06
Agglutinated foraminiferal counts

Sample Depth (cm)	Age (cal yr BP)	aderglom	amopseud	cribcras	cribjeff	cunart	recturb	reofusi	reograci	reopilu	sacdifli	spirobif	texear	trochjap
680	8168.2	0	0	0	0	1	0	0	0	0	0	3	0	0
688	8174.0	0	0	0	0	1	1	0	0	0	0	1	0	0
696	8189.8	0	0	0	0	0	0	0	0	0	0	5	0	1
704	8185.5	0	0	0	0	2	0	0	0	0	0	3	0	0
712	8191.3	0	0	1	0	2	0	0	0	0	0	9	1	0
720	8197.1	0	0	0	0	2	0	0	0	0	0	4	3	0
728	8202.9	0	0	1	0	1	0	0	0	0	0	3	0	0
736	8208.7	0	0	1	0	2	1	0	0	0	0	2	1	0
744	8214.5	2	0	0	0	2	0	0	0	0	0	6	2	0
752	8220.3	0	0	0	0	1	0	0	0	0	0	7	0	0
760	8226.1	1	0	1	0	1	0	0	1	0	0	1	0	0
768	8231.9	1	0	0	0	0	1	0	0	0	0	0	0	0
776	8233.7.7	0	0	0	0	1	0	0	0	0	0	3	0	0
784	8243.5	0	0	0	0	1	0	0	0	0	0	1	1	0
792	8249.3	0	0	0	0	2	0	0	0	0	1	5	0	0
800	8255.1	0	0	0	0	0	0	0	0	0	0	3	0	0
808	8260.8	0	0	0	0	0	0	0	0	0	0	2	0	0
816	8266.6	0	0	0	0	0	2	0	0	0	0	3	0	0
824	8272.4	0	0	0	0	1	0	0	0	0	0	4	0	0
832	8278.2	1	0	0	0	1	0	0	1	0	0	1	0	0
840	8284.0	1	0	0	0	3	0	0	0	0	0	2	0	0
848	8289.8	2	1	2	1	3	2	0	2	0	0	1	0	0

Appendix 3: Core DA00-06
Agglutinated foraminiferal counts

Sample Depth (cm)	Age (cal yr BP)	aderglom	amopseud	cribcras	cribjeff	cunart	recturb	reofusi	reograci	reopilu	sacdifli	spirobif	texear	trochjap
856	8295.6	0	0	0	0	0	0	0	1	0	0	0	0	0
864	8301.4	0	0	0	0	1	0	0	2	0	0	1	0	0
872	8307.2	1	0	2	0	1	1	0	0	0	0	0	1	0
880	8313.0	0	0	0	0	0	0	0	0	0	0	1	0	0
888	8318.8	0	0	2	0	0	1	0	0	0	0	4	0	0
896	8324.6	0	0	0	0	0	0	0	0	0	0	0	0	0
904	8330.3	0	0	1	0	0	0	0	0	0	0	0	0	0
912	8336.1	0	0	0	0	4	0	0	3	0	0	5	0	0
920	8341.9	0	0	0	0	1	0	0	2	0	0	3	0	0
928	8347.7	1	0	2	0	6	0	3	1	0	1	3	1	0
934	8353.5	0	0	0	0	5	0	0	1	0	0	5	0	0
944	8359.3	0	0	0	0	3	0	0	1	0	0	6	0	0

Appendix 4: Core DA00-06
Core foraminiferal analysis data

Sample Depth (cm)	Converted Age (cal yr BP)	% agglu	% calc	total benthic counted	aggul species > 5%	calc species > 5%	% species dominance	% ice proximal species	sediment volume	no forams	foram conc (tests/ml)	testline	% Arctic	% Atlantic
144	7803.3	22	77	261	10	9	26	40	5	262	52	3	47	34
152	7809.1	15	84	300	8	10	40	49	12	300	25	9	60	24
160	7814.9	12	87	300	6	10	26	41	11	300	27	4	55	25
168	7820.7	24	76	221	5	8	27	39	2	221	44	3	53	22
176	7826.4	24	76	302	6	10	26	38	10	302	30	8	53	31
184	7832.2	9	89	307	5	10	32	54	10	307	31	1	65	19
192	7838.0	15	84	300	7	9	31	53	10	300	30	0	73	14
200	7843.8	11	88	298	8	9	29	42	15	298	20	15	56	26
208	7849.6	6	91	139	4	8	31	49	10	139	14	0	50	34
216	7855.4	13	86	271	6	7	34	59	8	271	34	0	73	16
224	7861.2	11	87	158	4	9	45	58	10	158	16	6	68	24
232	7867.0	11	89	273	4	9	36	48	11	273	25	8	72	19
240	7872.8	15	83	307	6	9	40	60	10	307	31	0	77	14
248	7878.6	4	94	281	2	9	36	57	10	281	28	3	79	10
256	8784.4	14	86	266	5	8	29	50	11	266	24	9	63	12
264	7890.2	41	59	91	6	8	23	33	5	91	18	15	57	29
272	7895.9	26	72	145	8	7	28	39	11	145	13	14	59	18
280	7901.7	9	89	296	4	9	28	51	11	296	27	2	74	8
288	7907.5	28	72	162	5	7	27	44	7	162	23	17	81	9
296	7913.3	11	89	301	3	8	27	46	10	301	30	2	79	11
304	7919.1	14	86	302	4	7	28	46	10	302	30	1	82	4
312	7924.9	19	79	215	5	6	27	49	10	215	22	0	76	13

Appendix 4: Core DA00-06
Core foraminiferal analysis data

Sample Depth (cm)	Converted Age (cal yr BP)	% agglu	% calc	total benthic counted	aggul species > 5%	calc species > 5%	% species dominance	% ice proximal species	sediment volume	no forams	foram conc (tests/ml)	testline	% Arctic	% Atlantic
320	7930.7	9	88	300	3	8	24	45	12	300	25	0	73	7
328	7936.5	18	79	300	7	10	27	47	12	300	25	0	72	8
336	7942.3	12	86	282	5	8	27	51	8	272	34	0	82	9
344	7948.1	8	90	300	3	7	43	33	10	300	29	0	82	6
352	7953.9	11	86	301	6	7	41	33	10	301	29	0	78	6
360	7959.7	17	80	76	3	8	41	29	5	76	15	0	83	7
368	7965.5	10	88	280	3	6	53	25	10	280	28	0	84	5
376	7971.2	9	90	304	2	6	56	28	10	304	30	0	90	4
384	7977.0	12	87	238	3	8	40	68	8	238	30	0	82	8
392	7982.8	7	93	176	2	8	23	61	11	176	16	0	82	3
400	7988.6	7	91	299	5	9	27	52	20	299	15	0	76	10
408	7994.4	3	95	280	2	7	36	71	10	280	28	0	88	5
416	8000.2	3	96	298	2	6	37	51	10	298	30	0	88	5
424	8006.0	13	86	304	7	6	35	43	10	304	30	0	85	10
432	8011.8	14	85	206	5	5	32	48	5	206	41	0	84	10
440	8017.6	11	88	305	5	8	27	46	12	305	23	1	77	11
448	8023.4	10	88	300	5	7	34	37	11	300	27	0	73	14
456	8029.2	17	81	42	2	6	29	45	5	42	8	0	86	10
464	8035.0	10	89	301	4	8	33	42	14	301	22	0	79	15
482	8040.7	6	92	297	4	7	37	39	12	297	25	2	79	13
480	8046.5	14	85	145	6	8	29	41	7	145	21	0	74	12
488	8052.3	7	91	278	4	7	29	40	12	278	23	0	72	18

Sample Depth (cm)	Converted Age (cal yr BP)	% agglu	% calc	total benthic counted	aggul species > 5%	calc species > 5%	% species dominance	% ice proximal species	sediment volume	no forams	foram conc (tests/ml)	testline	% Arctic	% Atlantic
496	8058.1	11	87	300	5	8	23	44	14	300	21	1	71	17
504	8063.9	10	89	162	7	9	28	41	10	162	16	0	72	16
512	8069.7	10	88	299	6	8	30	39	13	299	23	0	72	16
520	8075.5	10	89	272	5	7	38	35	10	272	27	2	78	13
528	8081.3	14	84	302	7	7	29	42	10	302	30	0	73	12
536	8087.1	5	91	293	2	5	32	49	14	293	21	1	84	8
544	8092.9	4	94	300	4	6	41	50	11	300	27	0	85	8
552	8098.7	7	923	228	1	5	57	27	5	228	46	0	89	7
560	8104.5	11	88	300	5	8	34	43	12	300	25	0	82	9
568	8110.3	10	90	300	6	7	43	33	11	300	27	0	79	10
576	8116.0	14	83	304	6	7	33	38	10	304	30	0	75	12
584	8121.8	11	87	300	5	8	42	32	11	300	28	0	77	9
592	8127.6	9	90	300	4	6	48	32	12	300	25	0	83	9
600	8133.4	10	89	246	6	6	37	38	10	246	25	0	77	11
608	8139.2	10	89	298	6	8	49	27	14	298	21	0	77	12
616	8145.0	11	88	305	5	7	46	31	15	305	20	0	80	11
624	8150.8	28	70	227	8	6	37	22	10	227	23	0	68	18
632	8156.6	8	91	298	5	8	35	45	16	298	19	0	82	11
640	8162.4	9	89	295	4	7	33	47	15	295	20	0	83	12
648	8168.2	33	67	114	7	6	24	36	5	114	23	0	71	12
656	8174.0	6	94	304	4	7	43	44	10	304	30	0	90	5
664	8179.8	4	95	295	1	8	32	55	12	295	25	0	87	7

Appendix 4: Core DA00-06
Core foraminiferal analysis data

Sample Depth (cm)	Converted Age (cal yr BP)	% agglu	% calc	total benthic counted	aggul species > 5%	calc species > 5%	% species dominance	% ice proximal species	sediment volume	no forams	foram conc (tests/ml)	testline	% Arctic	% Atlantic
672	8185.5	7	92	236	2	5	31	60	10	236	24	0	89	8
680	8191.3	5	93	296	2	8	44	42	14	296	21	0	89	4
688	8197.1	4	95	604	3	4	43	47	13	304	23	2	92	2
696	8202.9	8	90	215	2	5	41	44	10	215	22	0	90	5
704	8208.7	6	92	305	2	7	46	41	12	305	25	0	89	5
712	8214.5	13	85	304	4	5	36	44	15	304	20	0	88	6
720	8220.3	10	89	208	3	6	32	51	10	208	21	0	87	5
728	8226.1	5	93	298	3	7	37	50	14	298	22	2	86	4
736	8231.9	6	92	300	5	7	37	50	14	300	21	0	87	5
744	8237.7	14	86	50	4	7	34	48	5	50	10	0	78	14
752	8243.5	9	86	96	2	7	35	54	11	96	9	0	82	6
760	8249.3	4	92	164	5	7	34	57	12	164	14	0	80	5
768	8255.1	3	95	79	2	6	44	66	10	79	8	0	87	6
776	8260.8	4	95	266	2	8	49	38	14	266	19	0	88	5
784	8266.6	3	97	300	3	7	34	63	11	300	27	1	89	4
792	8272.4	8	90	132	3	6	41	40	10	132	13	0	86	8
800	8278.2	4	93	287	1	6	45	42	15	287	19	0	90	5
808	8284.0	3	94	218	1	6	37	50	10	218	22	0	89	5
816	8289.8	7	90	92	2	9	27	45	5	92	18	0	70	9
824	8295.6	5	92	219	2	8	38	43	10	219	22	0	84	6
832	8301.4	6	93	294	4	6	36	45	12	294	25	0	82	8
840	8307.2	6	93	120	3	6	35	61	5	120	24	0	82	13

Sample Depth (cm)	Converted Age (cal yr BP)	% agglu	% calc	total benthic counted	aggul species > 5%	calc species > 5%	% species dominance	% ice proximal species	sediment volume	no forams	foram conc (tests/ml)	testline	% Arctic	% Atlantic
848	8313.0	13	84	187	8	5	31	51	11	187	17	0	75	11
856	8318.8	2	97	300	1	8	36	60	14	300	21	0	87	5
864	8324.6	5	95	111	3	7	35	54	5	111	22	0	83	10
872	8330.3	6	94	304	5	6	39	46	14	304	22	0	85	12
880	8336.1	3	94	252	1	9	37	65	14	252	18	0	70	14
888	8341.9	8	89	143	3	9	34	50	5	143	29	0	76	14
896	8347.7	2	97	300	0	7	34	66	15	300	20	0	86	9
904	8353.5	3	96	215	1	7	36	64	11	215	20	0	78	13
912	8359.3	14	82	166	3	6	25	46	5	166	33	0	72	10
920	8365.1	7	88	228	3	4	54	30	14	228	16	0	87	5
928	8370.9	23	76	270	8	7	25	32	14	270	19	0	44	38
934	8376.7	10	84	106	3	6	43	60	5	106	21	0	80	10
944	8382.5	10	86	69	3	5	45	38	10	69	7	0	88	4

Appendix 4: Core DA00-06
Core foraminiferal analysis data

Appendix 5: Core DA00-06
Individual species test counts for isotope analysis

DA/06 Sample No.	no of N. lab tests	no of C. ren. tests	no of L. nor. tests
2			
8			
16			
24			
32			45
40	8		40
48			30
56	4		45
64	19		100
72			20
78		25	
80		11	
88	6	28	
96			
104	5	20	
112	22	55	
120		6	20
128	10	50	23
136		40	10
144			32
152	7	45	18
160		40	20
168			29
176	5	60	22
184	6	50	45
192		22	7
200	9	26	43
208	9	17	33
216		27	17
224	2	16	22
232	5	22	30
240		35	13
248		45	25
256		11	14
264			
272			
280		75	11
288		12	
296		70	21
304		90	7
312		35	6
320	6	80	9
328	4	60	9
336		35	8
344	5	38	11
352		60	8
360			
368	5	40	7
376		40	6
384		20	
392	5	35	
400	10	45	14
408		25	6
416		50	9
424	6	40	12
432		15	
440	3	50	23
448	6	45	25
456			
464	8	47	17
472	4	37	21
480			
488	8	30	30
496		45	36
504		10	17
512	11	55	23
520	7	50	12
528		7	6
536		45	19
544		22	14

Appendix 5: Core DA00-06
Individual species test counts for isotope analysis

552			9
560	5	70	16
568		45	18
576		30	12
584	4	70	19
592		60	22
600		15	5 (not used)
608	7	80	12
616	12	90	
624		15	11
632	5	90	18
640		80	10
648		16	
656		80	13
664		75	13
672		40	11
680		60	6
688		80	
696		30	
704		70	
712		65	
720		35	
728		60	
736		70	
744			
752		32	
760		55	
768		18	
776		50	
784		65	
792		15	
800		70	7
808		50	
816		7	
824		40	
832		60	12
840			
848		30	10
856		130	27
864		2 (not used)	5 (not used)
872		110	34
880		30	32
888		9	15
896		90	36
904		70	20
912		4 (not used)	5 (not used)
920		40	9
928		30	45
936		20 (934 s.n)	
944		22	

Appendix 6: DA00-06
Individual species isotope data

Depth (cm)	Converted Age (cal yr BP)	$\delta^{13}C$ PDB N. lab	$\delta^{13}C$ PDB C. ren	$\delta^{13}C$ PDB I. nor
32	2229.4			-0.17
40	2579.7	-1.17		-0.16
48	2930.1			
56	3280.4	-2.23		-0.20
64	3630.7	-0.76		-0.32
72	3981.1			
88	4681.7	-1.45		-0.56
104	5382.4	-2.15		-0.86
112	5732.7	-1.53		-0.65
120	6083.1			
128	6433.4	-1.63	-1.62	-0.88
136	6783.8		TS	-1.21
144	7134.1			
152	7484.4	-1.85	-1.15	-0.61
160	7791.7		TS	-0.65
168	7797.5	-0.64		
176	7803.3	-1.23	-0.66	-0.48
184	7809.1		-1.13	-0.50
192	7814.9	-1.45		
200	7820.7	-1.38	-1.37	-0.58
208	7826.4		-1.15	-0.55
216	7832.2	TS		
224	7838.0	-1.97	-1.33	-0.72
232	7843.8		-1.38	-0.74
248	7855.4		-1.35	-0.81
240	7849.6			
256	7861.2		-1.19	-0.75
272	7872.8		TS	-0.97
280	7878.6		-1.36	LOST
288	7884.4			
296	7890.2		-1.46	-1.08
304	7896.0		-1.58	-1.31
312	7901.7			
320	7907.5	-2.10	-1.51	-0.95
328	7913.3	-1.70	-1.46	-1.36
336	7919.1			
344	7924.9	-1.46	-1.74	-1.26
352	7930.7		-1.75	-1.31
368	7942.3	TS	-2.06	-1.69
376	7948.1		-1.71	-1.93
384	7953.9			
392	7959.7	-2.29	-2.19	
400	7965.5	-2.15	-1.72	-1.11
408	7971.2			
416	7977.0		-1.71	-1.52
424	7982.8	-2.16	-1.46	-1.45
432	7988.6			
440	7994.4	-3.38	-1.94	-1.45
448	8000.2	-2.79	-1.96	-1.24
464	8011.8	-2.15	-2.02	-1.49
472	8017.6	-1.70	-1.67	-1.15
480	8023.4			
488	8029.2	-2.46	-2.15	-1.31
496	8035.0		-2.04	-1.58
504	8040.8			
512	8046.5	-2.56	-1.99	-1.63
520	8052.3	-3.21	-2.68	-2.22
528	8058.1			
536	8063.9		-1.66	-1.39
544	8069.7		TS	-1.69
552	8081.3			
560	8087.1	-3.40	-1.59	-1.21

Depth (cm)	Converted Age (cal yr BP)	$\delta^{18}O$ PDB N. lab	$\delta^{18}O$ PDB C. ren	$\delta^{18}O$ PDB I. nor
32	2229.4			2.81
40	2579.7	2.89		2.96
48	2930.1			2.61
56	3280.4	-0.87		3.20
64	3630.7	3.20		3.21
72	3981.1			2.88
88	4681.7	3.08		3.31
104	5382.4	3.23		2.91
112	5732.7	3.61		3.42
120	6083.1			1.90
128	6433.4	3.35	2.26	2.98
136	6783.8		TS	3.00
144	7134.1			2.98
152	7484.4	2.79	2.89	6.50
160	7791.7		TS	3.24
168	7797.5			3.15
176	7803.3	3.29	3.01	3.57
184	7809.1	3.47	3.29	3.54
192	7814.9		1.13	2.62
200	7820.7	3.57	2.90	3.57
208	7826.4	3.70	3.06	3.77
216	7832.2		-0.05	3.00
224	7838.0	TS	2.54	3.49
232	7843.8	3.36	3.07	3.32
248	7855.4		3.26	3.51
240	7849.6		1.74	2.87
256	7861.2		3.08	3.45
272	7872.8		TS	3.23
280	7878.6		3.39	LOST
288	7884.4		-0.41	
296	7890.2		3.33	3.51
304	7896.0		3.43	3.32
312	7901.7		1.52	2.75
320	7907.5	2.85	3.11	3.43
328	7913.3	2.71	3.15	3.11
336	7919.1		1.80	2.86
344	7924.9	2.21	2.84	3.08
352	7930.7		2.91	2.56
368	7942.3	TS	2.57	2.43
376	7948.1		2.73	2.14
384	7953.9		1.34	
392	7959.7	2.71	2.34	
400	7965.5	3.30	3.04	3.35
408	7971.2		1.54	2.82
416	7977.0		2.97	0.48
424	7982.8	2.41	3.11	3.13
432	7988.6		0.95	
440	7994.4	1.09	2.84	3.22
448	8000.2	2.61	2.81	3.20
464	8011.8	3.07	2.65	3.02
472	8017.6	3.15	3.26	3.40
480	8023.4		-0.20	2.96
488	8029.2	2.96	2.51	3.36
496	8035.0		2.81	3.36
504	8040.8			3.21
512	8046.5	2.41	2.70	3.01
520	8052.3	2.20	1.89	2.21
528	8058.1			1.84
536	8063.9		2.87	3.10
544	8069.7		TS	2.57
552	8081.3			1.62
560	8087.1	1.41	3.25	3.48

Appendix 6: DA00-06
Individual species isotope data

Depth (cm)	Converted Age (cal yr BP)	$\delta^{13}C$ PDB N. lab	$\delta^{13}C$ PDB C. ren	$\delta^{13}C$ PDB I. nor
568	8087.1		-1.52	-1.00
576	8092.9			
584	8098.7	-2.56	-1.59	-1.31
592	8104.5		-2.04	-1.65
600	8110.3			
608	8116.0	-3.66	-1.90	-2.12
616	8121.8	-3.98	-2.26	
624	8127.6			
632	8133.4	-3.76	-1.94	-1.25
640	8139.2		-2.04	-1.55
648	8145.0			
656	8150.8		-1.68	-1.65
664	8156.6		-1.91	-1.60
672	8162.4			
680	8168.2		-1.60	-1.35
688	8174.0		-1.49	
696	8179.8			
704	8185.6		-1.42	
712	8191.3		-1.51	
720	8197.1			
728	8202.9		-1.49	
736	8208.7		-1.37	
752	8220.3		-1.70	
760	8226.1		-1.79	
768	8231.9			
774	8236.2		-1.55	
784	8243.5		-1.87	
782	8249.3			
800	8255.1		-1.75	-2.50
808	8260.8		-1.41	
816	8266.6			
824	8272.4		-2.50	
832	8278.2		-2.18	-2.24
848	8289.8		-2.78	-1.61
856	8259.6		-1.76	-1.64
872	9307.2		-2.20	-1.66
880	8313.0		-2.67	-1.53
888	8318.8			
896	8324.6		-2.05	-1.77
904	8330.4		-2.43	-1.99
920	8341.9		-2.65	-3.33
928	8347.7		-1.93	-1.53
934	8352.1			
944	8359.3		-1.72	

Depth (cm)	Converted Age (cal yr BP)	$\delta^{18}O$ PDB N. lab	$\delta^{18}O$ PDB C. ren	$\delta^{18}O$ PDB I. nor
568	8087.1		3.26	3.63
576	8092.9		1.40	2.98
584	8098.7	3.24	3.24	3.66
592	8104.5		2.96	3.50
600	8110.3		-0.55	
608	8116.0	3.49	3.32	3.24
616	8121.8	3.54	3.20	
624	8127.6		1.31	3.07
632	8133.4	3.01	3.26	3.42
640	8139.2		3.21	3.16
648	8145.0		1.22	
656	8150.8		3.16	3.08
664	8156.6		2.92	2.99
672	8162.4		2.20	1.76
680	8168.2		3.51	2.89
688	8174.0		3.52	
696	8179.8		-0.26	
704	8185.6		3.54	
712	8191.3		3.55	
720	8197.1		2.48	
728	8202.9		3.53	
736	8208.7		3.57	
752	8220.3		3.14	
760	8226.1		3.26	
768	8231.9		1.86	
774	8236.2		3.37	
784	8243.5		3.39	
782	8249.3		1.16	
800	8255.1		3.38	1.93
808	8260.8		2.59	
816	8266.6		-1.78	
824	8272.4		2.48	
832	8278.2		2.98	2.72
848	8289.8		2.27	0.58
856	8259.6		3.18	3.37
872	9307.2		3.14	3.30
880	8313.0		2.56	3.46
888	8318.8		-0.70	2.74
896	8324.6		3.12	3.13
904	8330.4		2.64	2.52
920	8341.9		1.81	1.58
928	8347.7		2.21	3.58
934	8352.1		1.12	
944	8359.3		1.91	

Appendix 7: Core DA00-06
Composite isotope data

Depth (cm)	Converted Age (cal yr BP)	Composite d13C ratio
32	2229.4	-0.17
40	2579.7	-0.67
56	3280.4	-1.21
64	3630.7	-0.54
88	4681.7	-1.00
104	5382.4	-1.50
112	5832.7	-1.09
218	6433.4	-1.38
136	6782.8	-1.21
152	7685.5	-1.43
160	7791.7	-0.65
176	7803.3	-0.59
184	7809.1	-0.98
200	7820.7	-1.16
208	7826.4	-1.10
232	7843.8	-1.56
248	7855.4	-1.08
256	7861.2	-0.97
272	7872.8	-0.48
280	7878.6	-1.36
296	7890.2	-1.27
304	7895.9	-1.45
320	7907.5	-1.52
328	7913.3	-1.51
344	7924.9	-1.49
352	7930.7	-1.53
368	7942.3	-1.87
376	7948.4	-1.82
392	7959.7	-2.24
400	7965.5	-1.66
416	7977.0	-1.62
424	7982.8	-1.69
440	7994.4	-2.26
448	8000.2	-2.00
464	8011.8	-1.89
472	8017.6	-1.80
488	8029.2	-1.97
496	8035.0	-1.81
512	8046.5	-2.06
520	8052.3	-2.70
536	8063.9	-1.53
544	8069.7	-1.69
560	8081.3	-2.06
568	8087.1	-1.26
584	8098.7	-1.82
592	8104.5	-1.84
608	8116.0	-2.56
616	8121.8	-3.12
632	8133.4	-2.32
640	8139.2	-1.80
656	8150.8	-1.67
664	8156.6	-1.75
680	8168.2	-1.47
688	8174.0	-1.49
704	8185.5	-1.42
712	8191.3	-1.51
728	8202.9	-1.49
736	8208.7	-1.37
752	8220.3	-1.70
760	8226.1	-1.79
774	8237.7	-1.55
784	8243.5	-1.87
800	8255.1	-2.12
808	8260.8	-1.41
824	8272.4	-2.50
832	8278.2	-2.21
848	8789.8	-2.19
856	8295.6	-1.70
872	8307.2	-1.93
880	8313.0	-2.10
896	8324.6	-1.91
904	8330.3	-2.21
920	8341.9	-2.99
928	8347.7	-1.73
944	8359.3	-1.72

Appendix 7: Core DA00-06
Composite isotope data

Depth (cm)	Converted Age (cal yr BP)	Composite d18O ratio
32	2229.4	2.81
40	2579.7	2.93
48	2930.1	2.61
56	3280.4	1.17
64	3630.7	3.21
72	3981.1	2.88
88	4681.7	3.20
104	5382.4	3.07
112	5732.7	3.52
120	6083.1	1.90
128	6433.4	2.86
136	6783.8	3.00
144	7134.1	2.98
152	7484.4	3.06
160	7791.7	3.24
168	7797.5	3.15
176	7803.3	3.29
184	7809.1	3.43
192	7814.9	2.62
200	7820.7	3.35
208	7826.4	3.51
216	7832.2	3.00
224	7838.0	3.19
232	7843.8	3.25
240	7849.6	3.38
248	7855.4	2.87
256	7861.2	3.27
272	7872.8	3.23
280	7878.6	3.39
296	7890.2	3.42
304	7895.9	3.37
312	7901.7	2.75
320	7907.5	3.13
328	7913.3	2.99
336	7919.1	2.86
344	7924.9	2.71
352	7930.7	2.74
368	7942.3	2.50
376	7948.1	2.43
392	7959.7	2.53
400	7965.5	3.23
408	7971.2	2.82
416	7977.0	2.97
424	7982.8	2.88
440	7994.4	2.38
448	8000.2	2.87
464	8011.8	2.91
472	8017.6	3.27
480	8023.4	2.96
488	8029.2	2.94
496	8035.0	3.08
504	8040.7	3.21
512	8046.5	2.71
520	8052.3	2.10
528	8058.1	1.84
536	8063.9	2.98
544	8069.7	2.57
552	8075.5	1.62
560	8081.3	2.71
568	8087.1	3.44
576	8092.9	2.98
584	8098.7	3.38
592	8104.5	3.23
608	8116.0	3.35
616	8121.8	3.37
624	8127.6	3.07
632	8133.4	3.23
640	8139.2	3.19
656	8150.8	3.12
664	8156.6	2.95

680	8168.2	3.20
688	8174.0	3.52
704	8185.5	3.54
712	8191.3	3.55
728	8202.9	3.53
736	8208.7	3.57
752	8220.3	3.14
760	8226.1	3.26
774	8231.9	3.37
784	8237.7	3.39
800	8243.5	2.65
808	8260.8	2.59
824	8272.4	2.48
832	8278.2	2.85
856	8295.6	3.27
872	8307.2	3.22
880	8313.0	3.01
888	8318.8	2.74
896	8324.6	3.12
904	8330.3	2.58
920	8341.9	1.69
928	8347.7	2.89
944	8359.3	1.91

Appendix 8: Core DA00-05
Calcareous foraminiferal counts

Sample Depth (cm)	Converted Age (cal yr BP)	bolpseud	buctener	casrenif	casterit	elphex	elphexfc	globina	islanorc	melobarl	nonilabr	staincon	npachys
10	1302.4	0	0	0	0	0	0	0	0	0	0	0	0
20	1330.8	0	0	0	0	0	0	0	0	0	0	0	0
30	1359.2	0	0	0	0	0	0	0	0	0	0	0	0
41	1390.4	0	0	0	0	0	0	0	0	0	0	0	0
51	1418.8	0	0	0	0	0	0	0	0	0	0	0	0
60	14444	0	0	0	0	0	0	0	0	0	0	0	0
70	147.28	0	0	0	0	0	0	0	0	0	0	0	0
80	1501.2	0	0	0	0	0	0	0	0	0	0	0	0
90	1529.6	0	0	0	0	0	0	0	0	0	0	0	0
100	1558.0	0	0	0	0	0	0	0	0	0	0	0	0
110	1586.4	0	0	0	0	0	0	0	0	0	0	0	0
120	1678.4	0	0	0	0	0	0	0	0	0	0	0	0
130	1770.4	0	0	0	0	0	0	0	4	0	0	0	0
140	1862.4	0	0	0	0	0	0	0	0	0	0	0	0
151	1963.6	0	0	0	0	0	0	0	0	0	0	0	0
160	2046.4	0	0	0	0	0	0	0	0	0	0	0	0
171	2147.6	0	0	0	0	0	0	0	0	0	0	0	0
180	2230.4	0	0	0	0	0	0	0	0	0	0	0	0
190	2322.4	0	0	0	0	0	0	0	0	0	0	0	0
211	2515.6	0	0	0	0	0	0	0	0	0	0	0	0
220	2598.4	0	0	0	0	0	0	0	0	0	0	0	0
240	2782.4	0	0	0	0	0	0	0	0	0	0	0	0

Appendix 8: Core DA00-05
Calcareous foraminiferal counts

Sample Depth (cm)	Converted Age (cal yr BP)	bolpseud	buctener	casrenif	casterit	elphex	elphexfc	globina	islanorc	melobarl	nonilabr	staincon	npachys
260	2966.4	0	0	0	0	0	0	0	0	0	0	0	0
280	3105.8	0	0	0	0	0	0	0	0	0	0	0	0
300	3245.2	0	0	0	0	0	0	0	0	0	0	0	0
320	3384.6	0	0	0	0	0	0	0	0	0	0	0	0
340	3474.7	0	0	0	0	0	0	0	0	0	0	0	0
360	3538.3	0	0	0	0	0	0	0	0	0	0	0	0
380	3601.9	0	0	0	0	0	0	0	0	0	0	0	0
400	3665.5	0	0	0	0	0	0	0	0	0	0	0	0
410	3697.3	0	0	0	0	0	0	0	0	0	0	0	0
420	3729.1	0	0	0	0	0	0	0	0	0	0	0	0
430	3760.9	0	0	0	0	0	0	0	0	0	0	0	0
440	3792.7	0	9	3	0	9	0	2	30	0	5	2	0
450	38254.5	0	0	0	0	0	0	0	0	0	0	0	0
460	3856.3	0	0	0	0	0	0	0	0	0	0	0	0
470	3888.1	0	0	0	0	0	0	0	0	0	0	0	0
480	3919.9	0	0	0	0	0	0	0	0	0	0	0	0
490	3951.7	0	0	0	0	0	0	0	0	0	0	0	0
500	3983.5	0	0	0	0	0	0	0	0	0	0	0	0
510	4015.3	0	0	0	0	0	0	0	0	0	0	0	0
520	4047.1	0	0	0	0	0	0	0	0	0	0	0	0
530	4078.9	0	0	0	0	0	0	0	0	0	0	0	0
540	4110.7	0	0	0	0	0	0	0	0	0	0	0	0

Appendix 8: Core DA00-05
Calcareous foraminiferal counts

Sample Depth (cm)	Converted Age (cal yr BP)	bolpseud	buctener	casrenif	casterit	elphex	elphexfc	globina	islanorc	melobarl	nonilabr	staincon	npachys
550	4142.5	0	0	3	0	8	2	4	34	0	11	3	0
560	4174.3	21	5	4	0	14	5	5	9	3	11	0	0
570	4206.1	0	4	0	0	4	0	0	28	0	4	0	0
580	4237.9	0	0	0	0	5	0	13	32	0	6	0	1
590	4269.7	0	0	0	0	0	0	6	56	0	3	0	0
600	4332.7	0	0	0	0	0	0	5	38	0	3	0	1
610	4395.7	14	0	6	0	9	0	3	19	0	7	3	0
620	4458.7	0	2	0	0	12	0	0	31	0	16	0	0
630	4521.7	3	0	7	0	12	3	2	17	0	7	0	0
640	4584.7	12	4	0	0	0	0	0	26	0	6	5	0
650	4647.7	4	2	4	0	12	3	4	20	0	17	5	0
660	4710.7	0	5	0	0	16	0	2	0	0	14	4	0
670	4773.7	0	0	0	0	0	0	0	19	0	0	0	0
680	4836.7	0	0	6	0	15	0	3	25	0	10	2	0
690	4899.7	0	3	0	0	0	0	0	0	3	0	0	0
700	4962.7	0	0	0	0	0	0	0	0	0	0	0	0
710	5025.7	5	0	6	4	10	0	0	40	0	9	5	0
720	5088.7	0	0	11	3	14	4	4	40	0	7	3	0
730	5151.7	0	4	0	0	7	0	0	17	0	4	0	0
740	5214.7	0	11	0	6	4	1	3	47	0	4	3	0
750	5277.7	0	0	0	0	0	0	0	0	0	0	0	0
760	5340.7	0	5	0	0	2	0	0	56	0	3	0	2

Appendix 8: Core DA00-05
Calcareous foraminiferal counts

Sample Depth (cm)	Converted Age (cal yr BP)	bolpseud	buctener	casrenif	casterit	elphex	elphexfc	globina	islanorc	melobarl	nonilabr	staincon	npachys
770	5340.7	0	0	5	0	12	0	0	29	0	7	7	0
780	5403.7	0	0	0	0	0	0	0	3	0	0	0	0
790	5466.7	0	3	0	0	0	0	0	0	0	0	0	0
800	5529.7	0	4	6	2	16	0	0	44	0	3	3	1
810	5655.7	0	0	0	0	18	0	0	0	0	0	0	0
820	5707.9	0	23	0	0	0	0	0	0	0	0	0	9
830	5760.1	7	0	6	3	11	0	0	25	0	11	4	0
840	5812.3	0	0	11	0	16	0	0	36	0	13	5	0
850	5864.5	0	5	0	0	4	0	0	29	3	0	0	0
860	5916.7	0	0	0	0	0	0	0	0	0	0	0	0
870	5968.9	0	0	0	0	0	0	0	0	0	0	0	0
880	6021.1	0	4	3	0	0	0	2	58	6	6	0	0
890	6073.3	0	7	0	0	5	0	5	53	0	0	0	1
900	6125.5	14	0	9	0	11	0	2	14	0	12	2	0
910	6177.7	13	0	6	0	13	0	0	22	0	9	3	0
920	6229.9	0	0	0	0	17	0	0	14	0	8	0	0
930	6282.1	7	4	0	3	10	0	0	35	0	5	3	0
940	6334.4	0	0	0	4	0	0	0	35	0	2	0	0
950	6386.5	0	0	0	0	0	0	0	0	0	0	0	0
960	8438.7	0	0	0	0	12	0	0	4	0	4	0	0
970	6490.9	0	0	0	0	3	0	3	70	0	2	0	0
980	6543.1	0	3	0	0	0	0	13	54	0	2	4	0

Appendix 8: Core DA00-05
Calcareous foraminiferal counts

Sample Depth (cm)	Converted Age (cal yr BP)	bolpseud	buctener	casrenif	casterit	elphex	elphexfc	globina	islanorc	melobarl	nonilabr	staincon	npachys
990	6595.3	0	5	0	0	4	0	11	56	3	0	0	0
1000	6647.5	0	2	3	0	17	0	0	39	4	7	7	0
1010	6699.7	0	2	0	2	10	0	0	41	0	4	3	0
1020	6751.7	13	0	8	2	5	0	0	22	0	3	2	0
1030	6804.1	7	0	10	0	11	0	0	8	0	6	4	0

Appendix 9: Core DA00-05
Agglutinated foraminiferal counts

Sample Depth (cm)	Converted Age (cal yr BP)	aderglom	amopseud	cribcras	cunart	recturb	reofusi	reograci	reopilu	sacdifli	spiribif	tecear	textorq	trochjap	trochan
10	1302.4	34	0	2	7	0	6	8	0	7	5	7	9	6	2
20	1330.8	21	0	3	25	0	4	12	0	5	6	4	9	0	3
30	1359.2	18	0	0	15	0	0	30	1	0	8	0	18	0	0
41	1390.4	28	0	0	17	2	2	22	0	14	3	0	6	0	0
51	1418.8	15	0	0	18	0	0	34	3	10	0	0	10	0	0
60	1444.4	27	0	3	9	0	2	20	0	25	0	0	8	0	0
70	1472.8	30	0	4	16	0	0	16	4	13	0	0	8	0	0
80	1501.2	18	0	0	29	12	0	0	2	8	12	0	11	0	2
90	1559.6	31	3	4	12	0	0	15	3	19	0	0	5	0	3
100	1558.0	22	0	3	23	2	7	13	4	8	3	1	10	1	2
110	1586.4	11	0	4	41	0	0	15	3	2	13	0	3	0	3
120	1678.4	24	0	3	18	0	2	11	0	8	2	0	12	0	15
130	1770.4	19	0	5	21	0	0	10	3	13	5	0	10	0	0
140	1862.4	27	5	5	17	0	0	9	2	4	11	0	7	2	0
151	1963.6	19	0	4	19	0	4	10	6	7	4	0	12	0	8
160	2046.4	15	0	2	41	0	0	10	0	0	10	0	14	0	0
171	2147.6	4	3	3	34	0	2	33	0	0	8	0	6	5	0
180	2230.4	10	3	3	41	0	0	20	0	3	7	0	7	0	0
190	2322.4	8	0	7	35	0	0	31	0	0	5	0	4	3	0
211	2515.6	2	0	8	42	0	0	26	0	0	7	0	6	0	2
220	2598.4	14	0	7	29	2	5	18	3	4	3	0	3	6	0
240	2782.4	3	0	12	14	0	2	47	0	2	2	0	2	7	0

Appendix 9: Core DA00-05
Agglutinated foraminiferal counts

Sample Depth (cm)	Converted Age (cal yr BP)	aderglom	amopseud	cribcras	cunart	recturb	reofusi	reograci	reopilu	sacdifli	spiribif	tecear	textorq	trochjap	trochan
260	2966.4	3	0	7	51	0	0	0	0	5	8	0	13	6	0
280	3105.8	0	0	0	41	0	0	46	0	0	7	0	0	0	0
300	3245.2	2	0	9	30	0	0	24	0	0	10	0	8	6	0
320	3384.6	3	0	0	36	0	0	40	0	0	9	2	3	2	0
340	3474.7	3	6	5	14	0	7	11	4	29	7	0	4	4	0
360	3538.3	3	3	9	29	0	5	26	3	14	5	0	0	0	0
380	3601.9	6	2	9	24	0	3	15	0	13	13	0	3	4	0
400	3665.5	9	3	9	31	0	4	15	0	12	9	0	0	2	0
410	3697.3	7	7	19	16	0	3	17	0	20	3	0	3	0	0
420	3729.1	13	0	7	34	0	0	13	0	21	3	0	0	0	0
430	3760.9	12	7	12	15	4	0	9	0	16	11	0	4	6	0
440	3792.7	6	0	0	5	0	2	2	0	7	0	0	0	0	0
450	3824.5	14	4	4	27	3	3	18	0	10	8	0	4	3	0
460	3856.3	0	0	0	38	0	0	50	0	0	3	0	3	0	0
470	3888.1	14	3	0	32	5	0	14	3	6	15	0	3	3	0
480	3919.9	7	0	3	31	0	0	48	0	0	4	0	2	0	0
490	3951.7	5	0	2	36	0	0	42	0	0	5	0	2	0	0
500	3983.5	4	0	0	34	0	0	32	0	0	11	0	7	0	0
510	4015.3	5	0	0	36	3	0	39	0	0	0	3	4	0	0
520	4047.1	8	4	0	32	8	0	17	0	8	19	0	0	4	0
530	4078.9	0	0	0	28	0	0	56	0	0	7	0	0	0	0
540	4110.7	0	0	0	32	0	0	50	0	0	10	0	3	0	0

Appendix 9: Core DA00-05
Agglutinated foraminiferal counts

Sample Depth (cm)	Converted Age (cal yr BP)	aderglom	amopseud	cribcras	cunart	recturb	reofusi	reograci	reopilu	sacdifli	spiribif	tecear	textorq	trochjap	trochan
550	4142.5	0	0	2	8	0	0	6	0	0	5	0	2	0	0
560	4174.3	0	3	0	3	0	0	3	0	0	0	0	0	0	0
570	4206.1	5	3	2	15	0	3	13	0	0	4	0	6	0	0
580	4237.9	7	0	0	7	0	0	11	0	0	4	0	3	0	0
590	4269.7	3	0	0	8	4	0	5	0	0	0	0	3	0	1
600	4332.7	6	0	3	14	0	0	9	4	3	0	0	3	0	0
610	4395.7	4	0	0	4	0	0	3	0	0	0	0	0	0	0
620	4458.7	4	0	0	7	0	0	9	0	0	4	0	2	2	0
630	4521.7	3	0	4	8	0	0	6	0	0	0	0	3	0	0
640	4584.8	0	0	2	12	0	0	7	0	0	5	0	3	0	0
650	4647.7	3	0	0	4	0	0	3	0	0	4	0	0	0	0
660	4710.7	6	0	3	8	3	0	15	0	0	8	0	0	5	0
670	4773.7	17	2	9	8	6	0	6	6	3	4	0	3	3	0
680	4836.7	0	2	0	8	0	0	2	0	0	2	0	0	0	0
690	4899.7	9	0	6	17	0	0	15	9	6	10	0	0	0	8
700	4962.7	9	0	6	4	0	4	13	9	35	7	3	0	0	0
710	5025.7	0	0	0	3	0	0	2	0	0	0	0	2	0	0
720	5088.7	0	0	2	0	0	0	0	0	0	0	0	0	0	0
730	5151.7	0	0	4	17	0	0	12	4	4	4	0	2	3	0
740	5214.7	0	7	0	0	0	0	0	0	0	0	0	0	0	0
750	5277.7	18	11	11	11	0	9	0	11	20	0	0	0	4	0
760	5340.7	0	3	0	6	0	0	10	0	0	0	0	2	0	0

Appendix 9: Core DA00-05
Agglutinated foraminiferal counts

Sample Depth (cm)	Converted Age (cal yr BP)	aderglom	amopseud	cribcras	cunart	recturb	reofusi	reograci	reopilu	sacdifli	spiribif	tecear	textorq	trochjap	trochan
770	5403.7	2	0	4	6	0	0	13	0	0	2	0	0	0	0
780	5466.7	6	0	3	29	0	0	23	6	3	6	0	0	3	6
790	5529.7	3	5	8	23	0	0	24	3	14	0	0	3	6	0
800	5592.7	0	0	0	3	0	0	3	0	0	0	0	0	0	0
810	5655.7	9	0	18	9	0	0	18	18	0	0	0	0	0	0
820	5707.9	7	2	5	9	0	50	12	0	35	0	0	0	0	0
830	5760.1	0	0	0	2	0	0	4	0	0	0	0	0	0	0
840	5812.3	0	0	0	0	0	0	0	0	0	0	0	0	0	0
850	5864.5	2	0	0	7	0	11	25	0	10	2	0	0	0	0
860	5916.7	0	3	0	5	0	4	5	5	25	11	0	5	0	25
870	5968.9	4	0	0	11	0	0	22	4	26	0	0	11	0	19
880	6021.1	0	0	0	3	0	0	3	0	3	0	0	0	0	0
890	6073.3	0	0	0	2	0	0	0	0	9	0	0	0	0	4
900	6125.5	0	0	0	0	0	0	6	0	0	0	0	0	0	0
910	6177.7	0	0	0	4	0	0	7	0	0	0	0	0	0	0
920	6229.9	0	0	0	9	0	0	38	0	0	0	0	0	0	0
930	6282.1	0	0	0	6	0	0	12	0	0	0	0	0	0	0
940	6334.3	8	0	0	10	0	2	17	0	5	3	0	0	0	0
950	6386.5	10	0	4	29	0	0	36	5	5	5	0	0	2	0
960	6438.7	0	0	0	21	0	0	51	0	0	0	0	0	0	0
970	6490.9	0	0	0	6	0	0	4	0	0	0	0	0	0	0
980	6543.1	0	0	0	2	0	0	5	0	2	0	0	0	0	0

Sample Depth (cm)	Converted Age (cal yr BP)	aderglom	amopseud	cribcras	cunart	recturb	reofusi	reograci	reopilu	sacdifli	spiribif	tecear	textorq	trochjap	trochan
990	6595.3	0	0	0	0	0	0	0	0	5	0	0	0	0	0
1000	6647.5	2	0	0	4	0	0	3	0	0	0	0	0	0	0
1010	6699.7	2	0	0	7	0	0	7	0	0	2	0	0	0	0
1020	6751.9	0	0	0	4	0	0	4	0	0	0	0	0	0	0
1030	6804.1	0	0	0	6	0	0	2	0	0	3	0	0	0	0

Appendix 9: Core DA00-05
Agglutinated foraminiferal counts

Sample Depth (cm)	Converted Age (cal yr BP)	total agglu	total calc	total benthic species	npachys	testline	% ice proximal species	no agglu counted	no calc counted	total forams counted	sed volume	foram conc (tests/ml)	% agglu >5%	% calc >5%	species dominance	% Arctic	% Atlantic
10	1302.4	11	0	11	0	0	0	85	2	87	6	15	93	0	34	5	44
20	1330.8	10	0	10	0	6	0	158	1	159	5	32	91	0	25	6	29
30	1359.2	8	0	8	0	16	0	316	3	304	6	51	90	0	30	8	18
41	1390.4	8	0	8	0	28	0	272	0	272	5	54	95	0	28	3	42
51	1418.8	6	0	6	0	30	0	331	0	303	5	61	89	0	34	0	25
60	1444.4	7	0	7	0	42	0	307	0	300	8	38	93	0	27	0	55
70	1472.8	7	0	7	0	89	0	334	1	304	8	38	91	0	30	0	47
80	1501.2	8	0	8	0	26	0	300	0	300	6	55	95	0	29	12	27
90	1529.6	9	0	9	0	35	0	302	0	302	6	50	95	0	31	0	54
100	1558.0	13	0	13	0	0	0	167	0	167	10	17	98	0	23	3	33
10	1586.4	9	0	9	0	4	0	314	1	301	6	50	95	0	41	13	18
120	1678.4	9	0	9	0	43	0	300	0	300	7	43	95	0	24	2	35
130	1770.4	8	1	9	0	83	0	230	18	248	6	41	85	4	21	5	41
140	1862.4	10	0	10	0	12	0	329	0	302	12	25	91	0	27	11	36
151	1963.6	6	0	6	0	29	0	225	1	226	5	45	92	0	19	4	30
160	2046.4	6	0	6	0	18	0	293	1	294	6	49	91	0	41	10	17
171	2147.6	8	0	8	0	30	0	199	0	199	7	28	95	0	34	7	7
180	2230.4	8	0	8	0	26	0	218	2	220	9	24	95	0	41	8	15
190	2322.4	7	0	7	0	15	0	227	0	227	10	23	93	0	35	5	16
211	2515.6	7	0	7	0	16	0	195	1	196	10	20	93	0	42	7	10
220	2598.4	11	0	11	0	9	0	147	0	147	7	21	94	0	29	3	24
240	2782.4	9	0	9	0	32	0	91	1	92	6	15	91	0	47	2	17

Appendix 10: Core DA00-05
Core foraminiferal analysis data

Sample Depth (cm)	Converted Age (cal yr BP)	total agglu	total calc	total benthic species	npachys	testline	% ice proximal species	no agglu counted	no calc counted	total forams counted	sed volume	foram conc (tests/ml)	% agglu >5%	% calc >5%	species dominance	% Arctic	% Atlantic
260	2966.4	7	0	7	0	30	0	127	1	128	11	12	92	0	51	8	15
280	3105.8	3	0	3	0	21	0	284	3	287	6	48	93	0	46	7	0
300	3245.2	7	0	7	0	61	0	181	0	181	9	20	91	0	30	10	12
320	3384.6	7	0	7	0	92	0	253	3	256	10	26	95	0	43	9	3
340	3474.7	11	0	11	0	6	0	124	1	125	12	10	94	0	29	7	37
360	3538.3	9	0	9	0	24	0	158	0	158	16	10	96	0	29	5	25
380	3601.9	10	0	10	0	51	0	247	0	247	10	25	92	0	24	13	28
400	3665.5	9	0	9	0	29	0	137	1	138	12	12	95	0	31	9	30
410	3697.3	9	0	9	0	43	0	69	0	69	14	5	93	0	20	3	46
420	3729.1	6	0	6	0	28	0	119	0	119	10	12	92	0	34	3	41
430	3760.9	10	0	10	0	30	0	85	0	85	15	6	95	0	16	11	40
440	3792.7	5	7	12	0	8	12	87	218	305	15	20	22	60	30	17	56
450	3824.5	11	0	11	0	58	0	227	1	228	15	15	96	0	27	8	27
460	3856.3	4	0	4	0	23	0	264	0	264	14	19	94	0	50	3	0
470	3888.1	10	0	10	0	15	0	66	0	66	16	4	97	0	32	15	20
480	3919.9	6	0	6	0	30	0	172	0	172	14	12	96	0	48	4	10
490	3951.7	6	0	6	0	38	0	284	2	286	14	20	92	0	42	5	7
500	3983.5	5	0	5	0	110	0	266	2	268	9	30	88	0	34	11	4
510	4015.3	6	0	6	0	68	0	264	0	264	16	17	90	0	39	0	5
520	4047.1	8	0	8	0	10	0	53	0	53	12	4	98	0	32	19	15
530	4078.9	3	0	3	0	74	0	317	0	300	15	20	91	0	56	7	0
540	4110.7	4	0	4	0	47	0	301	0	301	11	27	94	0	50	10	0

Appendix 10: Core DA00-05
Core foraminiferal analysis data

Appendix 10: Core DA00-05
Core foraminiferal analysis data

Sample Depth (cm)	Converted Age (cal yr BP)	total agglu	total calc	total benthic species	npachys	testline	% ice proximal species	no agglu counted	no calc counted	total forams counted	sed volume	foram conc (tests/ml)	% agglu >5%	% calc >5%	species dominance	% Arctic	% Atlantic
550	4142.5	5	7	12	0	17	13	101	202	303	16	19	35	65	34	21	47
560	4174.3	3	10	13	0	0	23	33	280	313	13	25	8	89	21	35	29
570	4206.1	8	4	12	0	56	4	105	76	181	15	12	50	39	28	8	43
580	4237.9	5	4	9	1	9	5	121	182	304	15	20	32	55	32	9	44
590	4269.7	6	3	9	0	8	0	90	209	300	16	19	24	64	56	0	62
600	4332.7	7	3	10	1	40	0	122	139	263	14	19	42	46	38	0	54
610	4395.7	3	8	11	0	11	15	60	258	318	18	18	11	73	19	31	30
620	4458.7	6	4	10	0	53	12	84	166	250	14	18	28	60	31	15	52
630	4521.7	5	8	13	0	7	22	116	228	344	15	23	24	59	17	28	33
640	4584.7	5	6	11	0	12	0	119	194	313	8	39	30	58	26	15	38
650	4647.7	4	10	14	0	16	20	53	251	304	11	28	13	78	20	34	42
660	4710.7	7	5	12	0	83	16	113	112	225	14	16	47	42	16	28	28
670	4773.7	11	2	13	0	15	0	92	35	127	14	9	68	21	19	6	49
680	4836.7	4	7	11	0	26	21	76	238	314	15	21	15	64	25	28	36
690	4899.7	8	2	10	0	122	0	106	13	116	10	12	81	7	17	10	28
700	4962.7	9	0	9	0	5	0	68	0	68	14	5	91	0	35	7	50
710	5025.7	3	8	11	0	15	16	25	206	232	12	20	8	83	40	25	53
720	5088.7	0	9	9	0	7	28	25	277	302	14	22	2	88	40	34	52
730	5151.7	8	4	12	0	12	7	94	77	171	17	10	50	32	17	11	33
740	5214.7	1	8	9	0	9	4	21	159	180	16	11	7	78	47	7	67
750	5277.7	8	0	8	0	9	0	55	1	56	11	5	93	0	20	0	48
760	5340.7	4	8	8	2	22	2	25	60	86	6	14	22	66	56	2	64

Appendix 10: Core DA00-05
Core foraminiferal analysis data

Sample Depth (cm)	Converted Age (cal yr BP)	total agglu	total calc	total benthic species	npachys	testline	% ice proximal species	no agglu counted	no calc counted	total forams counted	sed volume	foram conc (tests/ml)	% agglu >5%	% calc >5%	species dominance	% Arctic	% Atlantic
770	5403.7	5	6	11	0	53	17	60	136	196	7	28	27	62	29	29	42
780	5466.7	9	2	11	0	31	0	28	3	31	5	6	87	10	29	13	16
790	5529.7	9	2	11	0	25	0	61	5	66	9	7	88	8	24	5	27
800	5592.7	2	8	10	1	16	23	31	273	306	5	61	5	82	44	30	53
810	5655.7	5	1	6	0	23	18	9	2	11	6	2	82	18	27	18	27
820	5707.9	7	1	8	9	9	0	32	10	43	7	6	74	23	35	0	70
830	5760.1	2	9	11	0	2	17	28	282	310	8	39	6	86	25	39	40
840	5812.3	0	6	6	0	3	27	15	291	306	7	44	0	85	36	35	50
850	5864.5	5	4	9	0	25	4	86	75	161	11	15	48	41	29	7	49
860	5916.7	9	0	9	0	12	0	59	2	61	10	6	95	0	25	11	25
870	5968.9	8	0	8	0	60	0	27	0	27	9	3	100	0	26	0	30
880	6021.1	3	6	9	0	26	3	33	271	305	7	47	9	83	58	7	76
890	6073.3	3	4	7	1	11	5	37	131	169	7	24	15	70	53	5	69
900	6125.5	1	8	9	0	5	20	27	273	300	10	30	6	86	22	44	26
910	6177.7	2	7	9	0	4	19	43	272	315	12	26	11	84	22	41	31
920	6229.9	2	4	6	0	33	17	155	151	306	6	51	47	42	38	19	23
930	6828.1	2	8	10	0	20	10	71	236	307	9	34	18	72	35	18	47
940	6334.3	6	4	10	0	25	0	47	45	92	6	15	46	42	35	4	54
950	6386.5	8	0	8	0	20	0	129	0	129	6	22	96	0	36	5	19
960	6438.7	2	4	6	0	4	12	60	21	81	5	16	72	25	51	17	7
970	6490.9	2	4	6	0	13	3	27	174	201	7	29	10	79	70	3	73
980	6543.1	3	6	9	0	4	0	31	216	247	9	27	9	79	54	7	61

Appendix 10: Core DA00-05
Core foraminiferal analysis data

Sample Depth (cm)	Converted Age (cal yr BP)	total agglu	total calc	total benthic species	npachys	testline	% ice proximal species	no agglu conuted	no calc counted	total forams counted	sed volume	foram conc (tests/ml)	% agglu >5%	% calc >5%	species dominance	% Arctic	% Atlantic
990	6595.3	1	5	6	0	9	4	21	205	227	8	28	5	78	56	4	69
1000	6647.5	3	8	11	0	12	20	40	263	303	10	30	9	81	39	29	53
1010	6699.7	4	7	11	0	11	10	44	132	176	8	23	19	69	14	21	52
1020	6751.9	2	8	10	0	1	12	40	260	300	6	50	9	83	27	42	28
1030	6804.1	3	7	10	0	13	21	60	246	306	7	44	11	70	25	54	13

Appendix 11: Core DA00-03
Calcareous foraminiferal counts

Sample Depth (cm)	Converted Age (cal yr BP)	ammogull	astrogal	bolpseud	bucfrige	casrenif	casterit	chilfim	ciblobat	dentbagi	elphask	elphbart
2	506.3	0	0	0	1	1	2	0	2	0	0	0
8	522.2	0	0	0	0	2	0	0	3	0	0	0
16	543.4	0	0	0	0	0	0	0	13	0	0	0
24	564.6	0	0	0	0	1	0	0	4	0	0	0
34	591.1	0	0	1	0	0	0	3	6	0	0	0
40	607.0	0	0	0	0	0	1	0	3	0	0	0
48	628.2	0	0	0	0	0	0	0	14	0	0	1
56	649.4	0	0	1	1	1	1	1	1	0	0	1
72	691.8	0	0	0	0	2	4	0	0	9	0	0
80	713.0	0	1	14	1	8	1	3	2	0	0	1
96	755.4	0	0	0	6	0	6	0	0	0	0	0
100	766.0	0	0	3	1	4	2	4	2	0	0	1
102	771.3	0	0	3	0	3	8	0	0	0	0	0
104	776.6	0	0	0	0	0	0	0	0	0	0	0
106	781.9	0	0	0	3	0	0	0	10	0	0	0
112	797.8	0	0	0	0	1	0	0	1	0	0	0
120	819.0	0	0	0	0	0	3	0	0	0	0	0
128	840.2	1	0	1	1	5	1	1	2	0	0	1
144	882.6	0	0	0	0	0	0	0	0	0	0	0
152	903.8	0	0	0	0	5	0	0	2	0	0	0
160	925.0	0	0	0	0	0	0	0	0	0	0	0
168	946.2	0	0	0	0	0	0	0	0	0	0	0

Appendix 11: Core DA00-03
Calcareous foraminiferal counts

Sample Depth (cm)	Converted Age (cal yr BP)	elphex	elphince	globina	hanesobi	islanorc	nonilabr	nonauric	staincon	stainfey	npachys
2	506.3	0	0	4	0	0	24	0	0	0	0
8	522.2	0	0	0	0	0	10	0	0	0	0
16	543.4	4	0	0	0	0	35	0	0	0	0
24	564.6	0	0	0	0	0	1	0	0	0	0
34	591.1	1	0	4	0	1	57	0	0	1	3
40	607.0	0	0	6	0	0	3	0	0	0	1
48	628.2	4	0	28	0	0	29	0	1	0	0
56	649.4	5	0	2	0	5	22	10	0	1	0
72	691.8	13	0	7	0	9	0	0	0	7	0
80	713.0	2	0	2	0	1	6	0	0	36	2
96	755.4	0	0	11	0	0	22	0	6	0	0
100	766.0	1	0	7	0	5	38	0	0	9	3
102	771.3	2	0	10	0	2	20	0	0	49	0
104	776.6	0	0	0	0	0	4	0	0	0	0
106	781.9	6	0	0	0	3	48	0	0	0	0
112	797.8	0	0	0	0	0	46	0	0	0	0
120	819.0	4	0	7	0	4	56	0	0	0	0
128	840.2	6	0	12	0	9	42	1	1	0	0
144	882.6	0	0	2	0	10	43	0	0	0	0
152	903.8	8	0	20	0	14	47	0	0	0	0
160	925.0	0	0	8	0	0	0	0	0	0	0
168	946.2	0	0	0	0	0	0	0	0	0	0

Appendix 11: Core DA00-03
Calcareous foraminiferal counts

Sample Depth (cm)	Converted Age (cal yr BP)	ammogull	astrogal	bolpseud	bucfrige	casrenif	casterit	chilfim	ciblobat	dentbagi	elphask	elphbart
176	967.4	0	0	0	0	0	0	0	0	5	0	0
184	988.6	0	2	2	1	7	0	1	6	0	0	1
192	1009.8	0	0	0	1	8	0	0	11	0	0	0
200	1031.0	0	0	0	0	0	0	0	0	0	0	0
208	1052.2	0	0	0	0	0	0	0	0	0	0	0
216	1073.4	0	0	0	0	0	0	0	0	0	0	0
232	1115.8	0	0	0	1	0	2	1	2	0	0	0
240	1137.0	0	0	0	0	1	3	0	2	0	0	3
248	1158.2	0	0	0	0	0	0	0	0	0	0	0
256	1179.4	0	0	0	0	0	0	0	0	0	0	0
264	1200.6	0	0	1	9	4	7	0	0	0	0	0
272	1221.8	0	0	0	1	2	1	0	1	0	0	0
280	1243.0	0	0	2	0	4	14	2	0	0	0	0
288	1264.2	0	0	4	1	15	0	0	5	0	0	1
296	1285.4	0	0	0	0	0	0	0	0	0	0	0
300	1296.0	0	0	0	1	8	1	1	3	0	0	2
304	1306.6	0	0	2	2	12	2	9	5	0	1	2
312	1327.8	0	0	0	0	4	0	0	7	0	0	0
320	1349.0	0	8	0	4	0	0	0	0	4	0	4
328	1370.2	0	0	3	1	13	1	6	7	0	0	1
336	1391.4	0	1	1	1	5	0	0	7	0	0	3
344	1412.6	0	0	0	4	4	0	0	4	0	0	0

Appendix 11: Core DA00-03
Calcareous foraminiferal counts

Sample Depth (cm)	Converted Age (cal yr BP)	elphex	elphince	globina	hanesobi	islanorc	nonilabr	nonauric	staincon	stainfey	npachys
176	967.4	0	0	0	0	0	0	0	0	0	0
184	988.6	6	0	7	0	11	17	0	0	0	2
192	1009.8	10	0	7	0	11	21	0	0	1	0
200	1031.0	0	0	0	0	0	75	0	0	0	0
208	1052.2	0	0	14	0	0	29	0	0	0	0
216	1073.4	0	0	0	0	0	3	0	0	0	0
232	1115.8	5	0	12	0	10	47	0	0	0	2
240	1137.0	2	0	14	1	9	52	0	10	0	5
248	1158.2	9	0	4	0	13	9	0	0	0	0
256	1179.4	0	0	0	0	50	0	0	0	0	0
264	1200.6	9	0	0	0	14	33	0	0	0	0
272	1221.8	8	0	1	0	3	20	0	0	0	0
280	1243.0	2	0	4	0	18	31	0	0	0	4
288	1264.2	4	0	9	2	6	42	0	0	0	3
296	1285.4	0	0	0	0	0	0	0	0	0	0
300	1296.0	4	0	0	1	4	18	6	1	3	1
304	1306.6	4	0	8	1	3	26	1	0	1	5
312	1327.8	4	0	17	0	16	48	0	2	0	0
320	1349.0	0	0	0	0	4	0	0	0	0	0
328	1370.2	7	0	0	1	6	15	3	0	5	4
336	1391.4	5	2	8	2	3	8	0	0	0	1
344	1412.6	4	0	4	0	17	38	0	0	0	4

Appendix 11: Core DA00-03
Calcareous foraminiferal counts

Sample Depth (cm)	Converted Age (cal yr BP)	ammogull	astrogal	bolpseud	bucfrige	casrenif	casterit	chilfim	ciblobat	dentbagi	elphask	elphbart
352	1433.8	0	0	7	0	10	3	3	4	0	2	2
360	1455.0	0	0	1	0	9	0	0	0	0	0	1
368	1476.2	0	0	3	2	13	0	4	2	1	0	6
376	1497.4	0	0	0	0	0	0	0	0	0	0	0
384	1518.6	0	0	0	0	0	0	0	0	0	0	0
392	1539.8	0	0	0	0	0	0	0	0	0	0	0
400	1561.0	0	0	0	0	9	1	0	5	0	0	0
406	1576.9	0	0	0	0	13	0	0	4	0	0	3
416	1603.4	0	0	0	0	0	0	0	0	0	0	0
424	1624.6	0	1	0	0	9	3	0	1	0	0	0
430	1640.5	0	0	0	0	0	0	0	0	0	0	0
440	1667.0	0	0	0	0	3	0	0	5	0	0	0
448	1688.2	0	0	1	0	10	1	1	3	0	0	3
454	1704.0	0	0	1	0	8	0	4	4	0	0	1
464	1730.6	0	0	1	3	14	1	0	1	0	0	0
472	1751.8	0	0	3	0	10	0	4	0	0	0	0
488	1794.2	0	0	1	0	5	0	0	1	0	0	1
496	1815.4	0	0	0	0	2	0	0	2	0	0	0
500	1826.0	0	0	3	3	10	2	4	1	0	0	1
502	1831.3	0	0	0	0	0	0	0	3	0	0	0
512	1857.8	0	0	1	2	12	0	2	5	0	0	2
526	1894.9	0	0	5	0	11	0	0	4	0	1	4

Appendix 11: Core DA00-03
Calcareous foraminiferal counts

Sample Depth (cm)	Converted Age (cal yr BP)	elphex	elphince	globina	hanesobi	islanorc	nonilabr	nonauric	staincon	stainfey	npachys
352	1433.8	2	1	0	8	1	10	2	0	36	0
360	1455.0	0	0	0	0	1	4	0	0	80	0
368	1476.2	2	1	9	0	7	21	5	0	7	2
376	1497.4	4	0	4	0	11	37	0	4	0	0
384	1518.6	0	0	0	0	0	0	0	0	0	0
392	1539.8	13	0	0	0	0	0	0	0	0	0
400	1561.0	10	0	26	0	5	33	0	1	0	1
406	1576.9	9	0	5	0	11	12	0	0	0	5
416	1603.4	0	0	0	0	0	25	0	0	0	0
424	1624.6	2	1	40	1	10	14	0	0	13	0
430	1640.5	0	0	0	0	0	0	0	0	0	0
440	1667.0	8	2	18	2	10	43	0	2	0	0
448	1688.2	6	0	14	2	9	37	0	1	4	5
454	1704.0	0	0	7	0	9	49	3	0	3	5
464	1730.6	17	0	10	0	4	37	0	0	8	1
472	1751.8	7	0	22	1	5	21	0	1	18	2
488	1794.2	8	0	20	0	26	26	1	2	0	1
496	1815.4	2	0	12	0	11	63	0	2	0	1
500	1826.0	8	0	13	0	8	28	0	3	6	5
502	1831.3	4	0	11	1	13	51	0	7	1	5
512	1857.8	6	0	21	0	10	26	1	6	3	0
526	1894.9	0	1	3	1	13	51	0	2	2	2

Appendix 11: Core DA00-03
Calcareous foraminiferal counts

Sample Depth (cm)	Converted Age (cal yr BP)	ammogull	astrogal	bolpseud	bucfrige	casrenif	casterit	chilfim	ciblobat	dentbagi	elphask	elphbart
536	1921.4	0	2	4	0	3	0	4	3	0	0	4
546	1947.9	0	2	12	0	7	3	2	3	0	0	2
560	1985.0	0	0	0	0	0	0	0	4	0	0	0
568	2006.2	0	0	11	0	3	1	6	3	0	0	0
574	2022.1	0	0	4	0	12	2	0	4	0	0	2
584	2048.6	0	1	1	0	6	3	1	0	0	0	1
592	2069.8	0	1	1	0	11	2	1	3	0	0	0
598	2085.7	0	0	1	0	11	1	0	0	0	0	4
608	2112.2	0	3	0	0	0	7	1	6	0	0	7
616	2133.4	0	0	0	0	5	5	0	0	0	0	14
622	2149.3	0	0	0	0	0	0	0	0	0	0	0
632	2175.8	0	0	0	0	0	0	0	0	0	0	0
640	2197.0	0	0	2	0	12	6	0	2	0	0	2
646	2212.9	0	0	0	0	0	0	0	2	0	0	1
656	2239.4	1	0	0	0	0	7	0	4	0	0	1
664	2260.6	0	0	0	0	1	13	0	7	0	0	2
670	2276.5	0	0	1	0	13	2	0	6	0	0	3
672	2281.8	0	0	0	0	0	0	0	0	0	0	0
680	2303.0	0	0	0	0	0	0	0	0	0	0	0
684	2313.6	0	0	0	7	0	0	0	2	0	0	0
688	2324.2	33	0	0	0	0	0	0	0	0	0	0
694	2340.1	0	0	0	0	0	0	0	0	0	0	0

Appendix 11: Core DA00-03
Calcareous foraminiferal counts

Sample Depth (cm)	Converted Age (cal yr BP)	elphex	elphince	globina	hanesobi	islanorc	nonilabr	nonauric	staincon	stainfey	npachys
536	1921.4	0	0	6	1	15	45	6	2	2	2
546	1947.9	5	0	12	0	22	9	5	1	8	3
560	1985.0	4	0	0	4	42	29	0	0	0	0
568	2006.2	3	0	10	0	16	27	2	2	9	3
574	2022.1	0	0	10	2	18	40	0	0	0	3
584	2048.6	5	0	24	3	23	21	0	1	1	4
592	2069.8	3	0	15	0	22	34	1	1	1	0
598	2085.7	0	0	0	0	19	58	0	0	0	3
608	2112.2	4	2	7	4	36	8	0	12	0	2
616	2133.4	0	0	9	0	18	23	0	0	0	0
622	2149.3	0	0	0	0	0	0	0	0	0	0
632	2175.8	0	0	0	0	0	0	0	0	0	0
640	2197.0	9	1	23	0	16	20	1	1	3	0
646	2212.9	7	0	8	0	26	49	0	0	0	0
656	2239.4	2	0	12	0	47	12	0	4	0	0
664	2260.6	0	0	17	0	30	12	1	6	0	1
670	2276.5	5	2	15	1	19	21	3	3	1	4
672	2281.8	5	0	42	0	18	24	0	0	0	0
680	2303.0	0	0	0	0	0	50	0	0	0	0
684	2313.6	2	0	12	0	0	0	0	0	0	0
688	2324.2	0	0	0	0	0	0	0	0	0	0
694	2340.1	0	0	0	0	0	0	0	0	0	0

Appendix 11: Core DA00-03
Calcareous foraminiferal counts

Sample Depth (cm)	Converted Age (cal yr BP)	ammogull	astrogal	bolpseud	bucfrige	casrenif	casterit	chilfim	ciblobat	dentbagi	elphask	elphbart
696	2345.4	0	0	0	0	1	0	0	4	0	0	1
702	2361.3	0	0	0	0	0	0	0	0	0	0	0
710	2382.5	0	0	0	0	0	0	0	0	0	0	0
720	2409.0	0	0	0	0	21	5	3	14	0	1	1
728	2430.2	0	0	0	0	0	0	0	0	0	0	0
736	2451.4	0	0	0	0	1	0	0	0	0	0	0
744	2472.6	0	0	1	1	26	1	0	14	0	0	4
752	2493.8	0	0	0	0	0	0	0	0	0	0	0
760	2515.0	0	0	0	0	0	0	0	0	0	0	0
768	2536.2	0	0	0	0	1	0	0	2	0	0	1
776	2557.4	0	0	0	0	0	0	0	0	0	0	0
792	2599.8	0	0	3	0	20	0	0	3	0	0	2
800	2621.0	0	0	0	0	0	0	0	0	0	0	0
808	2642.2	0	0	0	0	0	0	0	0	0	0	0
816	2663.4	0	0	6	1	27	0	0	4	0	0	1
824	2684.6	0	2	0	0	5	5	0	5	0	0	5
832	2705.8	0	0	0	0	0	0	0	0	0	0	0
840	2727.0	0	0	5	1	32	0	9	4	0	0	1
848	2748.2	0	0	2	0	12	0	2	12	0	0	11
856	2769.4	0	2	4	2	8	4	0	4	0	0	3
864	2790.6	0	0	0	0	11	0	0	5	0	0	2
872	2811.8	0	1	2	0	12	1	0	6	0	0	2

Appendix 11: Core DA00-03
Calcareous foraminiferal counts

Sample Depth (cm)	Converted Age (cal yr BP)	elphex	elphince	globina	hanesobi	islanorc	nonilabr	nonauric	staincon	stainfey	npachys
696	2345.4	0	0	38	0	6	44	0	1	0	0
702	2361.3	0	0	0	0	0	0	0	0	0	0
710	2382.5	0	0	0	0	0	0	0	0	0	0
720	2409.0	0	3	0	0	0	20	2	1	1	7
728	2430.2	0	0	0	0	0	0	0	0	0	0
736	2451.4	0	0	0	0	0	0	0	0	0	0
744	2472.6	1	3	31	1	5	0	0	1	0	5
752	2493.8	0	0	0	0	0	0	0	0	0	0
760	2515.0	0	0	0	0	0	0	0	0	0	0
768	2536.2	0	0	7	0	7	45	0	2	0	0
776	2557.4	0	0	0	0	0	0	0	0	0	0
792	2599.8	0	0	8	0	3	52	0	0	0	2
800	2621.0	0	0	0	0	0	0	0	0	0	0
808	2642.2	0	0	0	0	0	0	0	0	0	0
816	2663.4	2	0	5	0	2	11	0	0	36	3
824	2684.6	4	0	2	0	4	55	0	2	0	4
832	2705.8	0	0	0	0	13	0	0	0	0	0
840	2727.0	0	0	6	1	2	6	0	0	20	7
848	2748.2	5	0	12	2	3	17	2	9	2	8
856	2769.4	1	0	2	1	1	2	0	2	52	1
864	2790.6	3	0	21	0	10	13	2	2	15	2
872	2811.8	2	1	20	0	2	16	0	0	21	3

Appendix 11: Core DA00-03
Calcareous foraminiferal counts

Sample Depth (cm)	Converted Age (cal yr BP)	ammogull	astrogal	bolpseud	bucfrige	casrenif	casterit	chilfim	ciblobat	dentbagi	elphask	elphbart
880	2833.0	0	0	4	0	15	2	0	2	0	0	1
888	2854.2	0	0	0	0	0	0	0	0	0	0	0
896	2875.4	0	0	0	0	39	2	2	7	0	0	1
904	2896.6	0	2	2	0	10	0	0	5	0	0	0
912	2917.8	0	0	0	0	21	0	0	8	0	0	13
920	2939.0	0	1	3	0	22	2	0	6	0	0	0
928	2960.2	0	1	3	1	15	0	0	2	0	0	0
944	3002.6	0	0	0	0	6	0	0	4	0	0	0
952	3023.8	5	0	0	0	0	0	0	0	0	0	0
968	3066.2	0	0	0	0	0	0	0	0	0	0	0
972	3076.8	0	8	0	0	2	0	0	0	0	6	8
992	3129.8	0	0	0	0	19	2	0	11	0	0	7
1000	3151.0	0	1	2	0	11	4	1	8	0	0	0

Sample Depth (cm)	Converted Age (cal yr BP)	elphex	elphince	globina	hanesobi	islanorc	nonilabr	nonauric	staincon	stainfey	npachys
880	2833.0	10	0	7	0	5	13	1	2	10	4
888	2854.2	0	0	17	0	0	74	0	0	0	0
896	2875.4	11	0	15	3	2	5	1	1	1	11
904	2896.6	8	0	21	5	8	26	0	2	0	2
912	2917.8	4	0	13	0	0	21	0	8	0	0
920	2939.0	9	0	15	0	5	16	0	1	2	2
928	2960.2	5	0	4	1	3	6	0	1	3	1
944	3002.6	10	0	18	2	6	14	0	0	0	0
952	3023.8	0	0	0	0	0	0	0	0	0	0
968	3066.2	0	0	0	0	0	0	0	0	0	0
972	3076.8	6	3	21	18	0	18	2	5	0	0
992	3129.8	7	15	11	7	1	3	1	2	1	8
1000	3151.0	0	0	15	1	2	36	1	0	2	1

Appendix 11: Core DA00-03
Calcareous foraminiferal counts

Appendix 12: Core DA00-03
Agglutinated foraminiferal counts

Sample Depth (cm)	Converted Age (cal yr BP)	aderglom	cribcras	cribjeff	cunart	eggadv	recturb	reograci	reogutt	reopilu
2	506.3	0	1	0	22	0	0	34	0	0
8	522.2	0	3	3	27	0	0	31	0	0
16	543.4	0	0	4	17	0	0	17	0	0
24	564.6	0	2	0	30	0	4	51	0	0
34	591.1	0	3	0	14	0	0	4	0	0
40	607.0	0	12	16	12	0	6	15	0	0
48	628.2	0	8	1	0	0	0	8	0	0
56	649.4	0	7	1	12	0	4	27	0	0
72	691.8	0	0	0	11	0	2	26	0	0
80	713.0	0	0	0	8	0	0	5	2	0
96	755.4	0	6	0	28	0	0	11	0	0
100	766.0	0	3	0	12	0	0	3	0	0
102	771.3	0	0	0	0	0	0	0	0	0
104	776.6	0	1	0	27	0	0	16	0	0
106	781.9	0	0	0	19	0	0	6	0	0
112	797.8	0	0	0	31	0	0	4	10	0
120	819.0	0	0	0	13	0	0	15	0	0
128	840.2	0	1	2	6	0	0	5	2	0
144	882.6	0	17	0	10	0	10	0	0	0
152	903.8	0	2	0	0	0	0	0	0	0
160	925.0	0	15	0	31	0	0	38	0	8
168	946.2	0	9	0	34	4	4	40	0	0

Appendix 12: Core DA00-03
Agglutinated foraminiferal counts

Sample Depth (cm)	Converted Age (cal yr BP)	reoscorp	sacdifli	silicosi	spirobif	texear	textorq	trochjap	trochnan
2	506.3	0	0	0	4	1	0	0	1
8	522.2	0	0	0	15	0	0	6	0
16	543.4	0	0	0	9	0	0	0	0
24	564.6	0	0	0	7	0	0	0	0
34	591.1	0	0	0	1	0	0	0	0
40	607.0	0	0	0	18	0	0	8	0
48	628.2	0	0	0	1	0	0	0	0
56	649.4	0	0	0	2	0	1	4	1
72	691.8	0	0	0	2	0	4	0	2
80	713.0	0	0	0	2	0	0	0	0
96	755.4	0	0	0	6	0	0	0	0
100	766.0	0	0	0	0	0	0	0	0
102	771.3	0	0	0	0	0	0	0	0
104	776.6	8	0	0	42	0	1	1	0
106	781.9	0	0	0	3	0	0	0	0
112	797.8	0	0	0	4	1	0	0	0
120	819.0	0	0	0	0	0	0	0	0
128	840.2	0	0	0	1	0	0	0	0
144	882.6	0	0	0	7	0	0	0	0
152	903.8	0	0	0	0	0	0	0	2
160	925.0	0	0	0	0	0	0	0	0
168	946.2	0	0	2	8	0	0	0	0

Appendix 12: Core DA00-03
Agglutinated foraminiferal counts

Sample Depth (cm)	Converted Age (cal yr BP)	aderglom	cribcras	cribjeff	cunart	eggadv	recturb	reograci	reogutt	reopilu
176	967.4	0	9	0	27	0	9	36	9	0
184	988.6	0	7	1	12	0	0	6	6	0
192	1009.8	0	1	0	12	0	5	8	0	0
200	1031.0	0	25	0	0	0	0	0	0	0
208	1052.2	0	29	0	14	0	0	0	0	0
216	1073.4	0	11	0	31	0	0	56	0	0
232	1115.8	0	1	1	5	0	0	6	0	0
240	1137.0	0	3	1	0	0	0	1	0	0
248	1158.2	0	9	4	13	0	0	26	0	0
256	1179.4	0	0	0	50	0	0	0	0	0
264	1200.6	0	7	9	3	0	0	1	0	0
272	1221.8	1	5	7	22	0	5	10	0	0
280	1243.0	0	8	0	0	0	0	8	0	0
288	1264.2	0	0	0	0	0	0	7	0	0
296	1285.4	0	6	0	50	0	0	19	0	0
300	1296.0	5	2	0	14	0	2	20	0	0
304	1306.6	1	1	0	5	0	0	3	0	0
312	1327.8	0	1	0	0	0	0	1	0	0
320	1349.0	0	8	0	29	0	4	29	0	0
328	1370.2	0	1	0	7	0	0	6	0	0
336	1391.4	0	2	0	20	0	3	24	0	0
344	1412.6	0	0	0	4	0	0	4	0	0

Appendix 12: Core DA00-03
Agglutinated foraminiferal counts

Sample Depth (cm)	Converted Age (cal yr BP)	reoscorp	sacdifli	silicosi	spirobif	texear	textorq	trochjap	trochnan
176	967.4	0	0	5	0	0	0	0	0
184	988.6	0	0	1	0	0	0	0	0
192	1009.8	0	0	2	1	0	0	0	0
200	1031.0	0	0	0	0	0	0	0	0
208	1052.2	0	0	14	0	0	0	0	0
216	1073.4	0	0	0	0	0	0	0	0
232	1115.8	0	0	0	1	0	0	3	0
240	1137.0	0	0	1	0	0	0	0	1
248	1158.2	0	0	0	4	0	0	9	0
256	1179.4	0	0	0	0	0	0	0	0
264	1200.6	0	0	1	0	0	0	0	0
272	1221.8	0	0	1	3	0	1	9	0
280	1243.0	0	0	0	0	0	0	0	0
288	1264.2	0	0	0	0	0	0	0	0
296	1285.4	0	0	6	13	6	0	0	0
300	1296.0	0	0	0	1	0	1	1	0
304	1306.6	0	0	0	1	0	0	0	0
312	1327.8	0	0	0	0	0	0	0	0
320	1349.0	0	0	0	0	0	0	0	0
328	1370.2	0	0	0	4	0	0	0	0
336	1391.4	0	0	1	5	0	1	0	0
344	1412.6	0	0	8	4	0	0	0	0

Appendix 12: Core DA00-03
Agglutinated foraminiferal counts

Sample Depth (cm)	Converted Age (cal yr BP)	aderglom	cribcras	cribjeff	cunart	eggadv	recturb	reograci	reogutt	reopilu
352	1433.8	1	0	0	5	0	0	1	0	0
360	1455.0	0	1	0	0	0	1	0	0	0
368	1476.2	1	1	0	1	0	2	4	0	3
376	1497.4	0	22	0	7	0	4	7	0	0
384	1518.6	31	0	0	0	0	0	69	0	0
392	1539.8	0	25	0	13	0	0	13	0	0
400	1561.0	0	4	2	0	0	2	0	0	0
406	1576.9	1	20	0	7	0	7	0	0	1
416	1603.4	0	0	0	50	0	0	25	0	0
424	1624.6	0	1	0	0	0	2	0	0	0
430	1640.5	0	5	0	41	0	5	27	0	0
440	1667.0	0	3	2	2	0	0	0	0	0
448	1688.2	0	3	0	0	0	0	0	0	0
454	1704.1	0	0	0	1	0	0	3	0	0
464	1730.6	0	0	0	0	0	1	0	0	0
472	1751.8	0	0	0	1	0	0	3	0	0
488	1794.2	0	0	2	0	0	0	0	0	0
496	1815.4	0	0	0	0	0	0	1	0	0
500	1826.0	1	1	1	1	0	0	0	0	0
502	1831.3	0	0	0	2	0	0	0	0	0
512	1857.8	0	0	0	0	0	0	1	0	0
526	1894.9	0	0	0	0	0	0	0	0	0

Appendix 12: Core DA00-03
Agglutinated foraminiferal counts

Sample Depth (cm)	Converted Age (cal yr BP)	reoscorp	sacdifli	silicosi	spirobif	texear	textorq	trochjap	trochnan
352	1433.8	0	0	0	0	0	0	0	0
360	1455.0	0	0	0	0	0	0	0	0
368	1476.2	0	0	0	0	0	1	1	0
376	1497.4	0	0	0	0	0	0	0	0
384	1518.6	0	0	0	0	0	0	0	0
392	1539.8	0	25	13	0	0	0	0	0
400	1561.0	0	0	0	0	0	0	0	0
406	1576.9	0	0	0	0	0	0	0	0
416	1603.4	0	0	0	0	0	0	0	0
424	1624.6	0	0	0	0	0	0	0	0
430	1640.5	0	0	5	18	0	0	0	0
440	1667.0	0	0	0	0	0	0	0	0
448	1688.2	0	0	0	0	0	0	0	0
454	1704.1	0	0	0	0	0	0	0	0
464	1730.6	0	0	0	0	0	0	0	0
472	1751.8	0	0	1	0	0	0	0	0
488	1794.2	0	0	3	0	0	0	0	0
496	1815.4	0	0	0	0	0	0	0	0
500	1826.0	0	0	0	0	0	0	0	0
502	1831.3	0	0	0	0	0	0	0	0
512	1857.8	0	0	0	0	0	0	0	0
526	1894.9	0	0	0	0	0	0	0	0

Appendix 12: Core DA00-03
Agglutinated foraminiferal counts

Sample Depth (cm)	Converted Age (cal yr BP)	aderglom	cribcras	cribjeff	cunart	eggadv	recturb	reograci	reogutt	reopilu
536	1921.4	0	0	0	0	0	0	0	0	0
546	1947.9	0	0	0	1	0	0	1	0	1
560	1985.0	0	8	0	4	0	0	4	0	0
568	2006.2	0	0	0	0	0	0	1	0	0
574	2022.1	0	2	0	1	0	0	0	0	0
584	2048.6	0	0	0	3	0	0	1	0	0
592	2069.8	0	0	0	0	0	0	1	0	0
598	2085.7	0	0	0	0	0	0	0	0	0
608	2112.2	0	1	0	0	0	0	0	0	0
616	2133.4	18	5	0	0	0	0	0	0	0
622	2149.3	0	0	0	33	0	0	67	0	0
632	2175.8	0	0	0	0	0	0	0	0	0
640	2197.0	0	0	0	1	0	0	0	0	0
646	2212.9	0	3	0	0	0	1	0	0	0
656	2239.4	0	2	0	4	0	0	0	0	0
664	2260.6	1	1	0	0	0	0	0	0	0
670	2276.5	0	0	0	0	0	0	0	0	0
672	2281.8	0	5	0	0	0	0	3	0	3
680	2303.0	0	50	0	0	0	0	0	0	0
684	2313.6	0	7	0	22	0	0	29	0	0
688	2324.2	0	67	0	0	0	0	0	0	0
694	2340.1	0	0	0	50	0	0	50	0	0

Appendix 12: Core DA00-03
Agglutinated foraminiferal counts

Sample Depth (cm)	Converted Age (cal yr BP)	reoscorp	sacdifli	silicosi	spirobif	texear	textorq	trochjap	trochnan
536	1921.4	0	0	0	0	0	0	0	0
546	1947.9	0	0	0	0	0	0	0	0
560	1985.0	0	0	0	0	0	0	0	0
568	2006.2	0	1	0	0	0	0	0	0
574	2022.1	0	0	0	0	0	0	0	0
584	2048.6	0	0	0	0	0	0	0	0
592	2069.8	0	0	0	0	0	0	0	0
598	2085.7	0	0	0	0	0	0	0	0
608	2112.2	0	2	0	0	0	0	0	0
616	2133.4	0	5	0	0	0	0	0	0
622	2149.3	0	0	0	0	0	0	0	0
632	2175.8	0	0	0	0	100	0	0	0
640	2197.0	0	0	0	2	0	0	0	0
646	2212.9	0	0	0	0	0	0	0	0
656	2239.4	0	3	0	0	0	0	0	0
664	2260.6	0	0	0	0	0	0	0	0
670	2276.5	0	0	0	0	0	0	0	0
672	2281.8	0	0	0	0	0	0	0	0
680	2303.0	0	0	0	0	0	0	0	0
684	2313.6	0	0	0	0	7	0	0	0
688	2324.2	0	0	0	0	0	0	0	0
694	2340.1	0	0	0	0	0	0	0	0

Appendix 12: Core DA00-03
Agglutinated foraminiferal counts

Sample Depth (cm)	Converted Age (cal yr BP)	aderglom	cribcras	cribjeff	cunart	eggadv	recturb	reograci	reogutt	reopilu
696	2345.4	0	2	0	1	1	1	0	0	0
7002	2361.3	0	23	0	31	0	0	15	0	0
710	2382.5	0	64	0	18	0	0	9	0	0
720	2409.0	0	8	0	3	0	1	8	0	0
728	2430.2	0	33	0	17	0	17	17	0	0
736	2451.4	1	1	0	73	0	0	16	0	0
744	2472.6	0	0	0	1	0	1	3	0	0
752	2493.8	4	0	0	39	0	0	36	11	0
760	2515.0	0	2	1	78	0	0	9	0	0
768	2536.2	0	2	0	0	0	0	0	0	0
776	2557.4	0	0	0	0	0	0	50	0	0
792	2599.8	0	3	0	0	0	0	0	0	0
800	2621.0	0	0	20	30	0	0	30	0	0
808	2642.2	0	20	0	20	0	0	20	0	0
816	2663.4	0	0	0	1	0	0	0	0	0
824	2684.6	0	2	2	0	0	0	2	0	0
832	2705.8	13	25	0	13	0	0	38	0	0
840	2727.0	0	0	0	3	0	0	1	0	0
848	2748.2	0	0	0	0	0	0	0	0	0
856	2769.4	0	1	0	6	2	0	2	1	0
864	2790.6	0	7	0	5	0	0	0	0	0
872	2811.8	0	0	0	3	0	0	4	0	0

Appendix 12: Core DA00-03
Agglutinated foraminiferal counts

Sample Depth (cm)	Converted Age (cal yr BP)	reoscorp	sacdifli	silicosi	spirobif	texear	textorq	trochjap	trochnan
696	2345.4	0	0	0	0	0	0	0	0
7002	2361.3	0	0	0	31	0	0	0	0
710	2382.5	0	0	0	9	0	0	0	0
720	2409.0	0	0	1	0	0	0	0	0
728	2430.2	0	0	0	17	0	0	0	0
736	2451.4	0	0	0	4	0	2	0	1
744	2472.6	0	0	0	0	0	0	0	0
752	2493.8	0	0	7	4	0	0	0	0
760	2515.0	0	0	1	2	3	3	0	0
768	2536.2	0	0	0	0	0	0	0	0
776	2557.4	0	0	0	0	0	0	0	50
792	2599.8	0	0	0	0	0	0	0	0
800	2621.0	0	0	0	0	0	0	20	0
808	2642.2	0	0	0	20	0	20	0	0
816	2663.4	0	0	0	1	0	0	0	0
824	2684.6	0	0	0	0	0	0	0	0
832	2705.8	0	0	0	0	0	0	0	0
840	2727.0	0	0	1	1	0	0	0	0
848	2748.2	0	0	0	0	0	0	0	0
856	2769.4	0	0	0	1	2	0	0	0
864	2790.6	0	0	0	0	0	0	0	0
872	2811.8	0	0	0	0	0	0	0	0

Appendix 12: Core DA00-03
Agglutinated foraminiferal counts

Sample Depth (cm)	Converted Age (cal yr BP)	aderglom	cribcras	cribjeff	cunart	eggadv	recturb	reograci	reogutt	reopilu
880	2833.0	0	0	0	9	0	0	8	1	0
888	2854.2	0	0	0	6	0	0	0	3	0
896	2875.4	0	0	0	1	0	0	0	0	0
904	2896.6	3	0	0	5	0	0	2	0	0
912	2917.8	0	0	0	0	0	0	13	0	0
920	2939.0	0	0	0	5	0	2	4	1	0
928	2960.2	2	3	5	19	0	5	6	2	0
944	3002.6	0	2	2	4	0	0	20	2	0
952	3023.8	0	0	5	30	15	5	10	0	0
968	3066.2	0	33	0	33	0	0	33	0	0
972	3076.8	0	0	0	0	0	0	0	0	0
992	3129.8	0	0	0	0	0	0	1	0	0
1000	3151.0	0	5	0	0	0	0	2	0	0

Sample Depth (cm)	Converted Age (cal yr BP)	reoscorp	sacdifli	silicosi	spirobif	texear	textorq	trochjap	trochnan
880	2833.0	0	0	1	3	0	0	1	0
888	2854.2	0	0	0	0	0	0	0	0
896	2875.4	0	0	1	0	0	0	0	0
904	2896.6	0	0	0	2	0	0	0	0
912	2917.8	0	0	0	0	0	0	0	0
920	2939.0	0	0	0	0	0	0	1	0
928	2960.2	0	0	0	5	2	1	2	1
944	3002.6	0	0	0	4	2	0	0	2
952	3023.8	0	0	0	15	0	10	0	5
968	3066.2	0	0	0	0	0	0	0	0
972	3076.8	0	0	0	0	0	0	0	0
992	3129.8	0	0	0	0	0	0	0	0
1000	3151.0	0	0	0	1	0	0	0	1

Appendix 12: Core DA00-03
Agglutinated foraminiferal counts

Appendix 13: Core DA00-03
Core foraminiferal data analysis

Sample Depth (cm)	Converted Age (cal yr BP)	no. agglu species	no. calc species	total no. species	% agglu	% calc	%species dominance	ice proximal species	aggl count	calc count	total benthic counted	sediment volume	foram conc (tests/ml)	% Arctic	% Atlantic
2	506.3	6	6	12	65	35	34	1	102	55	157	25	6	6	27
8	522.2	6	3	9	85	15	31	2	53	9	62	6	10	16	13
16	543.4	4	3	7	48	52	35	4	11	12	23	5	5	13	35
24	564.6	5	3	8	94	6	51	1	105	7	112	5	22	8	3
34	591.1	4	8	12	22	75	57	1	17	58	75	6	13	5	61
40	607.0	7	4	11	87	12	18	0	94	13	107	7	15	18	16
48	628.2	4	6	10	19	81	29	4	14	58	72	8	9	6	37
56	649.4	9	13	22	59	41	27	6	102	71	173	9	19	9	34
72	691.8	6	7	13	48	52	26	15	22	24	46	6	8	24	13
80	713.0	4	13	17	18	80	36	10	55	240	295	15	20	62	8
96	755.4	4	5	9	50	50	28	0	9	9	18	6	3	6	33
100	766.0	3	12	15	20	77	38	5	46	180	226	8	28	17	48
102	771.3	0	8	8	0	100	49	5	0	209	209	7	30	58	30
104	776.6	7	1	8	96	4	42	0	76	3	79	6	13	42	5
106	781.9	3	5	8	29	71	48	6	9	22	31	6	5	10	52
112	797.8	5	3	8	51	49	46	1	36	34	70	7	10	6	46
120	819.0	2	5	7	28	72	56	4	15	39	54	6	9	4	61
128	840.2	6	13	19	17	83	43	11	29	142	171	8	21	12	53
144	882.6	4	3	7	45	55	47	0	19	23	42	8	5	7	69
152	903.8	2	6	8	3	97	47	12	2	64	66	7	9	12	62
160	925.0	4	1	5	92	8	38	0	12	1	13	6	2	0	15
168	946.2	7	0	7	100	0	40	0	53	0	53	5	11	8	25

Appendix 13: Core DA00-03
Core foraminiferal data analysis

Sample Depth (cm)	Converted Age (cal yr BP)	no. agglu species	no. calc species	total no. species	% agglu	% calc	%species dominance	ice proximal species	aggl count	calc count	total benthic counted	sediment volume	foram conc (tests/ml)	% Arctic	% Atlantic
176	967.4	6	1	7	95	5	36	0	21	1	22	5	4	0	25
184	988.6	6	11	17	34	63	17	13	28	52	80	5	16	16	35
192	1009.8	6	8	14	29	71	21	19	31	76	107	5	21	21	33
200	1031.0	1	1	2	25	75	75	0	1	3	4	6	1	0	100
208	1052.2	3	2	5	57	43	29	0	4	3	7	7	1	0	57
216	1073.4	3	1	4	97	3	56	0	35	1	36	7	5	0	14
232	1115.8	6	8	14	19	79	47	5	19	81	100	8	13	6	60
240	1137.0	5	10	15	6	89	52	3	8	125	133	7	19	3	66
248	1158.2	6	4	10	65	35	26	9	15	8	23	5	5	13	30
256	1179.4	1	1	2	50	50	50	0	1	1	2	6	0	0	50
264	1200.6	5	7	12	21	79	33	13	15	55	70	9	8	14	61
272	1221.8	9	8	17	63	37	22	10	97	56	153	11	14	13	29
280	1243.0	2	8	10	18	78	31	6	9	38	47	7	7	8	71
288	1264.2	1	10	11	7	90	42	19	12	153	165	6	28	24	48
296	1285.4	6	0	6	100	0	50	0	16	0	16	6	3	13	6
300	1296.0	8	13	21	47	52	20	12	80	90	170	7	24	16	25
304	1306.6	5	15	20	12	84	26	16	33	235	268	9	30	21	32
312	1327.8	2	6	8	2	98	48	7	2	81	83	6	14	7	65
320	1349.0	4	4	8	71	29	29	0	17	7	24	7	3	0	12
328	1370.2	4	13	17	21	75	15	20	44	154	198	7	28	32	24
336	1391.4	7	12	19	55	44	24	9	84	67	151	7	22	14	14
344	1412.6	4	7	11	21	75	38	8	5	18	23	6	4	12	54

Appendix 13: Core DA00-03
Core foraminiferal data analysis

Sample Depth (cm)	Converted Age (cal yr BP)	no. agglu species	no. calc species	total no. species	% agglu	% calc	%species dominance	ice proximal species	aggl count	calc count	total benthic counted	sediment volume	foram conc (tests/ml)	% Arctic	% Atlantic
352	1433.8	3	14	17	8	92	36	12	23	280	303	9	34	54	14
360	1455.0	2	6	8	2	98	80	9	7	286	293	7	42	91	7
368	1476.2	8	14	22	13	86	21	15	21	144	165	6	28	25	29
376	1497.4	4	4	8	41	59	37	4	11	16	27	5	5	4	70
384	1518.6	2	0	2	100	0	69	0	13	0	13	6	2	0	0
392	1539.8	5	1	6	88	13	25	13	7	1	8	7	1	13	50
400	1561.0	3	8	11	9	90	33	18	7	74	81	6	14	18	43
406	1576.9	4	7	11	36	59	20	22	27	45	72	6	12	22	42
416	1603.4	2	1	3	75	25	50	0	3	1	4	7	1	0	25
424	1624.6	2	11	13	3	97	40	11	3	91	94	5	19	23	28
430	1640.5	6	0	6	100	0	41	0	22	0	22	7	3	18	5
440	1667.0	3	9	12	7	93	43	12	4	56	60	6	10	12	57
448	1688.2	1	13	14	3	93	37	16	3	102	105	8	13	21	50
454	1704.0	2	10	12	4	91	49	8	10	213	223	8	28	12	57
464	1730.6	1	10	11	1	97	37	31	1	69	70	5	14	41	42
472	1751.8	3	10	13	4	94	22	18	7	181	188	7	27	39	26
488	1794.2	2	10	12	6	93	26	13	5	81	86	7	12	14	53
496	1815.4	1	7	8	2	96	63	5	2	80	82	6	14	5	73
500	1826.0	4	13	17	4	91	28	17	12	268	280	25	11	27	38
502	1831.3	1	8	9	2	92	51	4	2	84	86	7	12	5	64
512	1857.8	1	13	14	3	97	26	18	6	230	236	8	30	23	38
526	1894.9	0	12	12	0	98	51	11	0	166	166	9	18	18	64

Appendix 13: Core DA00-03
Core foraminiferal data analysis

Sample Depth (cm)	Converted Age (cal yr BP)	no. agglu species	no. calc species	total no. species	% agglu	% calc	%species dominance	ice proximal species	aggl count	calc count	total benthic counted	sediment volume	foram conc (tests/ml)	% Arctic	% Atlantic
536	1921.4	0	13	13	0	98	45	3	1	223	224	9	25	9	60
546	1947.9	3	14	17	3	94	22	12	8	286	294	10	29	32	35
560	1985.0	3	5	8	17	83	42	4	0	0	0	8	0	4	79
568	2006.2	2	12	14	2	95	27	6	4	20	24	7	3	26	45
574	2022.1	2	9	11	4	93	40	12	5	236	241	9	27	17	62
584	2048.6	2	13	15	4	93	24	11	10	242	252	7	36	14	46
592	2069.8	1	13	14	1	98	34	14	3	74	77	7	11	17	59
598	2085.7	0	6	6	0	97	58	11	3	204	207	8	26	13	78
608	2112.2	2	11	13	3	95	36	4	0	208	208	7	30	4	53
616	2133.4	3	6	9	27	73	23	5	3	99	102	6	17	5	55
622	2149.3	2	0	2	100	0	67	0	6	16	22	7	3	0	0
632	2175.8	1	0	1	100	0	100	0	6	0	6	7	1	0	0
640	2197.0	2	13	15	4	96	23	21	1	0	1	7	0	27	41
646	2212.9	2	6	8	6	94	49	7	6	151	157	6	26	7	78
656	2239.4	3	8	11	9	91	47	2	6	90	96	7	14	2	71
664	2260.6	2	9	11	2	96	30	1	9	91	100	8	13	1	57
670	2276.5	0	14	14	1	95	21	18	2	80	82	6	14	20	42
672	2281.8	3	4	7	11	89	42	5	3	289	292	8	37	5	47
680	2303.0	1	1	2	50	50	50	0	4	34	38	7	5	0	100
684	2313.6	4	4	8	76	24	29	2	1	1	2	5	0	2	7
688	23242.	1	0	1	67	33	67	0	31	10	41	7	6	0	67
694	2340.1	2	0	2	100	0	50	0	2	1	3	6	1	0	0

Appendix 13: Core DA00-03
Core foraminiferal data analysis

Sample Depth (cm)	Converted Age (cal yr BP)	no. agglu species	no. calc species	total no. species	% agglu	% calc	%species dominance	ice proximal species	aggl count	calc count	total benthic counted	sediment volume	foram conc (tests/ml)	% Arctic	% Atlantic
696	2345.4	4	7	11	6	94	44	1	2	0	2	8	0	1	52
702	2361.3	4	0	4	100	0	31	0	5	80	85	8	11	31	23
710	2382.5	4	0	4	100	0	64	0	13	0	13	6	2	9	64
720	2409.0	5	11	16	20	73	21	21	11	0	11	6	2	22	33
728	2430.2	5	0	5	100	0	33	0	31	112	143	7	20	17	33
736	2451.4	7	1	8	99	1	73	1	6	0	6	6	1	5	1
744	2472.6	3	12	15	5	90	31	28	81	1	82	7	12	29	6
752	2493.8	6	0	6	100	0	39	0	4	72	76	6	13	4	0
760	2515.0	8	0	8	100	0	78	0	28	0	28	8	4	2	2
768	2536.2	1	7	8	2	98	45	1	92	0	92	7	13	1	55
776	2557.4	2	0	2	100	0	50	0	5	198	203	6	34	0	0
792	2599.8	1	7	8	3	95	52	20	2	0	2	6	0	23	58
800	2621.0	4	0	4	100	0	30	0	0	0	0	5	0	0	0
808	2642.2	5	0	5	100	0	20	0	2	61	63	6	11	20	20
816	2663.4	2	10	12	2	95	36	28	10	0	10	6	2	72	12
824	2684.6	3	10	13	5	91	55	9	5	0	5	6	1	9	65
832	2705.8	4	1	5	88	13	38	0	6	286	292	6	49	0	38
840	2727.0	4	11	15	6	87	32	32	3	50	53	7	8	59	8
848	2748.2	0	13	13	0	92	17	17	7	1	8	5	2	20	20
856	2769.4	7	14	21	13	86	52	9	19	264	283	7	40	66	7
864	2790.6	2	10	12	11	87	21	15	0	60	60	7	9	30	30
872	2811.8	2	12	14	8	89	21	14	26	169	195	8	24	37	20

Appendix 13: Core DA00-03
Core foraminiferal data analysis

Sample Depth (cm)	Converted Age (cal yr BP)	no. agglu species	no. calc species	total no. species	% agglu	% calc	%species dominance	ice proximal species	aggl count	calc count	total benthic counted	sediment volume	foram conc (tests/ml)	% Arctic	% Atlantic
880	2833.0	6	12	18	23	73	15	26	7	53	60	8	8	43	21
888	2854.2	2	2	4	9	91	74	0	21	229	250	12	21	0	74
896	2875.4	2	13	15	1	87	39	50	69	221	290	9	32	51	9
904	2896.6	4	10	14	10	89	26	18	3	32	35	5	7	21	34
912	2917.8	1	7	8	13	88	21	25	2	160	162	6	27	25	21
920	2939.0	5	11	16	14	84	22	31	6	55	61	6	10	36	22
928	2960.2	12	12	24	53	45	19	20	3	21	24	7	3	30	12
944	3002.6	8	7	15	39	61	20	16	32	196	228	6	38	20	22
952	3023.8	8	0	8	95	5	30	0	153	130	283	7	40	15	0
968	3066.2	3	0	3	100	0	33	0	19	30	49	6	8	0	33
972	3076.8	0	10	10	0	100	21	8	19	1	20	6	3	8	18
992	3129.8	1	13	14	1	91	19	25	3	0	3	5	1	26	7
1000	3151.0	4	12	16	9	89	36	11	0	66	66	6	11	16	47

Appendix 14: DA00-03
Single species isotope data

Depth (cm)	Converted Age (cal yr BP)	No of *N. labradorica* tests used	$\delta^{13}C$ PDB	$\delta^{18}O$ PDB
8	522.2	4	-5.28	1.59
16	543.4	6	-3.96	2.71
34	591.1	30	-2.89	3.26
40	607.0	3	-4.60	1.88
48	628.2	17	-5.38	3.21
56	649.4	28	-5.18	2.66
72	691.8	15	-4.78	2.84
80	713.0	15	-5.61	3.01
106	781.9	12	-2.48	2.85
112	797.8	4	-2.14	3.09
120	819.0	17	-2.93	3.05
128	840.2	33	-1.75	2.76
144	882.6	15	-1.99	2.69
152	903.8	18	-4.16	2.22
184	988.6	10	-5.28	2.89
192	1009.8	16	-1.56	2.89
232	1115.8	14	-4.24	3.23
240	1137.0	21	-1.57	2.96
264	1200.6	9	-3.69	3.04
272	1221.8	10	-3.02	3.29
280	1243.0	9	-2.11	2.86
288	1267.2	30	-3.16	2.98
300	1296.0	12	-3.70	3.05
304	1306.6	15	-2.45	3.29
312	1327.8	30	-3.89	2.96
328	1370.2	12	-3.63	3.20
344	1412.6	8	-2.81	2.56
352	1433.8	15	-3.95	3.26
360	1455.0	10	-4.67	2.91
368	1476.2	25	-3.82	3.11
376	1497.4	7	-1.89	2.49
400	1561.0	19	-2.91	3.28
424	1624.6	10	-3.72	3.18
440	1667.0	14	-3.19	3.31
448	1688.2	21	-3.31	3.58
456	1709.4	30	-2.62	3.22
464	1730.6	20	-2.76	3.39
472	1751.8	35	-3.15	3.30
480	1773.0	30	-4.91	2.94
488	1794.2	16	-3.27	3.28
496	1815.4	12	-1.71	3.42
500	1826.0	12	-3.19	3.49
504	1836.6	13	-1.07	2.94
512	1857.8	38	-1.09	3.54
520	1879.0	31	-1.76	3.38
528	1900.2	30	-0.74	3.10
536	1921.4	30	-0.34	3.62
546	1947.9	20	-0.58	3.50
560	1985.0	6	-0.42	3.30
568	2006.2	20	-0.55	3.69
576	2027.4	30	-0.75	3.23
584	2048.6	10	-1.12	3.36
592	2069.8	26	-0.75	3.27
600	2091.0	30	-0.62	3.08
608	2112.2	8	-2.45	1.13
616	2133.4	6	-2.72	1.17
640	2197.0	24	-3.32	2.80
648	2218.2	28	-0.97	2.98
656	2239.4	11	-2.87	3.02
664	2260.6	22	-1.49	3.23
672	2281.8	30	-0.96	3.05
696	2345.4	26	-4.39	2.81
720	2409.0	8	-1.82	2.42
744	2472.6	30	-3.38	2.91
768	2536.2	25	-1.84	3.28
816	2663.4	30	-2.01	2.87
824	2684.6	9	-0.77	3.24
840	2727.0	3	-2.87	3.02
848	2748.2	24	-2.51	3.02

Appendix 14: DA00-03
Single species isotope data

Depth (cm)	Converted Age (cal yr BP)	No of *N. labradorica* tests used	$\delta^{13}C$ PDB	$\delta^{18}O$ PDB
856	2769.4	29	-3.69	3.28
864	2790.6	37	-3.59	3.34
872	2811.8	27	-3.65	2.82
880	2833.0	10	-3.81	3.18
888	2854.2	15	-3.14	3.04
896	2875.4	10	-3.41	2.81
904	2896.6	35	-4.29	3.13
912	2917.8	14	-3.72	3.12
920	2939.0	8	-4.78	2.72
928	2960.2	7	-3.37	3.00
936	2981.4	15	-1.55	2.81
944	3002.6	10	-0.86	2.95
960	3045.0	4	-2.01	2.22
976	3087.4	4	-2.21	2.76
984	3108.6	23	-3.90	3.19
992	3129.8	10	-3.47	2.63
1000	3151.0	35	-3.18	3.10